Australian Geomechanics Society

Soft Ground Engineering

Proceedings of the Sydney Chapter 2006 Symposium

Wednesday 11th October 2006

Platinum sponsor: Keller Ground Engineering

Gold Sponsors: Austress Menard, Avopiling, Coffey Geotechnics, Vibropile, VSL - Intrafor

Silver Sponsors: Coates Shorco, Franki, Jeffery & Katauskas, Parsons Brinckerhoff

ENGINEERS AUSTRALIA

AusIMM AUSTRALASIAN INSTITUTE OF MINING & METALLURGY

ISSN 0818-9110

Platinum sponsor

Gold sponsors

Silver sponsors

Photographs on Front Cover: on right a Keller vibroprober hard at work in Newcastle; on left a piling rig set-up for installation of "rigid inclusions".

ISBN 1 876775 65 3

SOFT GROUND ENGINEERING

PROCEEDINGS OF THE SYDNEY CHAPTER 2006 SYMPOSIUM

HELD IN

AUSTRALIAN NATIONAL MARITIME MUSEUM, DARLING HARBOUR, NSW

ON

October 11th 2006

Organising Committee : H.G. Buys, P. Hewitt and R.A. Moyle

Published by
The Australian Geomechanics Society,
National Secretariat,
P.O. Box 955, ST IVES, NSW 2075

The AUSTRALIAN GEOMECHANICS SOCIETY is jointly sponsored by:
Engineers, Australia and
The Australasian Institute of Mining and Metallurgy

Australian Geomechanics Society

Geomechanics is the application of engineering principles to the earth sciences to improve continually the accuracy, efficiency, cost-effectiveness and safety of construction projects both above and below ground, including the recovery of the earth's mineral resources. It remains an imprecise discipline due to the infinite variety of conditions in the earth's crust but correspondingly offers a fascinating and rewarding field of research and practice.

The Australian Geomechanics Society was founded in 1970. Its origins lie in the National Committee of Soil Mechanics of the Institution of Engineers, Australia, established in 1953 and the call for a corresponding society in rock mechanics. In 1973 the society was expanded to include the third discipline of engineering geology and has remained substantially unchanged since that date.

The society is affiliated to the International society of Soil Mechanics and Foundation Engineering (ISSMFE), the International Society for Rock mechanics (ISRM) and the International Association for Engineering Geology and the Environment (IAEG).

The AGS is jointly sponsored by the Engineers Australia and the Australian Institute of Mining and Metallurgy.

CORPORATE MEMBERSHIP OF THE AGS

$649.00 and look at what your organisation gets -
Membership for two nominees who each receive:

- Membership fee ($154)
- Membership of the three International Societies ($118.80)
- IAEG Bulletin ($39.60)

An extra copy of *Australian Geomechanics* for company library ($95)

Acknowledgement in front section of every issue of *Australian Geomechanics*

Total benefit is $719.80 All prices include GST.

Contact Peter Robinson on secretary@australiangeomechanics.org or go to www.australiangeomechanics.org **for application forms and more information**.

Australian Geomechanics Society

Sydney Chapter

ENGINEERS AUSTRALIA
SYDNEY DIVISION

2006 Symposium

Soft Ground Engineering

Wednesday 11 October 2006

Australian National Maritime Museum, Darling Harbour, Sydney

Program

8:30	Registration
9:00	Opening address **Graham Scholey**
	Session 1 - Overview
9:15	Why are there seashells in my alluvial valley? **Trevor Graham**
9:45	Preload design - what can go wrong? **Patrick Wong**
10:15	The development and application of grouting and ground treatment **David Lees**
10:45	Questions
10:55-11:10	Morning tea
	Session 2 – Investigation and Analysis
11:10	Soft soil site characterisation by in situ testing **Allan McConnell**
11:40	Deep excavations in soft ground using temporary structural steelwork **Christopher Daniel**
12:10	Settling and consolidation behaviour of dredged cohesive estuarine soil using column testing apparatus **SR Morrison, Andrew Tait**
12:40	Questions
12:50 - 13:35	Lunch
	Session 3 – Construction Methods and Case Histories
13:35	Lime Cement Mixing (LCM) – Applications of the Scandinavian Method **Marcus Dahlstrom**
14:05	Soft soil case history: Shellharbour sewage treatment plant upgrade **Philip Davies, Andrea Faulkner**
14:35	Jet grouting for Lisarow rail bridge renewal **Paul Hewitt, Charles Spaulding**
15:05	Questions
15:15-15:45	Afternoon tea
	Session 4 – Constitutive Modelling and Monitoring
15:45	Effects of clay structure degradation on settlement of embankment **Jidong Zhao, Daichao Sheng, Andrew Abbo, Scott Sloan**
16:15	Assessment of impacts of ground movements on existing structures adjacent to excavations **Jeff Hsi**
16:45	Questions
16:55	Closing address **Henk Buys**
17:10	Close

Australian Geomechanics Society

Sydney Chapter

2006 Symposium

Soft Ground Engineering

Program (Cont'd)

The following papers will also be included in the Proceedings.

Soft ground improvement – issues and selection – **Paul Hewitt and George Munfakh**

Sensitivities of braced deep excavations to jet grout pile applications - **Christopher Daniel**

Modelling of soft soil improvement induced by tree root suction - **Behzad Fatahi, Buddhima Indraratna**

Large-scale cyclic triaxial testing of soft clay - **Anass Attya, Buddhima Indraratna, Hadi Khabbaz**

The sensitivity framework: Behaviour of Richmond River estuarine clays - **Daniel Bishop, Stephen Fityus**

Performance & prediction of soft clay behaviour under vacuum conditions - **Cholachat Rujikiatkamjorn, Buddhima Indraratna**

Australian Geomechanics Society, ABN 89 615 696 393

Venue: ANZ Theatre, Australian National Maritime Museum, 2 Murray Street, Darling Harbour, Sydney NSW 2000. (02) 9298 3625

AGS committee reserves the right to change the program and /or the identity of the presenters at any time without notice.

SYMPOSIUM – WEDNESDAY 11 OCTOBER 2006

SOFT GROUND ENGINEERING

PREFACE

This document contains the papers for the 10th annual symposium organised by the Sydney Chapter of the Australian Geomechanics Society. It is hoped the symposium will keep practising geotechnical engineers, engineering geologists and other engineering professionals informed of recent developments in this field. It also recognises the need to gather together the experience of those practising throughout Australia and to allow transfer of knowledge and sharing of their experiences.

These symposia continue to be one of the best forums for bringing together the key stakeholders of the Australian geotechnical community. The objectives of the symposium held in Sydney on 11 October 2006 have been to advance the knowledge of soft ground engineering.

The symposium includes a number of themes including ground characterisation, investigation and analysis, case histories and construction. Contributors include owners, designers, suppliers and contractors. The papers present soft ground project challenges and solutions from throughout Australia and overseas.

This symposium is the cooperative effort of many authors. The Editors and organising committee wish to thank the authors, who have so generously contributed their time to prepare the various papers, and the employers of the authors, who have assisted with time, secretarial, drafting and photocopying facilities. Appreciation is also extended to our sponsors for their support. Without them, the AGS Symposium would not be one of the best ongoing forums for the Australian geomechanics community.

Henk Buys, Paul Hewitt, Richard Moyle

On behalf of the Australian Geomechanics Society, Sydney Chapter and
Sydney Chapter Symposium Organising Committee

Annual Seminars of AGS Sydney Chapter

No.	Date	Topic	Chairman & Organising Team
1	9 April 1997	Pavement Design Beyond 2000	Andrew Leventhal
2	1998	Recent Developments in Piling Practice in Sydney	Peter Andrews
3	11 August/1999	Flexible Retaining Walls: Design to Prevent Failure	Peter Andrews/Paul Hewitt
4	9 August 2000	Computer Methods	Paul Hewitt/John Carter
5	8 August 2001	Excavation Retention	T. Walker/P. Hewitt
6	2002	Landslide Risk Management	B Walker/T Walker
7	13 August 2003	Geotechnical Instrumentation and Construction works Compliance Testing	G Scholey/T Walker
8	12 October 2004	The Engineering Geology of the Sydney Region – Revisited	G Scholey/M Parmar /G Young/G McNally
9	12 October 2005	Geotechnical Aspects of Tunnelling	H Buys/T Gourlay
10	11 October 2006	Soft Ground Engineering	H Buys/P Hewitt/R. Moyle

CONTENTS

[All papers have been refereed in accordance with the full DETYA review process, unless stated otherwise.]

SOFT GROUND IMPROVEMENT – ISSUES AND SELECTION

Paul Hewitt and George Munfakh
Parsons Brinckerhoff

ABSTRACT

Issues that affect the successful application of ground improvement in soft ground are studied, with emphasis on the design, construction and long-term performance of the improved ground, and recent developments relevant to Australian geotechnical practice.

This paper discusses various technical issues affecting typical soft ground improvement techniques including: densification, consolidation, weight reduction, structural support and chemical treatment. Several factors that can influence the selection of a ground improvement technique, or a combination of techniques, are discussed. Case studies are provided to demonstrate the recent application of ground improvement techniques to the design and construction process.

1 INTRODUCTION

Ground improvement techniques applied in geotechnical engineering practice are tools used by the geotechnical engineer for "fixing" the problems of poor ground. By imaginative use of techniques, the engineer forces the ground to adapt to the project's requirements, by altering its natural state, instead of having to alter the design in response to the ground's natural limitations. Ground characteristics have affected the decisions made by builders since the days of early settlement. The location, height and configuration of some of the historic monuments and infrastructure seen today were influenced to a certain degree by the anticipated behaviour of the ground. Where poor ground existed at a project site, the early builder was faced with the following questions:

- Should the soft ground be removed and replaced with a more suitable material?
- Should the soft ground be bypassed laterally by changing the project's location, or vertically by the use of deep foundations? or
- Should the design of the facility (height, configuration, etc.) be changed to reflect the ground's limitations?

With the development of ground improvement, the modern builder has a fourth option - to "fix" poor ground, making it suitable for the project's needs - instead of having to alter the original plans to reflect the ground's limitations. The new questions facing the current builder are then:

- Should the problematic ground at the project site be fixed instead of bypassed?
- What are the critical issues that influence the successful application of a specific fixing tool? and
- Which fixing tool should be used out of the comprehensive and diversified set currently available in the toolbox?

Technical, practical, economical and political factors influence the answers to the first and third questions. In order to provide credible answers, the second question needs to be answered first. In this paper, the critical issues affecting the feasibility of the main ground improvement methods in the current state of the practice are evaluated from both design and construction points of view.

2 GROUND IMPROVEMENT IN SOFT SOIL

Ground improvement in soft soil has five major functions, namely to:

- increase the bearing capacity
- control deformations and accelerate consolidation
- provide lateral stability
- form seepage cut-off and environmental control and
- increase resistance to liquefaction.

These functions can be accomplished by modifying the character of the ground, with or without the addition of foreign material. Improving the ground at the surface is usually easily accomplished and relatively inexpensive. At depth,

however, the task becomes more difficult, usually requiring more rigorous analyses and the use of specialised equipment and construction procedures.

3 THE CURRENT STATE OF PRACTICE

The soft soil improvement methods most commonly used today can be divided into categories as follows:

- densification (vibrocompaction, dynamic compaction, blasting, compaction grouting)
- consolidation (preloading, surcharge, vertical (wick) drains, electro-osmosis, vacuum consolidation)
- weight reduction (wood chips, fly ash, slag, tyre chips, flowable fill, geofoam)
- reinforcement (reinforced soil wall systems, soil nailing, piles, stone columns, fibre reinforcement)
- chemical treatment (permeation, jet or fracture grouting, soil mixing, lime columns)
- thermal stabilization (ground freezing, vitrification).

Additional methods such as electrotreatment and biotechnical stabilization more applicable to other soils are addressed in Munfakh and Wyllie (2000).

Some the above methods are suited to a specific ground type, while others apply to a wide range of soils. Table 1 presents the ground improvement techniques used for granular and cohesive soils and the main objectives of their applications. This table is by no means completely comprehensive, as new methods and applications are constantly evolving. With the development of new machinery, inexpensive construction materials, geotechnical instrumentation techniques and flexible contracting policies and procedures, the application of innovative methods for improving the natural state of weak soils is limited only by the imagination of the engineer.

4 GROUND IMPROVEMENT ISSUES

Many issues affect the successful application of ground improvement; some of these require resolution by the designer and others by the contractor. While detailed studies and extensive research by government agencies, research institutions and academia have focused on the major issues, some equally important issues are not well recognised, except by specialty contractors. Such contractors have developed many of the ground improvement techniques currently used, including some that are still considered ‘state-of-the-art’.

When highway and railway embankments are built over compressible alluvial deposits, ground improvement is often required to ensure stability and allow construction of steep side slopes which, in turn, reduces cost and minimizes impact on adjacent facilities or encroachment on environmentally sensitive areas, such as wetlands. If the native soil is granular, the improvement usually consists of densification. If the soil is cohesive, the ground improvement techniques applied may include consolidation, weight reduction, or reinforcement using vertical reinforcing elements. Detailed discussions of the design and construction aspects of these methods can be found in Munfakh (1997), Munfakh (1999) and Elias *et al.* (1999). To follow is a brief description of the ground improvement methods currently on the market, and the key issues that affect their application.

4.1 GROUND IMPROVEMENT BY DENSIFICATION

Loose granular soils can be densified to increase their bearing capacity, reduce settlement and increase resistance to liquefaction. At the surface, densification is achieved through compaction with conventional or high energy impact compaction rollers. See Figure 1 which illustrates the use of impact compaction of loose sand at a high-rise, residential and commercial development site in Sydney. On this site, adoption of ground improvement techniques allowed use of an alternative stiffened raft foundation, instead of piles, to “fix” poor ground, making it suitable for the project’s needs.

When applied at depth, however, more complicated techniques are used, which often require specialist equipment.

Figure 1: Densification to increase the bearing capacity and reduce settlement in marine sand.

4.1.1 Methods of Application

Densification at depth is accomplished using the following methods:

- vibro-compaction
- dynamic compaction
- dynamic replacement
- blasting
- compaction (displacement) grouting.

During vibro-compaction, loose granular soils are densified at depth by insertion of vibrating probes into the ground. Compaction is achieved by impact and vibration, with or without the use of a water jet or compressed air and with or without the addition of granular material. Densification can be achieved to depths of 30 m.

During dynamic compaction, large weights are dropped repeatedly onto the ground surface over a predetermined grid pattern. The resulting high-energy impacts cause densification of the soil mass to depths from 3 m to 8 m. The drop heights are usually 12 m to 24 m, with drop points several metres apart in a grid pattern. Sometimes the generated craters are filled with select granular material.

Dynamic replacement uses large diameter stone columns driven into the ground using a 15 tonne to 30 tonne drop weight.

Densification by blasting is accomplished through the detonation of explosives buried in loose soils. The shock waves generated by the blast, break down the initial structure of the soil, and create a liquefaction condition, enabling the soil particles to rearrange themselves in a denser packing.

During compaction grouting, a very stiff mortar grout is injected into the ground under relatively high pressure to densify loose soil formations. The grout does not generally enter the soil pores, but remains in a homogeneous mass that displaces and compacts the surrounding soil. The grout mix typically consists of silty sand, cement, additives and water.

Table 1: Ground improvement methods and their main objectives.

GROUND IMPROVEMENT METHOD	Type of soil		Ground improvement objectives				
	Granular	Cohesive	Bearing Capacity	Settlement Control	Lateral Stability	Environmental Control	Liquefaction Resistance
Vibro-compaction (VC)	●		●	●			●
Impact compaction	●		●	●			●
Dynamic compaction (DC)	●		●	●		●	●
Dynamic replacement (DR)		●	●	●		●	●
Blasting	●		●	●			●
Compaction grouting	●			●			
Preloading/drains (VD)		●	●	●			●
Electro-osmosis		●	●	●			
Vacuum consolidation		●	●	●			
Lightweight fill	●	●		●			
Mechanical stabilization	●		●	●	●		
Soil nailing	●				●		
Soil anchoring	●				●		
Micropiles	●		●	●	●		
Stone columns (SC)		●	●	●	●		●
Fibre reinforcement	●		●	●	●		
Permeation grouting	●		●	●		●	
Jet grouting (JG)	●	●	●	●	●	●	●
Deep soil mixing (DSM)	●		●	●	●	●	●
Lime columns		●	●	●	●	●	●
Fracture grouting		●	●	●		●	
Ground freezing	●	●			●	●	
Vitrification	●	●				●	
Electro-kinetic treatment		●		●		●	
Electro-heating		●		●		●	
Biotechnical stabilization stabilisation	●				●	●	

Figure 2 illustrates the selection of soil treatment method as a function of soil type and the depth of compressible soil.

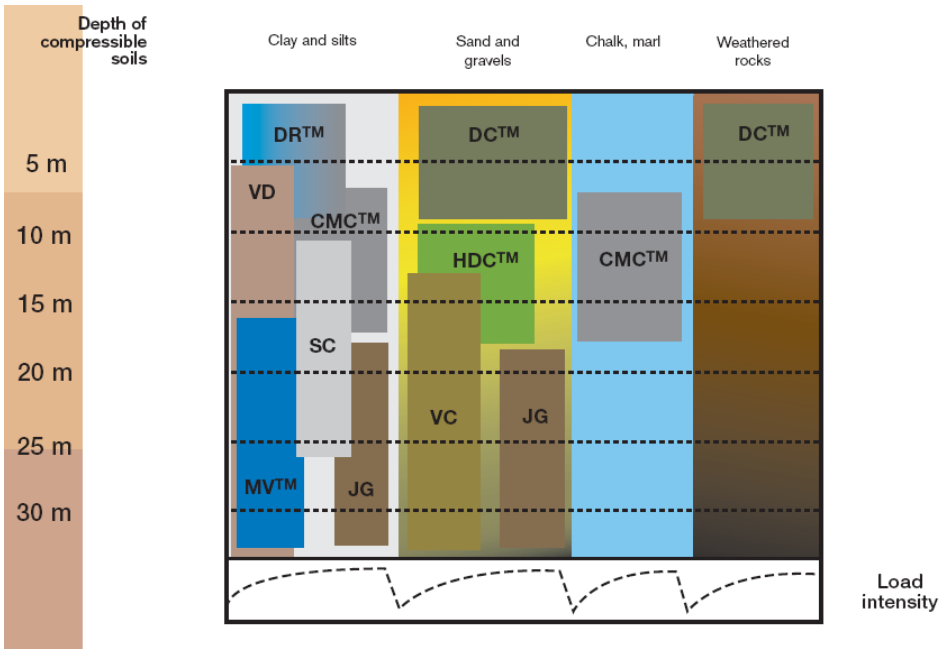

Legend:

SC	Stone columns	DR	Dynamic replacement
CMC ™	Controlled modulus columns	VC	Vibro-compaction
DC ™	Dynamic compaction	MV	Vacuum consolidation
VD	Vertical drains	JG	Jet grouting

Figure 2: Selection of ground treatment in soil (Menard, 2006).

4.1.2 Key Issues

The key issues influencing the effectiveness of soil densification include the:

- percentage of fines in the soil
- ability of the soil to dissipate excess pore water pressure
- energy felt by the soil
- presence of boulders, utilities and adjacent structures and
- the somewhat mysterious phenomenon of ageing.

Presence of Fines
The presence of fines has a negative impact on the densification process, as the fines act as lubricants, which reduce the frictional resistance between the rearranged soil particles within the densified mass. With vibro-compaction, for instance, a fines content of 20% renders the process ineffective. The amount of fines in the soil also affects soil drainage properties, which are a key factor when the densified soil is in a saturated state.

Pore Pressure Dissipation
When densification is applied to a saturated cohesionless material, a micro-liquefaction process takes place, allowing the soil particles to rearrange themselves. If excessive fines or cohesive soils are present, dissipation of the excess pore water pressure (generated by the densification process) is slowed down, or prevented. This can affect the feasibility of the applied method. To safeguard against this, pore pressure dissipation is facilitated by fissuring, or through the use of vertical drains, which are usually located equidistant from the points of densification application (the points of vibroprobe penetration, weight drop, blast holes, etc.).

Level of Energy
The level of energy applied in densification can be estimated from the characteristics of the equipment used (vibrating frequency, tamper weight, amount of explosives, etc.) and the configuration of application (probe spacing, drop height, depth of charge, etc.). The amount of energy actually felt by the soil is influenced by factors related to the ground

characteristics, the effectiveness of the applied procedures, and the experience of the equipment operator. In dynamic compaction, for instance, the depth of influence of the process is calculated using the weight and height of drops, and a soil-related empirical coefficient (Lukas, 1985; Mitchell and Jardine, 2002). This depth is also influenced by other factors like the stratigraphy of the soil, the degree of saturation and the method by which the weight is dropped. (A crane drop is less efficient than a free drop.) The presence of soft cohesive layers or peat has a damping effect on the dynamic forces penetrating the soil, and thus the depth of influence is reduced.

Proximity to Structures

The presence of utilities and buried structures affects the choice of densification used and the level of energy applied. The impact of the process on adjacent structures is a major concern and there are no set criteria in present practice to guide how close vibro-compaction or dynamic compaction can be implemented next to an existing structure without adverse effect. On a recent project involving the vibro-compaction of hydraulic fill adjacent to a bulkhead structure, inclinometer data near the bulkhead measured horizontal deflection of less than 10 mm when the vibroprobe was 3 m away from the bulkhead, increasing to more than 50 mm as the probe got within 2 m of the bulkhead. Therefore, a safe distance of 3 m was established for that project.

Ageing

Densification of the soil continues for a period of several weeks after "disturbance" due to the little-known phenomenon of "ageing". Mitchell and Solymar (1984) attribute the increase in strength and deformation modulus with time to the possible action of silica bonding between grains. Mesri *et al.* (1990) credit the phenomenon to the continued rearrangement of sand particles during secondary compression, which results in a gradual increase in particle interlocking. Debats and Sims (1997) illustrated the increase in strength with time as reported for various applications of vibro-compaction, blasting and dynamic compaction (see Figure 3). They reported a strength increase of 35% from the second to the sixth week after a major vibro-compaction application in Hong Kong. On a recent project in Norfolk, Virginia, in the United States, one of the authors of this paper (George Munfakh), measured a 15-30% increase in the relative density of a hydraulic fill, approximately 20 days after vibro-compaction, due to ageing.

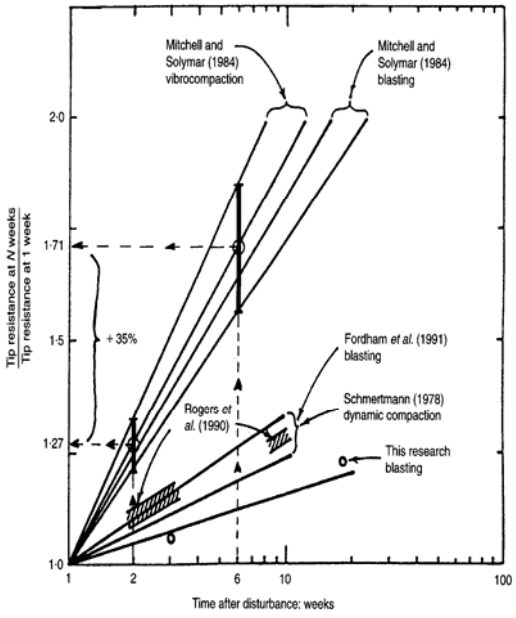

Figure 3: Strength gain due to ageing (Debats and Sims, 1997).

4.2 GROUND IMPROVEMENT BY CONSOLIDATION

Consolidation of a soft cohesive soil improves the engineering characteristics of the soil. Both the strength and unit weight of the soil are increased and hydraulic conductivity is reduced when the soil is consolidated. Unfortunately, these improvements are accompanied by a decrease in soil volume and ground deformation. To mitigate the impact of

deformation on the structure, the soil is often pre-consolidated under loads higher than the design load, so that design deformations occur prior to installation of the structure.

4.2.1 Methods of Application

There are three basic methods of ground improvement through consolidation:

- preloading with or without vertical drains
- electro-osmosis
- vacuum consolidation.

In Australia, preloading is the more commonly adopted method. Preloading is usually accomplished by placing surcharge fills which apply a load in excess of the permanent load to accelerate the rate of settlement. Controlled filling of tanks or lined ponds, electro-osmosis or vacuum consolidation are alternative means of preloading. To accelerate consolidation, vertical (sand or prefabricated wick) drains are often used with preloading.

Consolidation by electro-osmosis is the same in many aspects as consolidation under externally applied stresses, except that the driving force for drainage is induced internally by an electric field.

During vacuum consolidation, both liquid and gas (water and air) are extracted from the ground by suction induced through the creation of a vacuum on the ground surface and assisted by a system of vertical and horizontal drains. As illustrated in Figure 4, an airtight membrane is usually placed on the ground surface and in peripheral trenches to seal the soil from the atmosphere and allow the creation of the vacuum. For construction of a highway embankment over a compressible, highly organic, clay layer with a moisture content of 140% to 210%, vacuum consolidation was applied for a period of 3 months. The effect of vacuum consolidation was equivalent to that of preloading with 5 m of fill (Cognon *et al.*, 1994).

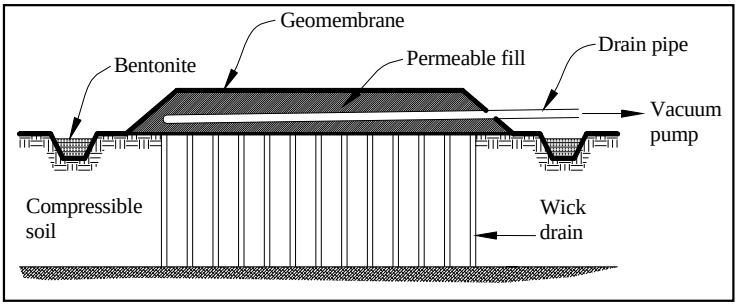

Figure 4: Vacuum consolidation concept.

Formatted: Font: 10 pt, Bold

4.2.2 Key Issues

The key issues associated with ground improvement by consolidation are:

- stability during surcharge placement
- clogging of vertical drains
- maintaining the vacuum.

System Stability

To safeguard against stability problems, surcharge loads are often placed in stages, with each stage added only after the soil has acquired sufficient strength, under the influence of the previous stage, to support the new load. A good knowledge of consolidation characteristics is needed, especially if timing is critical. The build up and dissipation of excess pore water pressure and the accompanying soil deformation are usually monitored to pinpoint the timing for stage placement. When electro-osmosis or vacuum consolidation is applied, no stability problem is anticipated and the staging requirement of preloading is eliminated.

Clogging of Drains

The clogging and smear of vertical drains is a key issue affecting the feasibility of ground improvement through consolidation. A major advantage of plastic wick drains over sand drains is their flexibility and their ability to sustain large deformations of the consolidating cohesive soil, which may otherwise shear and clog the sand drains, rendering

them ineffective. The hydraulic conductivity or discharge capacity of wick drains, on the other hand, is influenced by potential crimping of the material when large deformations take place, or clogging of drainage channels due to an ineffective filter jacket. A non-woven geotextile fabric is usually used to provide filtering and ensure the hydraulic conductivity of prefabricated drains.

Maintaining the Vacuum
The provision of an all-around seal to maintain the vacuum at ground level is critical for the successful application of vacuum consolidation. Resistance of the membrane to tearing during and after placement is an important factor affecting the ability of the system to do so. Often, the membrane is covered by a layer of soil or by water ponding to prevent tearing by vehicles, animal or bird attacks or vandalism. A new system developed recently in France eliminates the need for the membrane, as the required vacuum is generated by circulation of air through a series of specially designed drains installed to the depth of the layer to be consolidated (Robinet and Juran, 1999).

4.3 GROUND IMPROVEMENT BY WEIGHT REDUCTION

This method of ground improvement involves reduction of the weight applied to a soft compressible soil through the use of lightweight fill material. The lightweight material is either used as a fill placed on the ground surface, as in the case of embankment construction, or as a replacement to an excavated native soil layer, resulting in an overall reduction in the in situ stress on the soil beneath it.

The overall benefits gained from the use of lightweight fill materials include reduced settlement, increased slope stability, and reduced lateral earth pressure on retaining structures. A key benefit is the material's high resistance to earthquake effects. (The low unit weight results in lower seismic inertial forces.)

4.3.1 Methods of Application

The lightweight materials used most commonly in geotechnical applications are listed in Table 2, based on Stark *et al.* (2004), and Riad *et al*. (2004). The lightweight materials are placed over the native soil in one of three ways:

- spread in a loose form, then compacted
- cut in block forms, then stacked according to a certain arrangement or
- pumped in a flowable liquid form.

Table 2: Lightweight material used for ground improvement.

Fill material	Source/process	Dry unit weight (kN/m^3)
Wood fibres	Sawed timber waste	5.4 – 9.6
Shredded tyres	Mechanically cut tyre chips	5.9 – 10
Expanded shale/clay	Vitrified shale or clay	5.9 – 10.4
Fly ash	Residue of burned coal	11.2 – 14
Air-cooled slag	Blast furnace material	11 – 15
Flowable fill	Foaming agent in a concrete matrix	3.4 –7.7
EPS/Geofoam	Block moulded expanded polystyrene	0.12 – 0.32

4.3.2 Key Issues

The key issues associated with the weight reduction method of ground improvement are usually related to the method of placement of the fill material and the properties of the fill material used, namely the durability and long-term performance of the fill.

Material Placement
When fly ash is wet during placement, it may become spongy and difficult to compact. When dry, it may become too dusty and, therefore, environmentally unacceptable.

Durability
The flotation characteristics of geofoam, and its susceptibility to fire and deterioration from fuel spills or insect burrowing, are long-term durability issues that require special measures. Continued crushing and knitting of shells (oyster, or similar) under the influence of vehicular traffic may reduce the drainage potential of the embankment, thus resulting in ponding of water at the surface. Otherwise, it may reduce the frictional angle of the material, thus increasing its lateral pressure on supporting structures.

4.4 GROUND IMPROVEMENT BY REINFORCEMENT

In situ reinforcement of a poor soil is accomplished by the addition of reinforcing elements to the soil to improve its engineering characteristics. The soil and its reinforcing elements act in combination to increase the shear strength of the soil mass, reduce its settlement under load, and improve its resistance to liquefaction. The reinforcing element can be either inserted in the *in situ* soil or placed in the soil mass as it is constructed.

4.4.1 Methods of Application

Reinforcing the soil is usually accomplished by one of the following methods:

- mechanical stabilisation
- soil nailing
- soil anchoring
- micropiles
- stone columns and/or
- fibre reinforcement.

In mechanical stabilisation, the reinforcing elements are placed between layers of compacted soil. Different materials (metals, polymers, geotextiles, etc.) and shapes (strips, grids, sheets, rods, etc.) are used for reinforcement. When used in the construction of retaining walls or embankment slopes, the reinforcing elements are usually attached to facings that retain the compacted soil at the face and protect the reinforcing elements from weathering effects. The types of facing used include pre-cast concrete panels, cast-in-place concrete, metallic plates or baskets, geosynthetic grids or sheets, timber, modular blocks and rubber tyres. The backfill material usually consists of granular soil with high frictional resistance.

Used primarily to support excavations and reinforce slopes, the concept of ‘soil nailing’ involves placing closely spaced reinforcing elements *in situ* to increase the shear strength of the soil and to restrain its displacement during and after excavation. Construction is accomplished using a top-down process that involves three repetitive stages:

- excavation to a limited depth
- installation of nails and drainage
- placement of a facing.

The reinforcing elements (soil nails) are usually in the form of metal bars, tubes or rods, which are installed by driving, drilling and grouting, jet grouting, or firing (launched nails). The facing can either be built on-site (with shotcrete or cast-in-place concrete) or built from prefabricated steel or concrete panels. When excavating below the groundwater table, an appropriate vertical and/or horizontal drainage system should be installed behind the permanent facing. Figure 5 illustrates soil nailing to support an excavation on EastLink in Melbourne, and for road widening beneath a rail bridge on the Lane Cove tunnel project in Sydney.

Figure 5: Soil nailing on EastLink, Melbourne and Lane Cove tunnel project, Sydney.

During soil anchoring, pre-stressed soil anchors are installed in the ground to reinforce the soil and support vertical or inclined excavations. The anchors are attached at the surface to concrete panels or “elements,” forming what is sometimes called an element wall. As with soil nailing, the reinforcements and the soil form a coherent body that resists applied loads. To accomplish this, anchors are placed closer than in a typical anchored wall and the need for structural elements (soldier piles, lagging and walers) is avoided.

When micropiles are used for soil reinforcement, small-diameter, usually less than 300 mm, piles are installed vertically, or in a reticulated fashion, to support excavations, slopes or foundations. For these applications, the piles are spaced closer than in conventional pile foundations and the loads are supported by a complex soil-pile structure. The structure is analogous to reinforced concrete, with the ground acting like concrete and the micropiles acting like steel reinforcements. Micropiles are installed by drilling and grouting, displacement or jet grouting.

Although constructed using the same equipment and procedures as vibro-compaction, stone columns function as reinforcement rather than a method of densification. They are applied to soft cohesive soils in order to increase bearing capacity, reduce settlement and accelerate consolidation, improve slope stability and control liquefaction. The presence of stone columns transforms the ground into a composite mass of granular cylinders with intervening native soil, providing lower compressibility and higher shear strength than observed in the native soil alone. Stone columns can be installed using a variety of methods, including vibro-replacement, vibro-displacement, dynamic impaction, rammed columns, vibro-concreted columns and many others.

More recent concepts of earth reinforcement techniques involve the mixing of continuous polymer fibres (yarn), or elastomeric sprays with granular soil to form a composite material capable of resisting tensile forces. Individual fibres can also be mixed with the soil to improve strength and deformation characteristics. Although polyester fibres are generally used in actual applications, other materials, such as wood and rubber tyre chips, can be mixed with the soil to provide reinforcement. Reinforcement with these natural or processed elements is still in the experimentation stage. Recently, an elastomeric cementitious spray was used to address instability of a weathered sandstone batter at a former brickworks site in the Southern Highlands, New South Wales.

4.4.2 Key Issues

The key issues affecting soil reinforcement are:

- load transfer to the reinforcing elements
- failure surface of the reinforced soil mass
- strain compatibility between the soil and the reinforcement
- arrangement of the reinforcing elements
- durability and long-term behaviour of the reinforcements.

Load Transfer

In mechanical stabilisation design, the maximum tension in the reinforcing element is compared to the tensional capacity of the reinforcement, and the bond between the soil and the reinforcement (the pull-out capacity). The tension in the reinforcement is determined from the lateral earth pressure in the reinforced soil layer. The lateral earth pressure is calculated by multiplying the vertical earth pressure a coefficient (K) ranging from ‘at-rest’ to ‘active’, depending on the degree of restraint imposed on the soil by the reinforcing elements. When extensible reinforcing systems are used, such as those made by polymers or geotextiles, a substantial yield is allowed in the soil, resulting in lateral pressures that are closer to the active case. For fully restrained systems that include rigid reinforcing elements (metal strips, grids or bars), the soil yield is restricted and the developed earth pressures are closer to the at-rest condition at the surface. However, the pressures are gradually reduced with depth to values closer to the active case.

The stress transfer between the soil and the reinforcing elements is a critical factor affecting the method of reinforcement with stone columns and use of basal layers incorporating geotextile reinforcement. As the rigidity of the column is substantially higher than that of the surrounding soil, a larger portion of the applied load is transferred to the stone, which improves the load carrying capacity of the treated ground and reduces its settlement. The higher the ratio of stress in the stone column to the stress in the soil between the columns (the stress ratio), the more significant the ground improvement. Generally, stress ratio values lie between 2.0 and 5.0, with higher values corresponding to very weak soils and very close column spacings, and lower values representing stronger soils and wider spacings. Although theoretical solutions are available for predicting the stress ratio (Priebe, 1995), the value used in the design is usually based largely on experience. For preliminary design, a conservative stress ratio of 2.5 to 3.0 is often used.

When micropiles are used in soil reinforcement, they are placed closer than in conventional pile design, or arranged in a reticulated fashion so that the soil and the piles act as a monolithic unit to resist loads. In this case, it is assumed that the stresses are distributed to the soil and the piles, rather than the piles alone. To achieve this, a “knot effect” is assumed, by which the stress acting on the pile is partially transferred to the nearby piles, owing to the interaction between the piles and the ground generated by the high bond between them. The knot effect has been confirmed by both model and field tests (Lizzi, 1978; Plumelle, 1984).

The ability of the soil-pile system to generate this knot effect depends on the density and arrangement of the system. When a reticulated micropile system is used to support excavations and slopes, the density and configuration of the

piles should also be selected to minimise the possibility of plastic flow between the piles. The stability against plastic flow can be verified by comparing the horizontal pressure exerted by the soil mass with the limit resistance developed by the arching effect between two adjacent piles (Ito and Matsui, 1975).

A preliminary configuration of six to seven piles per linear metre is recommended for reticulated micropile walls (see Figure 6) to allow for generation of the knot effect.

Figure 6: Knot effect in a reticulated micropile system.

Failure Surface

The failure surface in the reinforced soil mass usually divides the soil into two zones: active and resistant. This is particularly important in mechanical stabilisation and soil nailing design, where the pull-out resistance of the reinforcing element is calculated along its embedded length in the resistant zone. When inextensible reinforcements are used for mechanical stabilisation, the failure surface is assumed to be bilinear. With extensible reinforcements, that surface coincides with the Coulomb or Rankine active failure plane. Figure 7 illustrates applications of reinforced soil wall systems on the Sydney Lane Cove tunnel and Melbourne Tullamarine-Calder Interchange projects.

Strain Compatibility

The behaviour of the reinforced soil mass is influenced by the 'strain compatibility' between the soil and the reinforcing elements. The influence of strain on the stress distribution and failure surface in reinforced soil wall systems was discussed above. Strain compatibility is also important in the selection of appropriate shear strength properties for the soil to be used in calculating the composite soil-reinforcement strength for use in the design of stone columns and basal reinforcement layers in embankments built over soft ground. Compatibility controls are also necessary to ensure that no greater load is transferred to the column than that which is assigned according to the stress ratio used in the design. As the soil between columns experiences larger strains than that of the columns, further transfer of the load takes place from the soil to the columns by arching, which increases the stress acting on the column.

Arrangement of Reinforcing Elements

When used for excavation support, the inclination of the reinforcing element (nail or micropile) affects the behaviour of the system. The direction of the reinforcement with respect to the potential failure surface plays a role in mobilising tension and shears and, therefore, in the overall shear strength of the reinforced soil. Inclining the inclusions downwards, for instance, would lead to an increased failure surface and reduced pull-out resistance. In a parametric study on the subject, Bang *et al.* (1992) presented optimum inclusion inclinations of 5 to 20 degrees for which the safety factor against pull-out resistance was the highest. It was also shown that, for shorter nail lengths, the optimum inclination angle was higher than that for longer nails.

The length and spacing of the inclusions also affect the behaviour of the reinforced-soil system. When the inclusion is relatively short, slippage is usually the dominant failure factor. When the inclusion is very long, breakage is the most probable cause of failure.

Bang *et al.* (1992) showed that the average measured safety factor gradually increased from 1.1 to 1.8 as the nail increased in length from 6 m to 18 m. The factor of safety becomes constant after a certain length, however, due to the yielding of the inclusions. Finally, as the spacing between inclusions increases, the contributions of the tensile forces in the inclusions to the global stability become smaller.

Figure 7: Reinforced soil wall installation using: (a) Inextensible reinforcement - Lane Cove tunnel project, Sydney, and (b) Extensible reinforcement - Tullamarine Calder Interchange, Melbourne.

Durability of Reinforcement

The service life of a reinforced soil depends to a great extent on the durability of the reinforcement and, to a lesser extent, on the durability of the facing elements. The durability of metallic reinforcements is usually measured by their resistance to corrosion. Geosynthetics are assessed by their resistance to hydrolysis (polyester), oxidation (polyethylene and polypropylene), stress cracking, biological degradation and ultraviolet light exposure (Sullivan *et al*., 1990). The choice of a reinforcing system and its design are sometimes influenced by long-term durability requirements. When geosynthetics are used for reinforcement, for instance, the tensile strength of the reinforcing element is divided by three reduction factors, representing creep, installation damage and durability. Depending on the material used, the creep reduction factor ranges from 2 to 5, the installation damage factor from 1 to 3, and the durability reduction factor from 1.1 to 2.0 (Munfakh *et al.*, 1999).

4.5 GROUND IMPROVEMENT BY CHEMICAL TREATMENT

Cement, lime, fly-ash, asphalt, silicate and other materials can be used to stabilise weak soils. These materials generally bind the soil particles together, resulting in higher strength and lower compressibility. For lime stabilisation, an ion exchange reduces the soil's plasticity and improves its workability. The ion exchange is then followed by a chemical reaction that increases the shear strength. In surface stabilisation, the chemicals are mixed with the soil and an appropriate amount of water, and then compacted using conventional compaction equipment and procedures. At depth, the chemicals are applied by injection, or by deep mixing methods. Further guidance is given in AustStab (2004), and Wong (2004).

4.5.1 Methods of Application

The chemical treatment methods discussed here are those applied at depth in soft ground. They are defined in Bruce (2005) and include:

- permeation grouting
- jet grouting
- deep soil mixing
- lime columns
- fracture grouting.

For permeation grouting, cement, lime, bentonite or chemical grouts (silicates, etc.) fill the voids in the soil, resulting essentially in increased strength and cohesion and reduced permeability, with no change in the volume or structure of the original ground. Organic compounds, or resins, are also used for special applications. Microfine and ultrafine cement grouts are the latest addition to permeation grouting. Grout additives may be used to enhance penetrability and strength and to control setting time. Grouting is performed by drilling holes in the ground and injecting slurry grouts through the end of a casing, or through the use of specialised equipment such as a tube-a-manchette.

Jet grouting uses high-pressure fluids, applied through a nozzle at the base of a drill pipe, to erode the soil particles and mix them with the cement grout as the drill bit is rotated and withdrawn, thereby forming hard, impervious columns. Excess soil cuttings are carried to the surface in the form of waste slurry. The grouted columns can be formed vertically, horizontally or at an angle. A row of overlapping columns forms a wall. Jet grouting is used mainly for excavation support, underpinning, tunnelling and groundwater cut-off. It is probably the most applied method of ground

improvement on soft ground tunnel projects. Jet grout columns are installed to provide barriers for the movement of soils and groundwater into the tunnel excavation, as well as, underpinning and support for existing structures and utilities in the vicinity of tunnelling.

For excavation support in water-charged, soft ground, jet grout technology has recently been used in projects in Sydney and the Gold Coast to form a seal between bored piles using a cement and bentonite mix to depths of 28m. For this application, a drill pipe was placed in the ground between the piles which rotates horizontally eroding the soil into which cement is pumped, mixing with the soil to create a seal between the structural members.

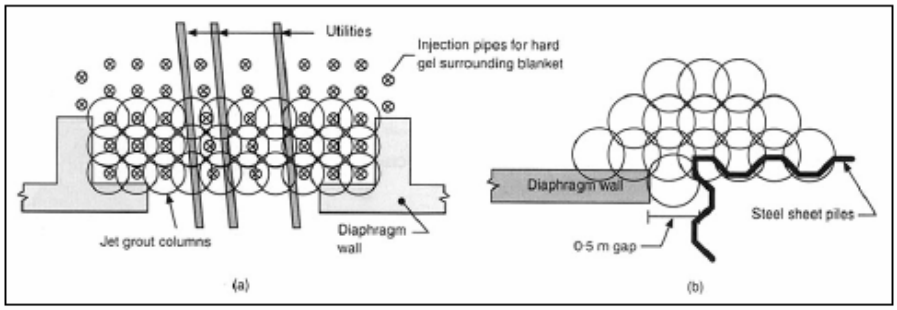

Figure 8: Miscellaneous jet grouting at Cairo Metro.

Figure 8 illustrates miscellaneous jet grouting applications on the Cairo Metro. In addition to providing ground treatment at the cross passages between adjacent tunnels, and at the departure and arrival points of the TBM out of, or into, the stations, it was also used to provide water cut-off at utility gaps in diaphragm walls and for underpinning of two buildings directly above the tunnel (Morey and Campo, 1999).

The deep soil mixing (DSM) technique involves mixing in-place soils with cement grout or other reagent slurries, through the use of multiple-axis augers and mixing paddles, to construct overlapping stabilised-soil columns. By arranging the columns in various configurations, the system can be used to strengthen weak soils, for groundwater cut-off, or liquefaction control. If required, steel reinforcement can be inserted into the column to provide bending resistance. When used for liquefaction control, the DSM system is performed in a block or lattice pattern to resist stresses associated with embankment or surcharge loading when loose cohesion-less soils liquefy during seismic ground shaking.

The lime column method is a variation of deep soil mixing, in which unslaked quicklime is used in lieu of, or mixed in with, the cement. The lime columns are suitable, at best, for stabilising deep, soft clay deposits. A pozzolanic reaction takes place between the lime and the clay minerals, resulting in a substantial increase in the soil strength and a reduction in the plasticity of the native material. The heat generated by hydration of the quicklime also reduces the water content of the clayey soils, resulting in accelerated consolidation and strength gain. Lime columns can be used for load support, for stabilising natural and cut slopes, and as an excavation support system.

Soil fracture grouting was developed to stabilise and consolidate cohesive soils that are not injectable by conventional permeation grouting techniques. The method involves controlled fracturing of the soil unit using a fluid grout, without significantly affecting the soil structure. Cementitious or chemical grouts are injected in a uniform fashion beneath structures to create a reinforced mass of soil and grout. Improvement of the soil follows three basic mechanisms: reinforcement, densification and ion exchange. Because the process requires that the soil be fractured and not permeated, fracture grouting can be used in all types of soil.

4.5.2 Key Issues

Chemical treatment is influenced by the following key issues:

- soil-grout compatibility and reactivity
- operational parameters
- column verticality
- weathering effects.

Soil-Grout Compatibility and Reactivity

The type of grout used and the make-up of the grout mix depend on the properties of the ground. Figure 8 illustrates the compatibility of the various grouting techniques with the grain size ranges of the grouted soils (Elias *et al.*, 1999). In

permeation grouting, the principal parameter affecting permeation is the size of the intergranular voids, which is usually represented by the soil's coefficient of permeability. As the grout permeates through the ground under pressure, it displaces water and air from the voids at a rate dictated by the ground permeability. In homogeneous, isotropic, uniform soils, a spherical flow of grout takes place. Normally, however, the ground is non-uniform, and the penetration depth is affected by the soil's stratigraphy.

Although jet grouting may work in most types of soil (see Figure 9), because the initial structure of the soil is broken down by the jetting process, its success is nevertheless influenced by ground characteristics, such as the size and frequency of boulders and the presence of peat or organic materials. The humic acids generated by these materials may affect the hydration of the cement and delay, or prevent, the hardening of the soil-grout mix. The presence of boulders or obstructions in the soil is even more limiting in the deep soil mixing method, since the columns are usually constructed to fixed dimensions; therefore, the cement grout cannot penetrate or engulf larger-diameter objects as is usually done in jet grouting. Recently developed equipment, however, allows the use of jetting or spreadable mixing tools at the tip of the auger to enhance the grout penetration and increase the column diameter at a specific depth (Probaha, 1998).

When using lime columns, the feasibility of stabilisation and the amount of lime needed to trigger the pozzolanic reaction are influenced by the type of soil being treated. In general, lime stabilisation is applied to cohesive soils (both inorganic and organic). For inorganic soils with low to medium plasticity, the lime content used is usually 6 to 8% of the dry unit weight of the stabilised soil. In highly plastic soils, more lime is added. When organic soils are treated, a lime content of 2 to 3% is required to neutralise the acidity of the organic matter. The remainder of the added lime (10 to 12% in total) is used to trigger the pozzolanic reaction (AustStab, 2004). Gypsum is mixed with unslaked lime to stabilise organic soils with high water content. In low-reactive clays, fly ash or kiln dust may be added to enhance the soil-lime pozzolanic reaction. Lime-cement mixes of equal proportions are used when higher strength is required.

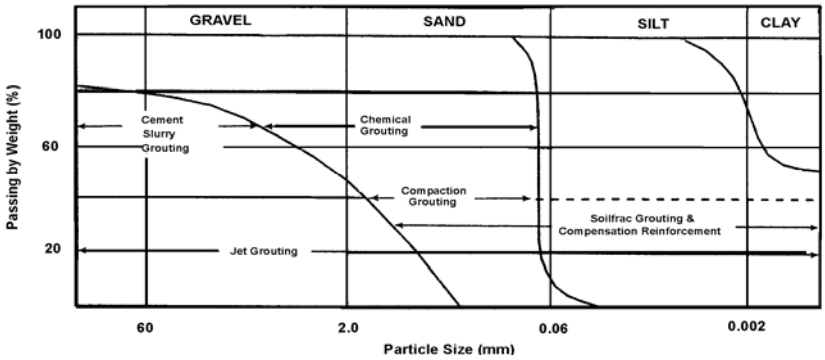

Figure 9: Range of groutable soils (Elias *et al*., 1999).

Operational Parameters

All deep chemical treatment methods are operator-sensitive and their success depends on 'operational parameters' controlled by the construction crew. Both the strength and the permeability of the treated mass, for instance, are influenced by the net amount of cement in the ground, which in turn is influenced by the controlled volumes of cement, water and additives mixed at the grout plant or at the top of the deep mix auger. They are also influenced by the level of the soil-grout mixing achieved *in situ*. In deep soil mixing, the grout flow is usually adjusted constantly to accommodate varying drill speeds in different soil strata, so that the design volume of grout per unit volume of the *in situ* soil is maintained.

The diameter of the column is a function of the method of installation used. It is influenced by a number of operating parameters, such as injection pressure, grout flow and rod withdrawal and rotation rates. A triple fluid system, for instance, produces a column with a larger diameter than that produced by a double fluid system. For a given soil type, the slower the withdrawal and rotation rates, the larger the column diameter that can be achieved. All operating parameters are usually determined through initial field trials at the beginning of construction (Hewitt and Spaulding, 2006).

When fracture grouting is applied, performance-type specifications are normally used and the grout mix is adjusted by the operator to provide the required performance. Portland cement is used in the grout mix, and additives are sometimes provided to control the grout gel time, so that controlled lifting of the ground in discrete areas under the structure is provided by repeated injections at short intervals. A detailed, high-precision, instrumentation monitoring program is

usually used as an integral part of the fracture grouting scheme. Continued monitoring of the movements of the structure and the ground allows the contractor to adjust the grouting operation to suit the project's performance requirements.

Column Verticality
The verticality of the constructed column is an important issue in jet grouting, particularly when the system is used to construct fluid barriers. When used for construction of a cut-off wall, multiple rows of overlapped columns are usually designed on the basis of the assumed permeability of the jet grouted column (a minimum overlap of 0.3 m is usually used). When two adjacent columns deviate from their vertical alignments in opposite directions, the required column overlap may not develop and voids (or windows) may occur in the jet grout wall, substantially increasing its hydraulic conductivity and rendering it ineffective as a cut-off wall.

The column's verticality is monitored by the operator, and the presence of windows is detected by a pumping test or exposure of the completed columns. The verticality and overlapping of the columns are less of an issue in deep soil mixing, since the columns are constructed to fixed diameters and the overlapping is ensured by the construction process.

Durability and Long-term Performance
Although the strength of the chemically-treated soil increases with time until a certain age, the long-term behaviour of the soil structure is influenced by weathering, particularly if there is continuous exposure to weathering elements such as water, wind or temperature. Test results on the subject show that lime-treated soils absorb less water with time than do untreated soils, and they also dry faster. Contrary to cement stabilisation, the frost heave in lime-stabilised soils is greater than that in untreated soils, particularly if the soils are frozen within one month of compaction. The resistance against frost-thaw effects, however, increases rapidly with curing time as the strength of the stabilised soil is increased. Generally, the depth and speed of frost penetration are reduced with the addition of lime, because the larger void ratio generated by flocculation allows less heat conduction through the soil. The resistance of the chemically treated soils to weathering effects is tested through durability tests involving wet-dry or freeze-thaw cycles.

4.6 GROUND IMPROVEMENT BY THERMAL STABILISATION

Although both heating and freezing can be used for ground improvement, soil heating is still in the experimental stage and has seen little application due to its cost. Ground freezing, on the other hand, has received wider acceptance as a temporary measure for excavation support especially in soft ground in urban areas. Examples include the 11 m diameter, 65 m deep Swan Street shaft, in permeable water-bearing gravel, on Melbourne CityLink (Tagaza, 2002), and the Kranji shaft on Singapore's Deep Tunnel Sewer System (Lees, 2006).

4.6.1 Methods of Application

The thermal stabilisation methods discussed in this paper are:

- ground freezing
- vitrification
- thermal desorption.

Ground freezing has two main functions: to prevent groundwater seepage into excavations and to increase the shear strength of the soil and improve its structural capacity. Two basic systems are usually followed in freezing. In an open system, the refrigerant (liquid nitrogen or carbon dioxide) is lost to the atmosphere after it has absorbed energy and vaporised. Alternatively, a closed-circuit hydraulic system uses conventional mechanical plant and a circulating coolant. In either case, the groundwater is frozen and prevented from entering the excavation. In addition, the shear strength of the soil is increased as the ice acts as a binding agent to the soil's particles. Ground freezing can be applied to a wide range of soils.

In vitrification, the soil is electrically melted at very high temperatures, typically in the range of 1,600 to 2,000° Celsius. This is accomplished through the use of graphite electrodes to conduct electricity through the soil. As the soil melts, the flowing electricity is converted into heat that moves outwards, melting new soil. The melted soil becomes electrically conductive and forms a heat-transfer medium, allowing the melt to move downward and laterally through the soil. The inorganic portion of the soil typically breaks down into major oxide groups, such as silica and alumina. Upon cooling, these groups form glass and crystalline products with excellent environmental properties.

Thermal desorption is generally classified as either indirect or direct. Direct thermal desorption separates contaminants from the soil matrix by directly exposing the soil to hot combustion gas. Following desorption, gas phase contaminants require treatment, which typically involves a secondary combustion step at temperatures greater than 1,000° Celsius. Indirect thermal desorption involves volatilisation of contaminants by indirect heating in a low oxygen atmosphere. Formation of dioxins and furans are avoided in the indirect method due to low oxygen levels and the absence of

combustion gases. In Australia, thermal desorption is being used at sites such as Homebush Bay in Sydney (Parsons Brinckerhoff, 2002) and trials have been undertaken at the former BHP Steelworks site and gasworks site in Newcastle.

4.7 GROUND IMPROVEMENT BY ELECTRO-TREATMENT

Developed mainly for use in the remediation of contaminated sites, electro-treatment methods involve the application of electric currents through the ground to remove contaminants in an unobtrusive fashion. These methods involve limited excavation and transport, and result in minimal environmental impacts. In Australia, electrical currents have been applied to the soils and wastes at Maralinga in South Australia to melt the toxic and radioactive components in the soils to form a solidified vitreous/ceramic mass with good physical, chemical and weathering properties. While this process was successful for a number of pits, the works were abandoned following damage to the electrical/vitrification unit and the uncertainties of the outcomes of the process (Commonwealth of Australia, 2003).

Further details of methods used in environmental applications are given in Munfakh and Wyllie (2000); and Holtz (1989).

4.8 GROUND IMPROVEMENT BY BIOTECHNICAL STABILIZATION

This form of ground improvement uses vegetation as reinforcing elements. It is used for stabilization of cut or fill slopes, or construction of earth-retaining structures on parkland and in environmentally-sensitive areas. Biotechnical stabilization is economical and more environmentally friendly than other forms of ground improvement. The biotechnical stabilisation techniques currently used include:

- brush layering
- contour wattling
- reed-trench layering
- brush matting
- live staking.

Of these, brush layering is the most commonly used. Descriptions of these methods are included in Gray and Leiser (1982), and RTA (1998). Coppin and Richards (1990) gave illustrative examples of slope stability analyses using the suction effect of vegetation both ways (i.e. as reduced pore water pressure and as increased artificial cohesion).

5 SOFT GROUND IMPROVEMENT SELECTION

The selection of a soft ground improvement method is a function usually provided by the design engineer. Owing to the proliferation of the available techniques on the market, the many benefits associated with each method and the rapidly developing nature of the ground improvement field, selection of the most appropriate method for a specific project is not an easy task. Selection can best be carried out through a thorough evaluation of many factors, and with extensive reliance on intuition and experience, so that the intended outcomes are achieved.

The key factors affecting the selection of a ground improvement method include:

- the ground
- the groundwater
- specification requirements
- construction considerations, including schedule, materials, accessibility, right-of-way, equipment and labour
- environmental and sustainability concerns
- durability, maintenance and operational requirements
- contracting, politics and tradition
- cost.

5.1 THE GROUND

The characteristics of the soil have a major impact on the effectiveness of the ground improvement technique adopted. Densification and reinforcement techniques, for instance, rely heavily on the internal friction between the soil particles, or the friction along the soil-reinforcement interface. So these methods are suitable for use with frictional soils such as sands and gravels. Some reinforcement methods (stone columns) and consolidation methods (preloading and vacuum consolidation) are suitable for use with fine cohesive soils. Strain compatibility is another factor affecting the design.

When the ground is reinforced with extensible elements such as geotextiles, the strain required to mobilise the full strength of the reinforcing elements is much larger than that needed to mobilise the full strength of the soil. Therefore, large internal deformations usually occur, and the soil design parameters are measured at large strains (residual strength). Obviously, these systems are less compatible with soils of relatively low residual strength.

Chemical stabilisation applies to a variety of soils. While permeation grouting is not suitable for fine-grained clayey soils, lime stabilisation is suitable for clayey soils, but only those that have enough silica and alumina constituents to induce the pozzolanic reaction. In jet grouting, the specific soil type is not as important as with other methods, since the in situ structure of the soil is broken down by the improvement process. The effectiveness of the method, however, is influenced by some soil elements, such as boulders and organic materials. In electrotreatment, soils with high levels of electric conductance produce better results. When biotechnical stabilisation is used, fertile soils are preferred.

5.2 GROUNDWATER

The level of groundwater and the degree of saturation of the soil affect many techniques. In the densification method, micro-liquefaction is induced in saturated soils below the groundwater table. Groundwater is also needed for ground freezing, or biotechnical stabilisation, to be effective. On the other hand, a high groundwater level may have a damaging effect on certain methods of ground improvement, such as soil nailing and the use of foam for weight reduction.

5.3 CONSTRUCTION CONSIDERATIONS

Schedule, materials availability, site accessibility, equipment and labour considerations are important factors affecting the selection of a ground improvement technique. Where preloading and wick drains are used, and to a lesser degree with lime stabilisation, time is of paramount importance. When the site is inaccessible to heavy equipment, such as in rough mountainous terrain or in soft ground, a method that can be implemented with a minimum of equipment, such as geotextile reinforcement, is preferred. On the other hand, labour-intensive systems, such as vacuum consolidation and biotechnical stabilisation, are usually not cost-effective in areas with labour shortage or strong labour union requirements. When low headroom does not allow the use of certain equipment, such as those required for deep soil mixing or stone columns installation, methods that can be implemented from remote areas, such as the various grouting or specialist low-headroom equipment techniques, are preferred (see Hewitt and Spaulding, 2006). Right-of-way and easement requirements may affect the feasibility of certain methods like mechanical stabilisation and soil nailing. The impact of construction on nearby facilities is an important factor in the selection. The use of the economical method of dynamic compaction, for instance, is precluded quite often because of its potential impact on existing structures and utilities.

Materials availability is an important factor in the selection of the preferred technique. When fill material is abundant, preloading is a very cost-effective method of ground improvement. If the required amount of surcharge material is not available within a short hauling distance, an alternative preloading scheme, such as vacuum consolidation, can be used. If industrial by-products, such as fly ash, kiln dust or slag, are available in large quantities, their use for enhancing lime stabilisation, or for weight reduction, may be cost-effective, as may be the use of waste materials such as shredded tyres or wood chips.

5.4 ENVIRONMENTAL AND SUSTAINABILITY CONCERNS

Sensitivity to environmental impacts is a key factor in the selection process. For contaminated sites, methods involving the discharge of large quantities of water, such as vibro-replacement, stone columns, vacuum consolidation and wick drains are avoided. On the other hand, methods that preserve the environment, such as geotextile reinforcement and biotechnical stabilisation, are welcome in environmentally-sensitive areas, such as parkland. Methods that allow construction of embankments with vertical faces (mechanical stabilisation) are preferred in or near wetland areas. Where a site is underlain by contaminated plumes, and if the contaminated site is to be cleaned and re-used instead of contained, electrotreatment or thermal consolidation techniques may be selected.

5.5 DURABILITY, MAINTENANCE AND OPERATIONAL REQUIREMENTS

The durability of materials used in ground improvement is a strong governing factor, particularly where the ground is exposed to heavy weathering elements. The use of metallic reinforcements, for instance, is avoided near stray currents or in highly corrosive soils. When geosynthetics are used, they require protection from the effects of heat, chemicals and exposure to ultraviolet light. Although all geosynthetic materials degrade upon exposure to ultraviolet radiation, their reaction to other durability effects varies. This should be taken into account in the selection process. For instance, although polyester is susceptible to hydrolysis and loss of strength when in contact with water, polyethylene and

polypropylene are not affected. However, these materials do tend to break down upon thermal oxidation in the presence of heat and oxygen, contrary to the behaviour of polyester.

The effects of wet-dry and freeze-thaw cycles are particularly important in chemical stabilisation. Extreme weather conditions, such as dry heat or ice, may have damaging consequences on biotechnical stabilisation. Thus, this technique should not be selected in areas with arid or frigid climates, and where there is a shortage of maintenance staff to take care of the foliage. The selection process is also influenced by the operational requirements of the facility. If there is ample time before the facility is operational, a rolling surcharge can be used. If the available time is relatively short, vertical drains and/or vacuum consolidation may be selected. To further reduce the ground improvement time, stone columns can be used, but at a relative cost penalty.

5.6 CONTRACTING, POLITICS AND TRADITION

Contractual requirements play a role in the selection process. Sometimes a method preferred by the design engineer cannot be specified because it is patented by a specialty contractor. National policies, free-trade agreements, labour union requirements, tradition and political influences sometimes affect the selection. Sometimes, certain methods of construction are not recommended, simply because they cannot be done by local contractors or because they require certain labour skills unavailable locally. One trend that will encourage adoption of new ground improvement techniques is the use of performance specifications, rather than process or product specifications.

5.7 COST

This is usually the most important factor in the selection process. If all other factors are satisfied, cost becomes the governing parameter. When analysing the cost, however, the long-term behaviour of the system and the required maintenance cost should be considered. A scheme with the lowest construction cost may not necessarily be the most economical, if it will require substantial maintenance and repair costs in the future. When different schemes are close to each other in cost, alternative ground improvement methods may be specified.

6 CASE STUDIES

The following case studies describe the use of a combination of ground improvement techniques on a single project. The factors affecting the selection of the multiple schemes are also discussed.

6.1 WHARF STRUCTURE

The expansion of the Norfolk International Terminal in Norfolk, Virginia, in the United States, involved the construction of a wharf structure and a storage area on land that had been previously reclaimed using dredged material placed over soft clays (Munfakh & Wyllie, 2000). Figure 10 illustrates a cross-section of the wharf structure and the storage area behind it. The 3 horizontal to 1 vertical slope under the wharf structure was established to minimise the width of the pile-supported platform and to avoid encroachment on existing facilities behind the wharf, including a sewer outfall pipe that could not be relocated.

As the new facility would place additional loads on the *in situ* soils, and the soft compressible soils were too deep to be practically or economically removed, ground improvement was needed at the site to: allow dredging of the soil to the required slope, minimise the soil's long-term settlement and down-drag impact on the piles, and reduce the lateral earth pressure on the bulkhead. Selection of an appropriate ground improvement method was a challenge. After evaluating the many selection factors discussed above, and to satisfy economical, operational, environmental and construction-related requirements, a combination of ground improvement techniques was adopted.

Preloading of the soft clay was the most economical solution. However, due to operational requirements, the wharf structure was positioned partly on land and partly over water. Since placing fill in the water was prohibited by environmental restrictions, the surcharge load had to be placed on the land side of the bulkhead. However, this preloading configuration was not adequate to achieve the minimum shear strength required for the stability of the dredged slope and the design of the bulkhead behind the structure. To accomplish that, a large enough section of the soft soil at both sides of the bulkhead was removed and replaced with sand forming a sand shear key. Preloading of the soft soil on land was still needed to allow safe excavation of that section for construction of the sand shear key. Furthermore, because the sand shear key material was placed underwater, it had a relative density of only 10 to 40%, which was substantially lower than the 70% relative density used in the design. To achieve the required relative density, the shear key material was densified using vibro-compaction.

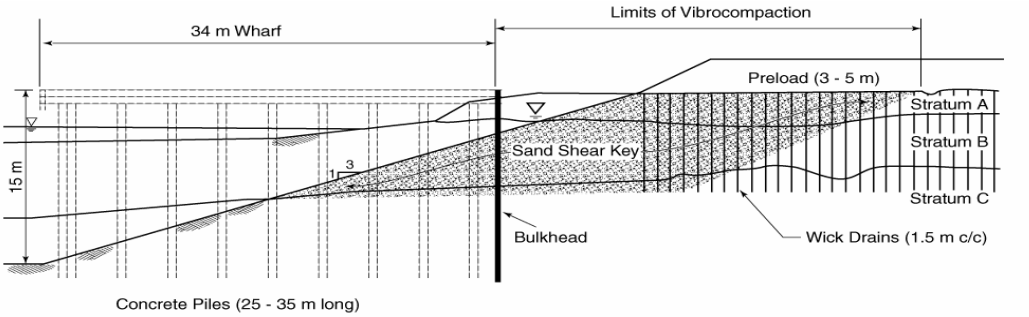

Figure 10: Cross-section of wharf at the Norfolk International Terminal.

Preloading was accomplished by placing 3 m to 5 m of surcharge fill. To accelerate consolidation, wick drains were installed to depths of 10 m to 17 m, at a spacing of 1.5 m centres, in a triangular array. The preloading program increased the shear strength of the soft clay from 10 kPa to up to 75 kPa, with over 90% of the long-term settlement completed within the 9-month construction period. Vibro-compaction was achieved with an electric vibroprobe, using water jetting and vibration. A probe spacing of 3 m was applied and sand was added during compaction to achieve the required 70% relative density.

The selection of ground improvement techniques was controlled by many factors, including the ground conditions, right-of-way limitations, operational requirements, environmental restrictions, construction issues, time constraints, and cost.

6.2 HIGHWAY EMBANKMENT

A significant part of the bridge approaches for a highway project in Eastern Australia was built over soft soils, with the prospect of significant settlement of the embankments. Building one particular approach over soft soils would have caused major stability issues and ongoing settlement problems. Following consideration of stability control methods such as staged embankment construction, vertical (wick) drains, geotextile reinforcement and stabilising berms and settlement control methods such as preloading and surcharge, ground treatment and timber and precast piles, blocks of light, high density foam blocks (geofoam) with transition treatment at bridges to reduce the settlement to an acceptable level was adopted. Prior to using 7,000 m^2 of geofoam fills, the original design consisted of various types of structures such as bridges, and fill over slab-on-piles.

Where the use of lightweight foam was not justified for cost or other considerations, the designs used combinations of piled embankments and wick drains at bridge approaches to ensure a smooth transition from piled bridge structures.

A typical example from a highway embankment built over soft compressible alluvial deposits is shown in Figure 11.

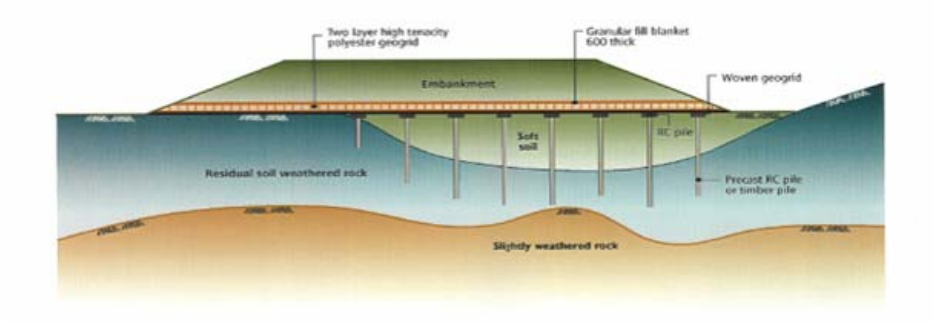

Figure 11: Piled embankment layout showing use of geotextile to transfer embankment load to pile caps.

On other sections of highways located over alluvial valleys in Eastern Australia, foundation treatment adopted in soft ground areas has included:

- staged embankment construction, to allow pore pressures to dissipate at each stage
- ground treatment using prefabricated vertical (wick) drains
- geotextile reinforcement
- stabilising berms
- preloading and surcharge and
- piled embankments using timber and precast piles at transition areas.

7 CONCLUSIONS

The successful application of ground improvement in soft soils is influenced by many technical issues related to the characteristics of the soil, the materials added to the soil and their interaction. Other technical issues affecting performance are subject to the equipment and procedures used, the skills of the operator and external factors, such as weather and proximity to existing structures. Technical, practical, economical, contractual and political factors affect the selection of a particular type of ground improvement for a specific site. The several factors discussed in this paper reflect the diversity of the ground improvement techniques available on the market and the complexity facing the design engineer in the attempt to select the most appropriate method, or combination of methods, to be applied to each project.

The following general conclusions can be drawn:

- the use of ground improvement in soft ground has clear advantages over conventional construction techniques and, sometimes, is necessary to make building of certain projects feasible and/or economical.
- the application of ground improvement techniques is almost a routine event on today's underground engineering projects in soft ground.
- one trend that will encourage adoption of ground improvement techniques to better suit a project's needs is the use of performance specifications, rather than process or product specifications.
- although ground improvement is still considered a novelty by some engineers and its applications are based, to a certain extent, on intuition and experience, the subject is rapidly evolving into a full-fledged field of geotechnical engineering with established analytical procedures, detailed construction specifications and documented, monitored performance.

5 ACKNOWLEDGEMENTS

This is an edited version of part 1 of a paper presented by Munfakh & Wyllie (2000) at GeoEng 2000. The original paper concentrated on ground improvement in both soil and rock, whereas this paper covers soft ground and recent developments relevant to Australian geotechnical practice.

6 REFERENCES

AustStab (2004). Lime stabilisation practice. AustStab Technical Note No. 1B, April 2004. Australian Stabilisation Industry Association, Artarmon (www.auststab.com.au). accessed May 2006.

Bang, S., Kroetch, P.P. and Shen, C.K. (1992). "Analysis of soil nailing system," *Proc. International Symposium on Earth Reinforcement Practice*, Hyushu University, Fukuoka, Japan

Bruce D A (2005). Glossary of grouting terminology. *Journal of Geotechnical and Geo. Eng Division*, ASCE, 131(12), 1534 – 1542

Cognon, J. M., Juran, I. and Thevanayagam, S. (1994) Vacuum consolidation technology- principles and field experience, *Proc. of conf. on vertical and horizontal deformations of foundations and embankments deformations*, Geotech, special publication SP40(2), ASCE, College station, Texas.

Commonwealth of Australia (2003) "Rehabilitation of former nuclear test sites at Emu and Maralinga (Australia) 2003", Department of Education, Science and Training, J.S. McMillan printing group, 456p

Coppin, N.J. and Richards, I.G. (1990). Use of vegetation in civil engineering, Butterworth, London

Debats, J.M., and Sims, M. (1997). "Vibroflotation in reclamations in Hong Kong," *Ground Improvement*, Vol. 1, No. 3, Thomas Telford Ltd., London

Elias, V., Welsh, J. Warren, J. and Lukas, R. (1999). "Ground improvement technical summaries," Volume II, Publication No. FHWA-SA-98-086, Federal Highway Administration, Washington, D.C.

Gray, D.H. and Leiser, A.J. (1982). Biotechnical slope protection and erosion control, Van Nostrand Reinhold, New York

Hewitt, P. and Spaulding C. (2006). Jet grouting for Lisarow rail bridge renewal. *Symposium on soft ground engineering*, Australian Geomechanics Society, Sydney chapter.

Holtz, R.D. (1989). Treatment of problem foundations for highway embankments. National Highway Research Program, Synthesis of Highway Practice 147, National Research Council, Washington DC.

Ito, T., and Matsui, T. (1975). "Methods to estimate lateral force acting on stabilizing piles." *Soils and Foundations*, 15, (4)

Lees, D (2006). The development and application of grouting and ground treatment. *Symposium on soft ground engineering*, Australian Geomechanics Society, Sydney chapter.

Lizzi, F. (1978). "Reticulated root piles to correct landslides." ASCE Convention & Exposition, Chicago, Il., October

Menard (2006). http://www.menard-soil treatment.com. accessed June 2006

Mesri, G, Feng, T.W., and Benak, J.M. (1990). "Postdensfication penetration resistance of clean sands," *Journal of Geotechnical Engineering Division*, ASCE, 112, No. 7

Mitchell, J.K. (1981). "Soil improvement methods and their applications in civil engineering." Sixteenth Henry M. Shaw Lecture in Civil Engineering, North Carolina State University.

Mitchell, J.K. and Solymar, Z.V. (1984). "Time-dependent strength gain in freshly deposited or densified sand," *Journal of Geotechnical Engineering Division*, ASCE, 112, No. 11

Mitchell, J M and Jardine, FM (2002), A guide to ground treatment. Construction Industry Research and Information Association publication C573.

Morey J. and Campo D W, (1999). Quality control of jet grouting on the Cairo Metro, *Ground Improvement (3)*, London.

Munfakh, G. A. (1997). "Ground improvement engineering – the state of the US practice: part 1. Methods." *Ground Improvement*, Thomas Telford Services Ltd, London, England

Munfakh, G.A. (1999) "Ground improvement engineering - yesterday, today and tomorrow," the 1999 Martin S. Kapp lecture, ASCE, New York

Munfakh, G.A., Samtani, N.C., Castelli, R.J. and Wang, J. (1999). Earth retaining structures, reference manual, publication no. FHWA NHI-99-025, Federal Highway Administration, Washington, D.C.

Munfakh, G. A. and Wyllie, D.C. (2000). Ground improvement engineering – issues and selection" *GeoEng 2000*, Melbourne

Plumelle, C. (1984). "Amelioration de la portante d'un sol par inclusions de froupe et. reseaux de micropieux." *Int. Symp. on In Situ Soil and Rock Reinforcement*, Paris, Oct

Parsons Brinckerhoff (2002). Environmental impact statement, Remediation of Lednez site, Rhodes and Homebush Bay.

Priebe, H.J (1995). The design of vibro replacement. *Ground Engineering*, Dec, pp 31-37

Probaha, A. (1998). Technical discussion, ground improvement, Vol. 2, No. 4, Thomas Telford Ltd, London

RTA (1998). Roadscape guidelines, NSW Roads and Traffic Authority Environment and Community Policy Branch

Riad H, Ricci A, Osborn P, D'Angelo D and Horvath J (2004), Design of lightweight fills for road embankments on Boston's Central Artery/ Tunnel project. *Proc. fifth int. conf. on case histories in geotech. engineering*, New York

Robinet, J.C. and Juran, I. (1999). "Dispostif d'Echange et de consolidation hydrique des sols." Traite de Cooperation en Matiere de Brevet /PET/ FR917/01863

Stark et al (2004). Geofoam applications in the design and construction of highway embankments. NCHRP Web Document 65 (Project 24-11), NCHRP Report 529, Washington, D.C.

Sullivan, D., Hausmann, M. R. and Hewitt, P (1991). Developing approval criteria for reinforced soil wall systems, *Sixth National Local Government Engineering Conference*, Hobart, 25-30 August 1991. Institution of Engineers, Australia, pp253-257.

Tagaza, E (2002). The story of the Melbourne CityLink. Institution of Engineers, Australia (Victoria Division).

Wong, P.K (2004). Ground improvement case studies – Chemical lime piles and dynamic replacement, *Australian Geomechanics*, v39 n2, pp47-60.

PRELOAD DESIGN, PART 1 – REVIEW OF SOIL COMPRESSIBILITY BEHAVIOUR IN RELATION TO THE DESIGN OF PRELOADS

Patrick K. Wong
Senior Principal, Coffey Geotechnics Pty Ltd

ABSTRACT

The method of treating soft soils by preloading has been used for over a century, and is still widely used today as one of most common form of ground improvement technique. Yet, every now and again, post-construction settlements have been observed to be more than those predicted after preloading. The author believes, in most cases, the poor preload performance is probably associated with lack of understanding of the time-dependent compressibility behaviour of the soft soils. And in particular, the behaviour of secondary consolidation (or creep) is still not well understood despite extensive research and numerous constitutive models that have been developed. The availability of powerful commercial computer programs does not help if they are used indiscriminately when the fundamental principles are not well understood.

Part 1 of this paper provides a review of the factors that influence creep. The dependency of creep on stress level and stress history expressed in terms of the over-consolidation ratio (OCR) is discussed, followed by a discussion on the commencement of creep. A brief overview of time-dependent consolidation and creep settlement analysis methods is provided, followed by a summary of the preload design approach given by Mesri (1991) that illustrates the possibility of the occurrence of higher creep rate some time following preloading.

In Part 2 of this paper, an analytical approach based on Bjerrum's (1967) time line model, or principle of "artificial aging" will be presented for preload design to limit post construction settlement, and a preload design example is discussed to illustrate the importance of geological and stress history on post-preload settlement behaviour.

1 INTRODUCTION

Preloading is one of most common and economical forms of ground improvement. If the intention of the preload is to eliminate the post-construction primary consolidation, the design of the preload is relatively straightforward. In this case, the preload must result in an effective stress increase, over the entire compressible stratum, that is, at least equal to the final effective stress expected under the design loading condition. However, if it is required to reduce post-construction secondary consolidation (creep) to a specified limit, a surcharge is required to be applied to preconsolidate the soil. The surcharge must produce a preconsolidation pressure greater than the final effective stress. The resulting over consolidation ratio will inevitably vary with depth and this complicates the preload design procedure, particularly for deep soft soil profiles. In this paper, the term "preloading" will be used interchangeably with the term "surcharging" to have the same meaning of preconsolidation to reduce post-construction creep settlement.

The author believes that one of the least understood aspects of soil behaviour in soil mechanics, creep, is responsible for either the success or failure of preloads. Of course, primary consolidation is also important, but at least its behaviour is better understood and more readily predictable and measured, unless masked by simultaneous creep during primary consolidation. Therefore, before launching into designing preloads, a good understanding of time-dependent settlement behaviour of soft clays, and the influence of geological and stress history on creep strain rates, is considered to be of critical importance.

Due to inconsistencies in published literature, text books and the test procedure of Australian Standard AS1289.6.6.1 (1998), the following terminology to describe creep will be used in this paper to avoid confusion:

C_α = creep index, and not the creep strain rate (or coefficient of secondary consolidation as defined in AS1289.6.6.1, 1998).

$C_{\alpha\varepsilon}$ = creep strain rate, or coefficient of secondary consolidation as defined in AS1289.6.6.1 = $\Delta H/H$ per log time cycle (note: some text books and AS1289.6.6.1 uses the symbol C_α for this quantity), $C_{\alpha\varepsilon} = C_\alpha/(1+e_o)$ where e_o = initial void ratio.

2 BACKGROUND INFORMATION

2.1 GEOLOGICAL HISTORY AND COMPRESSIBILITY OF SOFT CLAYS

Traditionally, time-dependent settlements of soft clays are separated into two components: (a) primary consolidation under increasing effective stress, and (b) secondary consolidation (or creep) under constant effective stress.

In relation to primary consolidation, Terzaghi first published his consolidation theory in 1925 (Terzaghi, 1925) which described pore water pressure dissipation. The end of primary consolidation for a soil sample at various effective stress levels is normally presented in the form of a void ratio versus log of applied effective stress (e – log p) plot, from which the re-compression and compression indices (C_r and C_c) may be obtained to describe the compressibility of the soil.

About a decade later, laboratory tests and field observations reported by Buisman (1936) and Taylor (1942) clearly indicated the effect of time on the compressibility of clays. Buisman found that settlements increased linearly with log of time under constant effective stress for clay and peat loaded in the field and in the laboratory. The diminishing consolidation with time under constant effective stress is referred to as creep.

It is well established that soft soils will undergo significantly greater consolidation when loaded beyond the preconsolidation pressure, p_c (or σ_c'). The preconsolidation pressure is defined as the effective pressure at which the break in slope occurs in the (e – log p) plot, and is also called the "yield stress" in some references. The latter term is used to avoid the common misconception that the presence of a preconsolidation pressure in soft clays is due only to past loading of the soil to a higher stress level (e.g. due to erosion). Chandler *et al.* (2004) concluded that the yield stress is a function of the structure of the clay, and suggested that it is likely to be greater than the maximum geological stress which it has sustained, whether the clay is normally or overconsolidated. In addition to geological stress history, the structure of the clay after deposition can be affected by environmental factors such as pore fluid chemistry (e.g. salinity), chemical and biological bonding and desiccation. The structure of clay deposits is also affected by creep and it has been shown (Taylor, 1942, Crawford, 1964 and Bjerrum, 1972) that the longer the soil is allowed to creep under constant stress after initial deposition, the higher its p_c will be.

2.2 THE CONCEPT OF PRELOADING

Although the term preloading may imply loading soft soils to a stress level equivalent to the in-service condition under self weight and design applied loading, it is also often used to describe the process of surcharging the soils above their anticipated in-service stress level so as to reduce post-construction creep as well as primary consolidation. The application of surcharge is inferred when the term preloading is used in this paper.

The ratio of the recompression index to the compression index, C_r/C_c is typically 0.1 to 0.2, and therefore, when a soil has previously been loaded to or beyond the final stress resulting from the proposed design load, the expected settlement due to primary consolidation when the design load is applied will be only 10% to 20% of that of a normally consolidated soil (i.e. reloading within the over-consolidated stress range). However, if the final stress is at or close to the preconsolidation pressure, significant creep settlement may still occur over time, and such creep settlement may not be acceptable over the design life of the development.

An important aspect to bear in mind when designing the preload is that the stress history and stress levels in a soil profile are not constant with depth. This is normally overcome by subdividing the soil profile into sub-layers and examining each of the sub-layers.

2.3 TIME-DEPENDENT CONSOLIDATION THEORY AND ITS APPLICATION IN PRELOADING

About a decade after Terzaghi presented his theory of one-dimensional consolidation, Taylor developed one of the first time-dependent consolidation models (Taylor, 1942). The early effort of Taylor attempted to model creep during primary consolidation. However, the effects of creep compression on preconsolidation pressure were generally not considered before Bjerrum's development of the time lines theory (Bjerrum, 1967; 1972). Bjerrum's conceptual model is often referred to as the concept of "artificial aging" as illustrated in Figure 1.

Figure 1 shows that if a soil sample in a laboratory oedometer test is loaded from its *in situ* effective stress value p_o at point "a" to point "c", which represents the end of primary consolidation and "d", which represents the point at which the surcharge is removed after a certain time period, then the stress level is reduced to that of point "e", the creep rate will now be significantly lower.

In Figure 1, Bjerrum showed parallel time lines for creep (i.e. independent with stress level) and a reducing creep strain rate equivalent to one order of magnitude reduction with each log time cycle. The validity of these assumptions will be explored later in this paper.

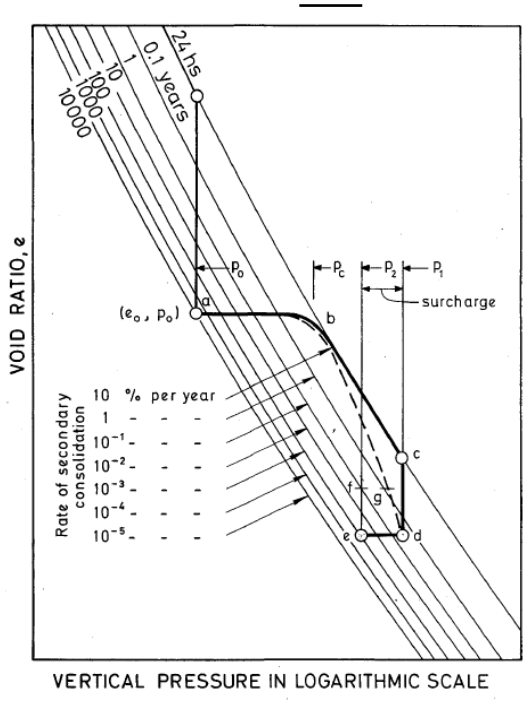

Figure 1: Principle of designing a preload to reduce the rate of creep (Bjerrum, 1967; 1972).

2.4 DEPENDENCY OF CREEP ON STRESS LEVEL

Just as soil compressibility during primary consolidation is stress level-dependent and history-dependent, such dependency also applies for creep. The creep dependency on stress level is true for all materials, including steel and plastic, and also stiff compacted fill as reported in Waddell and Wong (2005). The creep strain rates for most engineering materials are also strongly dependent on operating temperature (e.g. plastic, glass and metal). For soils below the ground, the temperature is relatively constant and the dependency of creep on temperature may therefore be ignored.

Examples of the dependency of creep on stress level in soft soils have been presented by Nash *et al.* (1992) and Ewers and Allman (2000). The test results by these researchers are reproduced in Figure 2 below.

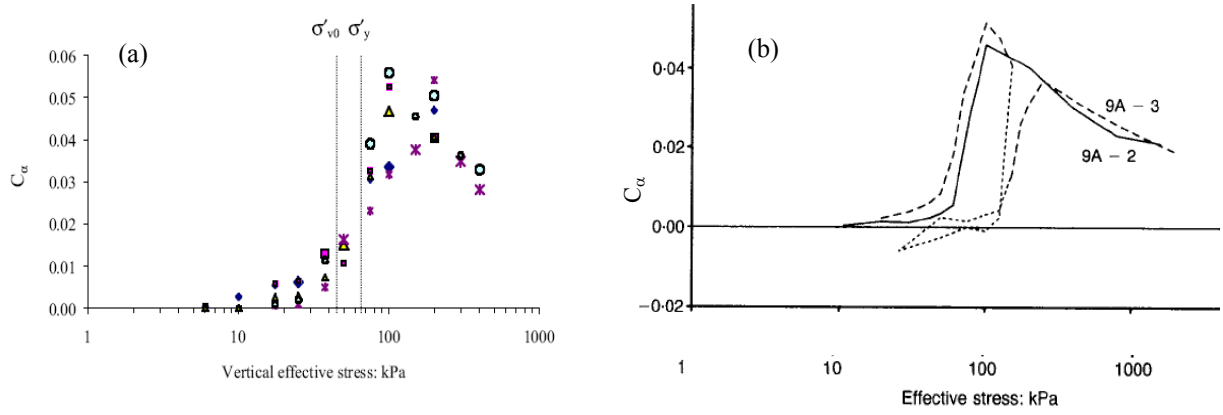

Figure 2: Dependency of Creep on Effective Stress (a) Ewers and Allman (2000) – soil samples from Teven Road site of Ballina Bypass Project, NSW, Australia (b) Nash *et al.* (1992) – soil sample from Bothkennar soft clay test bed, UK. (Note: Vertical Axis is C_α , not $C_{\alpha\varepsilon}$).

2.5 DEPENDENCY OF CREEP ON STRESS HISTORY

Compelling evidence has been presented by Mesri and Godlewski (1977) of the relationship between C_α and C_c. They found that at any (σ_v', t) during secondary compression, the ratio C_α/ C_c is a constant in both the recompression and compression ranges. In the above ratio C_α/ C_c, the value C_c is also used to describe the recompression index depending on the stress range. In other words, if C_c is replaced by C_r in the recompression range, and C_r is 0.1 to 0.2 times C_c, C_α will also reduce proportionally.

A clear illustration of the stress history dependency of creep has been presented by Magnan *et al.* (2001) as reproduced in Figure 3.

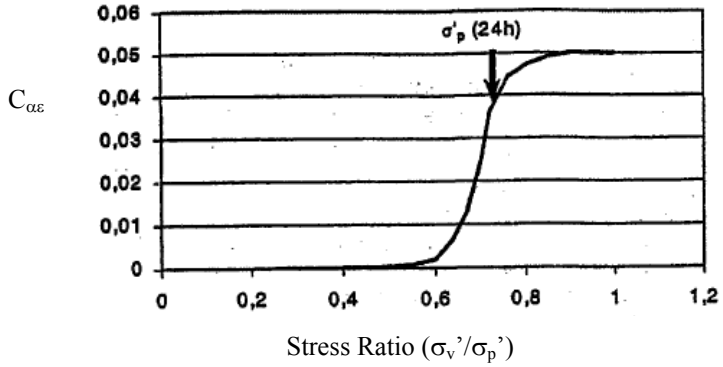

Figure 3: Stress History Dependency of Creep (Magnan, 2001).
(Note: $C_{\alpha\varepsilon}$ here is creep strain, not Mesri's Creep Index C_α)

The stress ratio reported by Magnan *et al.* is the inverse of the Over-Consolidation Ratio (OCR), and if an empirical exponential relationship such as Equation 1 below is used to describe varying $C_{\alpha\varepsilon(oc)}/C_{\alpha\varepsilon(nc)}$ with varying OCR, then one would obtain a gradual transition of creep strain rate near the preconsolidation pressure rather than an abrupt change from an overconsolidated value to a normally consolidated value.

$$\frac{C_{\alpha\varepsilon(oc)}}{C_{\alpha\varepsilon(nc)}} = \frac{(1-m)}{e^{(OCR-1)n}} + m \qquad \textbf{(1)}$$

In Equation 1 'm' and 'n' are constants. Constant 'm' represents the minimum value of $C_{\alpha\varepsilon(oc)}/C_{\alpha\varepsilon(nc)}$ or $C_{\alpha(oc)}/C_{\alpha(nc)}$ when the OCR is large. From Mesri (1991) 'm' will be equivalent to the ratio C_r/C_c. The magnitude of 'n' controls the rate of reduction of $C_{\alpha(o/c)}/C_{\alpha(n/c)}$ with OCR. Alonso *et al.* (2000) presented data for the reduction in the rate of creep with OCR for an inorganic clay from which the exponents 'm', and 'n' for Equation 1 to fit the data was found to be approximately 0.1 and 12. The creep reduction versus OCR relationship using 'm' = 0.1 and 'n' = 6 is shown in Figure 4 together with the back-figured data from Alonso *et al.* (2000). In the absence of data, the 'n' value of 6 is probably a reasonably conservative value for organic clays for preliminary assessment purposes. Of course, site specific data should be used if test data is available.

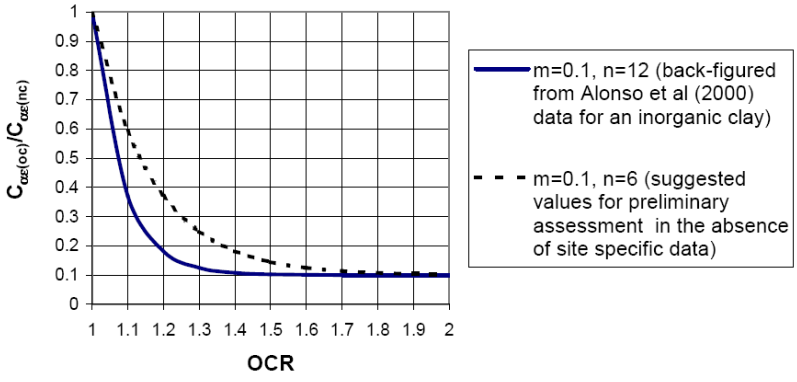

Figure 4: Creep versus OCR Relationships.

At this point, it is worth mentioning that the standard bilinear interpretation of recompression and compression in the typical (e – log p) plots is only a simplification for computational purposes. Real soils are likely to exhibit a curved transition below and above the preconsolidation pressure, (i.e. the slope describing the compression index is increasing gradually with increasing stress level around the preconsolidation pressure). In many soils the (e – log p) plot also flattens at high stress levels, and in such situations a secant C_c value may need to be used at the appropriate stress level. Therefore, Mesri and Godlewski's findings are indeed consistent with the creep - stress level/history dependency observations reported by others.

In other words, while C_α may be considered as a constant (and proportional to C_c or C_r) at any particular stress level and loading history, its magnitude does vary, depending on stress history, stress level and time. This finding contradicts with the parallel creep lines presented in Bjerrum's conceptual model shown in Figure 1. However, it does provide a clearer explanation for soft soils that have been deposited at relatively shallow depths (i.e. low stress levels) for tens of thousands of years but do not necessarily have high preconsolidation pressures as would otherwise be interpreted by using Bjerrum's figure. That is, at low stress levels, the creep strain rate is correspondingly low even when normally consolidated. Furthermore, creep itself causes an over-consolidation effect which further reduces the creep strain that is illustrated in Bjerrum's conceptual model of artificial aging. Although it is the author's view that the creep lines shown in Figure 1 are probably not parallel, Bjerrum's conceptual model is nevertheless very powerful for developing an understanding of the principle of artificial aging and preloading, and may be adopted provided the correct creep strain values are selected on the basis of stress level and stress history.

2.6 WHEN DOES CREEP COMMENCE?

For ease of computation, primary consolidation and creep are generally considered separately, and from the laboratory consolidation test result, commencement of creep is considered at the point of intersection of the straight line slopes drawn through the primary consolidation phase and creep phase of the test. This may be sufficiently accurate for a thin laboratory sample which may typically complete its primary consolidation phase in about 24 hours and during which the creep component is small. For a thick soft soil deposit in the field, this assumption may lead to errors in interpretation of monitoring results.

If we refer back to Sections 2.3 to 2.5 and consider the relationships between creep strain rate and "time lines", effective stress, and overconsolidation ratio, it would be intuitive that creep would commence as soon as additional effective stress is imposed, albeit it may be slow to start with due to the fact that an increase in total vertical stress produces an equal increase in porewater pressure initially. But as the pore pressure dissipates with time, the effective stress will increase and the effective stress state of the soil, "artificial age" and OCR will begin to alter according to Bjerrum's concept shown in Figure 1. It is also important to note that the dissipation of pore pressure (and therefore the rate of effective stress increase in creep) is non-uniform in a soil profile, with a faster rate of pore pressure dissipation near drainage boundaries. Therefore, the onset of creep is likely to commence sooner and at a faster initial rate near drainage boundaries than those further away. The concept of simultaneous creep and primary consolidation has been explored by many researchers, and Mesri *et al.* (1994) described the change in void ratio with time in the following equation:

$$\frac{de}{dt} = a_{vs}\frac{d\sigma_v'}{dt} + a_{vt} \qquad \textbf{(2)}$$

In Equation 2, the rate of compression de/dt is determined by the two compressibility parameters a_{vs} and a_{vt} which describe the rate of effective stress increase in the primary consolidation phase and the creep phase respectively in a simultaneous manner. It is only after all the excess pore pressure has dissipated and $d\sigma_v'/dt$ by definition is zero that the rate of compression is equal to a_{vt} alone during the creep phase.

Furthermore, because the rate of effective stress increase (i.e. $d\sigma_v'/dt$) is equal to the rate of pore pressure decrease ($-du'/dt$), Mesri *et al.* (1994) used this equality and rearranged Equation 2 to form Equation 3 as follows:

$$-\frac{du'}{dt} = \frac{\frac{de}{dt} - a_{vt}}{a_{vs}} \qquad \textbf{(3)}$$

Equation [3] shows that an increase in either a_{vs} or a_{vt} slows pore pressure dissipation. These simple equations clearly show that both primary consolidation and creep occur simultaneously and that they affect each other. They also provide conceptual explanations for the following common observations:

For pressure increments within the recompression range, the porewater pressures dissipate rapidly because a_{vs} is small.

As primary consolidation takes place and the effective stress increases with time, the effective stress may increase from within the overconsolidated range to the normally consolidated range, and the value of a_{vs} abruptly increases, and there is a dramatic reduction in the rate of porewater dissipation and primary consolidation.

As the effective stress increases, so does the creep rate, a_{vt}, which has the effect of delaying porewater dissipation according to Equation 3. This point is important as there is a common misconception that residual porewater pressures are being observed during the creep phase, when in fact primary consolidation is incomplete.

3 TIME SETTLEMENT ANALYSIS METHODS

As discussed in the preceding sections, preload involves loading, unloading and reloading and by doing so the soft soil profile undergoes a complex change in structure and porewater pressure dissipation and the inter-related primary consolidation and creep parameters will change with time.

Ideally, design of preloads should take into account the simultaneous nature of primary consolidation and creep. There has been significant progress in recent years towards development of time-dependent modelling of simultaneous primary consolidation and creep. The various approaches include:

- Macro-mechanical approach (also known as the phenomenological approach) based on fitting of mathematical expressions to experimental evidence (Feda, 1992).
- Micro-mechanical approach, which attempts to model soil behaviour at the particulate or molecular level (Mitchell *et al.*, 1968; Kuhn and Mitchell, 1992).
- Meso-mechanical approach, which combines the macro- and micro-mechanical approaches (Fox *et al*., 1994).
- Rheologic mechanical model such as the Rajot Model (Rajot, 1992) which uses a series of elastic springs and sliders to represent the primary consolidation component and a series of non-linear springs and non-linear dashpots to model the creep component.
- Elasto-visco-plastic approach based on a set of constitutive models including softening and hardening functions that describe the mechanical response of the soil based on experimentally observed soil behaviour. Early work in this approach included Perzyna's visco-plastic over-stress theory (1963) and Olaszak-Perzyna's (1966) theory of non-stationary flow surfaces. The latter included the concept of a yield surface that changes in time due to creep behaviour to model the time-dependent compression behaviour of soft soils. More recent developments include Modified Cam-clay model (Yin and Graham, 1999) and the "a,b,c Isotache" model (den Haan, 1996; den Haan and Sellmeijer, 2000). Most of these models use a hardening rule that is principally based on Bjerrum's time line concepts although, instead of using an instant time line model, either a total strain rate model or a creep rate model is used.

For readers who are interested in further details of various computer models for time-dependent analysis of simultaneous consolidation and creep of clay, a good summary of the types of analysis available and their capabilities has been provided by Perrone (1999), together with development of his computer model CONSOL97.

The commercially available PLAXIS finite element analysis program (PLAXIS Version 8, 2002) has a Soft-Soil-Creep model and utilises a form of strain rate controlled time-dependent consolidation and creep analysis that also incorporates concepts of Modified Cam-clay and viscoplasticity.

One advantage of using the Soft-Soil-Creep model of PLAXIS is that the input used may be obtained from the usual parameters that are measured by conventional one-dimensional laboratory testing. However, the constitutive model is not readily understood by practising engineers and it will be shown in Part 2 of this paper that the analysis results are dependent on the geological time assumed since deposition of the soft soil, as well as the initial OCR profile of the soil.

4 PRELOAD DESIGN FOR EMBANKMENTS CONSTRUCTED ON SOFT SOILS

Unfortunately, many of the time-dependent analysis models described in Section 3 are not easily understood by practising geotechnical engineers and some are still in the research stage and not available for commercial use. In any case, indiscriminate use of research or commercial software, without understanding the assumptions and limitations of these models, has the potential to result in serious errors.

Therefore, despite recent advances in time-dependent analysis of simultaneous consolidation and creep for soft soils, most settlement analysis and preload designs in practice are still being carried out using traditional analysis methods that treat primary consolidation and creep in separate, consecutive phases.

In the author's opinion, it is important to be able to use fundamental principles and conceptual models that are readily understood, for use as either a preliminary design tool, or as a check on more complex analysis methods that are more difficult to understand. Bjerrum's time line approach forms a readily understood conceptual model that may be used to gain insight into the stress path effect on post-surcharge compression behaviour of soft soils. This approach will be extended to include stress level and OCR dependency in Part 2 of this paper.

Mesri (1991) presented his design approach for surcharging to reduce post-construction creep that incorporates the use of a "secant" creep index, C_α" based on experimental results. Their method is summarised in Figures 5 and 6, and Equations 4 and 5.

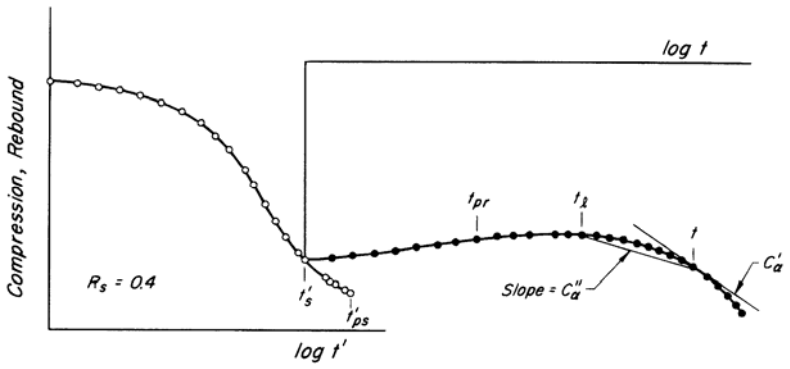

Figure 5: Settlement Behaviour – Surcharge Removal (Mesri, 1991).

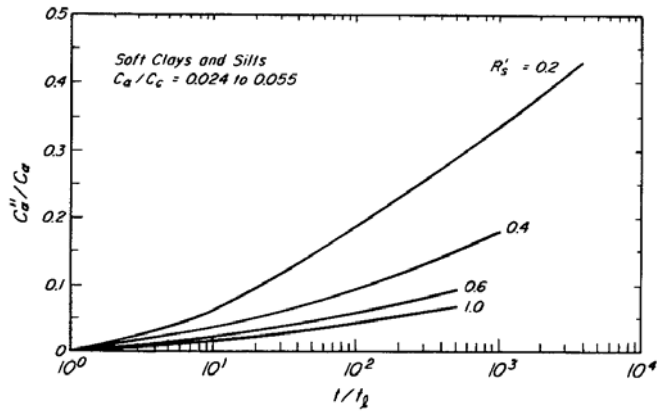

Figure 6: Post Surcharge C_α Relative to OCR and Time Effects (Mesri , 1991)

In Figures 5 and 6, Mesri (1991) defined the stress history and time-dependent parameters, R_s' and t_ℓ / t_{pr} that are used to assess the secant creep index, C_α" as follows:

$$R_s' = OCR - 1 \quad \textbf{(4)}$$

$$t_\ell / t_{pr} = 100(R_s')^{1.7} \quad \textbf{(5)}$$

In Equation 5, t_{pr} and t_ℓ are the time at completion of primary rebound and recommencement of creep, following removal of the preload. The time for completion of primary rebound (100% dissipation of negative porewater pressures) may be computed using traditional consolidation theory. The primary rebound time is generally fairly rapid due to unloading in the recompression range as discussed in Section 2.6.

By trial and error, using different surcharges, the final OCR and R_s' values may be calculated and once C_α" is obtained from Figure 5 and t_ℓ obtained from Equation 5, the post-construction creep settlement may be obtained from the equation:

$$s = \frac{C_\alpha''}{(1+e_o)} h_o \log \frac{t}{t_l} \quad \textbf{(6)}$$

Equation 6 should be integrated for all sub-layers that may have different h_o, C_α", and t_l values.

The possibility of relatively large on-going creep following preloading is fairly obvious from Figure 5, although the underlying reasons are still not readily conceptualised via Mesri's experimental data. In Part 2 of this paper, the use of Bjerrum's time line concept will be discussed and applied on an example problem to illustrate the likely reason for observed post-construction being greater than that predicted following preloading.

5 CONCLUSION

In designing a preload to reduce post-construction settlement, it is important to have a good basic understanding of the principles involved and soil consolidation behaviour. The following points have been highlighted in this paper:

- The geological history as well as loading history has a strong influence on compressibility behaviour of soils.
- Creep behaviour is one of the most important, yet least understood, aspects in preload design.
- Creep is dependent on stress level, geological and stress history.
- It is likely that creep occurs simultaneously with consolidation, particularly with thicker soft soil deposits.
- Various constitutive relationships using time-dependent, simultaneous consolidation and creep models, have been developed, ranging from fitting mathematical expressions to experimental data, to complex numerical models using elasto-visco-plastic models that can be used for assessing preloading and post-preload settlement behaviour.
- Despite recent advances in time-dependent settlement analysis and the availability of powerful commercial software, the underlying assumptions and basis of such software may not be readily understood by practising engineers. The author believes that in order to reduce the risk of serious errors in preload design, it may be better to use simpler models that incorporate more readily understood soil behaviour. Bjerrum's time line model provides such an approach that is still widely used for preload design today.
- Mesri's experimental data (Mesri, 1991) shows the potential for increasing rate of creep sometimes following preloading, under certain time and surcharge ratio conditions.

In Part 2 of this paper, an analytical approach based on Bjerrum's time line model (Bjerrum, 1967; 1972) is developed for preload design, and a preload design example is discussed to illustrate the importance of geological and stress history on post preload settlement behaviour.

6 REFERENCES

Alonso, E.E., Gens, A. and Lloret, A. (2000), "Precompression design for secondary settlement reduction" Geotechnique, 50, No. 6, pp. 645-656.

Australian Standard AS 1289.6.6.1 (1998), "Method of testing soils for engineering purposes. Method 6.6.1: Soil strength and consolidation tests-determination of the one-dimensional consolidation properties of a soil-standard method', Standards Australia

Bjerrum, L. (1967). "Engineering geology of Norwegian normally consolidated marine clays as related to settlements of buildings", 7th Rankine Lecture, Geotechnique, 17(2), pp. 81-118.

Bjerrum, L. (1972). "Embankments on Soft Ground", Proceedings of Speciality Conference, Performance of Earth and Earth-Supported Structures, American Society of Civil Engineers, New York, NY., Vol II, pp 1-54.

Buisman, L. (1936) "Results of long duration settlement tests", Proceedings, First International Conference on Soil Mechanics and Foundation Engineering, Cambridge, Massachusetts, Vol. 1, pp. 103-107.

Chandler, R.J., de Freitas, M.H. and Marinos, P. (2004) "Geotechnical Characterisation of Soils and Rocks: a Geological Perspective" The Skempton Conference, Thomas Telford, London, pp 67-102.

Crawford, C.B. (1964) "Interpretation of the consolidation test", Journal of the Soil Mechanics and Foundations Division, Proceedings of the ASCE, 90(5), pp. 87-102.

den Haan, E.J. (1996) "A compression model for non-brittle soft clays and peat" Geotechnique 46(1), pp. 1-16.

den Haan, E.J., and Sellmeijer, H.J.B. (2000) "Calculation of Soft Ground Settlement with an Isotache Model" Geotechnical Special Publication Number 112, Soft Ground Technology, Edited by James L. Hanson and Ruud J. Termaat, Proceedings of the Soft Ground Technology Conference, the Netherlands, pp. 94-104.

Ewers, B. and Allman, M.M. (2000) "Secondary Compression of Soft Clay from Ballina" GeoEng 2000

Feda, J. (1992) “Creep of Soils and Related Phenomena” Elsevier Science Publishing Co., New York.
Fox, J.P., Edil, T.B., Malkus, D.S. (1994) “Discrete element model for compression of peat” Computer Methods and Advances in Geomechanics, Siriwardane and Zaman (editors), Balkema, Rotterdam.
Kuhn, M.R. and Mitchell, J.M. (1993) “New Perspectives on Soil Creep”, Jnl. of Geotechnical Engineering, 119(3), pp. 507-524.
Magnan, J. P., Bertaina, G., Khemissa, M., and Reiffsteck, Ph. (2001). À propos des indices de fluage déterminés à l’œdomètre, *15th International Conference on Soil Mechanics and Geotechnical Engineering*, Istanbul, vol. 1, Balkema, pp. 203-206.
Mesri, G. (1991) “Prediction and performance of earth structures on soft clay”, Proceedings of The International Conference on Geotechnical Engineering on Coastal Development, Yokohama, 2, G2.1-G2.16.
Mesri, G., and Godlewski, P.M. (1977) “Time and Stress-Compressibility Interrelationship”, Jnl of the Geoltechnical Engineering Division, ASCE (103), No. GT5, pp. 417-430.
Mesri, G., Lo., and Feng, T. (1994). *ASCE Specialty Conference on Geotechnical Engineering,* Special Publication No. 40, vol. 1, pp. 8-76.
Mitchell, J.K., Campanella, R.G., and Singh, A. (1968) “Soil Creep as a rate process”, Jnl. Geotech. Engineering Division, ASCE, 94(1), pp. 232-253
Nash, D.F.T., Sills, G.C. & Davision, L.R. (1992) “One-dimensional consolidation testing of soft clay from Bothkennar” Geotechnique 42, No. 2, pp 241-256.
Olaszak, W. and Perzyna, P. (1966) “The constitutive equations of the flow theory for a non-stationary yield condition”, Applied Mechanics, Proc. Eleventh International Congress of Applied Mechanics, pp545-533, Springer – Ver lag.
Perrone, V. (1999) “One Dimensional Computer Analysis of Simultaneous Consolidation and Creep of Clay”, phD Thesis, Virginia Polytechnic Institute and State University, Blacksburg, Virginia.
Perzyna, P. (1963) “Fundamental Problems in Viscoplasticity”, Advances in Applied Mechanics, Vol. 9, pp243-377, Academic Press, New York
PLAXIS (Version 8, 2002) Finite Element Code for Soil and Rock Analysis, User Manual
Rajot, J.P. (1992) “A theory for the time dependent yielding and creep of clay”, Ph.D. Thesis, Virginia Polytechnic Institute and State University, Blacksburg, Virginia.
Taylor, D.W. (1942) “ Research on Consolidation of Clays”, Department of Civil and Sanitary Engineering, Massachusetts Institute of Technology, Cambridge, Massachusetts, Serial 82.
Terzaghi, K. (1925) Erdbaumechanik, Franz Deuticke, Vienna.
Waddell, P.J. and Wong, P.K. (2005) “Settlement of Deep Compacted Fill” Australian Geomechanics Jnl. Dec 2005 pp57-72.
Yin, J.H. and Graham, J.(1999) “Elastic viscoplastic modelling of the time dependent stress-strain behaviour of soils” Canadian Geotechnical Jnl., 36, pp736-745.

PRELOAD DESIGN, PART 2 – AN ANALYTICAL METHOD BASED ON BJERRUM'S TIME LINE PRINCIPLE AND COMPARISON WITH OTHER DESIGN METHODS

Patrick K. Wong
Senior Principal, Coffey Geotechnics Pty Ltd

ABSTRACT

Following a review of time-dependent settlement behaviour and preload design methods presented in Part 1 of this paper (Wong, 2006a), Part 2 of this paper presents the development of an analytical approach for preload design based on Bjerrum's (1967; 1972) time line model, or principle of "artificial aging". This analytical approach can be readily coded using an Excel spreadsheet for assessing the required preload thickness to limit post-construction settlement to a specified value.

A worked example is presented and compared with other methods (Mesri, 1991; Poulos, 2004; PLAXIS Version 8, 2002) to illustrate the importance of geological and stress history on post-preload settlement behaviour.

The dependency of creep on stress level and stress history is used in the analytical approach introduced in this paper, and the results of the worked example clearly show the reasons for the possibility of significant post-preload creep settlement if the amount and/or the degree of consolidation during surcharging were insufficient.

The purpose of this paper is not to suggest any preference for a particular preload design method with respect to either correctness or accuracy in predicting post-construction settlement performance following preloading. Rather, through the worked example, it highlights the dependency of the results on certain assumptions used in the models, and perhaps also highlights the importance of being able to follow the stress path and applying fundamental principles to explain the predictions and their limitations.

1 INTRODUCTION

In Part 1 of this paper (Wong, 2006a), the stress level-dependency and stress-history dependency of creep was introduced, and the following equation was suggested by the author for assessing the creep strain ratio of an over-consolidated soil:

$$\frac{C_{\alpha\varepsilon(oc)}}{C_{\alpha\varepsilon(nc)}} = \frac{(1-m)}{e^{(OCR-1)n}} + m \qquad \textbf{(1)}$$

where:

OCR = over-consolidation ratio (whether due to past higher stress, creep or "aging process", or other factors.

$C_{\alpha\varepsilon(oc)}$ = creep strain rate per log time cycle for an over-consolidated soil at a particular OCR.

$C_{\alpha\varepsilon(nc)}$ = creep strain rate per log time cycle for a normally consolidated soil (i.e. OCR =1) and is stress level dependent (see Figure 2 of Wong, 2006a).

m and n = constants depending on soil type, values of m = 0.1 and n = 6 are considered by Wong (2006a) to be reasonable values for organic soils in the absence of site specific data (see Figure 4 of Wong, 2006a). It is possible that higher "n" values may be possible based on back analysed data from Alonso *et al.* (2000).

Based on a modified form of Bjerrum's time line approach, Wong (2005) presented an analytical method for preload design that could be incorporated into a simple spreadsheet to assess the preload thickness required to achieve a given design embankment height and post-construction settlement limit. This approach incorporates the weight of the embankment fill, including the settled fill below the ground level and buoyancy effects of the settled fill.

The main difference in the method described by Wong (2005) and Bjerrum's time line approach (Bjerrum (1967; 1972) is that there is no need to assume that the lines representing the creep characteristics of a soil are parallel in the e –log (p) plot. While the varying creep rates shown by the "splaying out of the creep lines" with increasing effective stress in Figure 1 appear to be a very bold deviation from the parallel creep lines shown in Bjerrum's conceptual model, they represent a conceptual model that takes into account the dependency of creep strain with stress level. In the analytical approach that is described below, it does not really matter whether the creep lines are drawn parallel or splayed,

provided the appropriate creep strain value is selected, depending on stress level and stress history. In other words, the key is to have a reasonable assessment of the appropriate creep strain value for long-term post surcharge settlement assessment purposes, which is also true for the preload design method described by Mesri (1991).

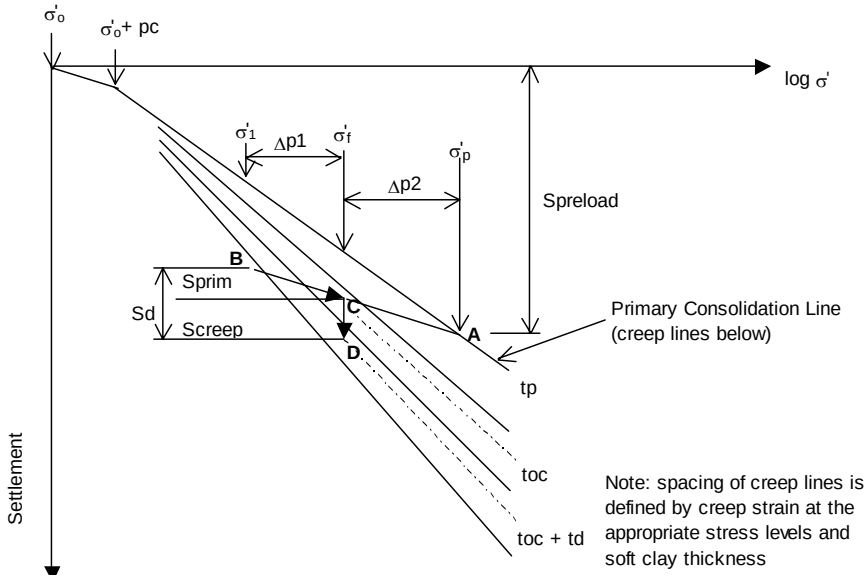

Figure 1: Development of Analytical Approach Using a Modified Form of Bjerrum's Model.

The points in Figure 1 are defined as follows:

Point A = Effective stress σ'_p reached after preloading with degree of consolidation U_p

Point B = Effective stress σ'_1 after removal of preload and rebound has occurred

Point C = Effective stress σ'_f after final design stress applied and primary consolidation S_{prim} occurred

Point D = Final settlement including creep after design life of t_d

Sd = Design post-construction settlement limit after ground improvement by preloading

Sprim = Primary consolidation component of S_d (reloading after preloading)

Screep = Creep component of S_d (over-consolidation creep after preloading)

Δp_1 = Design stress increase after preloading from project loads

Δp_2 = Effective stress increase above final stress, σ'_f , from preload at degree of consolidation, U_p

tp = Reference time for primary consolidation to occur (or primary rebound after surcharge)

toc = Equivalent "artificially aged" time after preloading

td = Design life after application of final stress increase associated with project.

In this approach, a key parameter (besides the other soil compressibility values) is the choice of the creep strain rate, $C_{\alpha\varepsilon(oc)}$, at the appropriate stress level and OCR corresponding to the final stress following removal of the surcharge and after application of the design load to account for the lower creep strain due to the artificial aging process in a similar way as the secant C_α" value used by Mesri (1991), reproduced as Figure 5 in Wong (2006a). It should be pointed out here that $C_{\alpha\varepsilon(oc)}$ used in this paper is equivalent to Mesri's C_α"/(1+e_o)

Another key parameter which will have an influence on the analysis result is the reference time, t_p , which is used to assess creep at a constant effective stress, and the equivalent "artificially aged" time, "toc" following removal of the surcharge and application of the final loading. This reference time is referred to as the instantaneous compression line in Bjerrum's original time line diagram (reproduced as Figure 1 in Wong (2006a), and is shown as a 24 hour line in keeping with the time for each load increment in the standard oedometer test. In preload assessment in the field, however, the onset of significant creep generally occurs much later than 24 hours even though the author believes that creep occurs simultaneously with primary consolidation as discussed in Wong (2006a). This is usually the case even if wick drains are used to accelerate primary consolidation. From the author's experience, a t_p value of 1 year appears to be reasonable for most practical projects when used with the analytical method described in this paper.

2 ANALYTICAL SOLUTION

Using the modified time line concept, a set of equations have been developed for the general case of a soft ground that requires filling to form a final construction platform followed by the application of development loading as shown in Figure 2.

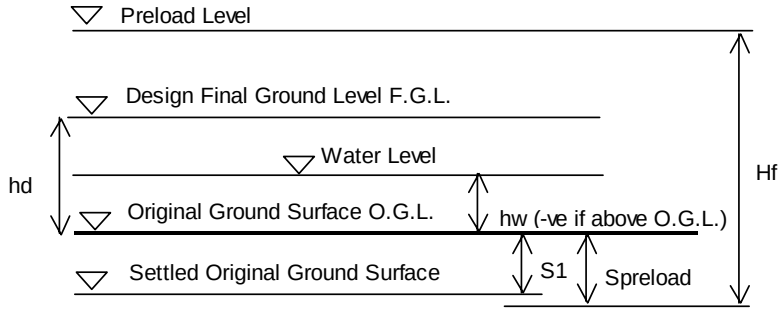

Figure 2: Problem Definition for Development of Preload Design.

The formulation of the preload design calculations takes account of the following:

- Settlement of the preload fill or working platform
- Buoyancy of the fill that settles beneath the ground water level
- Percentage consolidation under the preload (stress increase is assumed to be proportional to percentage consolidation)
- Dependency of creep strain rate on stress level and stress history.

An iterative approach is adopted, requiring an initial estimate of the settlement under the preload. The initial estimate is then checked against the computed value until a match is found that provides the corresponding preload fill thickness. The steps in the analytical approach (modified from Wong (2005) by iterating against an initial trial preload effective stress (rather than settlement during preloading to make spreadsheet computation easier) are as follows:

Step 1

Divide the soft soil profile into sub-layers, and for a given time available for preloading, calculate the degree of consolidation, Up, achievable under the preload for each sub-layer using the traditional one-dimensional consolidation theory and the diagram shown in Figure 3.

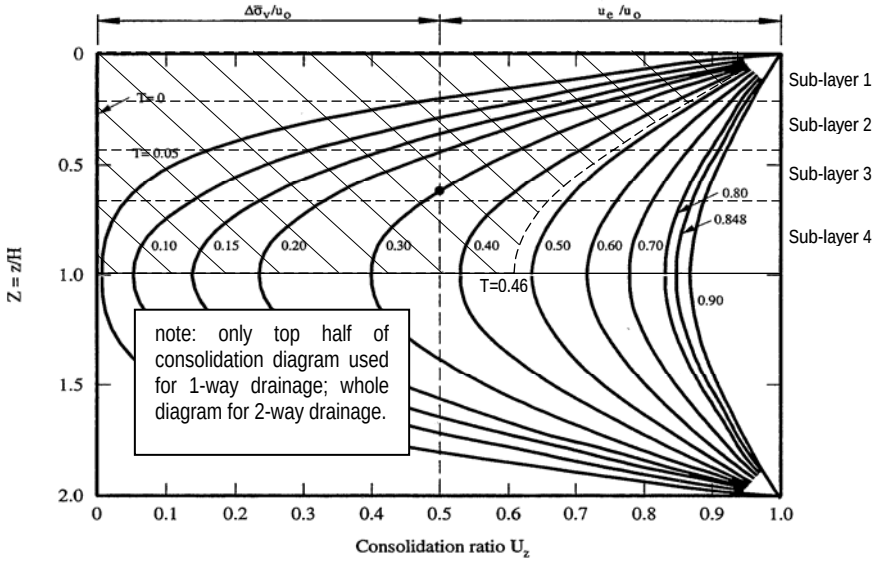

Figure 3: Degree of Consolidation as a Function of Depth and Time Factor (Lambe and Whitman, 1969).

Step 2

Trial an initial effective stress (including buoyancy effects) applied by the preload including the embankment and surcharge filling (note: a trial and error approach is not necessary if Excel's "SOLVER" function is used (see Step 11). The effective stress at the end of preloading, σ'_p is defined for each layer as:

$$\sigma'_p = U_p \times p'_{trial} \times I_z \quad \textbf{(2)}$$

where: U_p degree of consolidation from Step 1
p'_{trial} = trial initial stress applied at original ground level
I_z = depth influence factor to take into account of 2D or 3D loading conditions

Step 3

The settlement, S_A, for each sub-layer is calculated by applying the classical one-dimensional settlement equation:

$$S_A = h_o\left[\frac{C_r}{1+e_o}\log\left(\frac{\sigma_o'+p'_c}{\sigma_o'}\right)+\frac{C_c}{1+e_o}\log\left(\frac{\sigma'_p}{\sigma_o'+p'_c}\right)\right] \quad \textbf{(3)}$$

and the total settlement during preloading is integrated over the profile to obtain $S_{preload}$.

Step 4

Knowing the total settlement, $S_{preload}$ during preloading, the equivalent preload thickness, H_f , corresponding to the trial effective stress, is calculated based on the input target degree of consolidation and buoyancy effect due to the settled fill using the unit weight of the fill and water level information as defined in Figure 2.

Step 5

The final effective stress following removal of the surcharge to the design embankment height and the rebound, S_r , is calculated for each sub-layer so that the net settlement at point B (Figure 1) is $S_B = S_A - S_r$.

The amount of surcharge fill to be removed at this step is:

$$H_r = H_f - S_{preload} - h_d \quad \textbf{(4)}$$

But it should be pointed out that the stress decrease due to surcharge removal in each sub-layer for calculation of rebound needs is not $H_r \times \gamma_f$ unless the degree of consolidation during preloading has reached 100% for that sub-layer. The stress change from point A to point B may be calculated as follows:

$$(\Delta p_1 + \Delta p_2) = \sigma'_p - (h_d \times \gamma_f + S_{preload} \times \gamma'_f) \times I_z \quad \textbf{(5)}$$

where: $S_{preload}$ and I_z are as defined in the previous steps, and
γ_f and γ'_f = bulk unit weight and buoyant weight of the embankment fill respectively.

If $(h_d \times \gamma_f + S_{preload} \times \gamma'_f) \times I_z < \sigma'_p$, the rebound from point A to point B may then be calculated as follows:

$$S_r = h_o\left[\frac{C_r}{1+e_o}\log\left(\frac{\sigma'_p-(\Delta p_1+\Delta p_2)}{\sigma'_p}\right)\right] \quad \textbf{(6)}$$

It can be seen from Equations 5 and 6 that if $(h_d \times \gamma_f + S_{preload} \times \gamma'_f) \times I_z > \sigma'_p$, $(\Delta p_1 + \Delta p_2)$ will be negative and further primary consolidation will occur even after unloading. In this situation of insufficient preloading, Equation 6 should not be used, and S_r should be set to zero for that sub-layer and the future primary consolidation, S_{prime} , may be calculated as follows:

$$\text{For } (h_d \times \gamma_f + S_{preload} \times \gamma'_f) \times I_z > \sigma'_p \rightarrow S_{prim} = h_o\left[\frac{C_c}{1+e_o}\log\left(\frac{\sigma'_p-(\Delta p_1+\Delta p_2)}{\sigma'_p}\right)\right] \quad \textbf{(7)}$$

In the latter situation, not only is S_{prim} positive (i.e. further settlement rather than rebound), the magnitude is 5 to 10 times (i.e. ratio of C_c/C_r) higher than S_r compared to the case of sufficient preloading.

Step 6

The final effective stress following application of the design load and the corresponding primary consolidation component, S_{prim} is calculated. As discussed in Step 5, depending on the degree of preloading achieved at the time of removal of the surcharge, S_{prim} may undergo reloading (sufficient preloading) or virgin loading (insufficient preloading) or a combination of both.

For each sub-layer, the settlement at point C (Figure 1), S_C, is now calculated as $S_B + S_{prim}$.

Step 7

The settlement at σ_f' on the primary consolidation line directly above point C (Figure 1), if preloading had not been carried out, is calculated as S_{CO} as follows:

$$S_{co} = h_o\left[\frac{C_r}{1+e_o}\log\left(\frac{\sigma_o'+p'_c}{\sigma_o'}\right)+\frac{C_c}{1+e_o}\log\left(\frac{\sigma'_f}{\sigma_o'+p'_c}\right)\right] \quad \textbf{(8)}$$

Step 8

The OCR value after Step 6 is calculated and the new $C_{\alpha\varepsilon(oc)}$ value is assessed using Equation 1. The procedure for calculating the final OCR is relatively simple (i.e. σ'_p/σ'_f). However, incremental OCR values are required to enable the "artificially aged" time, "toc", to be calculated because the creep strain rate is not constant with time. That is, the spacing of the creep lines is reducing with each log time cycle because the process of creep causes an increase in the preconsolidation pressure as discussed in Wong (2006a). By dividing the difference in effective stress between σ'_p and σ'_f in to a number of increments (say "N" equal increments; N=5 is generally sufficient), it is possible to compute the creep strain rate and "toc" as follows:

$$\text{Average OCR at increment "i"} \rightarrow \quad OCR_{(i)} = \frac{\sigma'_f+(i-0.5)\left(\frac{\sigma'_p-\sigma'_f}{N}\right)}{\sigma'_f} \quad \textbf{(9)}$$

$C_{\alpha\varepsilon(oc)(i)}$ at this increment → calculate creep strain rate according to Equation 1 using $OCR_{(i)}$

$$S_c \text{ at this increment} \rightarrow \quad S_{c(i)} = S_{co} + h_o\left(\frac{C_c-C_r}{1+e_o}\right)\log\left(\frac{\sigma'_f+i\left(\frac{\sigma'_p-\sigma'_f}{N}\right)}{\sigma'_f}\right) \quad \textbf{(10)}$$

$$\text{"Aged" time at this increment} \rightarrow \quad toc_{(i)} = toc_{(i-1)}10^{\left[\frac{Sc(i)-Sc(i-1)}{C_{\alpha\varepsilon(oc)(i)}(h_o-S_{c(i-1)})}\right]} \quad \textbf{(11)}$$

Equations [9] to [11] are repeated from i = 1 to N to obtain the final "toc". In the above procedure, if $\sigma'_p < \sigma'_f$, then $C_{\alpha\varepsilon(oc)}$ should be set to $C_{\alpha\varepsilon(nc)}$ and "toc" should be set to "t_p" (i.e. normally consolidated condition).

Step 9

The final OCR and $C_{\alpha\varepsilon(oc)}$ are then calculated using OCR = σ'_p/σ'_f for each sub-layer, and the long-term creep settlement, S_{creep} can now be estimated as follows:

$$S_{creep} = C_{\alpha\varepsilon(oc)}(h_o - S_C)\log\left(\frac{toc+t_d}{toc}\right) \quad \textbf{(12)}$$

Step 10

Integrating over the soft soil profile, the total post-construction settlement is estimated from Steps 6 and 9 as (S_{prim} + S_{creep}).

Step 11

Steps 2 to 10 are then iterated, or Excel's SOLVER function is used until the following conditions are satisfied:

- $(S_{prim} + S_{creep}) \le S_d$, and **(13)**
- $(H_f - S_{preload}) \ge h_d$ **(14)**

It should be stressed that the above analytical procedure is not a time-dependent analysis and does not include the effect of simultaneous consolidation and creep. Compared to more complex time-dependent simultaneous consolidation and creep models, however, this simplified procedure does allow a ready visualisation of the stress path that the various sub-layers in the soil profile undergo in either Bjerrum's original time line model shown in Figure 1 of Wong (2006a), or the modified model shown in Figure 1 of this paper.

3 COMPARISON OF ANALYTICAL METHOD WITH OTHER METHODS

The analytical method described in Section 2 above is used in the following example which is also compared with analysis results carried out using (a) the approach of Mesri (1991), (b) a finite difference program CAOS-1D developed by Poulos (2004), and (c) simultaneous consolidation and creep model of the commercially available program PLAXIS (Version 8, 2002).

3.1 EXAMPLE PROBLEM

A proposed road embankment having a design height of 3 m constructed over 9 m of soft soil is used in this example:

Soft clay profile = 9 m thick
Groundwater level at surface
Bulk unit weight = 15 kN/m^3
0 m to 2 m OCR = 10
2 m to 4 m OCR = 4
4 m to 6 m OCR = 2
6 m to 9 m OCR = 1.2
$C_c/(1+e_o) = 0.3$
$C_r/C_c = 0.1$
$C_{\alpha\varepsilon(nc)} = 0.015$ at an effective stress level of approximately 100 kPa (if normally consolidated)
c_v = 15 m^2/yr (one way drainage with impermeable base)
Design embankment height, h_d = 3 m
Bulk unit weight of embankment fill and surcharge = 20 kN/m^3
Design load = 8 kPa (reduced live load factor of 0.4 × design traffic loading of 20 kPa)
Available surcharge time = 2.5 yrs
Road to open approximately 0.5 yr following removal of surcharge.

For this example, we will consider that the task is to find the required fill thickness, H_f , (including embankment fill, settlement, and surcharge) to limit post-construction settlement to 0.1 m in 20 years after construction.

3.2 ANALYTICAL APPROACH USING THE TIME LINE CONCEPT AS DESCRIBED IN SECTION 2

Within an available preload time of 2.5 yrs, the dimensionless time factor is calculated to be $T_v = c_v.t/H^2 = 0.46$, and an average degree of consolidation of 73% of the entire profile may be inferred from 1D consolidation theory. However, if we subdivide the profile into four sub-layers having thicknesses of 2 m, 2 m, 2 m, and 3 m, the degree of consolidation may be read from Figure 3 as approximately 93%, 80%, 70%, and 62% in each of the four sub-layers respectively.

The need to place more fill than the design height to compensate for settlement and surcharge causes additional loading and settlement, making it difficult to achieve high OCR for the soft soil without placing large amounts of preload fill. Staged construction is normally required to maintain adequate stability although not discussed in this paper.

Using a simple spreadsheet developed based on the analytical procedure described in Section 2, and adopting a reference time, t_p , of 1 year, the amount of preload fill required is assessed to be 6.4 m, with an estimated settlement of 1.04 m during preloading, leaving an excess fill of 2.36 m (i.e. 6.4 m-3 m-1.04 m) to be removed. However, this surcharge is found to be only partially effective due to the limited preload time and percentage consolidation achieved as indicated above.

The stress paths, assessed creep strain values and post-surcharge settlement for each of the sub-layers have been summarised in Table 1.

It can be seen from Table 1 that the majority of the estimated post-construction settlement of 0.1 m in 20 years is from the bottom two sub-layers which, through the process of the surcharging, have in fact become virtually “normally consolidated”.

Table 1: Summary of Preload Analysis Results for Example Problem from Analytical Procedure Described in Section 2

	Sub-layer	1	2	3	4
Initial Condition	Thickness (m)	2	2	2	3
	Initial Effective Stress (kPa)	5	15	25	37.5
	OCR	10	4	2	1.2
	Pre-consolidation Pressure (kPa)	50	60	50	45
After 2.5 years Preload	Degree of Consolidation (%)	93	80	70	62
	Effective Stress Achieved (kPa)	113.7	108.5	106.9	110
Final Condition after Surcharge Removal and Application of Design Load	Final Effective Stress (kPa)	83.2	93.2	103.2	115.7
	Final OCR	1.37	1.17	1.04	1.00
	Final $C_{\alpha\varepsilon}$(oc) (from Equation [1] with m=0.1, n=6	0.003	0.007	0.013	0.015
	Primary Consolidation due to applied load (m)	0.002	0.002	0.002	0.018
	Artificially aged time, "toc"	4.6E+5	65	2.1	1(1)
	Creep settlement in 20 yrs (m)	0.000	0.001	0.022	0.052
	Post-surcharge settlement in 20 yrs (m)	0.002	0.003	0.024	0.070

(1) Artificially aged time becomes the reference time of measuring creep (i.e. t_p =1 year used for this example) due to final effective stress being higher than effective stress achieved during preloading of this sub-layer.

Sensitivity analyses carried out indicate that the assessed post-construction settlement would be 20% higher if the reference time, t_p is halved from 1 year to 0.5 year.

3.3 COMPARISON USING MESRI (1991)

The same example problem is assessed using the experimental data of Mesri (1991) as reproduced in Figures 5 and 6 of Wong (2006a). However, rather than using a trial and error approach to calculate the required preload thickness, the results from Section 3.2 have been adopted for comparison of the assessed post-construction settlement as presented in Table 2.

The interesting point to note in this comparison is that the creep strain values obtained using Mesri's approach are generally less than those using the approach adopted by the author of this paper using Equation 1, with m and n coefficients of 0.1 and 6 respectively. However, the calculated long-term creep is similar for both cases because the difference in $C_{\alpha\varepsilon(oc)}$ is offset by the difference in the treatment in equivalent time of creep commencement following surcharging. For the example considered, the assessed post-construction settlement using Mesri's approach is only 3% higher than the method described in Section 2. It should be pointed out that Mesri's data on creep strain (Mesri, 1991) do not cover the situation of OCR values less than 1.2.

In this example, we have adopted a primary rebound time, t_{pr} , of 0.5 year following removal of the surcharge, based on the assumption that during unloading, c_v would be about 5 times higher than the value for virgin compression. In Mesri's approach, a greater time delay for on-set of creep and lower post-construction creep settlement would be assessed if a longer primary rebound time is used. Conversely, higher post-construction creep settlement would result if a lower primary rebound time is used.

Table 2: Summary of Preload Analysis Results for Example Problem from Using Mesri (1991) Approach.

	Sub-layer	**1**	**2**	**3**	**4**
Initial Condition	See Table 1	Same values from Table 1 adopted			
After 2.5 years Preload	See Table 1	Same values from Table 1 adopted			
Final[(1)] Condition after Surcharge Removal and Application of Design Load	Final Effective Stress (kPa)	83.5	93.5	103.5	116.0
	Final OCR	1.41	1.20	1.06	1.00
	R'_s = OCR – 1	0.41	0.2	0.06	0
	$t_f / t_{pr} = 100(R_s')^{1.7}$	22	6.5	0.8	0
	t_f based on t_{pr} = 0.5 yr (i.e. relatively quick rebound due to unloading range) (years)	11	3.3	0.4	0
	t/ t_f (for t = 20 years)	1.82	6.1	50	∞
	New $C_{\alpha\varepsilon}$(oc) Mesri (1991)	0.0002	0.0006	0.004[(2)]	0.015[(3)]
	Primary Consolidation due to applied load (m)	0.002	0.002	0.002	0.011
	Creep settlement in 20 yrs (m)	0.000	0.000	0.014	0.072[(4)]
	Post-surcharge settlement in 20 yrs (m)	0.002	0.002	0.016	0.083

(1) Refer to Mesri (1991) or as reproduced in Figures 5 and 6 in Part 1 of this paper (Wong, 2006a) for definitions of t_f, t_{pr}, R_s' etc.

(2) R'_s beyond data range presented by Mesri (1991) – value extrapolated from Mesri data as reproduced in Figure 6 of Wong (2006a).

(3) R'_s beyond data range presented by Mesri (1991) – value assumed to be the same as normally consolidated value.

(4) For t_f = 0, Mesri's equation for computing creep settlement as reproduced in Equation [6] of Wong (2006a) is undefined, and as recommencement of creep in this situation is expected to occur soon after removal of the surcharge, the reference time, 0.5 yrs from surcharge removal to opening of the road to traffic is used instead to calculate post-construction settlement in a further 20 years.

3.4 COMPARISON USING CAOS-1D (POULOS, 2004)

CAOS-1D is a one-dimensional finite difference program formulated for the consolidation analysis of soils under one-dimensional conditions, although stress influence factors with depth can be used to model the effect of two dimensional loading at a particular location say across the width of an embankment. Bjerrum's time line concept is used for the treatment of creep, but a constant ratio $C_{\alpha\varepsilon(oc)}/C_{\alpha\varepsilon(nc)}$ is used (usually the same ratio of C_r/C_c) at any particular point and time within the soil profile.

Layered soil profiles may be analysed and commencement of creep may be nominated at either a user-assigned absolute time following commencement of load application, or at a user assigned degree of consolidation. For example, if 90% consolidation is assigned as the commencement of creep, then creep will initiate at the sub-layers closest to drainage boundaries. The latter option is used for the comparison study, and the results from the CAOS-1D analysis indicate the following:

- Degree of consolidation after 2.5 years preload period = 73%
- For a preload thickness of 6.4 m, settlement during the preload period of 2.5 yrs = 1.05 m
- Rebound after unloading to the design embankment height of 3 m = 0 m
- After removal of the surcharge and 8 kPa of reduced live load applied, post-construction settlement from 3 yrs to 23 yrs = 0.07 m.

The results of the CAOS-1D analysis during the preloading phase are similar to those calculated using the procedures described in Sections 3.2 and 3.3, but the post-surcharge creep was computed to be 30% less. The author believes that this difference is in part caused by the use of a constant $C_{\alpha\varepsilon(oc)}/C_{\alpha\varepsilon(nc)}$ ratio in the program formulation. Closer agreement would have resulted if a $C_{\alpha\varepsilon(oc)}/C_{\alpha\varepsilon(nc)}$ ratio less than C_r/C_c was used.

A different result would also be obtained by CAOS-1D if creep is assumed to start at a lower percentage consolidation (e.g. 80% instead of 90%), which will result in higher settlement during the preload period and lower post-preload creep settlement.

3.5 PLAXIS ANALYSIS USING SOFT SOIL CREEP MODEL

PLAXIS (Version 8, 2002) has a Soft-Soil-creep model that utilises a form of strain rate controlled time-dependent consolidation and creep analysis that also incorporates concepts of Modified Cam-clay and viscoplasticity. The required input parameters are derived from conventional laboratory consolidation parameters as follows:

Modified Compression Index $$\lambda^* = \frac{C_c}{2.3(1+e_o)} = 0.13 \text{ (for this example)} \quad \textbf{(15)}$$

Modified Swelling Index $$\kappa^* = \frac{2}{2.3}\frac{C_r}{(1+e_o)} = 0.026 \text{ (for this example)} \quad \textbf{(16)}$$

Modified Creep Index $$\mu^* = \frac{C_\alpha}{2.3(1+e_o)} = 0.00652 \text{ (for this example)} \quad \textbf{(17)}$$

PLAXIS also allows the user to either define the initial OCR profile, or to generate the initial OCR profile by allowing the soil to creep over a user-specified geological time. To account for over-consolidation effects other than those generated by creep under self-weight, it is possible to select the OCR profile option (e.g. to account for erosion, desiccation, chemical bonding etc), and in addition, allow the soil profile to initialise over a geological time which will be nominated as t_i in this paper. This latter option has been adopted for the example problem to demonstrate that depending on the selection of t_i, PLAXIS will generate different results and may over-estimate the creep settlement if t_i is too low.

The PLAXIS analysis results are presented in Figure 4 together with those from the CAOS-1D analysis. It can be seen that when t_i is set to zero, the calculated settlement during the preload period of 2.5 years is about 30% higher than those calculated using conventional consolidation theory, and the post-surcharge settlement in 20 years is almost double those calculated using the methods described in Sections 3.2 to 3.4. With increasing t_i, the calculated settlement during preload, and the post-surcharge settlement reduce, and become 15% and 30% higher than those calculated using the procedure described in Section 3.2 when a t_i value of 10,000 years is used.

The difference in results caused by the use of different t_i values highlights the need for appreciating the importance of the geological time history, and the way in which computation methods deals with this issue. The dependency of the results on t_i is not unexpected when the more easily understood time line concept is used.

Another interesting observation from the PLAXIS analysis results is the relatively large post-surcharge settlement for this example. The majority of the settlement was indeed from the lower soil profile which did not achieve sufficient consolidation during the preloading stage, and this supports the observations made by the author using the stress path/time line approach.

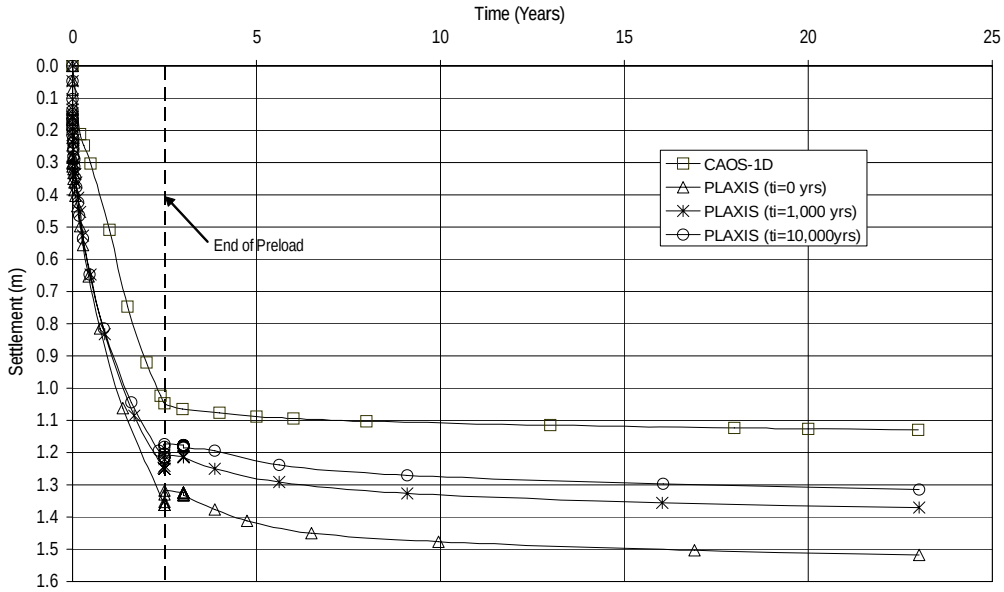

Figure 4: Results of Numerical Analysis (CAOS-1D & PLAXIS).

4 CONCLUSION

A modified form of Bjerrum's time line model for design of preloads has been developed with the introduction of stress level and stress history dependency based on the discussions given in Wong (2006a). A worked example has been used, and compared with other design methods (Mesri, 1991, Poulos, 2004, and the Soft-Soil-Creep Model of PLAXIS Version 8, 2002). The results indicate the following for the example problem described in this paper:

- Calculated post-construction settlements in 20 years for the various methods are ±30% compared to the analytical spreadsheet approach outlined in this paper.
- The method of Mesri (1991) gives close agreement (3% difference) although the treatment of creep strain rate and equivalent creep commencement time are different between the two methods.
- CAOS-1D by Poulos (2004) gives the lowest post-construction settlement, which is partly caused by the use of a constant $C_{\alpha\varepsilon(oc)}/C_{\alpha\varepsilon(nc)}$ ratio, rather than a variable ratio depending on OCR as suggested by Wong (2006a).
- PLAXIS (Version 8, 2002) gives the highest consolidation during preloading and post-construction settlement, and the results are dependent on the initial geological time, t_i , used to initialise the soil profile in addition to the OCR profile used. The greater t_i, the lower will be the calculated settlement due to the geological time history dependency of creep.

More importantly, the analysis results support the following observations:

- Post-construction settlement of preloaded soft ground is highly dependent on initial and final stress levels and OCR. This is particularly important for embankments with large anticipated settlements due to significant fill loading.
- Use of the time line or "artificial aging" principle in preload design can provide readily understood concepts and reasons for significant post-construction settlement following preloading in situations where a significant portion of the soft soil profile has not been preloaded to sufficiently high OCR.
- Special care needs to be given in preload design of thick soft soil deposits, particularly if only one way drainage is available. This may also be the case even if wick drains are used, and if the lower part of the soft soil profile is not adequately drained for reasons such as smearing, kinking or clogging of the wick drains.

5 REFERENCES

Alonso, E.E., Gens, A. and Lloret, A. (2000), "Precompression design for secondary settlement reduction" Geotechnique, 50, No. 6, pp. 645-656.

Bjerrum, L. (1967). "Engineering geology of Norwegian normally consolidated marine clays as related to settlements of buildings", 7th Rankine Lecture, Geotechnique, 17(2), pp. 81-118.

Bjerrum, L. (1972). "Embankments on Soft Ground", Proceedings of Speciality Conference, Performance of Earth and Earth-Supported Structures, American Society of Civil Engineers, New York, NY., Vol II, pp 1-54.

Lambe, T. W. and Whitman, R.V. (1969) "Soil Mechanics", (Pub.)John Wiley, New York.

Mesri, G. (1991) "Prediction and performance of earth structures on soft clay", Proceedings of The International Conference on Geotechnical Engineering on Coastal Development, Yokohama, 2, G2.1-G2.16.

PLAXIS (Version 8, 2002) Finite Element Code for Soil and Rock Analysis, User Manual

Poulos, H.G. (2004) "Consolidation Analysis of Soils" User Manual for Computer Program CAOS-1D.

Wong, P.K. (2005) "Application of Analytical Method for Preloading Design of Selected Case Studies", Ground Improvement - Case Histories, edited by Buddhima Indraratna and Jian Chu, (Pub.) Elsevier, London, 2005, Chapter 8, pp 231-246

Wong, P.K. (2006a) "Preload Design, Part 1 – Review of Soil Compressibility Behaviour In Relation to the Design of Preloads" Australian Geomechanics Society Sydney Chapter, Symposium on "Soft Ground Engineering", 11 October 2006.

THE DEVELOPMENT AND APPLICATION OF GROUTING AND GROUND TREATMENT

David Lees
Grouting and Foundation Works Australia Pty Ltd

ABSTRACT

Grouting and ground treatment is the application of engineering practices to provide improvement to the ground. These practices have been developed over the last 200 years. This paper will look at the development of these techniques and some of their recent application to the success of major engineering projects

1 INTRODUCTION

Grouting and ground treatment in particular is an art form. Why? Not because of the civil engineers who do not understand it, and mockingly suggest the addition of a few bats wings and frogs legs to the grout mix will overcome all problems. But because although we can put some numerical applications to our treatment of the ground, how the ground actually reacts to our treatment will vary and requires experienced personnel at the face to ensure the intended outcomes are achieved.

2 BRIEF HISTORY OF GROUTING AND GROUND TREATMENT

The first recorded application of grout injection to stabilise civil structures is by Charles Berigny in 1802 for the Port of Dieppe in France. Berigny went on to develop various injection processes in soft ground following the patenting of Portland Cement in 1824 developments of grouting occurred both sides of the Channel. At the turn of the Century cement grouting was used extensively as a remedial measure to deal with water ingress in the coalfields of France, Belgium and Germany and mines in the USA. Silicate and chemical grouts were introduced by Lemaire and Dumont and others at the turn of the 19th Century with the introduction of dilute silicate and acid solution into finer grained sandstones. This was then developed further by a Dutch engineer Hugo Joosten (1954).

Tube-a-manchettes were introduced by Swiss engineer Ischy in 1933 permitting grouts of different properties to be injected in any order at any interval of time in the same borehole. In the same period Maurice Lugeon (1933) published borehole watertightness criteria which is still the basis of our grouting definitions today. With the invention of the shear viscometer and the Marsh cone in 1931, engineers were able to determine better the flow characteristics of grouts to permeate fracture in rocks or soil panes.

The invention of the colloidal mixer by J.P. Morgan in 1934, manufactured by Colcrete in England from 1937, was a major result for grouting. Its high speed high shear action removed air from the cement, improved wetting and increased the proportion of fine cement particles, resulting in a grout that required less dilution with reduced segregation, lower bleed and higher strength. Much experimentation was carried out by the USBR from 1942 to 1944 on the physical properties of grout and in particular the flow properties of Portland Cement grout.

Developments of sodium silicate grouting in the 1950's included Soletanche's hard silicate gel. In 1957 the ASCE published state-of-the-art data on chemical grouting. By the 1960's grouting of alluvium was accepted worldwide and included construction of the new Blackwall Tunnel in London and the Whiteinch tunnel near Glasgow. By mid 1960 the grouting limits for common grout mixes were well appreciated.

In the 1970's concern over health and environmental pollution led to a ban on many chemical grouts, particularly in Japan. CIRA produced guidelines on the safe use of chemical grouts in the UK in 1982.

Our own Australian guru Clive Houlsby greatly improved the interpretation of the multi-pressure Lugeon tests in his publication in the Quarterly Journal of Engineering Geology in 1976.

Jet grouting emerged as an alternative to chemical grouting in the 1970s. Real time monitoring was introduced in the 1980's and in 1989 the success of microfine cements was recorded in material with otherwise poor penetration. Lombardi and Deere (1985) devised the grout intensity number and new admixtures, such as stabilizers and activators, are recorded in the 1990s with successful backfilling of the Channel Tunnel.

3 DETERMINATION OF GROUND TREATMENT NEEDS

Biggart (1984) presented a table of ground treatment based on soil grain size (Figure 1):

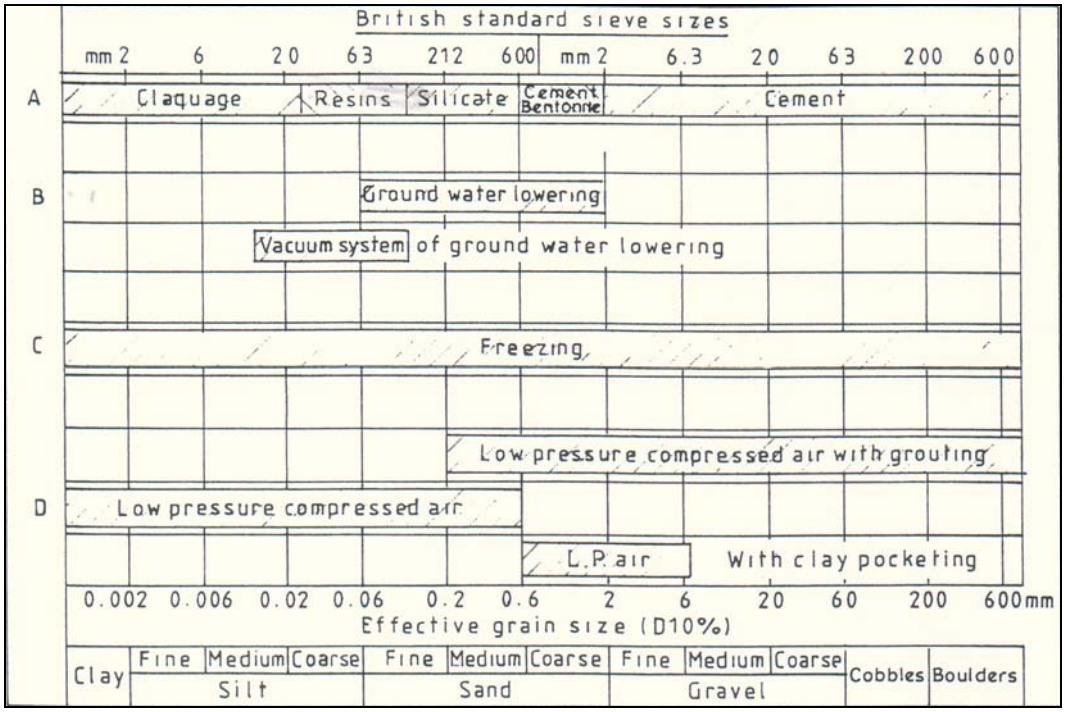

Figure 1: Ground treatment based on soil grain sizes (Biggart, 1984).

Dewatering should be the first choice of any ground treatment in soft waterlogged ground to stabilize the ground or stop groundwater entering an excavation. Well points are installed around the area. A wellpoint is a tube approximately 7 m long and 50 mm in diameter. The bottom one-metre length forms a screen through which the ground water enters. Wellpoints are usually jetted into place, a technique in which water at high pressure loosens the ground to aid penetration of the tube.

Jetting is suitable for soils of moderate to low permeability such as fine sand and sandy silt with an average permeability in the range 10-4 m/s to 10-6 m/s. Twenty-five to 50 wellpoints are usually connected to a single 25-50 m^3/hr pump header.

A filter well consists of a screened casing inserted into a drilled hole with a graded filter material packed around the screen. For temporary installations, the usual diameter of casing is 0.3 m to 0.4 m.

Usual limit conditions to groundwater lowering are

- K between 10-1 m/s to 10-6 m/s
- Substantially uniform soil conditions
- Total drawdown less than 30m
- Total outflow less than 5000 m3/hr
- Residual height H/4 for an aquifer in a given bed

Freezing is an alternative to dewatering where water logged ground is stabilized by introducing freezing material such as liquid nitrogen along tubes into the ground.

Grouting is often discussed in terms of the permeability of a soil or rock mass. Grouting is used to fill pores, fissures or voids in soil or rock to reduced water ingress, to provide increase in strength or stability of the ground, or to reduce ground movements or settlement. For planning purposes neat cement grout can achieve unconfined compressive strengths of 7-10 MPa and chemical grout can develop up to 3.5 MPa.

For rock practical limits for grouting may be set as:

- 5x10-4m/s for cement based grouts
- 5x10-5m/s for clay chemical grouts
- 5x10-5 to 5 x10-6m/s for chemical grouts

But as defined by Todd (1960) permeability is a medium's ability to transmit a fluid and takes no account of the property of the fluid. Todd goes on to say that few formulas give reliable estimates of results because of the difficulty of including all possible variables in porous media. For an ideal medium, such as an assembly of spheres of uniform diameter, hydraulic conductivity can be accurately evaluated from known porosity and packing conditions. Because of the problems inherent in formulas, other techniques for determining hydraulic conductivity are preferable for hydrogeological application.

In particular whilst soils may be more uniform in nature, as determined by the soil grading curves, and ground water flow through it may be represented as an average permeability, ground water flow through a fractured rock cannot be defined in terms of average permeability. The permeability of a rock mass is determined by the fractures, joints and bedding planes within it. Where the rock is not fractured it will be relatively impermeable but where a single open fracture occurs flows may be as high as several litres per second. Hence even determining the RQD of a rock mass may not necessarily determine the water ingress or its groutability.

As stated by Terzaghi "*No fissure can be cemented with a width of less than about 0.1 mm. For the same reason no fine sand or gravel can be grouted if the effective size of a compact sand is smaller than about 1.4 mm or that of a loose sand smaller than 0.5 mm – the grout merely replaces the material.*"

In this line the Groutability Ratio was presented by Mitchell (1970) as

$$GR = \frac{D_{15}}{D_{95}}$$

Where D_{15} is the particle diameter of the soil to be grouted 15% of which is finer by weight and D_{95} is the particle diameter of the grout 95% of which is finer by weight.

Weaver summarizes the possibility of grouting a soil for GR ranges as

GR>24 usually, GR< 19 not likely and GR< 11 not possible

However still the most practical method of determining groutability is still the water test. After all if the ground will take water it may take grout but if the ground will not take water then there is no point in trying to get grout into it. Maurice Lugeon's unit still used international today for grouting:

1 Lugeon unit is defined as water take of 1 litre per metre of test length of hole per minute at 10 bars (1,000 kPa or 150 psi). The Lugeon scale is sensitive at low values between 1 to 5 but with higher values of 50 or more and accuracy of +/- 10 Lugeons is adequate, and at more than 100 Lugeons an accuracy of +/- 30 Lugeons is appropriate.

Lugeon's 1933 work was further developed by Houlsby (1972) and may be summarized as follows:

- 1 Lugeon indicates almost no grouting is required
- Lugeons requires some light grouting
- 10 Lugeons indicates heavy grouting
- 20 Lugeons indicates extensive grouting

Houlsby also interpreted the data to help determine the ground characteristics as shown in Figure 2 .

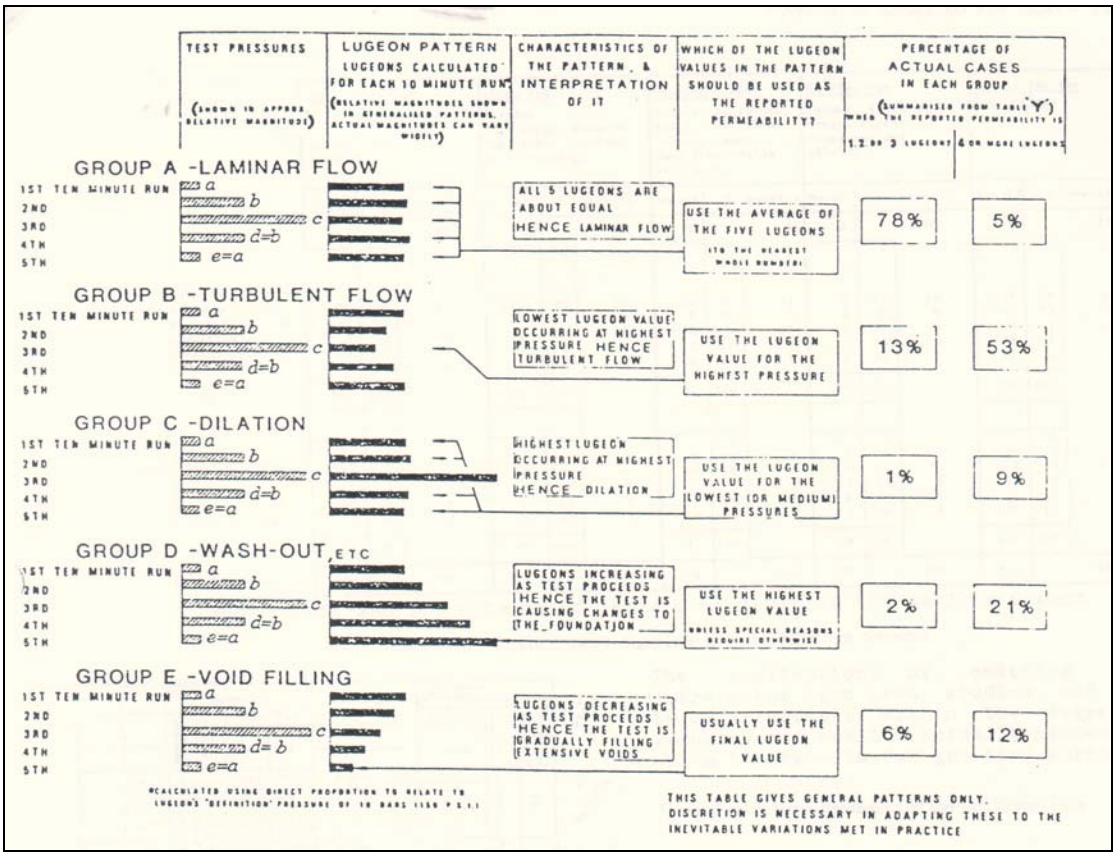

Figure 2: Interpretation of water pressure test results (Houlsby, 1972).

4 GROUND TREATMENT TECHNIQUES

Permeation Grouting – is the filling of interstices of the rock or soil, using appropriate materials and techniques to control water or to improve the structure of the ground. Vibrocompaction uses this aspect to compact the soil particles closer together.

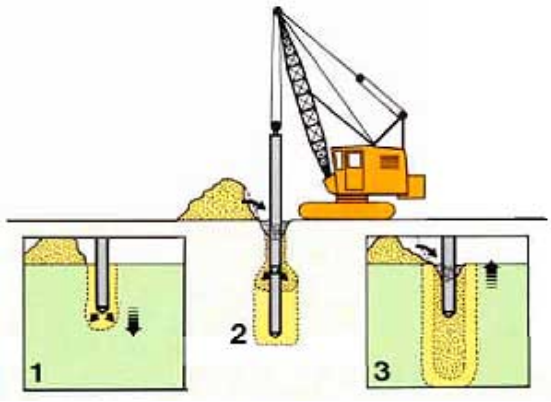

Figure 3: Compaction grouting.

Compaction grouting (Figure 3) – is the injection, under relatively high pressures, of a thick mortar. Because the grout is so thick it is unable to enter the pore space of the soil allowing displacement to compact the ground surrounding it. Stone columns are a further development of this process where granular material is injected into the ground to create a matrix of piers in an area of soft ground.

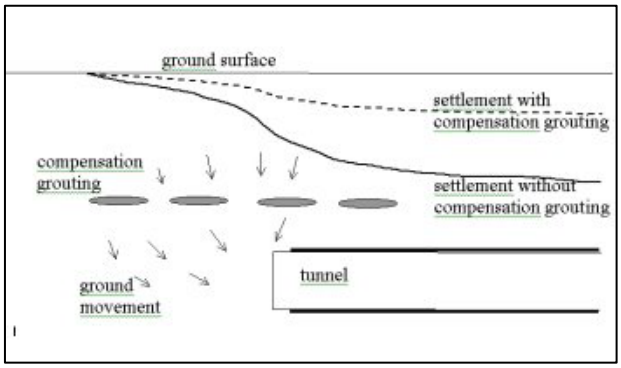

Figure 4: Compensation grouting.

Compensation grouting (Figure 4)– is essentially conducted through sleeved grout pipes or tube-a-manchettes to adjust ground levels as tunnels pass through compressible ground and was used extensively on the Jubilee Line Extension project in London.

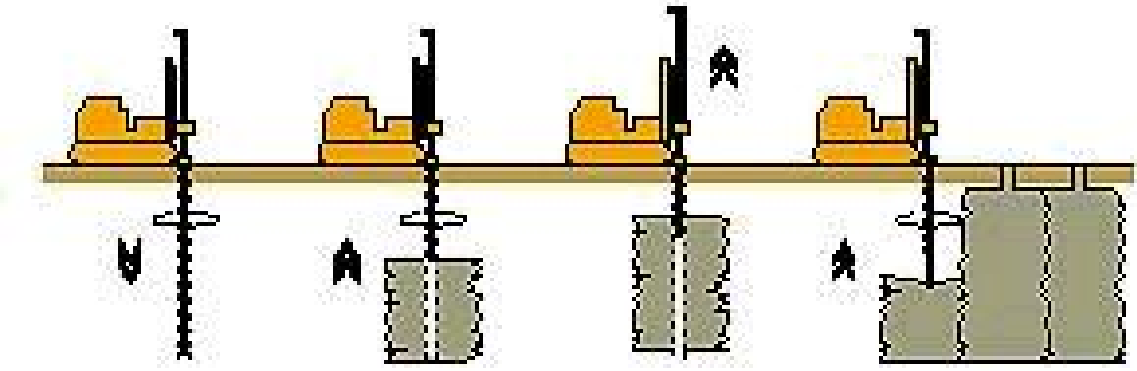

Figure 5: Jet grouting.

Jet grouting (Figure 5) – In jet grouting grout is passed at a very high pressure out of the side of a rotating tube. This grout cuts into the ground around the central hole and mixes this material to form a cylinder of grouted ground It is a grouting process developed in Germany and Japan for uniform sands and silts using very high pressures to provide pile columns up to 1.5 m in diameter. A lower pressure form of this technique is soil mixing.

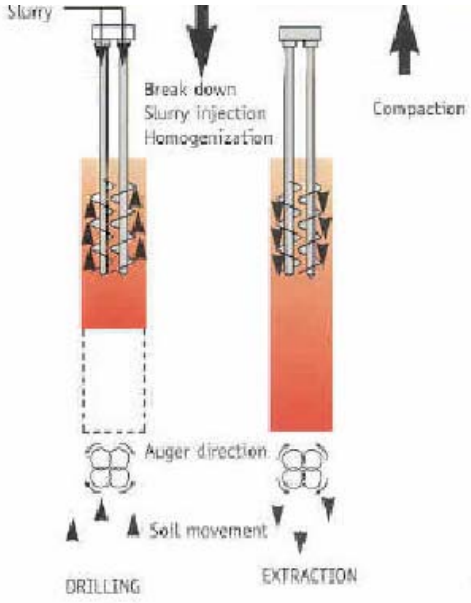

Figure 6: Colmix®.

Soletanche-Bachy have been responsible for developing soilmixing with their patented system Colmix® (Figure 6). It is a technique for consolidating face slopes in cut and fill in inaccessible or restricted places and is suitable for very poor engineering ground. The loose soil is stabilised and compacted with the aid of two or more augers which first break up the material before adding a special binder and recompacting the resulting pile.

Consolidation grouting – involves the filling of open joints, bedding planes, fault zones, cavities and other openings up to some distance beyond the excavation hence strengthening the ground and reducing groundwater flow.

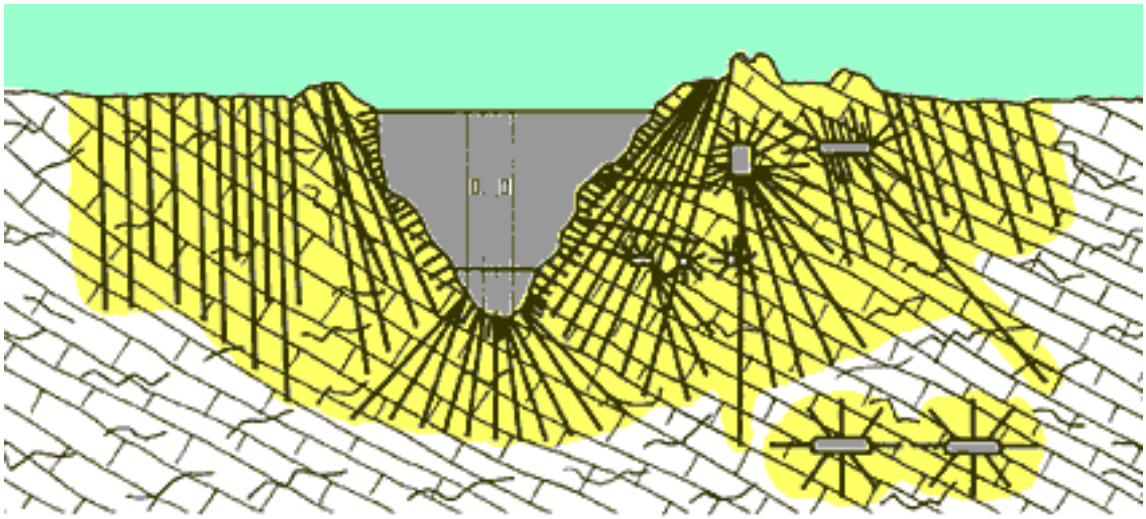

Figure 7: Curtain grouting.

Curtain grouting (Figure 7) – is the creation of an impermeable cut off usually radially around a shaft, tunnel or cavern to reduce the inflow of groundwater or the outflow of stored fluids such as LPG. Generally the grouting is carried out by widely spaced primary holes then infilled with secondary and tertiary holes until the barrier to water flow is fully achieved.

5 GROUTS AND GROUTING

There are essentially four groups of grouts, particulate grouts, colloidal solutions, pure solutions and others.

Particulate grouts are the most commonly used. These are essentially suspended mixtures with Bingham properties. This group consists of neat cement grouts (including microfine cements), clay/bentonite cement grouts and cement grouts with other additives to enhance penetration. Depending on the mix, the grout may be stable or unstable (having significant bleed). Water to solids ratio is the prime determinant of their properties and basic characteristics of stability, fluidity, strength and durability. These grouts are generally unsuitable for sealing high water flows, or high head conditions where they are likely to be diluted or washed away prior to setting

Colloidal solutions are evolutive Newtonian fluids in which viscosity increases with time. They comprise of mixtures of sodium silicate and reagent solutions which can change in viscosity over time to produce a gel. These grouts are generally unsuitable for providing permanent barriers against high-flow/high-head conditions because of their relatively long setting time, low strength and poor durability.

Pure solutions are organic resins. Their viscosity remains essentially consistent with the adjustable setting time. These are non-aqueous solvents capable of forming a gel or foam with specific mechanical properties under normal temperature conditions and in a closed environment such as poly-urethane, poly-acrylamide and epoxies. Resins are used where particularly low viscosity is required and fast strength gain. They are particularly resistant to high groundwater flows.

Miscellaneous grouts include other organic compounds which, in addition to providing waterproofing and strengthening, also provide qualities such as resistance to corrosion. These may be limited in their application due to their toxicity.

6 APPLICATION

6.1 DEWATERING – NEW SOUTHERN RAILWAY

The New Southern Railway is a 10 km twin track underground rail tunnel linking the Sydney Central Railway Station with the Kingsford Smith Airport and the previously existing East Hills Line. Five new stations were provided along the route. Bachy were responsible for the construction of the TBM launch shaft at Tempe, the new station box at Green Square and grouting behind the concrete tunnel lining segments.

Figure 8: Dewatering excavation for New Southern Railway.

The tunnel boring machine was 10.75 metres in diameter and over 75 metres long, the largest ever used in Australia and at that time the fourth biggest diameter tunnel in the world. The assembly shaft for the TBM was located in waterlogged ground adjacent to the Alexandria Canal. Bachy's engineers introduced an innovative slurry wall and dewatering system around the diaphragm wall box to assist in control in the high water table and ease construction (Figure 8).

6.2 FREEZING - DEEP TUNNEL SEWER SYSTEM SINGAPORE

The decomposed granite interface at the T05 shaft intersected the tunnel horizon. Shaft sinking was completed without the need for freezing but during blasting excavation of the tunnel horizon a major collapse took place. Soletanche-Bachy was asked to stabilize the area. Soletanche-Bachy used liquid nitrogen to provide the freezing medium. Freezing took approximately 3 ½ weeks for each section. Freezing was then switched to "maintenance mode" after the proper temperatures were reached to decrease nitrogen consumption. About 8 tanker trucks per day of nitrogen were delivered each day for initial freeze, maintenance dropped to 2 tankers per day

Excavation of the tunnel then continued with drill and blast of the frozen ground and shotcrete support (Figure 9).

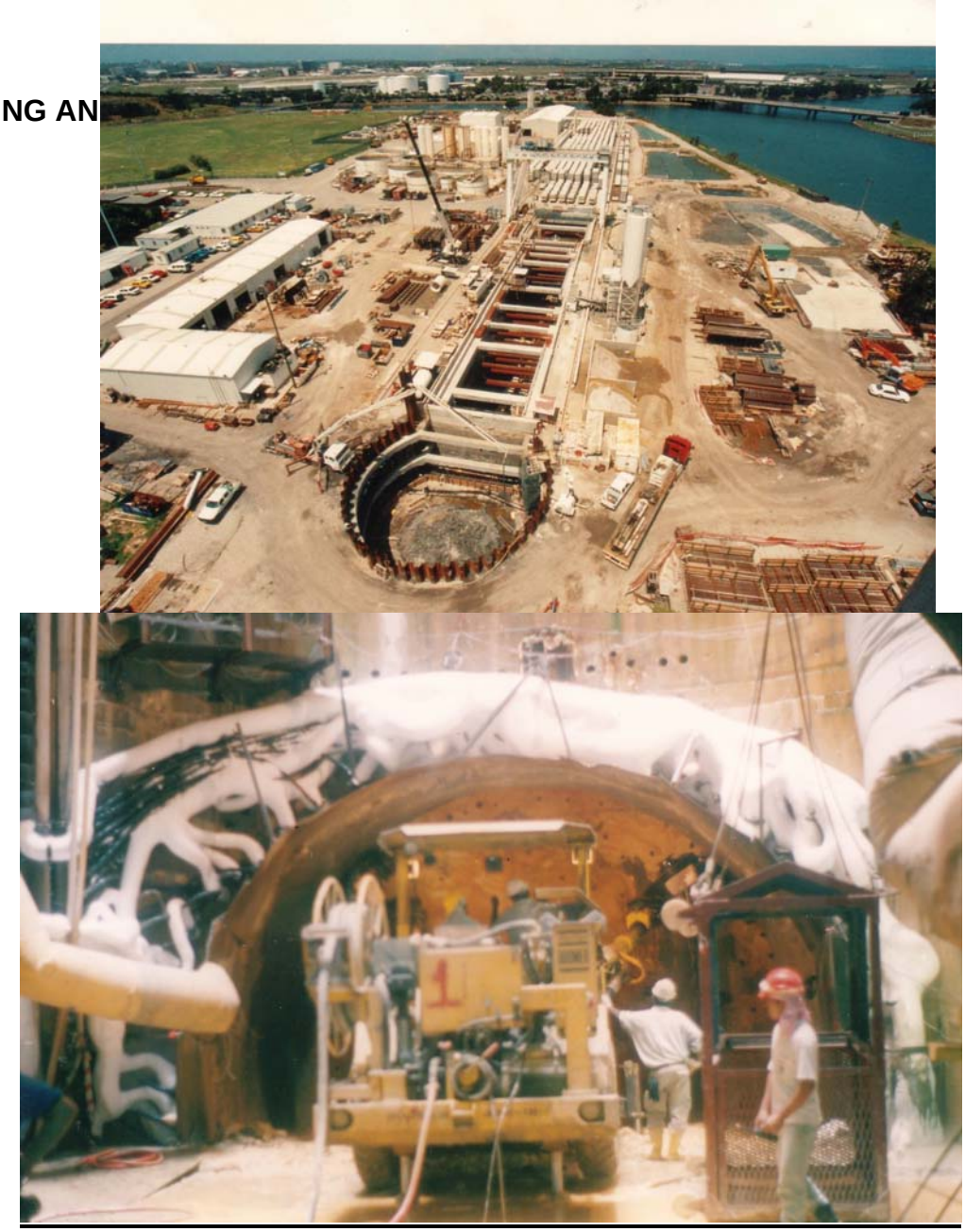

Figure 9: Freezing deep tunnel system, Singapore.

6.3 PERMEATION GROUTING – TRANSGRID CABLE 41 SUPPORT

TransGrid's Cable 41 is a high voltage supply for Sydney's CBD that comes through Arncliffe and crosses the Cooks River from south of the city (Figure 10). The cable consists of 1600 mm^2 stranded copper core with a flexible corrugated aluminium sheath, with fluid filled paper insulation and a PVC outer cover. The cables are rated at 750 MVA continuous or 900 MVA cyclic loading.

Figure 10: Location of cable crossing

Following the construction of a new sewer main in Arncliffe Street in Arncliffe, TransGrid were concerned that the founding sediments beneath the cable had become disturbed and that the cable could potentially settle and bend causing it damage.

Figure 11: Ground treatment at Arncliffe.

GFWA were asked by the geotechnical engineers to determine a grouting method to stabilize the ground with minimum risk to the 330kV cable. A system of permeation grouting using microfine cements was suggested and trials were carried out with a number of different types of product to determine an optimum spacing of grout holes and mix details (Figure 11).

Figure 12: Grouting for manhole construction.

The original contractors needed to carry out some additional manhole constructions in the street and asked us to assist. The excavations needed to be 7 m deep and due to our concerns over the silty peat layers within the sand we proposed to carry out a soil mixing process where grout was injected through nozzles as the drill bit was put into the ground. Intersecting grout holes of about 150 mm diameter were created around the perimeter of the excavation in two rows (Figure 12). When the excavation was carried out shoring was still required but the excavation was dry and no further undermining of the TransGrid cables occurred.

6.4 VIBROFLOTATION AND STONE COLUMNS – DARWIN EAST ARM PORT

The Darwin East Arm Port project forms part of the second stage of the East Arm Wharf Development. The project is being carried out for Department of Transport and Works, Northern Territory Government by Thiess Contractors. The $54M contract will involve extensive piling and concrete works and include the construction of a 110 m extension to the common user wharf, and a 160 m long bulk liquids and multi-user wharf. The project was to be completed in August 2004 to meet the needs of the AustralAsia railway (Figure 13).

Figure 13: Darwin East Arm Port.

Stage 2 consists of construction of a 16 m wide railway access causeway to link the Adelaide to Darwin railway and national rail network to an Internodal Container facility incorporating 200 m of wharf with priority access for container vessels, common user berth facility with capacity for the provision of 3 quay cranes able to handle third generation container vessels. The project included reclamation of a nominal 4 hectares for an internodal container terminal with capacity to handle in excess of 250,000 TEU per year. The facility has provision for two rail sidings and mobile terminal operating equipment. GFWA carried out the vibrocompaction of the backfill over a treatment area of 110 m x 28 m (3080m^2) x 16 m deep (Figure 14).

Figure 14: Ground improvement by vibrocompaction.

6.5 SOIL MIXING – PORTLAND LANDSLIDE, NEW ZEALAND

The Portland Project on New Zealand's North Island was a combination of a slip with settlement issues attributable to poor ground conditions. Ground investigation boreholes were carried out to determine the failure mechanisms, followed by design of a Colmix column layout to stabilise the slipping and settlement movements. The designed layout was four rows of columns with 2.5 m spacing between rows and columns at 2.5 m centres over the 50 m length of road (Figure 15).

Treatment of the Portland slip took several days longer than anticipated to complete due to the necessity to construct additional columns in one area of the slip where the ground conditions were exceptionally poor. This additional work was performed within the lump sum price provided for the design and construction of the Colmix columns. Even though the duration of the work was extended by several days, the work was still completed inside program due to the relative swiftness of constructing Colmix columns versus traditional slip repair solutions.

Due to the difficult nature of the job, the fact that the slip was a long standing maintenance issue for TNZ and also high profile being on SH 1, Portland was selected as a site to be monitored on a long term basis for any signs of further settlement or movement. Approximately every three months a series of monitoring pins, installed after Colmix, are surveyed for position and level to provide precise records of any movement that occurs. To date no movement has occurred as we pass the two year mark after completion of Colmix

Figure 15: Treatment of Portland Landslide by Colmix.

7 REFERENCES

ASCE (1957) "Chemical Grouting" Proceedings ASCE No. 83

ASCE (1962) "Cement Grouting" Proceedings ASCE No. 88.

Berigny, C. (1832) "*Memoire sur un procede d'injection a prevenir au arreter les filtrations sais les foundation des ouvrages hydrauliques*" Paris August 1832

Biggart, G. (1984) "Ground Improvement for Tunnelling". BTS meeting. Tunnels and Tunnelling June 1985

Bradt. E.F. (1909) "Crevices in a salt shaft". Mining World Vol 30 (12) 20th March 1909.

Bruce D.A. (2005). "Glossary of grouting terminology". J. Geotech and Geo.Eng. ASCE, 131(12) 1534 – 1542

CIRIA (1982) "Health and Safety Aspects of Ground Treatment Materials" Report No 95. London

Clarke, W., Boyd, M.D., and Helal, M. (1992) "Ultrafine Cement Tests and Dam Test Grouting". Proceedings ASCE Conference on Grouting in Geotechnical Engineering. W.H.. Baker.

Deere, D.U. and Lombardi, G. (1985) "Grout slimes – thick or thin?". Proceedings ASCE Conference on Grouting in Geotechnical Engineering. W.H.Baker

Gause, C. and Bruce, D.A. (1997) "Control of Fluid Properties of Particular Grouts" ASCE Geotechnical Special Publication No 66.

Glossop, R. (1961) "The Invention and Development of Injection Processes

Glossop, R. (1962) "Opening Address." Symposium on Grouts and Drilling Muds in Engineering Practice. Butterworth, London

Henn, R.W. (1996) " Practical Guide to Grouting of Underground Structures". Thomas Telford. London

Houlsby, A.C., (1972) "Construction and Design of Cement Grouting." John Wiley and Sons New York.

Ischy, E. and Glossop, R., (1962) "An Introduction to Alluvial Grouting" Proceedings Institute of Civil Engineers 21st March 1962

Janin, J.J. and Scielleur, J.F. (1970) "Chemical Grouting for Paris Rapid Transit Tunnels" Proceedings ASCE No. 96.

Joosten, A.J. (1954) "The Joosten Process for chemical soil solidification and sealing and it's development from1925 to date." N.V. Amsterdansche Ballast, Mjaatschappij

Karol, R.H. (1983) "Chemical Grouting". Marcel Dekker, New York

Karman, M. (1997) "Effect of Grouting and DMM on big Construction Projects in Japan and the 190 Hyogken-Nambin Earthquake" Grouting and Deep Mixing Balkema Rotterdam, Vol 2

Knight-Hassell & Tan (2000) " Tunnelling through challenging ground conditions in Singapore" Tunnels & Underground Structures, Ed: J Zhao, N. Shirlaw & R Krishnan

Lugeon, M. (1933) "*Barrage et Geologie*". Bulletin Technical Swisse Remande Lucerne

Mitchell, J.K. (1970) "In-placement treatment of foundation soils". Journal of the Soil Mechanics and Foundations Division, ASCE No 96

Shibazaki, M. (2003) "State of Practice of Jet Grouting" Proceedings of 3rd International Conference of Grouting and Ground Treatment ASCE New Orleans, February 2003

Todd, D.K. (1960) "Ground Water Hydrology". John Wiley and Sons,

Weaver, K.D. (1991) "Dam foundation grouting". ASCE. New York

SOFT SOIL SITE CHARACTERISATION BY *IN SITU* TESTING

Allan McConnell
McConnell GeoServices (MGS) & Insitu Geotech Services (IGS), Brisbane, Qld

ABSTRACT

The most commonly used *in situ* testing tool in site characterisation, the SPT, is more than 100 years old. While it's still a useful tool for many purposes there have been significant advances in technology over those 100 years, including advances in the tools that can be used for geotechnical site characterisation. Some very useful tools have evolved.

This paper discusses some up-to-date methods of site characterisation, focusing on those up-to-date tools that are now available in Australia and some that will be arriving soon. The paper also provides beginners-level guidance on "where to go" regarding interpretation of data that comes from these tools.

1 INTRODUCTION

Site characterisation is the most important step towards the design or construction of any geotechnical project. In the author's opinion it is also the step that has highest potential to be poorly done and, if poorly done, it makes the whole of the rest of the processes of analysis, design, documentation and tendering dubious.

Sophisticated analytical tools exist and are used by geotechnical engineers on a day-to-day basis, but these tools are only as good as the data that is input to them. This paper is about:

- Improving the data we input into soft soil geotechnical models.
- Reducing our reliance on field interpretations that are open to error, such as borehole logging from drill wash, cuttings and spaced-out samples.
- Markedly speeding-up the process of site characterisation and getting better site coverage.
- Improving the quality of life of the young geotechnical professionals who usually get the job of supervision of field testing work.

All of which are related to *in situ* testing in one way or another.

2 *IN SITU* TESTING – A BRIEF HISTORY AND OVERVIEW

2.1 THE STANDARD PENETRATION TEST (SPT)

The most commonly used in situ testing tool in site characterisation, the Standard Penetration Test (SPT), is more than 100 years old. It was invented by the Raymond Piling Company around 1903 to provide a tool that could be used to help predict the depth of their piles. It is a very simple test that we all know well; a thick-walled sampler of set proportions is driven into the soil from the bottom of a borehole using a hammer of set proportions. It is not intended to discuss this tool to any extent within this paper other than to say here that the author believes:

- It will be around for a long time yet and that it has legitimate application, particularly in probing very dense granular soils.
- It is used to interpret many soil parameters by correlation, some of which correlations are incongruous when one considers the actual process of the test (banging a sampler into the ground): strength, modulus, OCR, etc. In soft soils this is particularly incongruous, given that often the N-value from the test may be 0, 1 or 2.
- It is a remarkably un-repeatable and imprecise test when one compares tests by differing operators using differing rigs, rods and hammers (all "standard" and all meant to give the same result). Some comparative tests reported by Dr Paul W Mayne (Mayne 2004) are shown in Figure 1.
- It requires a drilling rig and must be supervised in the heat or cold or rain; it is expensive, noisy and uncomfortable to implement. Minor flaws in the drilling process can lead to major undetectable flaws in measured SPT N-Value.

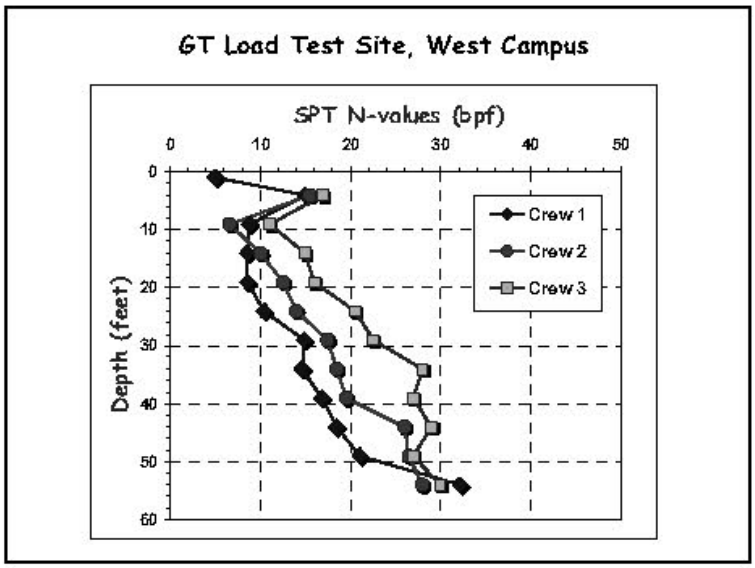

Figure 1: Comparison of SPT N-Values at a Test Site (Mayne 2004)

2.2 THE VANE SHEAR TEST

The vane shear test appears to have been invented in 1919 by John Olsson in Stockholm (Brand and Brenner, 1981). So it is almost as old as the SPT. However, while not new, vane shear testing will be promoted within this paper as this test varies from the SPT in that it does not try to be all things for all purposes, and because it is still a valid test for measuring clay shear strength, particularly the strength of soft clays, and because it has "evolved". It is a simple tool that is commonly cited by geotechnical engineers as being more-or-less "pure" in its measurement of shear strength of clay; it is often cited as the benchmark when comparing other methods to their correlations. However it is typically a clumsy and slow tool to use.

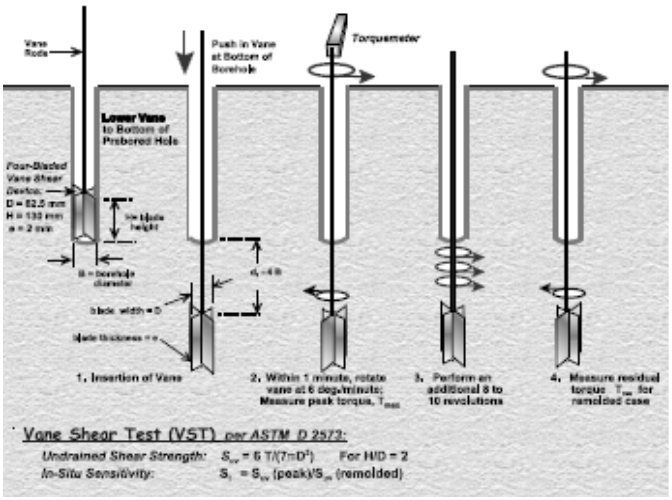

Figure 2a. Vane Shear Test Principles

Figure 2b. Geomil'sElectrical Vane

The CPT manufacturing company Geomil (Netherlands based) has recently made a significant advance in the evolution of the vane shear tool, developing a system intended to be pushed using a CPT rig, with inner torque rods protected against friction by the CPT rods as a casing. The system is fully automated and data logged and compensates for rod friction. Other similar systems exist and at least one specialist contractor in Australia offers vane shear at this time.

2.3 THE CONE PENETROMETER TEST (CPT)

Various forms of penetration tests have been around for a long time, one of the earliest being a reported 12 m steel rod pushed into the ground in Norway in 1736. The first description of a Dutch Cone Penetrometer (forerunner of the modern CPT) appears to have been in 1936, and the general proportions of the current CPT applied at that time (Brand and Brenner, 1981).

This first simple Dutch Cone Penetrometer has gradually evolved into the current CPT which is usually fitted these days with sensitive electronic load cells and often with a piezometer to measure pore pressure at the cone tip. As far as the author can ascertain the first electric cone penetrometer was introduced in 1948 but this technology did not come into use until the late 1960s (Meigh, 1987). The piezo-cone (CPTu) started to evolve in the early 1970s but, in the author's experience, has only really become a commercially useful and readily available tool in Australia during the last 10 years or so.

It is the author's view that the piezo-cone (CPTu) is one of the most valuable advances in characterisation of soft soil sites. It certainly replaces the SPT in terms of quality and repeatability of data, and it is now commercially available on a day-to-day basis. It is currently clearly the best tool available for developing a profile of site conditions but, because of its availability, it is at risk of also replacing the SPT as the "all things for all parameters" tool. The author believes that the geotechnical community should take care that this wonderful tool, with its many correlations against many parameters, does not become degraded by over-reliance. There are some tools that can perform some tasks better, or in concert with the CPTu.

Figure 3a. IGS 20t All-Terrain Test Rig

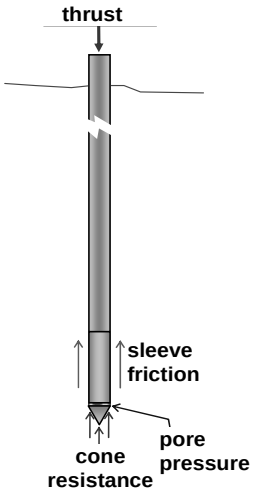

Figure 3b. CPTu – General Principles

The CPT "format" has become the vehicle for a number of other useful tools that can sometimes be used in conjunction with the CPT or sometimes are simply pushed into the ground using the CPT's rods and pushing system. These include: seismic cone (fitted with a geophone behind the usual CPT device); video cone (you can look at the soil, see some grain sizes and observe colour changes and other things); moisture content cone (self-explanatory); a range of "enviro cones" such as: pH and Redox Potential; Hydrocarbon Fluorescence; Electrical Conductivity, Magnetometer (useful for unexploded ordinance); Hydraulic Conductivity; etc.

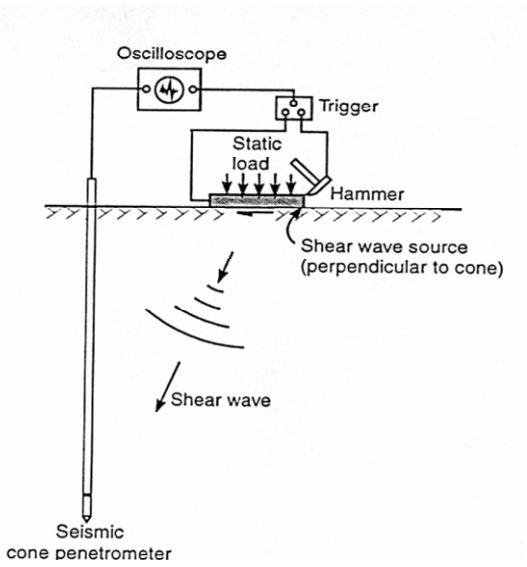

Figure 4a. Seismic CPT

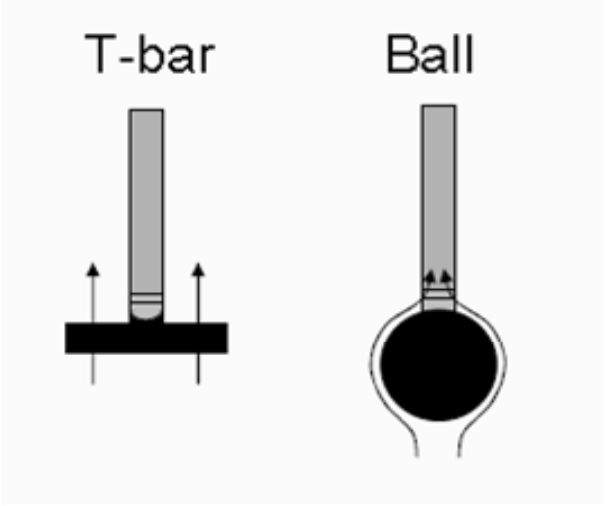

Figure 4b. T-bar and Ball Penetrometer s

So, the CPT has been around for 60 years or so – hardly new in concept – but has recently evolved into a very powerful site characterisation tool in the form of the CPTu and has in the last few years become readily available to geotechnical engineers for day-to-day use in Australia. Figure 3a shows IGS's 20 t capacity test rig. The author is a director of IGS.

A soft criticism of the CPT or CPTu is that it relies on factors or correlations for determination of soil properties and that some of these cannot be verified analytically. One recent evolution to overcome this criticism as it applies to measuring strength of very soft soils is the "flow penetrometer" that has two main types – a Ball Penetrometer (a ball of relatively large diameter replaces the usual conical tip) and a T-Bar Penetrometer (where a horizontal steel bar about 150 mm or 250 mm long x 40 mm diameter replaces the tip). The author anticipates that these two innovations, both being researched in Australia and internationally, will soon be available from at least some specialist contractors.

Figure 5a. NewSyd CPT Truck

Figure 5b. Lankelma (UK) Subsea Crawler (working in surf zone)

Figure 6a. CPTS Truck Rig

Figure 6b. CPTS Tracked Rig

2.4 THE FLAT DILATOMETER TEST (DMT)

The DMT is a type of simplified, low-cost, highly efficient, very robust, push-in pressuremeter, that is well-suited to use in characterisation of soft soil sites (and other sites). It can be pushed into the ground by a CPT rig or alternatively by a drilling rig, by pushing below the base of a borehole. The test principles are shown in Figures 7a & 7b.

The DMT was introduced to geotechnical engineering via a paper by its creator Professor Silvano Marchetti in 1980 (Marchetti, 1980). In 1986, under Dr John Schmertmann's chairmanship, an ASTM subcommittee developed a "Suggested Methodology" and in 1997 and 2001 Eurocode 7 and ASTM published standards for the test procedure.

The DMT is thus a more recent development than any of the preceding discussed *in situ* test methods, but it is still more than 20 years old and has certainly been in use commercially for 20 years.

There have been two international conferences that focused specifically on the DMT. The most recent of these was in Washington DC, earlier this year (April 2006) and was attended by the author who has a great interest in this tool and its evolution. At this conference Professor Marchetti released the first commercial Seismic DMT (SDMT, See Figure 8). This new tool is fitted with two geophones above the DMT testing blade and the author can announce here that this new site characterisation tool will become commercially available for day-to-day use in Australia in the very near future (possibly before the date of this symposium).

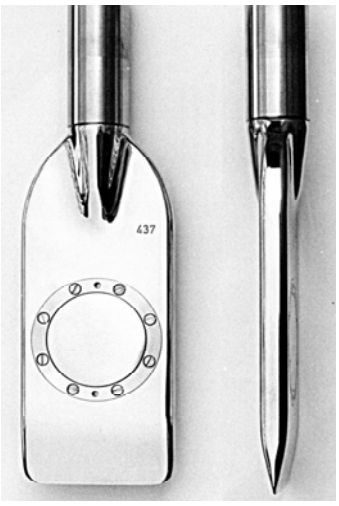

Figure 7a. DMT Blade Showing Diaphragm

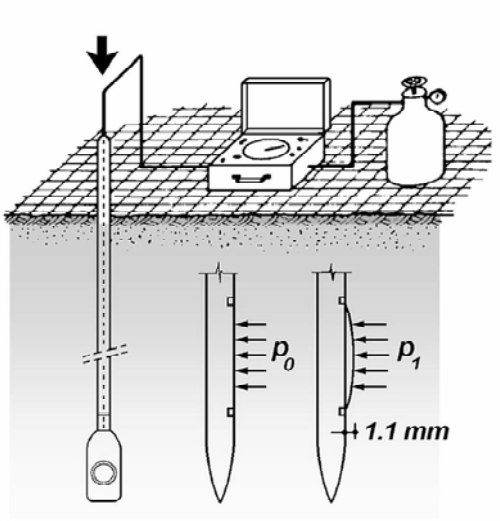

Figure 7b . DMT Operating Principle

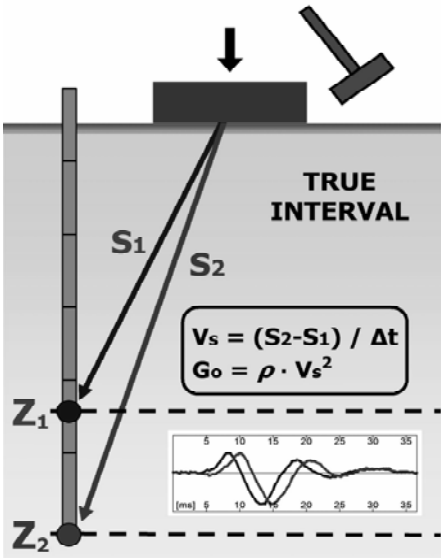

Figure 8a. SDMT Principles

Figure 8b. The Author With Dr Paul Mayne Inspecting SDMT No 1 (Washington 2006)

3 WHY USE *IN SITU* TESTS? - WHAT'S IN IT FOR YOU?

3.1 TIME & COST SAVINGS AND/OR BETTER SITE COVERAGE

Compared to the alternative approach to site investigation, boreholes, sampling and laboratory testing, the *in situ* tests that are discussed in this paper offer any or all of the following:

(a) The process overall is significantly quicker. Usually *in situ* tests provide a test data sheet or report more-or-less immediately they are completed, whereas a borehole takes much time and samples taken are typically sorted then chosen for laboratory testing that can take days and sometimes weeks.

(b) The daily cost of a field team undertaking *in situ* tests is about the same as the cost of a drilling rig and crew. However test productivity is usually much higher. Typically a well-organised CPTu testing rig and team can accomplish around 100-150 m of site testing per day (e.g. 6 x 20 m tests), which is about 4-5 times faster than a usual careful geotechnical drilling operation. Thus the cost per test is much lower.

(c) The corollary to (b) is that it has become possible to plan for much better site coverage using *in situ* testing than would normally be accomplished by drilling and sampling. In about the same time, for about the same budget, 4-5 times more tests can be done. A common approach is to "grid" a site with CPTu tests, then to choose just one or

two locations to drill boreholes, whereas past practice would have been a few more boreholes, but nowhere near as many as will now be tested by CPTu.

3.2 MORE PRECISE PROFILING

Using CPTu, site profiling is now very precise. The CPTu test equipment typically "samples" ground conditions each 20 mm vertically, allowing delineation of thin strata and precise determination of depths at which strata change.

With boreholes, samples can be taken as frequently as decided; however usual practise is to take SPTs or sometimes undisturbed samples at 1.5 m intervals and rely on the supervisor's impressions and interpretations of stratum changes that might occur between these test intervals.

It is common to find, where CPTu and boreholes are made adjacent to each other, that the borehole might have completely missed some thinly bedded strata and also that stratum change levels have been misinterpreted.

Following on from the strategy mentioned in Section 3.1(c), boreholes can be very strategically used if drilled after CPTu tests. Sample and test types and depths can be pre-decided based on the CPTu data and thus less sampling is needed and sample usefulness can be maximised.

3.3 BETTER DATA?

The author does not represent that in all cases and for all purposes *in situ* testing will be technically better than some other form of site investigation. The author acknowledges that it is "horses for courses":

- There are some situations where samples must be taken and laboratory tests must be made to achieve certain results. One case is secondary consolidation characteristics of soft clays; no *in situ* test that the author knows can measure C_{α}. Neither can any normal *in situ* test penetrate into bedrock and sample it for its engineering properties. Nor can normal *in situ* tests quantify soil plasticity or shrink-swell potential.
- However for a high percentage of sites and ground conditions there is a valid argument that *in situ* tests will probably provide better data than drilling and sampling can and, as described above, if drilling and sampling is needed for some reason (even just for confirmation), then at least the locations and numbers of boreholes and samples can be reduced.
- There will always be debate about the correlation factors to apply to *in situ* test values to convert these values to geotechnical design parameters. But frankly the same debate occurs in regard to laboratory measured soil properties. A mature view is that almost all geotechnical tests yield "index" parameters that must be used with intelligence and with the wisdom of experience. It is the same with *in situ* tests as it is with other methods; the difference is that with *in situ* tests you usually have more precise data and very much more of it to consider.

Certainly one can be confident of the following from *in situ* testing (focusing on soft soil sites):

- Site profiling will be very much better due to almost continuous "sampling" from CPTu testing (see example plot in Figure 9). Also due to the likelihood of better site coverage associated with lower cost.
- Knowledge of the *in situ* strength of soft soils will be much better, particularly when comparing *in situ* test methods with SPTs. An SPT N-Value of zero could mean a shear strength anywhere between 1 kPa and (say) 15 kPa; a CPTu will define this much better even using correlations, and an *in situ* vane shear will quantify it very precisely.
- CPTu equipment can be used to measure *in situ* permeability of low permeability soils by Pore Pressure Dissipation testing (the CPTu advance is halted and the rate of pore pressure decay is monitored). While debate could easily apply to the precision of such tests they must be more meaningful than laboratory tests on tiny samples, as they take into some account the influence of structure in the soil such as thin sandy lenses.

To conclude this section the author advises that his experience-based opinion is that, while nothing is perfect, *in situ* testing is in many ways more perfect than other methods at measuring the properties of soft soils.

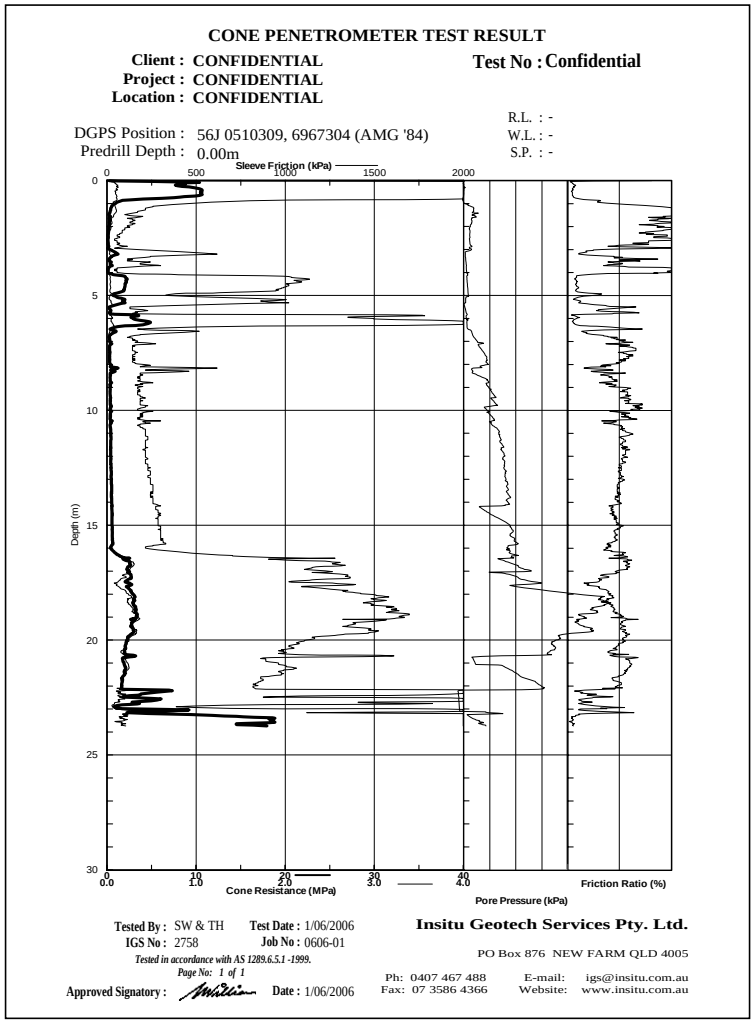

Figure 9. Example of CPTu Plot – Demonstrating Precise Profiling

4 SO - ARE THESE TESTS AVAILABLE LOCALLY?

A number of geotechnical consultants have *in situ* testing tools of their own, in-house. For instance the author is aware that CPT and CPTu have been used by several of the leading consultants since well before these tests were available from specialist contractors. The same applies to vane shear, in many differing forms (because of its misleading simplicity), and at least one consultant has had DMT for quite some years.

What has happened is that a few specialist geotechnical contractors have learned from the consultants and purchased equipment, set up testing systems and now offer these services to all who want to use them. It is the author's opinion that, on the whole, this is a better solution for the industry, as consultants usually don't seem to like to own costly equipment that requires maintenance and calibration, and certainly they don't seem to like to own very costly, heavy and complex testing vehicles.

Table 1 lists specialist *in situ* geotechnical testing contractors on the east coast of Australia that are known to the author, along with a list of the *in situ* tests that they offer to the marketplace.

Table 1: Geotechnical Contractors and *in situ* test methods offered.

Company & Base	**In Situ Tests Offered**	**Comment**
GeoPave, Melbourne	CPT, CPTu, DMT	Division of VicRoads, truck rig
NewSyd, Newcastle (research & contracting)	CPT, CPTu, Seismic CPT, Conductivity Cone	Collaboration between University of Newcastle and Sydney University, truck rig
Insitu Geotech Services (IGS), Brisbane	CPT, CPTu, DMT, Vane Shear (2006), Seismic DMT (2006)	All-terrain balloon tyred testing machine
Cone Penetration Testing Services (CPTS), Brisbane	CPT, CPTu, Seismic CPT, Vane Shear	Truck rig and all-terrain track rig

5 CHARACTERISING A SOFT SOIL SITE

It is this author's view that the most rational and solution-focused approach to characterising a soft soil site is as follows:

Step 1:	Undertake a grid or pattern of CPTu testing to profile the site and determine any patterns to soil variability. Often this may be enough; data from CPTu testing is commonly used by correlation to determine relevant soil properties; strength (C_u or ∅), compressibility (M, M_v, or E), permeability (k or C_v).
Step 2:	If compressibility is critical, particularly in soft-firm clays or in sands, undertake DMT profiles at selected locations, based on the CPTu data. Seismic CPT and Seismic DMT can be introduced to enhance compressibility data, or (particularly) if liquefaction is deemed a potential issue, or if cyclic loads will apply. If consolidation time is important, undertake some pore pressure dissipation tests using the CPTu, at selected locations. If possible make these tests long enough to measure t_{50} at least. Overnight testing is possible. In very soft to firm clays, if shear strength is critical, undertake vane shear profiles at selected locations. Note that vane shear testing can be misleading in fibrous soils (eg peaty stuff) or soils with shells or significant granular content.
Step 3:	Consider the data. If sampling and laboratory testing is still necessary (which may sometimes be the case), then select one or two locations based on the CPTu data, and undertake sampled boreholes. Use the CPTu data to pre-determine stratum boundaries and sampling depths and types. Note that some of the *in situ* testing contractors also have push samplers that can take useful samples in some conditions.

The above site characterisation process is not only possible, it is rational, best-for-project and very cost-efficient. Any one of the specialist contractors listed above can provide a range of the test methods needed.

6 INTERPRETING THE *IN SITU* TEST DATA

Most up-to-date geotechnical texts have valuable information on interpretation of *in situ* test data. For a sound starting point, the author recommends the following sources:

Cone Penetration Testing	Lunne Robertson & Powell (1997)
Geotechnical and Geophysical Site Characterisation	Proceedings ISC'2 (2004)
Flat Dilatometer Testing	Proceedings of 2nd International Conference on the Flat Dilatometer (2006)
Professor Marchetti's Web Site (DMT Papers)	www.marchetti-dmt.it/

7 REFERENCES

Brand, W. and Brenner, P (1981). Soft Clay Engineering. Developments in Geotechnical Engineering 20. Elsevier Scientific Publishing Company.

Failmezger, R.A. and Anderson, J.B. (2006). Flat Dilatometer Testing. Proceedings from the Second International Conference on the Flat Dilatometer, Washington DC.

Lunne, T., Robertson, P.K. and Powell, J.J.M. (1997). Cone Penetration Testing In Geotechnical Practice. E & F N Spon.

Marchetti, S. (1980). In Situ Tests by Flat Plate Dilatometer. ASCE Journal GED, Volume 106, No. GT3, March, 299-321.

Marchetti, S. and Monaco, P. (2001). Short Course on Flat Dilatometer. International Conference on In Situ Measurement of Soil Properties and Case Histories. Bali.

Marchetti, S. (2006) Web Site Containing Many Papers on DMT. www.marchetti-dmt.it

Mayne, P.W. (2004). Geotechnical Site Characterisation By Enhanced In Situ Testing. Short Course. The University of Sydney Centre For Geotechnical Research.

Meigh, A.C. (1987). The Cone penetration Test – Methods and Interpretation. CIRIA Ground engineering Report: In-situ Testing. Butterworths.

Trevor, F.A. and Mayne, P.W. (2004). Undrained Shear Strength and OCR of Marine Clays From Piezocone Test Results. Proc. ISC'2 Oporto. Geotechnical and Geophysical Site Characterisation. Millpress.

DEEP EXCAVATIONS IN SOFT GROUND USING TEMPORARY STRUCTURAL STEELWORK

Christopher Daniel
Parsons Brinckerhoff

ABSTRACT

In many city areas, ground anchors and soil nails cannot be used for deep excavation retention in soft ground for various reasons. The solution is often braced excavations involving temporary structural steelwork, serving multiple functions, like strutting, waling, lagging, traffic and construction decking. Based on the author's design and supervision experience on underground metro station, rail, expressway and commercial mall projects, this paper discusses the design, construction and monitoring of steelwork applications in deep excavation environments.

1 INTRODUCTION

Deep excavations in cities are often constrained by physical and statutory limitations which restrict the use of ground anchors and soil nails. Examples include:

a. Deep excavations adjacent to existing structures like basements, foundations, or tunnels;
b. Underground structures having statutory reserves surrounding them, within which works are either forbidden or permitted under rigorous constraints and
c. Land acts, building or environmental statutes forbidding the installation of temporary works under or at the perimeter of adjacent properties, when these cannot be reliably, safely and completely removed later. Where safe removal techniques exist, their cost and program implications may be prohibitive.

Temporary structural steelwork avoids these limitations and fulfils other roles. These include:

a. Traffic decking for bottom-up and top-down construction methods, maintaining traffic flows and facilitating deep excavation approvals;
b. Lagging at gaps in walls for underground services;
c. Utility support frames, avoiding expensive and time-consuming utility diversions;
d. Construction platforms over excavations, expediting construction work and top-down construction;
e. Flexibility in changing traffic decking openings - expediting excavation and concreting;
f. Cost-effectiveness due to steelwork's capacity for multiple reuse, cutting/welding to suit and modifications;
g. Its ductility enabling visual monitoring, forewarning overloading and verification of instrumentation readings and
h. Its flexibility to be locally strengthened on an *ad hoc* basis – critical to handling ground conditions found more severe than at the design stages and if an observational approach is adopted.

2 TYPICAL STRUCTURAL ELEMENTS

Typical steelwork elements are schematically shown in Figure 1:

a. Walls are braced by steel struts and walers. S2 and W2 denote second layer struts and walers respectively;
b. Struts and walers are restrained against buckling by bracing systems involving the vertical H piles or kingposts (KPs) and other steelwork;
c. KPs transmit vertical loads from decking to the ground below formation level;
d. Struts and walers are structural steel beam and column sections (Figure 2), their major axes oriented in the respective principal loading directions;
e. Struts and walers may be single beams (Figure 2), battened double beams (Figure 3) or laced beam girders (Figure 4);
f. Decking may cover any required proportion of the excavation area. Figure 1 shows a half cover, but full cover is possible, with openings at strategic locations to facilitate mucking out and concreting;

g. The vertical load path is: deck → S1→ longitudinal beams → KPs → ground;

h. The transverse load path is: deck → S1→ walls;

i. Struts are often preloaded. Preloading effectively 'pushes' walls into the soil, by axially compressing the struts. It is done at strut installation at each level, when the excavated ground is at strut soffit, to reduce wall deflections and ground movements;

j. Utilities like the 66 kV cable shown are suspended within the excavation and

k. Traffic decking elements (Figure 5) comprise steel beams welded together to increase bending and shear resistances. Their spans govern S1 spacing ('2000 c/c' in Figure 1).

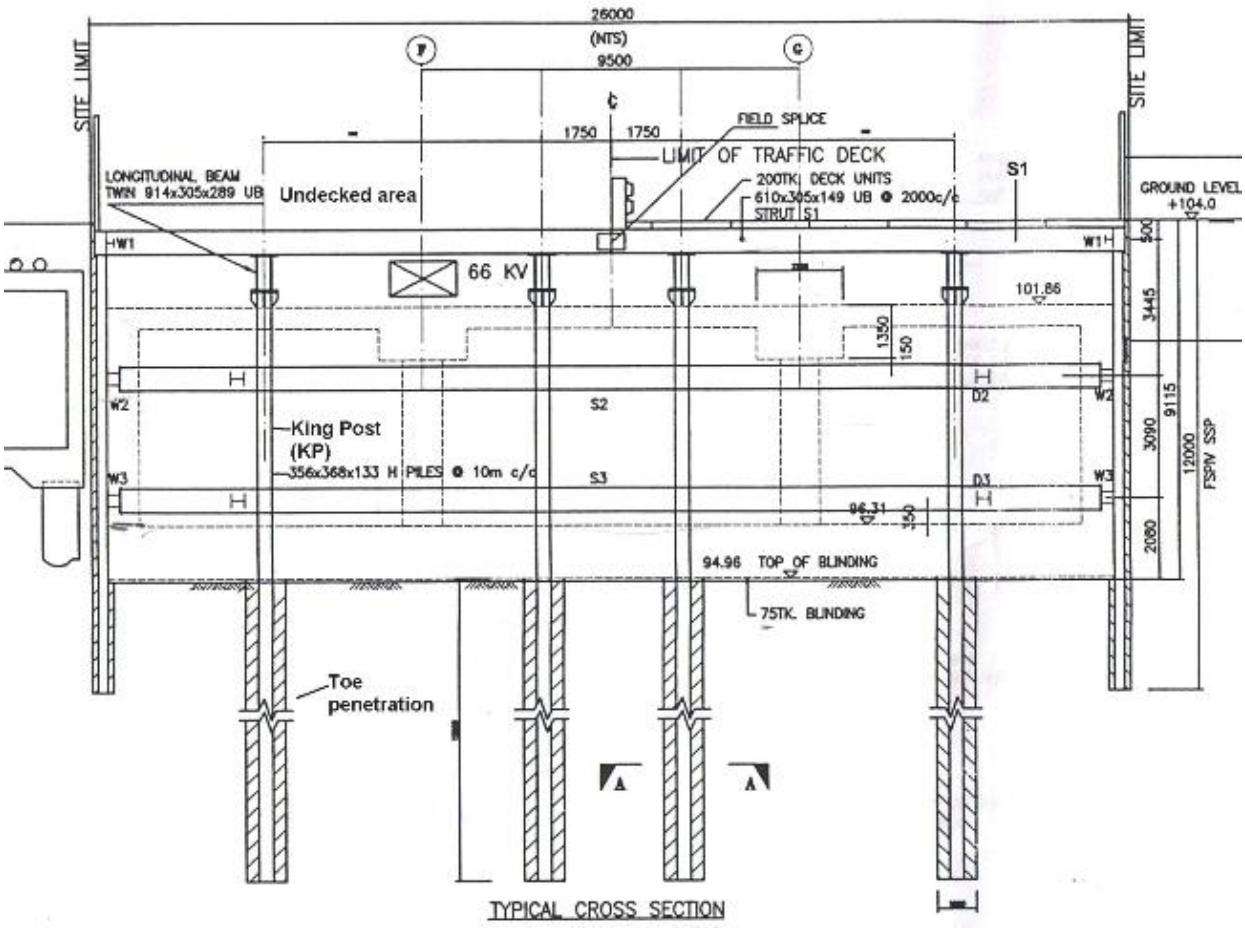

Figure 1: Typical section characteristics.

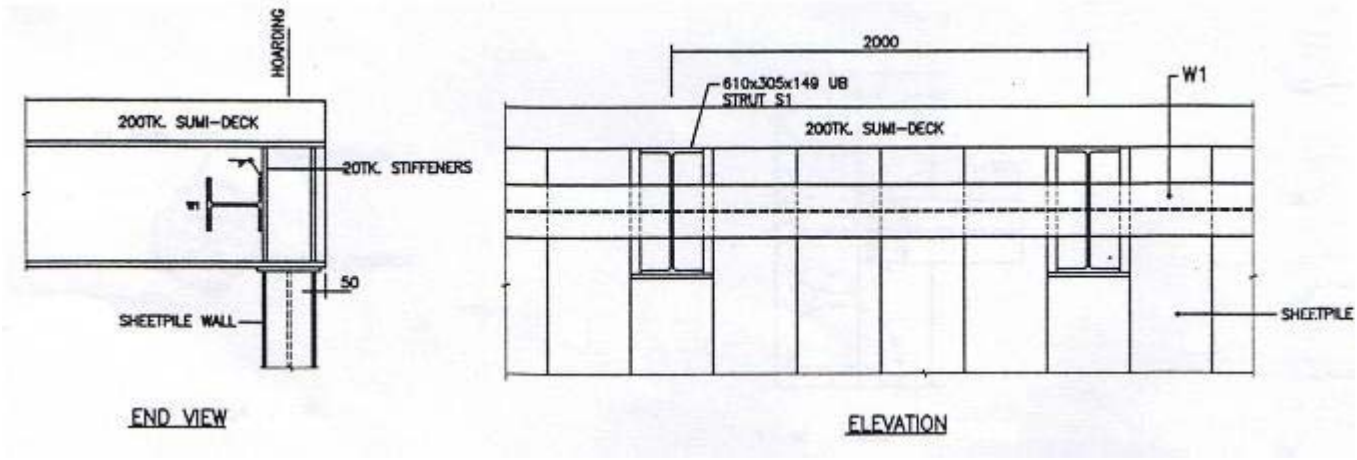

Figure 2: Typical strut/waler sections and orientations.

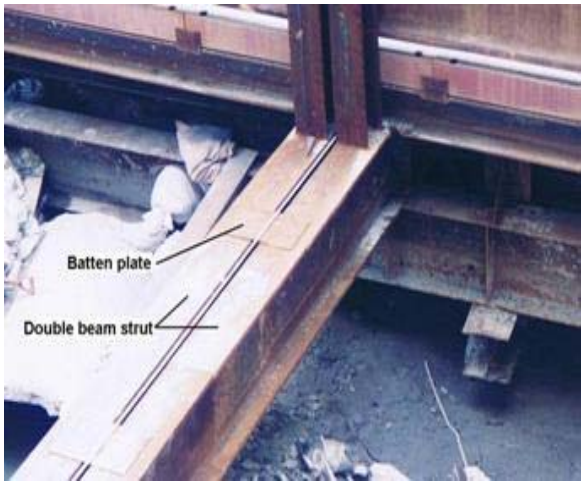

Figure 3: Battened double beams.

Figure 4: Laced beam girder struts.

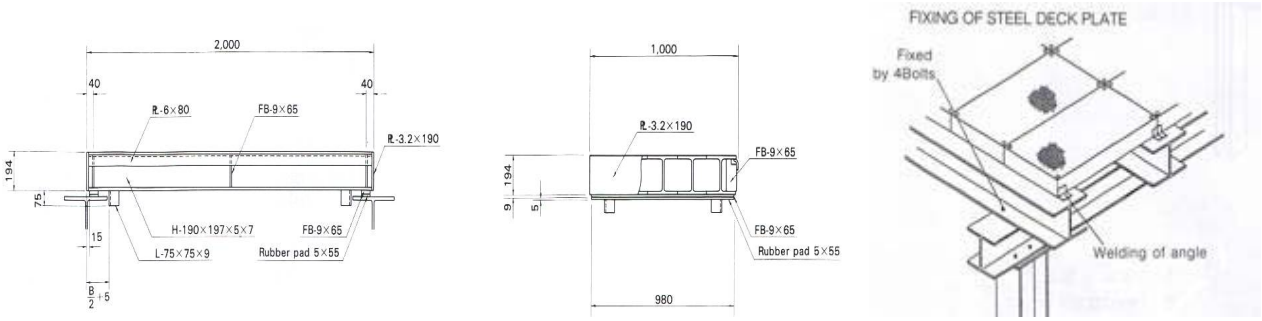

Figure 5: Typical steel decking elevation (L), end view (C) and installed (R) (Hirose, c.1996).

3 CONSTRUCTION ASPECTS

a. Before design, constructors must first plan steelwork areas, extents and timings. Planning starts with land parcel boundary lines, existing feature and utility locations (Figure 6a). The author suggests the principal drivers are minimising utility relocations, phased traffic management and section hand-over dates (to and from clients);

b. Struts, sheet piles and KPs are then initially-positioned (Figure 6b). Positioning is iterative as it affects the loads applied to the steel elements, and element capacities vary according to section size selection;

c. Decking construction is done in sections to limit traffic disturbance. In Figure 1, excavation and steelwork are done for half the section width, which is subsequently opened to traffic. The other half is then worked on (note Undecked Area shown). Figures 7 and 8 clarify;

d. For sheet pile hammers, driveability data should exist, often correlated to SPT N values. Reference should be made to geotechnical investigation data, to determine if sheet piling appears feasible to at least 4 m below formation level (author's typical toe penetration initial estimate);

e. To extend to full depth, sheet piles are welded together using full butt or fillet welds with splice plates (Figure 7) via manual electric arc welding. These welds resist earth pressures in shear and bending. Newly-formed welds require cooling times of about 45 minutes and affect driving times;

f. Where sheet piles attain refusal above final formation level, the down-the-hole hammer is effective in breaking up isolated obstructions, if noise pollution is not an issue. Other solutions are partial preboring (Figure 8), and 'berm-and-lag' (author's term – see g). Preboring at intervals enables sheet piles or box sections to attain design penetration below formation level at those intervals. This prebore is grouted with a weak mix to enable sheet piling later. Outside of the prebored locations, sheet piles are driven to refusal;

g. In 'berm-and-lag', excavation proceeds after sheet piling regardless of the high sheet pile toes, leaving an earth berm at the problem location. The berm is then excavated, exposing the pile toes and standing soil faces, in safe stages. The gap is then lagged or shotcreted. Watertightness, lagging, berm slope and soil face stabilities need additional design and supervision work. Program impacts include delayed strutting and staged slab casting;

h. KPs' steel sections are inserted into prebored holes drilled from the surface (Figure 10c) and concreted up to formation level (Figure 1);

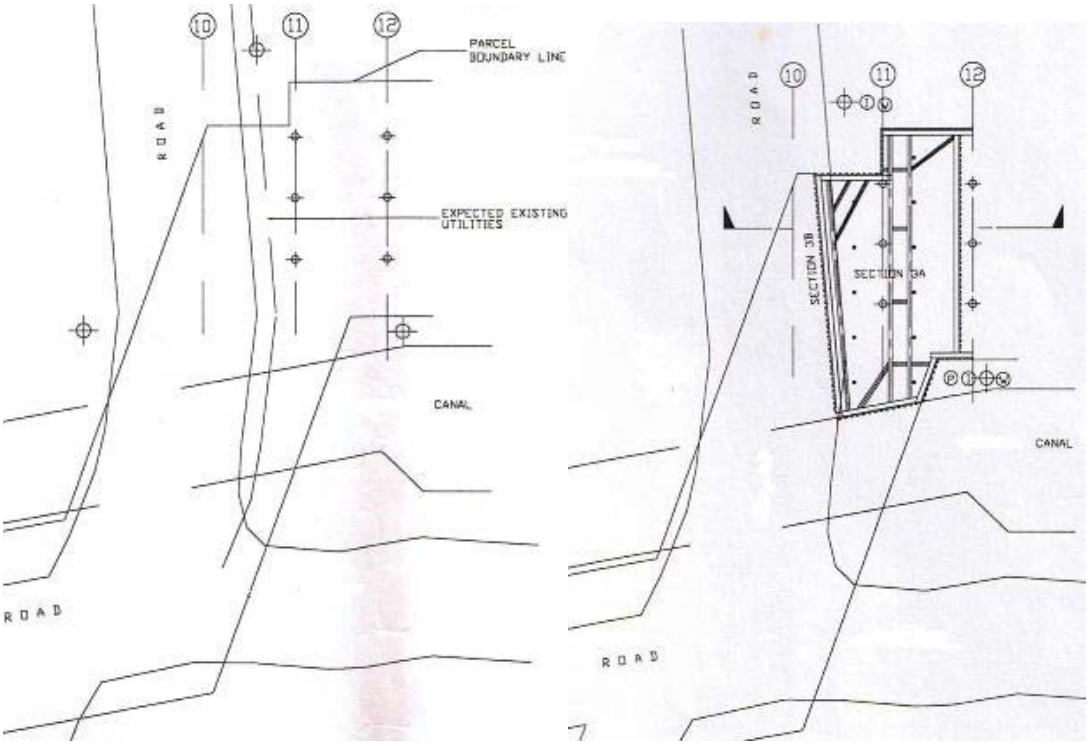

(a) (b)

Figure 6: (a) Existing features and land parcel line; (b) planned excavation steelwork (first phase)

Figure 7: Steelwork construction with traffic on the right.

Figure 8: Traffic switched to left after steelwork completion, work proceeds on right.

i. Temporary construction decking is installed in the undecked area of Figure 1 (Figure 11a). It is narrower than traffic decking to maximise open excavation and concreting access areas;

j. For bottom-up construction (Figure 1), the initial excavation is to S1 soffit level, S1 and W1 are installed and S1 preloaded. This is repeated at each level. After the lowest level strut is preloaded, the base slab and wall stumps to strut soffit (dotted) are cast (Figure 11b), then S3/W3 removed. Wall casting proceeds up to S2 soffit, followed by S2/W2 removal. Finally, the roof slab and roof-wall joints are cast (Figure 11c), and backfilling is done close to ground level. Steelwork is removed progressively. Traffic is then switched over to the left, and the same construction sequence proceeds on the right;

k. For top-down construction the permanent walls are installed first, from ground level. Traffic decking, S1/W1 and KP steelworks are installed halfway across, as for bottom-up. The other half is excavated to roof slab soffit level, and the roof is cast. Backfilling and half-road reinstatement may or may not take place above this slab, depending on whether the roof slab is designed to span wall to wall. If it is not, steel KPs may be installed before

slab casting, to support the roof during top-down excavation, until the required roof support walls are built bottom-up from lower floor slabs;

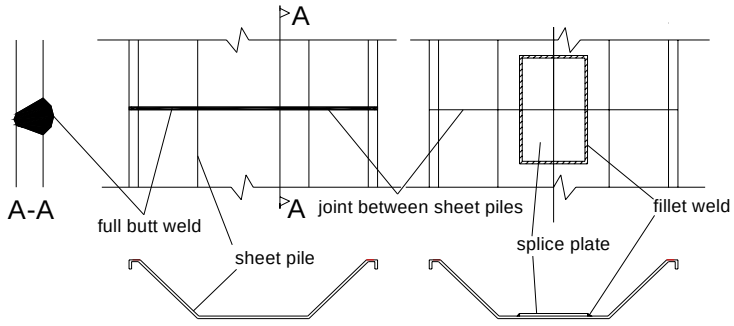

Figure 9: Full-butt weld sheet pile connection and fillet weld joint with splice plate.

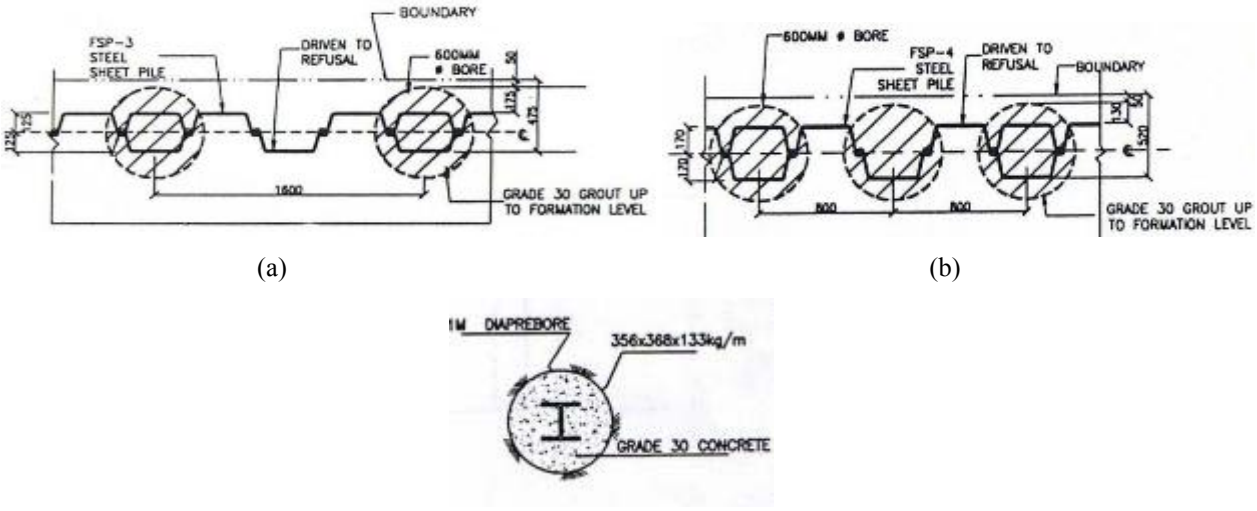

(a) (b)

(c)

Figure 10: Partial boring solutions – (a) preboring only for 1 in 4 'box' sections, (b) preboring for both alternate piles and 1 in 4 'box' sections, (c) KP toe section.

l. Figures 11 and 12 indicate the extent of transverse and longitudinal vertical cross bracings required for decking stability. There are also horizontal cross bracings not shown. Excavation and RC work methods/sequences need planning as bracings limit plant manoeuvrability and clearances. Usage of mini-excavators and skips is likely;

m. Struts in braced soft soil excavations are preloaded to limit wall deflection and ground movement. Hydraulic jacks are used to preload struts (Figure 13) to the design preload (often 30 to 50% of the design strut load) or design wall preload deflection. Note that preloading using in-strut jacks (as shown) is the more versatile of the two preloading methods generally used. The other uses jacks placed between struts and walers. In both cases, steel elements replace the jacks and enable jack removal after preloading. Preloading significantly increases construction time and strut loads;

n. The effects of temporary structural steelwork on permanent RC works must be considered. As per Figures 1, 11 and 12, steelwork penetrates RC elements during construction, but some elements cannot afford this intrusion for waterproofing or load-bearing reasons. Steelwork must then be positioned accordingly. Constructors should note the cost and program implications of rectification works to the RC elements after steelwork removal and

o. Steelwork and construction sequences affect each other. For example, in Figures 1 and 11, KPs function as piles and strut bracing until permanent roof slabs achieve their required strength. KPs are then cut between the roof soffit and top of base slab (Figure 11), to transfer their vertical loads to the roof slab. Backfilling and road reinstatement proceed after decking is gradually removed and KP lengths above roof slab are cut off. Short lengths of KPs remain within both roof and base slabs, for which rust proofing must be done. KP cutting and removal also affect roof slab waterproofing and structure internal works scheduling.

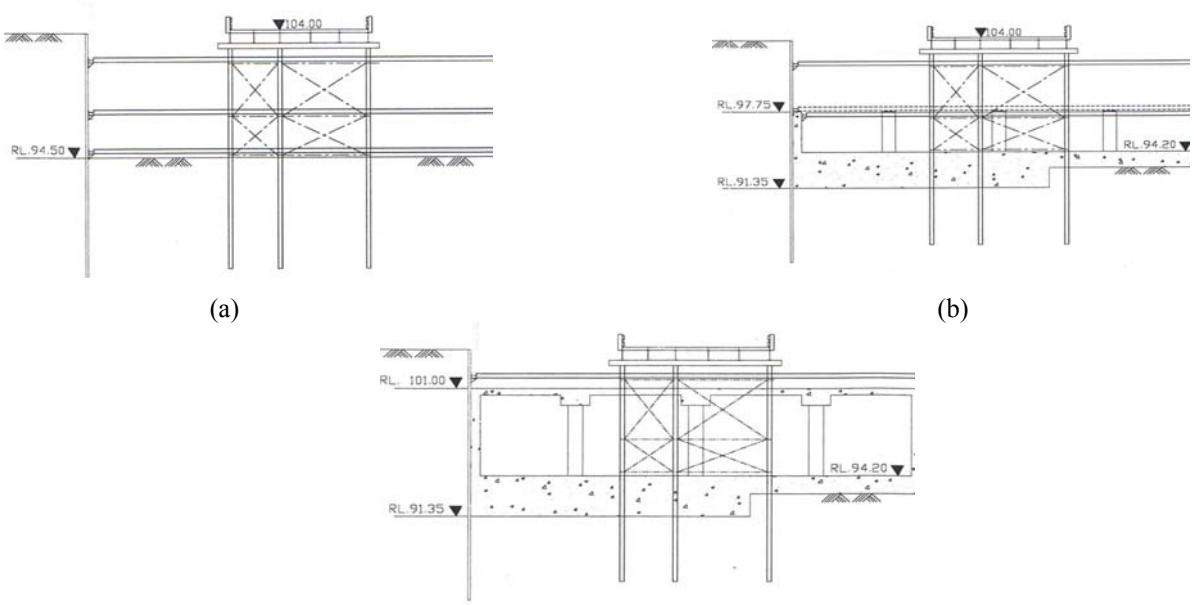

(a) (b)

(c)

Figure 11: Temporary construction decking and bottom-up sequence stages.

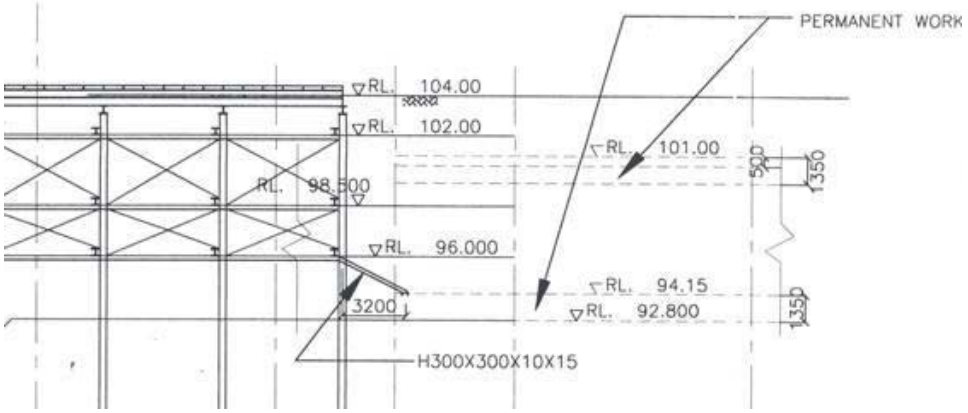

Figure 12: Construction decking longitudinal vertical cross bracing.

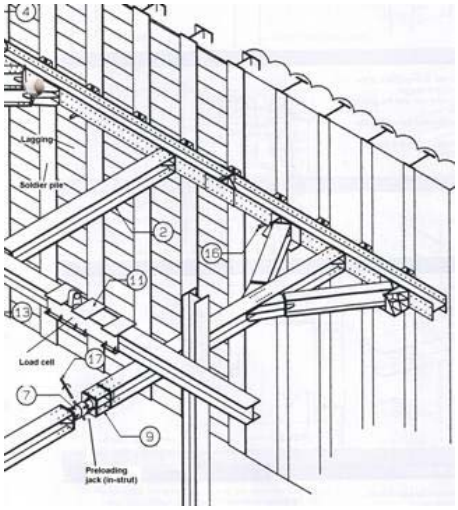

Figure 13: Preloading jack (in-strut), strut load cell (Hirose, c.1996).

4 DESIGN ASPECTS

4.1 LOADING AND SEEPAGE CALCULATIONS

a. Detailed understanding of the geology and groundwater conditions is critical. Design will normally utilise finite-element/finite-difference (FEM/FDM) software, for sensitivity analyses, ground movement, groundwater flow modelling and optimisation of strut spacings and wall type selection;

b. The appropriateness of software soil models and parameters should be understood. Program manuals may suggest non-typical parameter values to prevent ill-conditioning of the stiffness matrix and numerical problems. Examples include 'cohesion' for cohesionless soils, Poisson's ratio and permeabilities (Brinkgreve *et al.,* 2004);

c. The author recommends manual checking using Terzaghi *et al.* (1967), Peck (1969) or Xanthakos (1994) apparent earth pressure diagrams (including surcharge and water pressures). These provide trapezoidal pressure distributions for each brace level, to calculate moments and axial loads in elements. Clough *et al.* (1990), Mana *et al.* (1981) and Bowles (1996) suggest how to estimate ground movements and sheet pile deflections;

d. Similarly, seepage calculations using manual flow net calculations can verify seepage estimates, boiling and piping likelihoods;

e. Unplanned excavation (over-excavation) should be accounted for in the modelling, even if not specified in the appropriate code;

f. If using foreign specialist contractors, their steelwork design approaches must be reconciled with local standards;

g. Appropriate highway codes will supply traffic design loading information. Loads will often be functions of lane numbers and road geometry - hence, the significance of construction aspect 3a and

h. Construction decking load cases should include peak operational track pressures on decking elements and KPs.

4.2 WALLS

a. In wall modelling, the author suggests neglecting KPs due to their typically large spacings in both directions. Lee *et al.* (2003) conclude that, in soft ground, wall deflections would not be accurately predicted by incorporating KPs;

b. Borin (1996) suggests wall deflection reduction is not significant until strut preloading is dramatically increased, at which point the maximum strut loads have also jumped – preloading may not be particularly efficient and

c. The author recommends the highest level strut be placed within 2 m of ground level to limit maximum wall cantilever length and ground movement within tension crack zones.

4.3 STRUTS

a. The principal failure modes are shear, lateral torsional buckling, axial compressive buckling, local web and flange buckling and crushing in bearing;

b. To control lateral torsional buckling in struts, lateral restraints are provided. These need to resist a shear force proportional and transverse to the force in the strut. Lateral restraints are provided by a combination of KPs (vertical and horizontal support) and C-channels (horizontal shear force transmission). In Figure 12, the 'I' struts (projecting out of plane) are restrained at common points by KPs and three tiers of horizontal channels. Horizontally, these transmit restraint forces resulting from transversely restraining each strut;

c. These restraining forces are cumulative and require transmission to adequate anchorage points like walls. The author designed regularly-spaced 'towers' (Figure 14) for this purpose. Towers are completely cross-braced internally and externally, using channels. They collect and transmit restraining reactions from struts and KPs to the walls via cross-bracing. Traction and centrifugal loads from traffic decking are similarly transmitted;

d. With great excavation widths, struts often comprise two columns battened together (Figure 3) to increase axial stiffness and reduce slenderness ratios. Due to self-weight, struts are slightly predisposed to buckle in the vertical direction. Lateral restraint and vertical support are provided by the KPs via brackets (Figure 15);

e. Struts can be simply-supported or continuous beams atop KPs or their brackets, depending on specific location;

f. Note the usage of diagonal struts at corners (Figure 16). They differ from typical transverse struts only in the axial horizontal load component they transmit to walers;

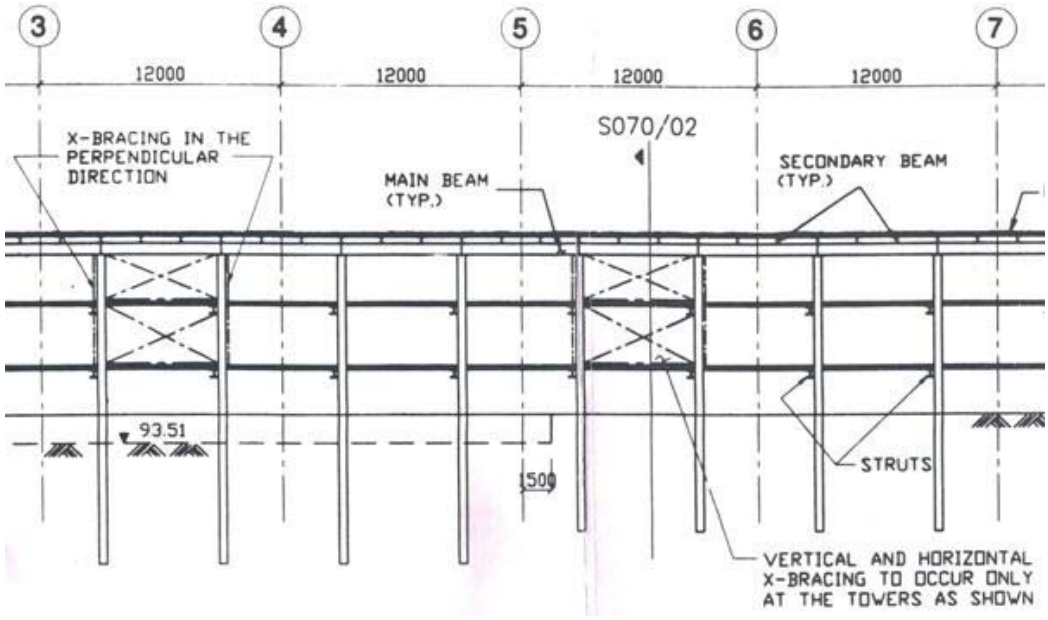

Figure 14: Longitudinal section showing towers to collect and transmit strut/KP restraint forces to walls.

g. Figure 16 displays the detail required at excavation junctions, and the impact of utilities on steelwork. Note the strut (1S3) strengthened with an additional beam and the additional diagonal struts (1DS4) and KP. All these are required to support the water main (Figure 17) and manhole (Figure 18). The cross beams serve three functions - propping the wall, splitting the manhole's load between the KP and the 1S3 and supporting traffic decking;

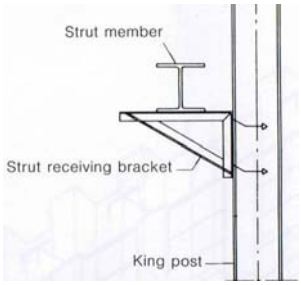

Figure 15: KP bracket (Hirose, c.1996).

h. Many top-down structures have large slab openings for escalators or architectural features. These slabs act as struts later, but these gaps impair this ability during construction. Temporary steel struts 'fill the void' and

i. Element design must include thermal effects. These generate additional strut axial forces and moments at KPs. For example, Ho *et al.* (1994) reported load variations in steel struts due to daily temperature changes of the order of 400 kN in a three-level excavation.

4.4 WALERS

a. Walers generally act only in bending. Effective lengths in buckling often need to be reduced by diagonal strut-waler connections as shown in Figure 13 and

b. Discontinuities in the linearity of the wall (Figure 16) produce axial forces in walers. Waler-wall connection design here should account for this.

4.5 LONGITUDINAL BEAMS

a. For design, primary and secondary longitudinal beams are assumed simply-supported due to varying KP positions. Rows of KPs are generally not straight throughout the excavation – refer to Sections 3a, 3b and 3n.

4.6 KINGPOSTS (KPS)

a. KP layout design is iterative and based on experience and output from Sections 3a, 3b and 3n. Tributary area loads are checked against section axial capacity, considering likely vertical unbraced lengths. The author suggests universal columns of 350 mm depth, 275 MPa steel grade, at 6 m spacings and 3-4 m unbraced length to start and

b. KPs are geotechnically designed as vertically and laterally-loaded piles and structurally as steel columns.

4.7 CONNECTIONS

a. All steelwork connections need rigorous design, with larger safety factors where connection is difficult, for example, overhead welds. Bolting and welding design calculations, particularly for eccentric loads like brackets (Figure 15) are critical.

4.8 UTILITIES AND UTILITY GAPS

a. Utility support loads affect all decking and wall elements. Figures 16 to 18 illustrate this and were discussed earlier;

b. Utility gaps often involve soldier piles to enable safe clearances on both sides of the utility. Soldier piles behave as vertical beams under shear forces from lagging element ends. Soldier pile-lagging wall sections are modelled by averaging the flexural rigidities of the pile and lagging sections, or manually designed as per Section 4c and

c. Lagging is generically represented in Figures 13 and 19. Elements can be sheeting, channels, angles or I-beams, and are designed as simply-supported beams resisting a tributary area of earth and hydrostatic pressures.

4.9 PLANNING CONSTRUCTION SEQUENCES

a. Bottom-up construction requires the progressive casting of wall sections to the soffits of struts, followed by strut removal. The newly-cast wall then behaves as a cantilever. Where slab-wall reinforcement design does not permit this, 'replacement struts' (author's term) are required. These could be typical horizontal struts similar to the ones removed, but their lengths complicate their eventual removal. The author has used inclined replacement struts as shown in Figure 16 to support cantilever walls off base slabs.

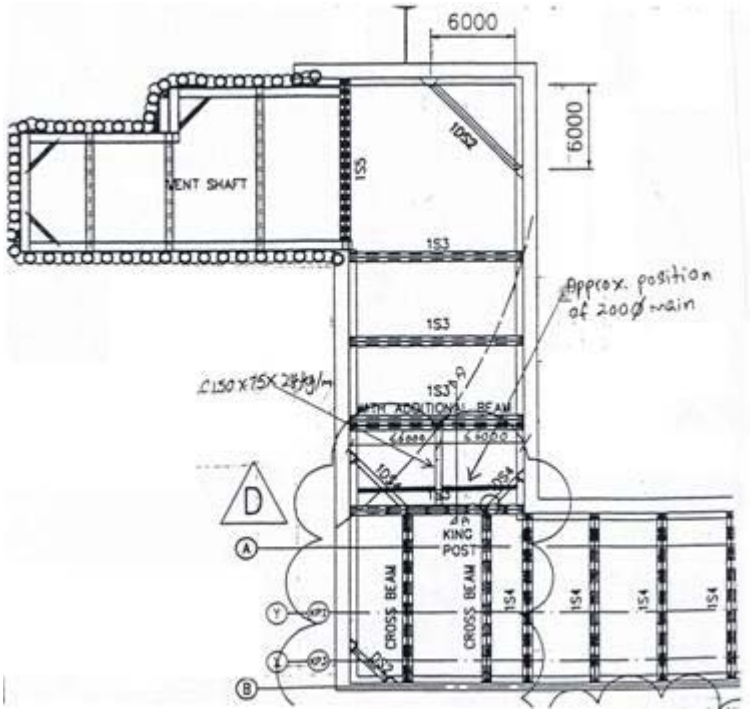

Figure 16: Corner struts, struts/KP supporting water main and manhole.

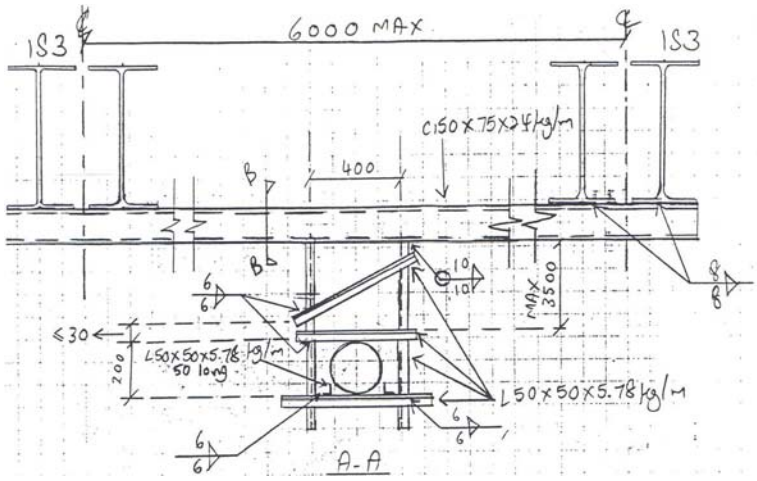

Figure 17: Typical utility support frame and connections.

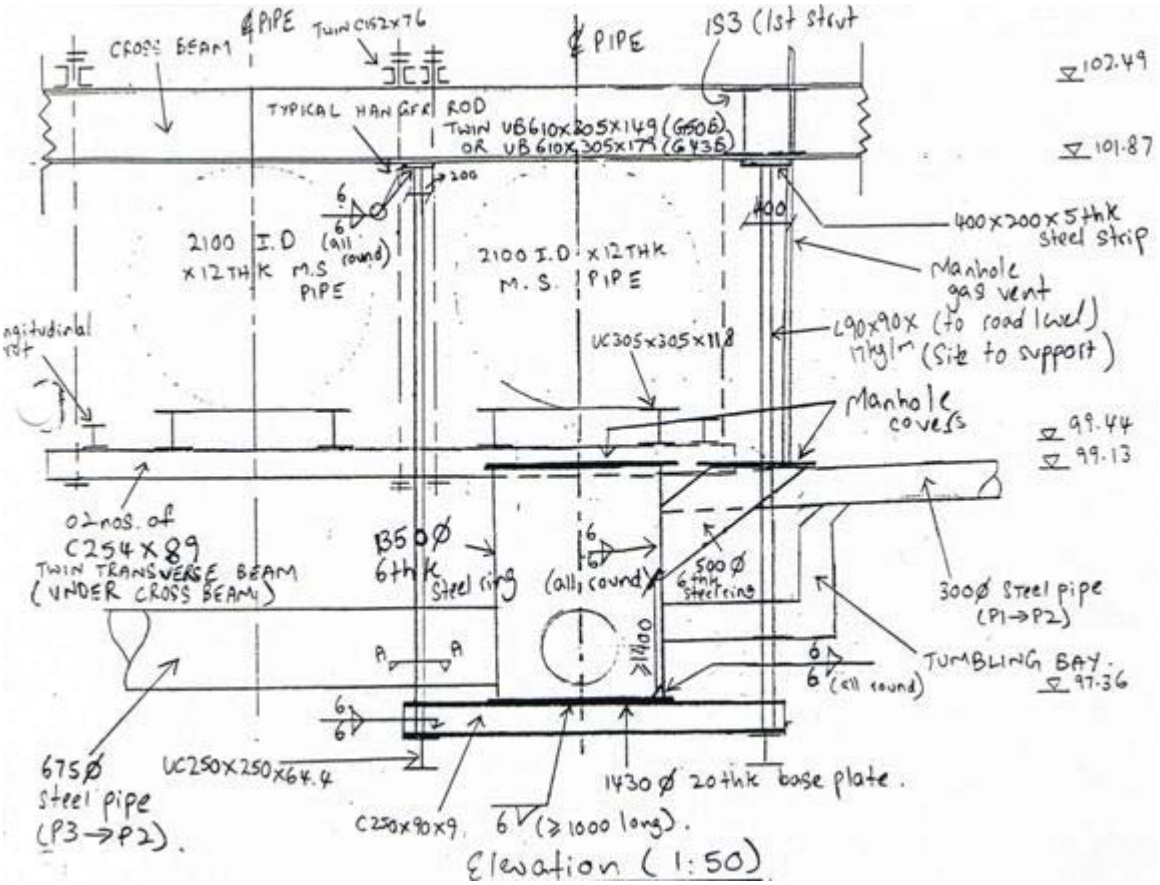

Figure 18: Manhole supported by same strut as water pipe (Figure 17) and cross beam (Figure 16).

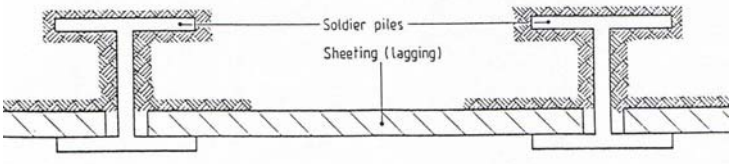

Figure 19: Schematic representation of soldier piles and lagging at utility gaps (BS 8002 : 1994).

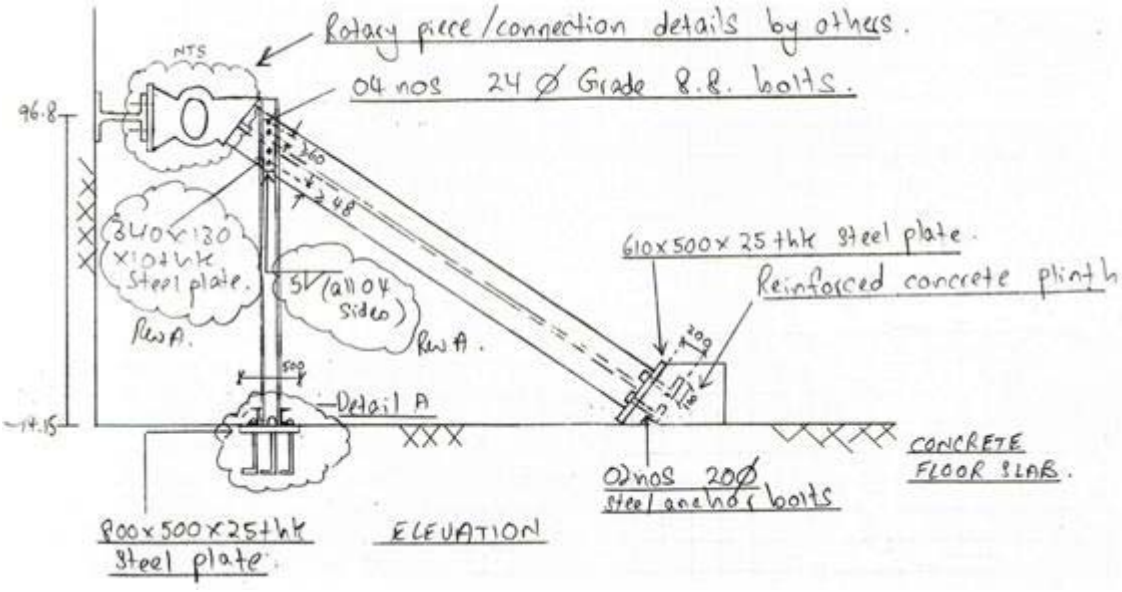

Figure 20: Inclined replacement strut to support RC cantilever walls during bottom-up construction.

4.10 AUTHOR'S STRUCTURAL STEELWORK DESIGN RECOMMENDATIONS

a. The author suggests maintaining excess capacities of 15% in each ultimate limit state (bending, shear and axial) and overall buckling/combined bending capacity checks. Site steelwork change requests by clients, utility/other authorities and constructors are unavoidable and often overstress lean elements. Strengthening incurs delays and costs and

b. Due to the large loads involved, the author suggests designers start sizing steelwork elements by considering connection requirements. Weld and bolt connection designs require minimum edge distances, parent metal and flange/web thicknesses, thereby often governing section size selection.

5 INSPECTION AND INSTRUMENTATION

The author strongly recommends that regular visual monitoring complements instrumentation monitoring. Designers should also prepare instrumentation arrays for constructors to install on site prior to excavation. These arrays capture ground movements, strut loads and wall deflections, at locations where design predictions exist. The instruments are settlement markers, load cells/strain gauges mounted in/on struts and inclinometers inserted in/behind/on walls respectively (Figure 21).

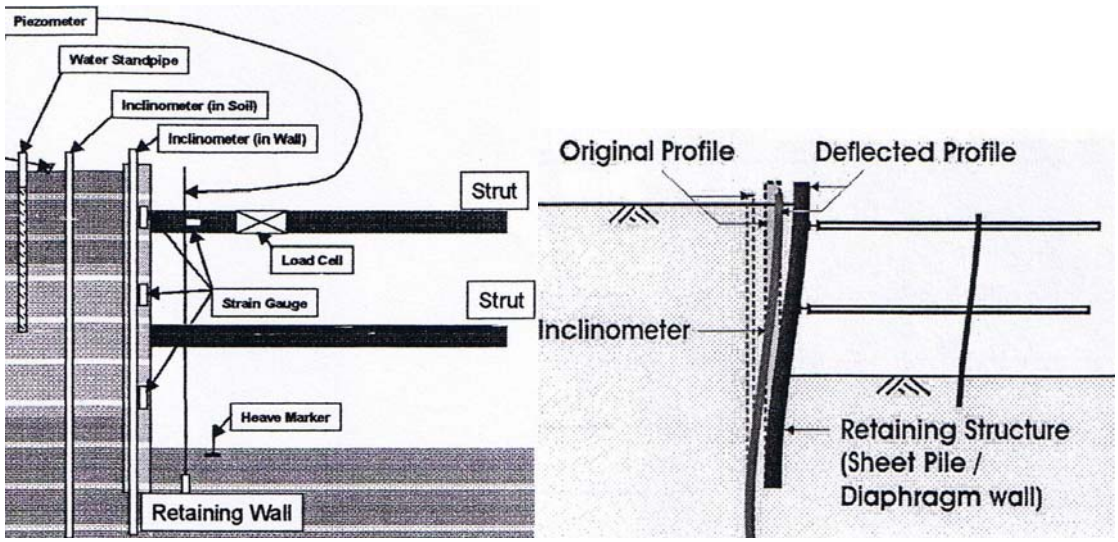

(a) (b)

Figure 21: Schematics of (a) instrumentation (Orihara, 2003) and (b) inclinometer (Ganeshan, 2003).

5.1 VISUAL INSPECTION CHECKLIST

a. Pre-existing adjacent ground and steelwork defects, to avoid undue alarm later;
b. Sheet pile deflections at the cantilever top and between strut levels, visibly in excess of those predicted;
c. Localised flange, web and lateral torsional buckling of bracing elements;
d. Coloured staining of steelwork inside the shaft signalling soil or groundwater ingresses;
e. Weeping along sheet piles and ponding on walers;
f. Cracking or subsidence in adjacent ground;
g. Surcharge from construction materials and equipment, obviously in excess of design assumptions and
h. Over-excavation (each stage).

5.2 GENERAL CHECKS

a. Steelwork inspections should verify that both sections and steel grades are as designed. Steel mill and heat test certificates should be available and
b. All elements should obviously be oriented (major axis) correctly.

5.3 STRUTS, WALERS, BRACING AND SHEET PILES

a. Visual inspections of struts, bracing and walers ensure buckling is not impending. This includes batten plates, lacing (Figure 3) and splice joints (Figure 9);
b. Baseline readings for strut strain gauges and load cells should be taken before preloading. This enables preload verification and correct axial load monitoring;
c. Connections need close inspection and testing at agreed frequencies and
d. Strut and waler installation should be done promptly.

5.4 STRUCTURAL INSTRUMENTATION (FIGURE 21)

a. Strain gauges enable axial load monitoring of struts – necessary at each stage. Peak loads are expected when excavation has been completed to the next strut level, just before its installation.

5.5 GEOTECHNICAL INSTRUMENTATION (FIGURE 21)

a. Inclinometers enable comparison between actual and predicted sheet pile deflection profiles. Biaxial movements should be indicated and the instrument should extend below formation level to the depth (predicted by design) where deflection is expected to cease and
b. Pneumatic and vibrating-wire piezometer readings indicate GWT variations via inferences from porewater pressure data. Drops in porewater pressure often herald impending settlement.

The author highlights the following pointers gleaned from multiple projects:

a. Attention should focus on trends rather than raw data value variations, because instruments, data processing, readers or other factors occasionally deliver unusual but isolated readings;
b. Current accredited and certified calibration of instruments provided by the equipment suppliers is critical;
c. Baseline readings for all instruments must be taken at the correct time - not always immediately after installation. Examples include recharge well activity masking accurate piezometer readings, or taking baseline inclinometer readings before the casing grout has set;
d. Readings must be taken at the specified frequency and construction stages;
e. Suspect readings in one instrument can be investigated using other instruments' data. For example, an inclinometer profile deflecting unexpectedly should be matched by settlement observed at markers either simultaneously or slightly later. Paper prisms on the same walls act as double-checks on inclinometer movements and
f. Inclinometer readings are often read focusing on the value of the observed deflections compared to the design predicted deflection. However, curvature is inversely proportional to bending moment. The author notes cases where observed deflections were within prescribed limits, but 'sharp bumps' occurred along the vertical deflection profile (Figure 21(b)). The author suggests these bumps reflect high localised wall moments, warranting monitoring, particularly for compliance to crack width requirements in tanked structures.

6 CONCLUSIONS

The author regards temporary structural steelwork as a rational and flexible solution for deep excavations in soft ground especially where conventional earth retention measures utilising ground anchors and soil nails cannot be used. Steelwork support methods also readily accommodate site/authority-requested deviations on utility, manhole, crane platform and other positional changes after steelwork completion via economical *ad hoc* element strengthening.

There are other economies, particularly for structures built bottom-up, due to wall cost savings. These economies depend on labour costs as steelwork is labour-intensive, but this applies equally to all temporarily-braced excavations.

Internal bracing of excavations especially lends itself to situations where traffic staging requires traffic to cross the excavation. The obvious disadvantage of internal excavation support is space restriction for permanent works construction and the management of temporary works elements incorporated into the permanent works.

7 ACKNOWLEDGEMENTS

The author gratefully acknowledges the support and contributions of Paul Gunson, Alan Garrard and Paul Hewitt of Parsons Brinckerhoff.

8 REFERENCES

Borin, D.L. (1996) WALLAP Version 4.0 User's Manual, Geosolve, pp 9-2.

Bowles, J (1996) Foundation Analysis and Design, Fifth Edition, McGraw-Hill, pp 803 – 806.

Brinkgreve, R.B.J. and Broere.W.(2004) Plaxis, 2D - Version 8, Plaxis bv, pp 3-39, 3-42, 3-43, 3-52.

British Standard 8002 (1994) Code of Practice for Earth Retaining Structures, Figure 41.

Clough, G.W. and O'Rourke, T.D. (1990) Construction-Induced Movements of In-situ Walls, *Design and Performance of Earth Retaining Structures,* ASCE Special Publication No. 25, pp 439-470

Ganeshan, V (2003) Seminar on Geotechnical Instrumentation, Institution of Engineers Singapore

Hirose & Co., Ltd (c.1996) Product Information

Ho, C.E. and Wallace, J.C. (1994) Geotechnical Aspects of a Deep Basement Construction in Soft Ground, *Journal of the Institution of Engineers, Singapore* Vol 34 No 5

Lee, F.H, Tan, S.A and Dasari, G. (2003) Seminar on Application of FEM in Geotechnical Engineering

Mana, A.I. and Clough, G.W. (1981) Predictions of movements for braced cuts in clay, *Journal of Geotechnical Engineering, American Society of Civil Engineering,* Vol 107, No GT6 pages 759-777

Orihara, K. (2003) Seminar on Geotechnical Instrumentation, Institution of Engineers Singapore

Peck, R.B. (1969) - Deep excavations and tunnelling in soft ground, *State of the art report. Proc. of VIIth International Conference on Soil Mechanics and Foundation Engineering, Mexico, 1969*

Terzaghi, K. and Peck, R.B. (1967) Soil Mechanics in Engineering Practice 2nd Ed

Xanthakos, P.P. (1994) - Ground Control and Improvement.

SETTLING AND CONSOLIDATION BEHAVIOUR OF DREDGED COHESIVE ESTUARINE SOIL USING COLUMN TESTING APPARATUS

S. R. Morrison[1] and A. M. Tait[2]
[1]*Senior Geotechnical Engineer, Coffey Geotechnics Pty Ltd, Wollongong*
[2]*Engineering Geologist, Coffey Geotechnics Pty Ltd, Newcastle*

ABSTRACT

Consolidation testing on *in situ* normally or over consolidated cohesive soils is commonly used to assess engineering parameters such as C_v, C_c and $C_{\alpha.}$ However, the application of conventional consolidation tests to reconstituted soil slurries is often unachievable. A column testing method for assessing the settling and consolidation behaviour of dredged soils was devised and applied to five samples of estuarine soil in a brackish (somewhat salty) water environment sourced from the South Coast of N.S.W, Australia. Test results show that void ratio and bulk density values after the settling phase of the test were comparable with results of *in situ* soil at the initial stage of standard laboratory oedometer testing. Calculation of compressibility coefficients C_c and C_α after the loading stage of the test revealed similar results to oedometer testing on the soils in the *in situ* state. The testing method was assessed to provide results within a more reasonable timeframe with sample thicknesses of approximately 100 mm. It was assessed that soil thicknesses greater than 100 mm in the columns were influenced by simultaneous primary and creep settlement and that an unreasonable test duration would be required to achieve meaningful results in an economic timeframe.

1 INTRODUCTION

Consolidation parameters such as C_v, C_c and C_α are commonly derived from laboratory oedometer tests such as AS1289 6.6.1 (1998) on 'undisturbed', 50 mm or 63 mm diameter soil samples retrieved from site investigation techniques. Frequently these samples show some degree of over–consolidation, enabling the test to be carried out in small diameter ring apparatus without compromising consolidation data. However, consolidation testing of soils that have been reconstituted to a suspension and subsequently settled often cannot be successfully tested using conventional testing methods (Krizek, 2004; Sridharan and Prakash, 1999).

Accessible land with favourable geotechnical properties is becoming limited in society and increasingly areas of reclaimed and contaminated land are being used for infrastructure purposes. Also the offshore disposal of dredged soil is less widely accepted by the community as an acceptable use of dredged soil. The viability of reuse of dredged cohesive soils onland is increasing where previously the cost of reuse of this type of material was considered prohibitive.

In many cases, developing reclaimed or contaminated land often requires the dredging of soils from marine, alluvial and estuarine environments or dredging from mining tailings or contaminated land. In most cases this dredged material is deposited in a holding area (i.e. tailings dam) to be subsequently used as reclaimed land. The nature of the soil as it settles from suspension and various properties such as the rate and magnitude of consolidation settlement must be assessed for decisions to be made as to whether the dredged soil can be reused as reclaimed land.

This paper presents the results of testing performed on cohesive soils sourced from an estuarine environment located on the South Coast of N.S.W, Australia. Significant research has previously been carried out on testing of dredged soil materials in freshwater environments (Krizek, 2004; Sheeran and Krizek, 1971). This paper discusses the settling behaviour of the dredged slurry suspension in brackish water for different soil to water ratios. It also provides assessment of ρ_d and e_o during the settling phase, assessment of consolidation parameters C_v, C_c and C_α. A comparison is also made between the results of the column testing for 'dredged' soil and conventional oedometer testing values from three samples of 'undisturbed' soil.

2 METHODOLOGY

The assessment of settling and consolidation behaviour of the soils was conducted using testing apparatus constructed exclusively for the test. The testing consisted of two phases, named Phase 1 and Phase 2. Phase 1 involved observation of the settling of the slurry suspension, and Phase 2 involved observation of the rate of consolidation over time with the addition of different surcharge weights. Australian Standard AS 1289 6.6.1 (1998) was used as a general reference for testing the procedure; however several modifications were made due to the unique nature of the testing.

2.1 APPARATUS

Fifteen clear Perspex columns with an inner diameter of 94 mm were used and each column had a Perspex base fixed with 'Acrifix' Adhesive and a reinforced collar to maintain a water tight seal and integrity of the joint under additional pressure. A plastic tube was drilled into the side of the column 10 mm from the base, with an outlet fixed to the top of the column.

The columns were firmly fixed to a wall using a metal collar placed near the top of the column to prevent movement (accidental or intentional) during the course of testing.

Prior to the settling phase of the testing, a 20 mm layer of sand was placed at the base of each Perspex column and filter paper was placed over the sand. This provided "two-way drainage" to facilitate consolidation in the laboratory condition. This was carried out in an attempt to quicken the rate of settlement with the knowledge that a theoretical correction can be applied to settlement estimates if only "one-way" drainage exists in the field.

After the settling phase of the testing was completed, an additional filter layer was constructed on the top of the settled soil surface. This included placing a layer of filter paper over the soil surface and a 20 mm thick layer of sand over the paper to facilitate drainage. An additional layer of filter paper was placed on top of the sand drainage layer prior to surcharge load being added.

Surcharge loads were constructed from concrete, pre-cast into PVC pipe with an external diameter of 90 mm. The weights were cured for seven days then weighed and measured to calculate load. The surcharge loads were cut to size to meet target preload pressures that were nominated for the testing procedure. The difference in annulus between the column diameter and the surcharge weight provided a drainage path for pore water to pass out of the consolidating soil, into the upper filtration layer and subsequently add to the column of 'free water' that existed above the consolidating soil.

A schematic diagram of the column testing apparatus is presented in Figure 1 and Figure 2.

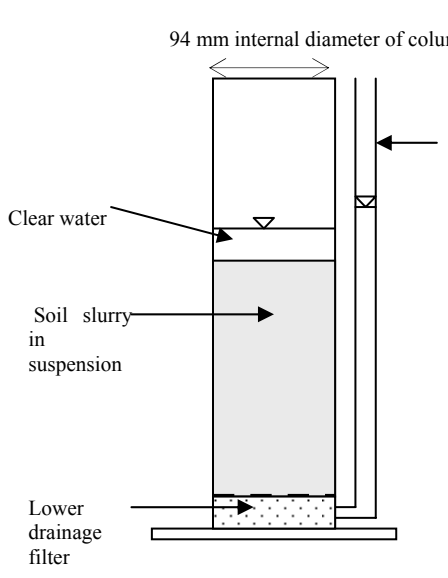

Figure 1: Phase 1.Settling of slurry suspension.

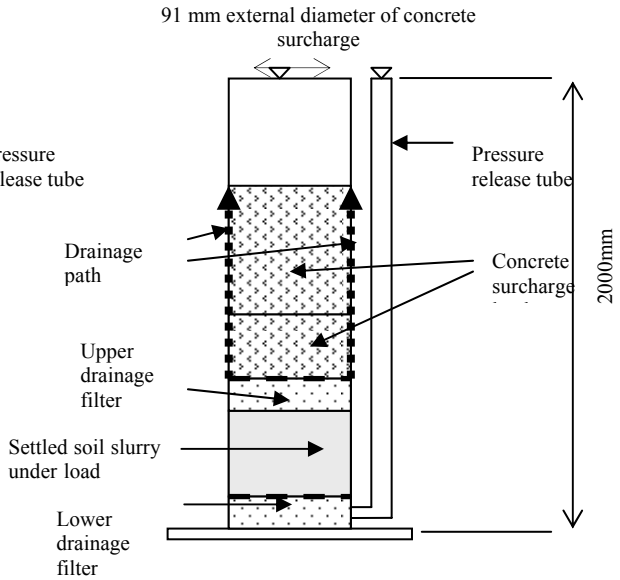

Figure 2: Phase 2 Settled soil under load.

2.2 MATERIALS

The soils used for this testing program were sourced from an estuarine environment located on the south coast of New South Wales. The soils were generally described as sandy clayey silts or silty clays and are typical of Holocene aged estuarine soils found in the region. The natural (initial) moisture content of the five samples of estuarine soils used for this column test ranged between 48% and 133%. No Atterberg Limit testing was carried out on the five estuarine soil samples prior to column testing, however twelve Atterberg Limit tests had been previously carried out on the clayey or silty estuarine soils at the site. Results from these twelve nearby tests are considered to be generally representative of the estuarine soil properties at the site. The Plastic Limit of the twelve nearby soil samples ranged between 15% and 39%, and the Liquid Limit of the twelve samples ranged from 39% to 78%.

To source material for the column test trial, six test pits (designated CGTP21 to CGTP26) were excavated on the 20 January 2004 and six samples were collected that generally represented a variety of estuarine soils at the site. The

particle size distributions of the tested samples are presented below in Figure 3. Standard Particle Size Distribution testing including hydrometer analysis according to AS 1289.3.6.2 (2000) was used to assess the silt and clay fractions below 75µm.

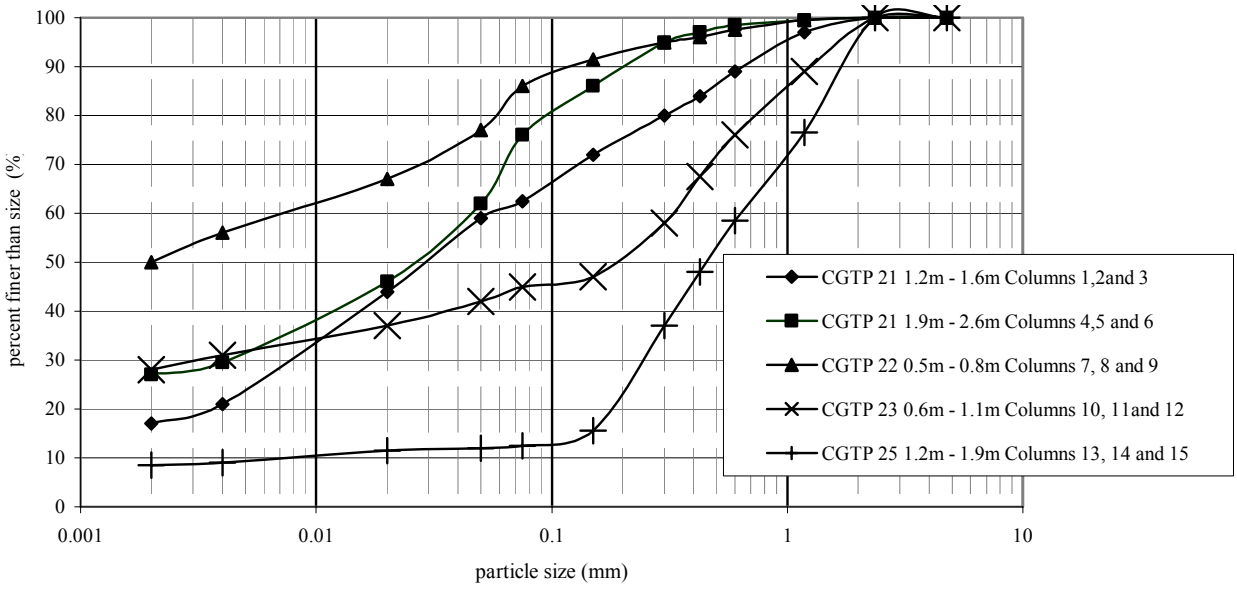

Figure 3: Particle size distributions of tested samples.

Water from the existing swamp on the site was collected for use in the testing procedure. The water was collected approximately 500 m inland and was generally brackish (somewhat salty) with a pH of 6.32. Following collection, the water was immediately taken to the laboratory for testing.

2.3 PROCEDURES

Phase 1 – Settlement of Slurry under self weight

A bakery 'Hobart' mixer was used to mix the samples. The soils were mixed to moisture contents of 233%, 300% and 400%. The initial void ratios (e_o) of the slurried material ranged between 5.14 and 10.04. The Hobart mixer provided a generally homogenous and consistent mix in a controlled condition with minimal sample loss. The mixed slurry suspension was siphoned into the column using a plastic hose placed near the base of the column and this was raised as material filled the column. Standard testing sheets were developed to record relevant data and observations during the testing procedure. Data was recorded during the mixing and dispensing of the slurry. The height of settled soil was recorded at 10 minute intervals up to about 40 minutes, then at 60 minute intervals for 4 hours, then twice daily for the duration of the test.

Measurements were taken at the interface of the settling slurry suspension and clear water above the suspension. The test was continued generally until less than 1 mm to 2 mm of reduction in the height of the settled soil was achieved over two consecutive days.

Some deviations to this general procedure occurred in columns 6 and 13 for the 1000 mm thickness soil samples. Higher rates of settlement of between 3 mm and 16 mm per day were reported in these columns at the completion of the test.

Periodic pH measurements of the water above the slurry were also made using an electronic pH probe calibrated to pH 4 and pH 7 reference solutions on the day of testing.

Phase 2 – Consolidation of slurry under vertical stress

Following completion of the Phase 1 testing, water was siphoned out of the column (taking care not to disturb the settled soil), leaving about 50 mm of water covering the settled soil. The upper sand filter layer was placed over the settled soil. The amount of sand used was weighed and then placed without disturbing the settled soil. The column was carefully filled with water to the top of the column, adding water with as little turbulence as possible. The level between the settled soil and the bottom layer of sand was recorded relative to the base of the column. Phase 2 of the testing commenced with the sample being loaded with a 2 kPa surcharge load. Measurements were taken immediately after the positioning of the surcharge load at time intervals of 6 sec, 15 sec, 30 sec, 1 min, 2 min 15 sec, 4 min, 6 min

15 sec, 9 min, 12 min 15 sec, 16 min, 20 min 15 sec, 25 min then once daily until measurements of less than 1 mm difference in reduction of sample height was recorded over three to eight rounds of monitoring (indicating completion of primary consolidation settlement under the given load increment). Placement of surcharge load weights was continued in this manner until between about 5 kPa to 30 kPa of load was applied to the sample.

For the columns with soil slurry heights of greater than 100 mm (thicknesses generally 300 mm and 1000 mm in this test), completion of >90% primary consolidation was not achieved after several months of monitoring. Even though >90% primary consolidation had not been achieved in these columns, another load increment was added to check that settlement under the given loads was indeed slow and was not due to other factors such as friction. For these columns with thicker soil slurry heights, in all cases it was assessed that >90% primary consolidation had not been achieved even after 6 months to 9 months of testing under the stated loads.

3 RESULTS

3.1 PHASE 1 – SETTLEMENT OF SLURRY UNDER SELF WEIGHT

Settling of the slurry suspension was generally achieved between 0.1 day and 28 days following placement of the soil slurry into the columns. For two columns some higher rates of settlement were reported after 8 days to 35 days of settlement under self weight. A reduction in void ratio of up to 77% was achieved at the completion of the Phase 1 testing.

Table 1: Phase 1 test results.

Sample Number	Sample Diameter (mm)	Before Phase 1 Consolidation					After Phase 1 Consolidation* under self weight				
		Initial Sample Thickness (mm)	Initial M.C.(%)	Initial ρ_w	Initial ρ_d	Initial e_o	Final Sample Thickness (mm)	Final M.C.(%)	Settled ρ_w	Settled ρ_d	Final e_o
Column 1	94	205	400	1.21	0.24	9.24	120	111	1.69	0.80	2.15
Column 2	94	825	300	1.20	0.30	7.39	562	194	1.30	0.44	4.72
Column 3	94	1240	233	1.26	0.33	5.68	968	175	1.33	0.48	4.22
Column 4	94	205	400	1.21	0.24	9.42	97	182	1.44	0.51	3.93
Column 5	94	1290	300	1.20	0.30	7.37	763	164	1.35	0.51	3.95
Column 6	94	1219	233	1.35	0.41	5.20	753	139	1.57	0.66	2.83
Column 7	94	220	400	1.24	0.25	9.14	94	169.6	1.57	0.58	3.33
Column 8	94	820	300	1.24	0.31	7.10	439	151	1.44	0.55	3.34
Column 9	94	1273	233	1.29	0.39	5.52	768	131	1.48	0.64	2.93
Column 10	94	220	400	1.14	0.23	10.04	144	249	1.22	0.35	6.23
Column 11	94	785	300	1.24	0.31	7.11	474	173	1.40	0.51	3.90
Column 12	94	1190	233	1.41	0.42	4.97	1107	217	1.44	0.45	4.56
Column 13	94	1191	233	1.37	0.41	5.14	1120	218	1.39	0.44	4.77
Column 14	94	780	300	1.25	0.31	7.03	585	220	1.34	0.42	5.03
Column 15	94	177	400	1.51	0.30	7.34	127	307	1.71	0.42	4.99
Oedometer 1	46.0	-	68.2	1.61	0.96	1.86	-	-	-	-	-
Oedometer 2	46.5	-	111.2	1.29	0.61	2.77	-	-	-	-	-
Oedometer 3	46.0	-	130.0	1.24	0.54	3.06	-	-	-	-	-
Oedometer 4 (Golder)	50	-	46.6	1.73	1.18	1.21	-	-	-	-	-

- ** - After Phase 1 Consolidation is defined as completion of primary consolidation settlement under self weight. These are slightly different to the values shown for 'Before Phase 2 Consolidation' in Table 2, below.*
- *ρ_w – wet or bulk density, tonnes/m^3. ρ_d – dry density, tonnes/m^3. e_o – void ratio*

A direct correlation between settling time and soil/water content could not be identified from the Phase 1 testing. Correlation of settling time and soil/water content would require a consistent slurry height (say 100 mm) to be used for the 20%, 25% and 30% soil/water ratios.

The pH of the water above the slurry dropped from 6.32 to between about 2.5 and 3.3 within about 5 days to 7 days following placement. This is due to the oxidation of the known Acid Sulfate Soil materials within the estuarine soil.

The implications of this change in pH along with other changes in soil chemistry are beyond the scope of this paper but would need to be addressed for developments where dredging of known Acid Sulfate Soil slurry materials occurs.

Table 1 presents a summary of the results from the Phase 1 Laboratory Testing, along with a comparison of results from Oedometer testing of U_{50} tube field samples taken from the estuarine soil unit.

3.2 PHASE 2 – CONSOLIDATION OF SLURRY UNDER VERTICAL STRESS

For the Phase 2 testing, values of $C_c/(1+e_o)$ ranged between 0.180 and 0.425 and for the oedometer tests the $Cc/(1+e_o)$ values ranged between 0.179 and 0.592. For the Phase 2 testing, values of $C_\alpha/(1+e_o)$ ranged between 0.0069 and 0.0110 and for the odometer tests the values of $C_\alpha/(1+e_o)$ ranged between 0.0067 and 0.0138. It is assessed that a general correlation between column testing and conventional odometer testing can be made.

Meaningful results were only recorded from the 100 mm (approximate) height soil columns. It was found that soil heights greater than 100 mm were continuing to record primary consolidation settlement after 10 months of testing. It is expected that results for soil heights greater that 100 mm may take many years to achieve meaningful results for the Phase 2 testing.

It should also be pointed out that sample thickness does have an influence on the consolidation characteristic of soils as hypothesised by Jamiolkowski *et al.* (1985), and as observed by other researchers in subsequent development of time-dependent models for simultaneous consolidation and creep compression.

Table 2: Results of Phase 2 testing.

Sample Number	Sample Diameter (mm)	Before Phase 2 Consolidation Testing*			After Phase 2 Consolidation Testing			
		Initial Sample Thickness (mm)	Initial Moisture Content (%)	Initial e_o	Final Sample Thickness (mm)	Final e_o	$C_c/(1+e_o)$	$C_\alpha/(1+e_o)$
Column 1	94	120	228.2	5.10	74	2.76	0.425	0.0110 (0.0110 - 0.0053)
Column 4	94	97	181.9	3.93	41	1.08	0.250	0.0093 (0.0012 - 0.0093)
Column 7	94	94	169.6	3.33	64	1.95	0.180	0.0069 (0.0008 - 0.0069)
Oedometer 1	46.0	17.29	68.2	1.86	-	1.05	0.310	0.0067 (0.0012 - 0.0067)
Oedometer 2	46.5	16.15	111.2	2.77	-	1.15	0.566	0.0111 (0.0000 - 0.0111)
Oedometer 3	46.0	16.62	130.0	3.06	-	1.68	0.592	0.0138 (0.0110 - 0.0053)
Oedometer 4 (Golder)	50	-	46.6	1.21	-	0.73	0.179	0.0110 (0.0000 - 0.0138)

- ** - Before Phase 2 Consolidation testing (for the Column tests 1, 4 and 7 only) is defined as after primary consolidation settlement under self weight, placement of sand drainage layer over surface of slurry, addition of a water up to the brim of the 2m high column and immediately after placement of initial concrete weight over the settled soil slurry.*
- *e_o – void ratio*

Plots of thickness of soil (slurry) height versus log time were prepared based on the readings taken during the course of monitoring. Due to space restrictions there is not sufficient room for presentation of these results, however an assessment of the coefficient of vertical consolidation, C_v, was made based on an assessment of t_{50} (the time for completion of 50% primary consolidation) and standard methods contained in AS 1289 6.6.1 (1998). The results for C_v for the 100 mm thick soil height columns displayed some scatter and ranged between 0.06 m^2/year and 30.36 m^2/year, however most results ranged between 0.3 m^2/year and 1 m^2/year.

Table 2 presents a summary of the results from the Phase 2 Laboratory Testing, along with a comparison of results from oedometer testing of U_{50} tube field samples taken from the estuarine soil unit.

Results from Table 2 show that the test methods used seem effective for assessment of $C_c/(1+e_o)$ and $C_\alpha/(1+e_o)$ for materials that are reconstituted and placed at low effective stresses (<30kPa) and high initial void ratios (e_o ranging between 9.14 to 9.42).

Figure 4 plots void ratio versus normal effective stress for the Phase 2 column testing and oedometer test results. The slope of the primary consolidation portion of the oedometer curves appears similar to the slope of the primary consolidation curves for the Phase 1 and 2 column testing. The results for the column testing confirm the absence of pre-consolidation pressure, which is expected for these reconstituted soils. Values of $C_c/(1+e_o)$ and $C_\alpha/(1+e_o)$ appear similar for both test methods where a 100 mm soil thickness for the column testing has been used.

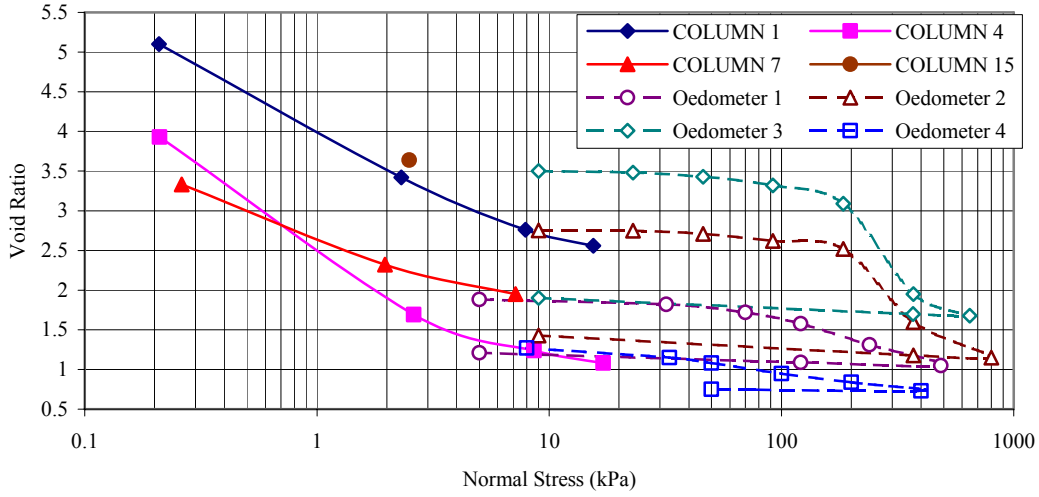

Figure 4: Comparison of Phase 2 column testing results and oedometer testing results for void ratio versus normal effective stress.

4 CONCLUSIONS

The results show the test method adopted for the assessment of settling under self weight and consolidation under load is generally suitable for dredged or reconstituted estuarine type soils in a brackish (somewhat salty) water environment. The test appears suitable for soil thicknesses of about 100 mm. Testing of thicknesses greater than this would require onerous timeframes or a modified testing method. For a 100 mm thickness, results show that a timeframe of 9 months to 12 months would be required for adequate results. Results of thick samples greater than about 100 mm are also likely to be affected by simultaneous primary consolidation and secondary consolidation (creep) behaviour and would require different test methods to provide meaningful results in an economic timeframe.

5 REFERENCES

AS 1289.3.6.2 (2000), 'Method of testing soils for engineering purposes. Method 3.6.2: Soil classification tests – determination of the particle size distribution of a soil – analysis by sieving in combination with hydrometer analysis', Standards Australia

AS 1289.6.6.1 (1998), 'Method of testing soils for engineering purposes. Method 6.6.1: Soil strength and consolidation tests-determination of the one-dimensional consolidation properties of a soil-standard method', Standards Australia

Jamiolkowski, M., Ladd, C.C., Germaine, J.T. and Lancellotta, R., (1985) "New developmens in field and laboratory testing of soils: general report." Proceedings Eleventh Int. Conf. Soil Mech. Fndn. Engng., San Francisco, 1, pp.57-153.

Krizek, R. J. (2004) 'Slurries in Geotechnical Engineering', the Twelfth Spencer J Buchanan Lecture, Texas A&M University.

Sheeran, D.E. and Krizek, R.J. 'Preparation of Homogeneous Soil Samples by Slurry Consolidation', Journal of Materials, JMLSA, Vol. 6, No. 2, June 1971, pp 356-373.

Sridharan, A and Prakash, K (1999) 'Simplified Seepage Consolidation Test for Soft Sediments', Geotechnical Testing Journal GTJODJ, Vol. 22, No. 3, September 1999, pp. 235-244.

LIME CEMENT MIXING (LCM) – APPLICATIONS OF THE SCANDINAVIAN METHOD

M. Dahlström
Senior Design Engineer, LCM AB/ KELLER, SE-437 34 Lindome, Sweden/ 4 Burbank Place, Baulkham Hills, NSW, Australia.

ABSTRACT

Since the introduction of the Scandinavian Lime/Cement Column Method of Soil Mixing (LCM) in the late sixties and early seventies, applications have experienced a major increase. Experience from different applications in Scandinavia and the United Kingdom is presented in this paper. Considered case histories refer to ground improvement, foundation support for light buildings, support for temporary sheet pile walls, permanent application to reduce the active earth pressure behind a mass gravity wall and support for deep excavations. The applications demonstrate the flexibility of the LCM method, which can be applied as a competitive solution to a number of different geotechnical challenges.

1 INTRODUCTION

In situ Soil Mixing (SM) is rapidly increasing in Europe as a method for stabilising soft soils to increase the engineering properties. Soil Mixing is a widely used name and the applications, installation methods and design issues have major differences. The differences and applications have recently been reviewed by Massarsch and Topolnicki (2005). This paper will focus on Soil Mixing using the Scandinavian Dry Deep Mixing (DDM) Method, also known as Lime/Cement Column Mixing (LCM).

The Scandinavian method was originally developed in Sweden in the late sixties and early seventies by Prof. B. Broms and engineer K. Pause (Bredenberg *et al*., 1999). The first equipment used for production of DDM Columns was developed by LCM´s predecessor company, the Swedish contractor BPA in 1976. Figure 2 shows a later model of the installation equipment.

LCM columns were originally developed for foundations of light buildings and for the reduction of settlements in low embankments and parking lots resting upon very soft inorganic clays. In the early projects the mixing additive was quick lime with a typical dosage of 60 kg/m^3 to 90 kg/m^3, the column diameter was 500 mm with a typical column depth of up to 10 m. The design undrained shear strength ($c_{u,col}$) ranged from 60 kPa to 100 kPa. Early development was focused on larger diameter columns, deeper columns, higher strength columns and increased production. Typical column diameters today are 600 mm to 800 mm and maximum installation depth is approximately 25 m. The design undrained shear strength ($c_{u,col}$) is today in the range of 100 kPa to 200 kPa (limited to a maximum of 150 kPa in stability analysis). New additives and mixtures of additives have been used. These are commonly blended as a combination of cement, quick lime, blast furnace slag or fly ash. New additives, various column diameters and more powerful equipment have developed a larger range of applications where LCM columns are applicable.

Typical main applications of LCM columns today are:

- Soil improvement for road and railroad embankments on soft soils.
- Improvement of stability.
- Foundation of houses and light warehouses.
- Reduction of ground vibration.
- Mass treatment of very soft soils such as peat, gyttja (a Scandinavian soil with very high organic and moisture contents) and dredged marine sediments.

Other applications include:

- Increase of passive and/or reduction of active earth pressure for sheet pile walls and retaining systems in soft clay.
- Preventing liquefaction in seismic hazard areas.
- Solidification and remediation work on contaminated soil.
- Support for temporary working platforms.

In the following section, selected examples of applications where LCM columns have been constructed are presented and illustrated. The examples are based on experience on LCM-columns in Scandinavia and the United Kingdom. The considered case histories refer to ground improvement for road embankments, foundations for houses on a uniform

floor slab, support for temporary sheet pile walls to reduce the active earth pressure behind a mass gravity wall and as support for a deep excavation. The applications demonstrate that Soil Mixing using LCM-columns can offer a competitive solution for a number of different geotechnical applications.

2 APPLICATIONS

2.1 GROUND IMPROVEMENT FOR A ROAD EMBANKMENT

LCM-columns of 600 mm and 800 mm diameter were applied to support a road embankment overlying very soft and soft clay and partly peat. The soft clay had typical undrained shear strengths of 12 kPa to 25 kPa and a thickness of 5 m to 20 m.

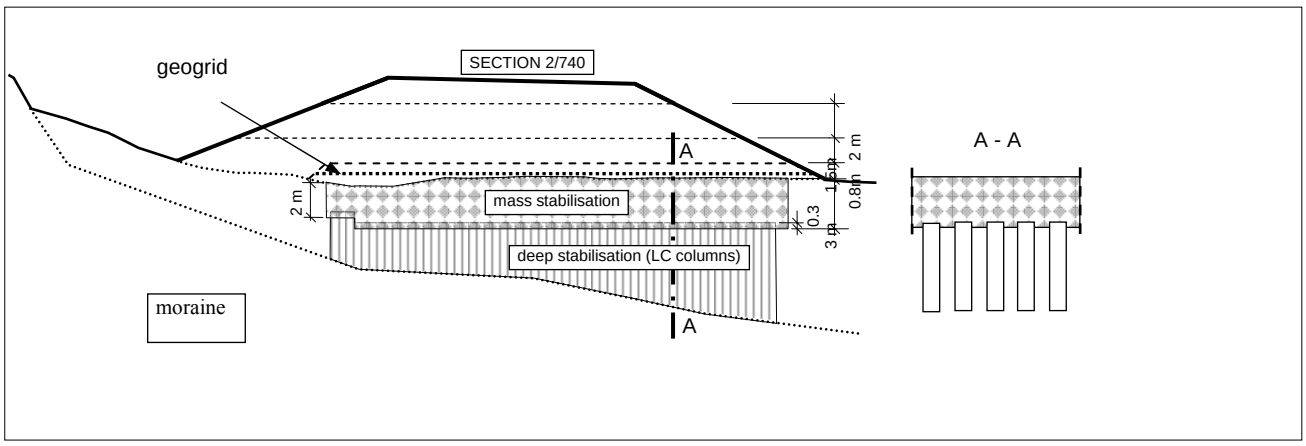

Figure 1: Cross section of a road embankment stabilised with DDM and mass mixing (Moraberg, Sweden, 2004).

On a section of approximately 500 m of the embankment, 0.5 m to 2.6 m of peat overllay 0.3 m to 0.5 m of gyttja above the soft clay deposit. The peat deposit had a typical water content of 500-1200% and the gyttja deposit had a typical water content of 100% to 300% and undrained shear strength of 3 kPa to 7 kPa. Mass treatment (so called mass stabilisation) was used in the peat and gyttja deposits.

In the soft clay LCM-columns were installed to a maximum depth of 15 m, acting as floating columns, on a square grid of between 1.0 m and 1.8 m centres depending on the height of the embankment. In areas where the factor of safety (FOS) was less than 1.0 for the untreated embankment, the columns were installed to interlock, with a spacing of 0.7 m between the columns (0.1 m overlapping), in perpendicular panels under the embankment. This increased the shear resistance and provided a FOS of 1.5. Single columns are sensitive to horizontal forces, hence the installation of interlocking columns to form panels. The additive used was a quick lime and standard Portland cement blended 50/50, and a dosage of 90 kg/m^3. Design undrained shear strength of the columns was 150 kPa (UCS=0.3 MPa). In stability analysis the design undrained shear strength was limited to 100 kPa. Drained parameters were evaluated as an internal friction angle $\varphi'_{col}=35^o$ and cohesion $c'=0.35*c_{u,col.}$ In the LCM columns the Young's modulus in the columns was calculated as 30 MPa increasing to 80 MPa at depth. Altogether 16,200 columns with a total length of 119,850 linear metres were installed. Construction of the embankment started 2 weeks after the columns had been installed.

In the part of the embankment where peat and gyttja were overlying soft clay, mass soil treatment was also performed to reduce future settlements and increase the compressive strength in the peat and gyttja deposits.

Installation of single columns in soils with low effective stress such as in peat and gyttja is not recommended as the bearing capacity of single columns is depending on the support from the confinement in the soil deposit. Standard Portland cement was used as additive with a dosage of 175 kg/m^3 in the mass treated soil volume. Design undrained shear strength was 50 kPa in the mass treated soil block. Directly after mixing an early embankment load of crushed stone of 0.8 m was placed on the mass treated soil volume. Between the mass treated soil volume and the embankment fill a geotextile was placed to separate the crushed stone (fraction 0-100 mm) from the mass treated soil. One to two months after the first load was applied a second load increment step to the full embankment height of 2 m was placed (Figure 1). Settlement was measured by horizontal inclinometers.

Measured settlements in the mass treated soil volume supported by underlying LCM columns were in the range of 150 mm cm to 350 mm during the construction time of 1.5 years, with 60% to 80% of the settlement developed within the first month. Measured settlements in soft clay stabilised with LCM columns were in the range of 50 mm to 100 mm during the construction time of 1.5 years. Quality assessment using Column Penetration Tests (CPT) showed an undrained shear strength in the columns of 150 kPa to >400 kPa. In the mass treated peat and gyttja undrained shear strengths varied between 25 kPa to 100 kPa, with an average of 75 kPa.

Figure 2: LCM rig and mass mixing rig at Moraberg (2003).

Settlements have been measured 2.5 years after the road was opened for traffic the measured settlements were <30 mm in all eight measured horizontal inclinometers in both mass treated and column treated areas.

2.2 LCM COLUMNS SUPPORTING SLAB FOUNDATIONS

A 52 house development in Gothenburg, Sweden, was located in an area with deep soft clays, locally extending to >30 m. Piling costs for the building were prohibitive and LCM columns provided an economical solution for the foundations. The soil conditions were typically a 1 m dry crust clay overlying very soft clays, increasing to soft and medium soft clays at depth. The top 5 m to 8 m of the very soft clay was normally consolidated (OCR~1.0), at greater depth the soft clay became over-consolidated with the OCR increasing with depth.

Analysis was performed of the current and proposed stress distributions, where the additional load of 13 kPa from the houses was considered. The analysis showed that with the additional load the effective stress situation at 10 m depth had an OCR=1.25. At OCR≥1.25 creep settlement can be neglected. Therefore the solution adopted was to transfer the load from the houses by using LCM columns to depths greater than 10 m to provide a technical and economical solution as an alternative to friction piles.

DDM columns with a diameter of 500 mm were selected as the solution to transfer the additional stresses from the houses to 10 m depths. The spacing between the columns varied depending on the load situation from the floor slab. For each house an average improvement ratio of a=0.196 (or 19.6%) was adopted. The maximum design load on a single column was limited to 40 kN, corresponding to a compressive strength of 205 kPa, including a safety factor of 1.8. The Young's modulus in the columns was calculated as 24 MPa at 1 m depth, increasing to 42 MPa at 10 m depths due to increased confinement at depth.

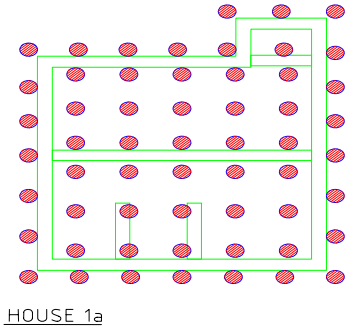

Figure 3: Column layout for a typical house (Hildedal, Gothenburg, Sweden).

The compression modulus M_L in the very soft and soft clay deposit was 0.25 MPa to 0.38 MPa. The combined compression modulus in the stabilised soil volume with an improvement ratio of 0.196 was calculated as 4.8 MPa at 1 m depth increasing to 8.4 MPa at 10 m depth. The calculated settlement was 25 mm for the stabilised 10 m soil volume. The additive used was a 50/50 lime/cement blend and a dosage of 100kg/m^3. 2824 Columns were installed for the 52 houses.

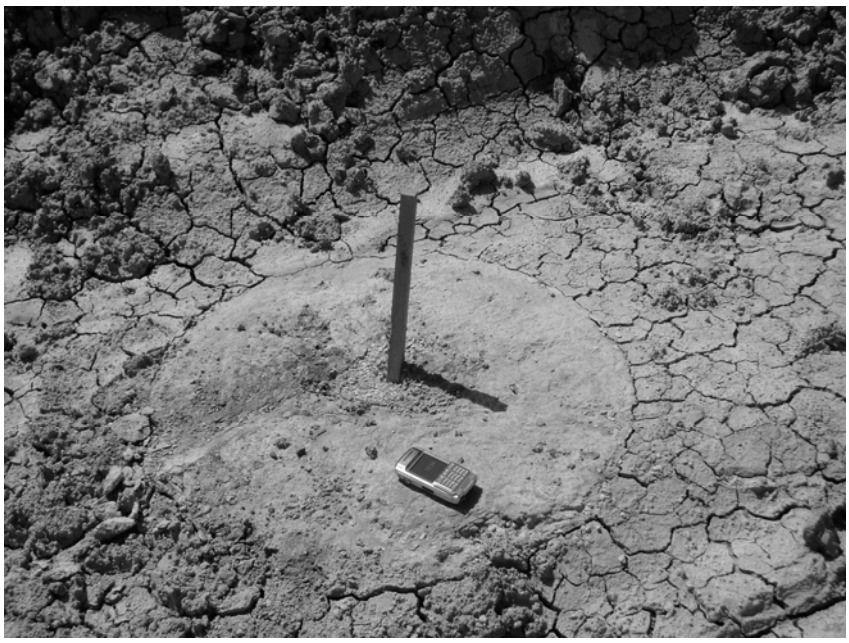

Figure 4: Exposed DDM-column.

2.3 SUPPORT FOR TEMPORARY AND PERMANENT RETAINING SYSTEMS

Retaining systems, predominantly sheet pile walls, can effectively be supported by DDM columns in order to reduce the active earth pressure and/or increase the passive earth pressure. In the last 5 years several of these applications have been effectively used in Scandinavia and United Kingdom.

Columns installed on the passive side (Figures 5 & 6) support the sheet piled wall by increasing the passive earth pressure. As a result of the installation of the LCM columns the shear strength in the soil volume increases. Due to increased undrained shear strength $c_{u,col}>c_{u,soil}$, there is an increased cohesion $c'_{col}>c'_{soil}$ and increased friction angle $\varphi'_{col}>\varphi'_{soil}$. To support a retaining structure columns are installed in panels or blocks perpendicular to the retaining wall system. Other vital requirements for successful support are a high degree of homogeneity in the columns and sufficient interlocking between the columns to transfer the load through a panel or block.

The column panels or blocks increase the average shear strength in the soil volume on the passive side, which increases the passive earth pressure acting toward the retaining structure. There are several advantages provided by installing passive columns: panels, together with a 100 mm to 200 mm concrete slab can usually reduce one level of anchors for

the retaining structure. Buildings with a basement can be founded on the LCM-columns as a compensation foundation. The risk for bottom heave also decreases, due to increased shear strength in the soil block.

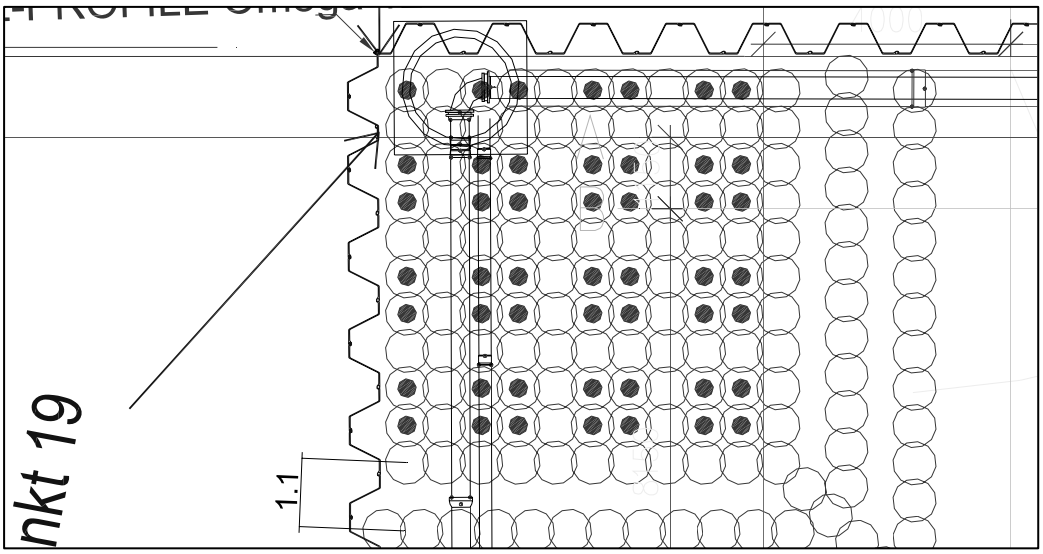

Figure 5: Plan drawing for LCM-columns to passive support a sheet pile wall at Sörkedalsvien in Oslo, Norway.

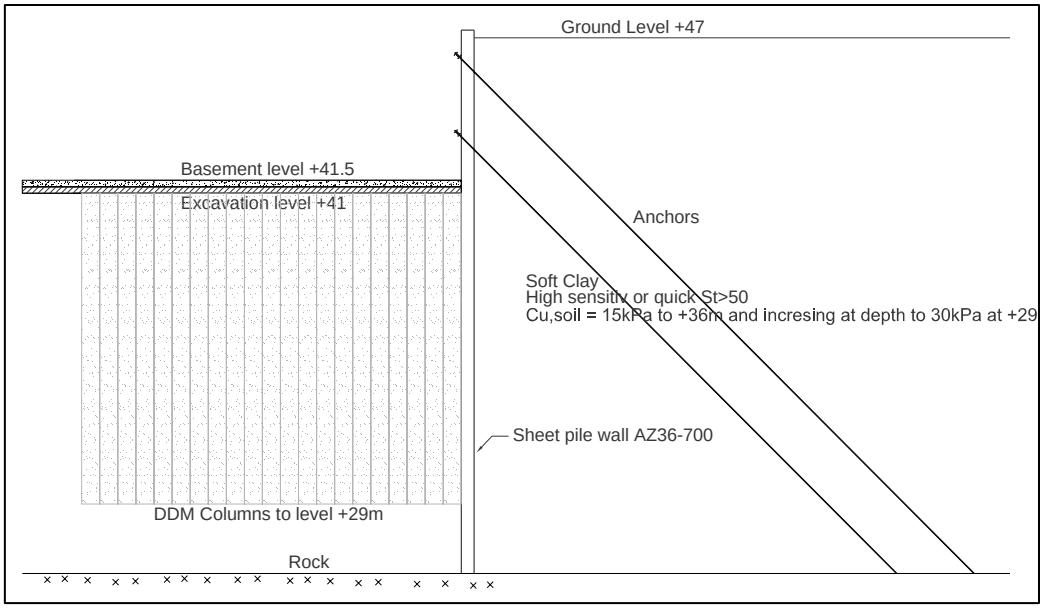

Figure 6: Cross section passive support to sheet pile wall at Sörkedalsvien in Oslo, Norway.

In Oslo, Norway, a deep excavation in a highly sensitive soft clay, at depth becoming quick S_t>50, was supported by a sheet piled wall. The excavation depth was approximately 6 m. The soil conditions were typically 0 m to 3 m of fill overlying 2 m to 3 m of soft clay overlying 5 m to 15 m of very soft and highly sensitive clay improving to soft at depth.

A system of interlocking columns installed in panels perpendicular to the sheet piled wall was submitted. In the corners a high degree of improvement was needed. Therefore a block of columns were installed (Figures 5 & 6). Depending on the excavation depth the improvement ratio in the stabilised soil volume varied between 31% and 57%. In the corner a zone with 100% improvement was needed.

The columns had a diameter of 0.7 m and were installed in 15 m long panels with a 0.1 m overlap to the underlying morain, or to maximum 13 m under the excavation level. The increased passive support from the panels together with a 200 mm concrete slab reduced the number of tieback anchors from 3 levels to 2 levels and at the same time reduced the dimensions of the sheet pile wall.

Figure 7: Installation of LCM Columns for passive support on a sheet pile wall in Asker, Norway.

Similarly, in Barking, London, LCM columns were used to support an existing quay wall in poor condition. As the existing wall was partially continuing to perform its function, it was decided to retain the wall and build a new wall unit immediately behind. The newly formed wall would be independent of the existing wall. The site lies upon geologically recent alluvial deposits of the River Roding. overlying Eocene deposits of London Clay. LCM columns were installed perpendicularly and alongside the existing quay wall to form a mass gravity structure for support. Two vertical panels of 800 mm diameter columns were installed nearest to the existing wall to an average depth of 7 m. Behind the front panels six inclined columns in panels with a centre spacing of 1.4 m between the panels to an average depth of 7 m were installed. Between the inclined panels an interlocking vertical column was installed to support a tieback rod, supporting the existing wall face.

Figure 8: LCM mass gravity block behind existing quay wall at Barking, United Kingdom

The poor condition of the existing wall was assumed to be an imminent risk of failure during installation. A collapse of the wall would allow the river to rise into housing areas and create damage to existing buildings. A survey program was implemented to observe every movement during installation to ensure that failure did not occur during installation. The design undrained shear strength was 150 kPa for columns installed in perpendicular inclined panels to the existing wall. Columns installed along the wall had design undrained shear strengths of 300 kPa. To achieve 300 kPa the columns

were mixed twice with 150 kg/m^3 cement at each mixing. Column strength was validated using pull out resistant tests (PORT). Test results varied between 150 kPa and 500 kPa shear strength in the columns.

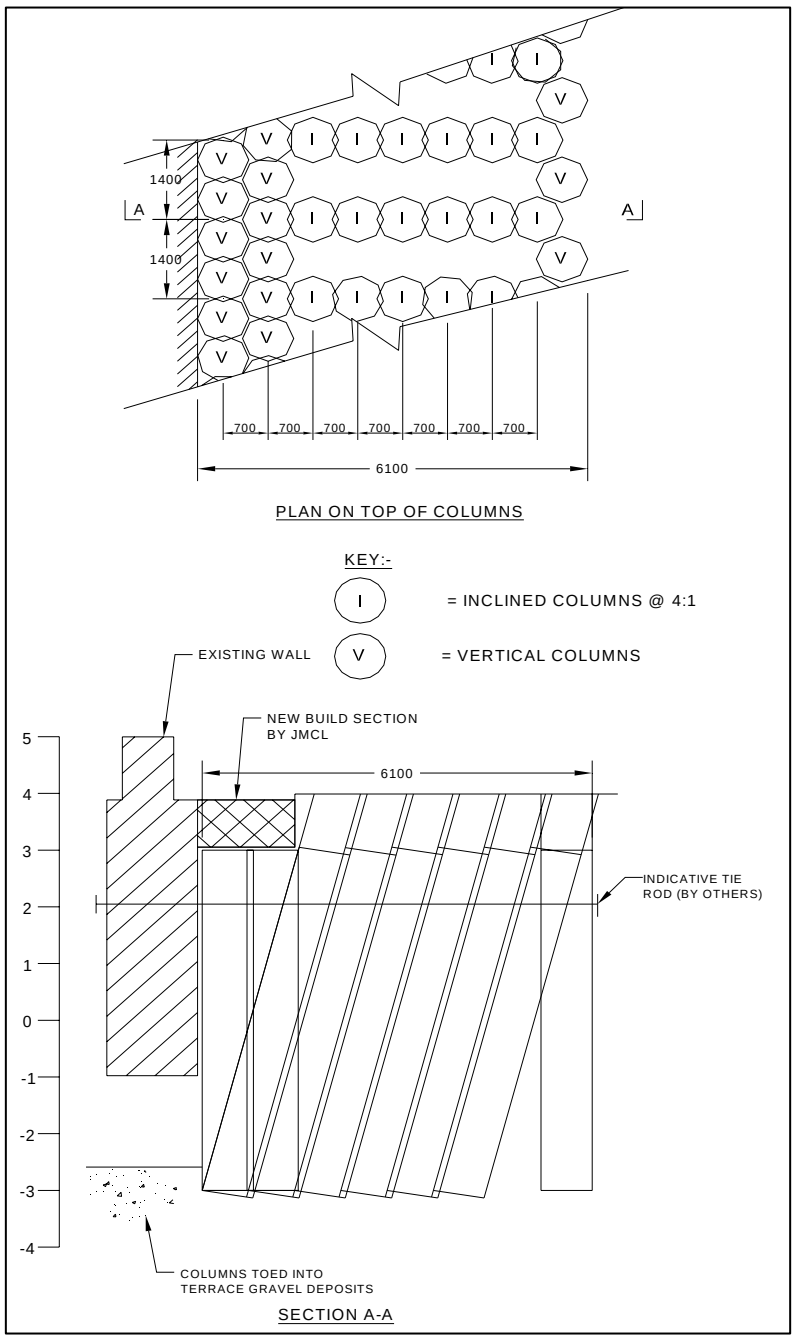

Figure 9: Plan and section drawing for columns installed to support a mass gravity wall at Barking, United Kingdom.

3 CONCLUSION

The development of the LCM method, since it was first used in the seventies, has allowed new and varied applications offering innovative solutions to engineering challenges. The increase in applications has raised interest in using the method outside Scandinavia. Today the LCM system is a well known ground improvement technique worldwide and has successfully been used in Central Europe, United Kingdom, United States, Asia and most recently in Australia. The LCM method forming columns with undrained shear strengths of 100 kPa to 300 kPa has proven to be an economical and technically sound solution in very soft clays worldwide. It is however of great importance to keep in mind that LCM or DDM is a soil improvement system using combined parameters where column and soil interact, and that the method has been developed in Scandinavia for Scandinavian soils. The development of new applications and the

introduction into untested soils requires a wide experience of the developed methodology and the achievable parameters and a careful evaluation of and respect for the local soil conditions on every project.

In the future applications using LCM columns will continue to be developed and new areas and countries will adopt the method.

Applications where the LCM method can be considered and extended include stabilising contaminated soils, wider use of high strength columns, for mitigation of vibration from high speed trains or plant and stabilisation of flood protection embankments. Areas where the method could be employed are in all types of soft soils especially in flood deltas and clay deposits of great depth.

As the DDM method is developing worldwide new requirements regarding design QA/QC control and performance will be a major task for the LCM method in the future to support the design and development of applications.

4 REFERENCES

Bredenberg, H., Holm, G. and Broms, B. (1999). *Dry mix methods for deep soil stabilization.* Proc. of Int. Conference on Dry Methods for Deep Soil Stabilization, Stockholm, Balkema, 358pp.

Broms, B. and Boman, P. (1978) *Stabilization of soil with lime columns*, Design Handbook Second edition, Department of Soil and Rock Mechanics, Royal Institute of Technology.

Dahlström, M. and Eriksson, H. (2005) *Mass stabilisation in Smista allé (2002) and Moraberg (2003) by the cell and block stabilisation methods.* Proc. Of Int. Conference on Deep Mixing – Best Practice and Recent Advances, Stockholm, state of practice report.

EuroSoilStab (2002 *Development of design and construction methods to stabilise soft organic soils. Design guide soft soil stabilisation.* CT97-0351. Project No BE-96-3177. European Commission. Industrial and Materials Technologies Programme (Brite-EuRam III), Brussels, 94pp.

Larsson, S. (2005) *State of practice Report – Session 6 Execution, monitoring and quality control.* Proc. Of Int. Conference on Deep Mixing – Best Practice and Recent Advances, Stockholm, state of practice report .

Massarch, M. and Topolnicki, M. (2005) *Regional Report: European Practice of Soil Mixing Technology,* Proc. Of Int. Conference on Deep Mixing – Best Practice and Recent Advances, Stockholm, Vol. 1, pp. R19-R45.

prEN 14679 (2005) *Execution of special geotechnical works – Deep mixing.* CENT C 288, AFNOR, Approved standard, 50pp.

SGF (2000) *Lime and lime cement columns. Guide for design, construction and control.* Report 2:2000, Swedish Geotechnical Society, Linköping, 111pp (in Swedish).

Topolnicki, M. (2004) *In situ soil mixing.* Chapter 9 in Ground Improvement 2nd Editors M. Moseley and K. Kirsch, Spon Press, Oxon, pp 331-428.

SOFT SOIL CASE HISTORY: SHELLHARBOUR SEWAGE TREATMENT PLANT UPGRADE

P.R.E Davies[1] and A. Faulkner[2]
[1] Senior Geotechnical Engineer, Golder Associates, [2] Geotechnical Engineer, Sinclair Knight Merz

ABSTRACT

This paper describes ground engineering challenges and solutions employed at a soft ground site near Shellharbour, New South Wales. Geotechnical issues encountered during the sewage treatment plant upgrade project included:

- Deep peaty soils at the backfilled swamp site
- High groundwater level and potentially high inflows through permeable fill
- Large clarifier tank excavations (approx 80 m x 80 m x 5 m deep)
- Flooding and acid sulphate soils
- Potential settlement impacts on existing infrastructure.

Ground engineering risks were successfully managed through adequate scoping of investigations, numerical modelling of designs and involvement of geotechnical engineers during construction. A comparison of actual versus predicted behaviour for an anchored sheetpile wall is presented, enabling an evaluation of WALLAP and PLAXIS software. The value of geotechnical observations and monitoring during construction is also discussed.

1 INTRODUCTION

This case history provides a summary of design and construction techniques used in soft ground conditions for the upgrade of Shellharbour Sewage Treatment Plant (STP) in New South Wales, Australia. In particular, this paper describes the design and behaviour of a large, sheetpiled excavation at the site and draws conclusions about the performance and possible improvements that may be achieved on similar future projects.

The site is situated in a low-lying area behind the dune environment of Shellharbour Beach, about 1 km north of the town of Shellharbour. Prior to the 2005 upgrade, the treatment plant was constructed in two phases during the 1970s and 1980s. Figure 1 shows the layout of the site.

The site was originally part of Barrack Swamp, which was reclaimed by backfilling with gravelly coal wash reject material. Construction drawings showed that early excavations for in-ground tanks and lagoon structures utilised a perimeter clay cut-off wall to limit groundwater inflow (dashed line around existing structures in Figure 1). Anecdotal evidence indicates that this was not entirely successful and that steel sheet piles were used to provide additional groundwater cut-off and improve excavation stability.

The recent upgrade was commissioned by Sydney Water in late 2004 under a Design and Construction Contract, awarded to United Group (Formerly UKG) as the Contractor and Sinclair Knight Merz as Designer. The $25M augmentation comprised construction of 4 x 30 m diameter buried clarifier tanks, control and distribution chambers, a buried pump station, chlorination and grit facilities, ancillary buildings, tanks, biofilter beds and associated roads, embankments and retaining structures. The focus of this paper includes the investigation, design and construction of the in-ground clarifier tanks.

2 SURFACE AND SUBSURFACE CONDITIONS

The landscape surrounding the extensively filled Shellharbour STP site comprises gently undulating and mounded grassland and bushes, with relief to 3 m. Low lying parts of the site are subject to periodic flooding, associated with the tidal Tongarra Creek running along the western and part of the southern site boundary. The average ground surface level of the site is RL 3 m AHD, which is above the 1 in 100 year flood level (RL 2.8 m AHD). However, a large depression covering much of the area of the proposed clarifier tanks was as low as RL 1 m AHD in places, and frequently flooded.

Adjacent to the creek, the ground surface comprises marshland vegetation of Barrack Swamp and the nearby Shadforth compensatory wetlands. An adjacent cricket oval was located on a former landfill, which was a potential source of contaminated groundwater.

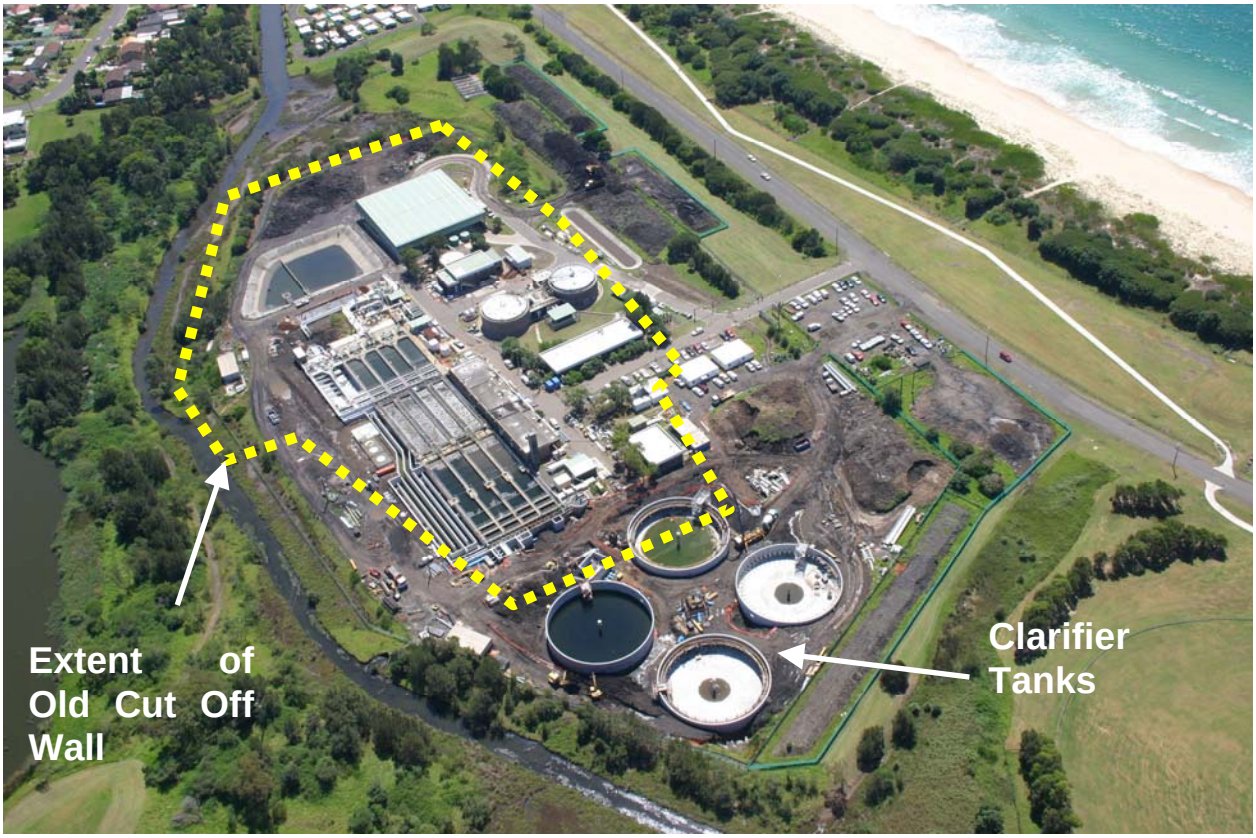

Figure 1: Site layout (during construction).

A geotechnical investigation was carried out by SKM in 2004 with the objective of collating existing information and gathering additional information for detailed design. Additional investigation included:

- Desk study, review of existing information including information from four previous investigations, which included 22 boreholes, 2 CPTs and 10 Test Pits;
- Drilling of 9 additional cored boreholes, with *in situ* strength testing and acid sulfate screening;
- Excavation of 9 exploratory test pits using a backhoe and a groundwater pump-out test;
- Installation of 3 standpipe piezometers for groundwater monitoring and falling head tests and
- Geotechnical laboratory testing including classification tests, oedometer tests, triaxial strength tests, aggressivity tests, POCAS tests, organic content tests and Californian Bearing Ratio (CBR) testing.

Table 1: Summary of Ground Profile.

Unit	Depth to top of unit (m)	Thickness (m)	Origin / Type	Description
1	0	1 – 5	Fill	FILL: comprising asphalt paving or topsoil over a highly variable mixture of sandy GRAVEL (coal wash reject), with cobbles of slag and zones of gravelly CLAY.
2	1 – 5	0 – 5	Estuarine Swamp	Clayey PEAT / Peaty CLAY low to medium plasticity, with fibrous material, brown and black. Very soft and highly compressible, odorous.
3	3 – 6	1 – 4	Estuarine	Organic Silty CLAY, medium plasticity, grey. Very soft and compressible. Locally interbedded with Unit 2.
4	6 -9	2 – 5	Alluvial (possibly estuarine)	Sandy Silty Clay, medium to high plasticity, grey with yellow brown. Highly variable mixture of sandy CLAY or clayey SAND. Sand is fine to medium grained.
5	8 – 14	0.5 – 4	Residual	Sandy Silty Clay, medium to high plasticity, grey mottled yellow brown or orange brown stained. Sand is generally fine to coarse grained.
6	10 – 15	-	Bedrock	SANDSTONE, fine to medium grained, volcanic/tuffaceous, distinctly weathered and medium to high strength.

The investigation showed that the uppermost ground profile comprised widespread fill of mostly slag and coal wash reject (also called 'chitter'). Natural soils comprised recent swamp deposits including organic peat and organic clays over soft estuarine clay and stiffer sand/clay mixtures of Quaternary age. The lower alluvial material was judged to be overconsolidated and deposited during an earlier geological epoch. Bedrock was identified in all cored boreholes as Budgong Sandstone, at an average depth of 12 m in the area near the proposed clarifier tanks.

Six geotechnical units were used to build the geotechnical model, which is summarised in Table 1.

A cross section through the site is shown on Figure 2 which illustrates this ground profile in the vicinity of the proposed clarifier tanks. It is worth noting a few additional characteristics of the upper soil units to illustrate the challenging nature of the soft ground conditions and how they affected the design of the proposed clarifier tank excavation.

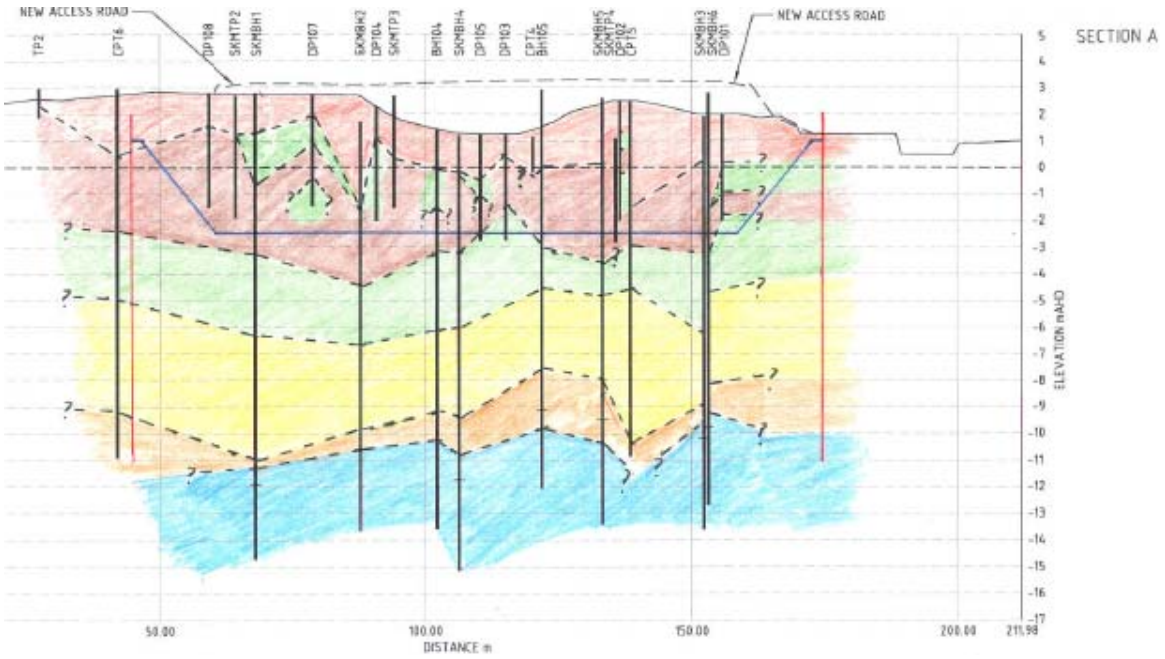

Figure 2: Cross Section through Clarifier Tanks.

The Unit 2 peaty soils were typically dark brown and where encountered, varied from pure peat of almost completely un-humified, fibrous plant remains to highly amorphous peat and clay mixtures. The Unit 2 soils were typically 3 m thick with a very high acid sulfate soil potential upon oxidation. Unit 2 peaty soils were found to vary from very soft to soft and spongy. Tree trunks and obstructions were also identified in the upper swamp deposits and fill. Corresponding organic content test results in Unit 2 soils varied from 60% to less than 10%. Samples having a high percentage of organic matter had high moisture contents of up to 339%, and material density as low as 11.6kN/m^3.

Below peaty soils, a layer of very soft to firm grey silty clay of high plasticity (Unit 3) was observed. To illustrate the low strength of these soils, the authors noted during investigation that the consistency of the estuarine clay in the softest, low lying areas was similar to toothpaste. In some areas, shells and shell fragments were observed, indicating an estuarine alluvial origin.

The thickness of this silty clay unit was about 3 m on average, although in many cases there was no clear boundary with the underlying alluvial unit. Permeability and therefore excavation inflows associated with this unit were expected to be low.

The clarifier excavation works had significant potential to generate acid sulphate soil and groundwater due to:

- Oxidation of potential Acid Sulfate Soils (ASS) exposed in excavation spoil and side walls of excavations and
- The oxidation of potential ASS soils due to changes in groundwater level.

An acid sulfate management plan was developed to prevent migration of impacted groundwater to off site receptors and control the handling and disposal of acid sulphate spoil, leachate and excavation water. The plan incorporated avoidance and mitigation strategies and detailed the management of stockpiles, neutralisation of impacted water and included a monitoring program and contingency measures.

3 GROUNDWATER

Groundwater exists at shallow depth throughout the low-lying site and its behaviour is influenced by the surrounding tidal creek. Groundwater levels measured during fieldwork were commonly in the range 1.0 m to 1.5 m AHD and high groundwater inflows were expected for excavations intersecting the highly permeable gravelly fill. In particular, control of groundwater at the large clarifier tank excavation (up to 6.5 m deep) was identified as a major issue at tender stage.

The reference design at tender stage included groundwater cut-off works comprising an 80 m length of sheet piling along the creek boundary adjacent to the clarifier excavation, with the objective of reducing groundwater inflow to a limit of 1 ML per day. An additional rate item was included with the tender to cover additional sheet piling if required. Subsequent analysis carried out as part of design estimated inflows of up to 2.2 ML/day for an open cut clarifier excavation, which led to the adoption of a circumferential cut-off wall to reduce groundwater inflow.

Following award of the tender, it was necessary to check the hydraulic connection between the tidal creek and the permeable fill and refine likely groundwater inflows and control options. Groundwater response in standpipe piezometers within the fill was periodically measured during the site investigation and compared against tidal variations. However, no consistent relationship was established between the groundwater and tidal fluctuations, probably due to the irregularity of manually read piezometer data.

Additional groundwater observations, including falling and rising head tests and pump out tests from pits during the investigation, indicated that the transmissivity of the fill was very high. It was inferred that significant recharge would occur in this layer, given the proximity to the tidal creeks and likely degree of hydraulic connection.

Despite the high transmissivity, it later became apparent that the fill was not so well connected to the creek and that once drained, the long term, steady state recharge of the gravel aquifer was less than expected. In this regard, a longer term pumping test utilising a production well and monitoring bores along with continuously datalogged piezometers would have been beneficial.

4 DESIGN PARAMETERS

The soil and rock design parameters adopted for analysis are shown on Table 2. These were based on a moderately conservative design line selected through combined test results and correlations for all available investigation data (current and historical). The corresponding anchor loads and bending moments from WALLAP analyses were treated as working load values to which appropriate safety factors were then applied.

Preliminary anchor design was carried out using limit state design methods according to the Australian Standard for Earth Retaining Structures (AS4678, 2002).

Table 2: Soil and Rock Design Parameters.

Unit	SPT 'N'	Bulk Density, γb (kN/m3)	In-situ Stress, K'o	Undrained Modulus Eu (MPa)[1]	Friction Angle, ϕ' (Deg)	Drained Cohesion c' (kPa)	Undrained Shear Strength Su (kPa)[1]	Permeability, K (m/s)
1. Gravelly FILL	3 - 29 Ave 14	18	0.44	2Z	34	0	0	1×10^{-3}
2. Estuarine Clayey PEAT / Peaty CLAY	0 - 4 Ave 1	14	0.69	1+0.35Z	18	2	3+1.2Z (Ave 8)	1×10^{-5}
3. Estuarine Organic Silty CLAY	0 - 5 Ave 4	16	0.62	2+0.34Z	22	2	6+1.1Z (Ave 14)	1×10^{-8}
4 & 5 Alluvial / Residual SAND & CLAY.	5 - 22 Ave 12	18	0.56	4.5+0.75Z	26	2	15+2.5Z (Ave 40)	1×10^{-8}
6. Tuffaceous SANDSTONE Bedrock	Refusal	24	-	100	42	200	-	1×10^{-7}

Note:

1. Where Z is depth measured below ground surface

5 DESIGN APPROACH

This section deals with the soft ground engineering issues relating to the large temporary excavation containing the four circular concrete clarifier tanks. Final excavation levels varied from RL -2.5 m at the outer edge of the tanks to -3.5 m AHD at the central sump of each tank. An additional 1 m of over-excavation was required for an under-tank drainage layer. Resulting excavation depths in the area of the buried clarifiers varied from 4.5 m to 6.5m.

During tender and preliminary design stages of the project, the following main excavation options were identified:

- Open cut (approx 100 m x 100 m x 5 m average depth) with shallow treatment / cut-off to reduce inflow;
- Secant piled tank structures installed from ground surface;
- Cantilevered sheet pile retaining wall around perimeter with supporting berm and
- Anchored sheet pile wall around perimeter without supporting berm.

Secant piles were eliminated at the pre-tender stage, due mainly to cost. The open cut option without cut-off walls was impractical due to space restrictions, dewatering impacts and slope instability associated with high slope pore pressure. Much of the design effort therefore went into developing a cost effective perimeter wall solution.

The cantilever wall with internal buttress berm was initially favoured to save on the cost of anchors. A sub-option of vinyl sheet piles to provide groundwater cut-off was considered, but wall displacements and space restrictions were problematic. To reduce movements of the cantilever wall to an acceptable level it was necessary to install the wall close to rock surface in combination with an internal berm (1V:4H). A series of limit equilibrium analyses were carried out using the software package SLOPE/W to optimise the slope geometry and check the internal berm stability (See Figure 3).

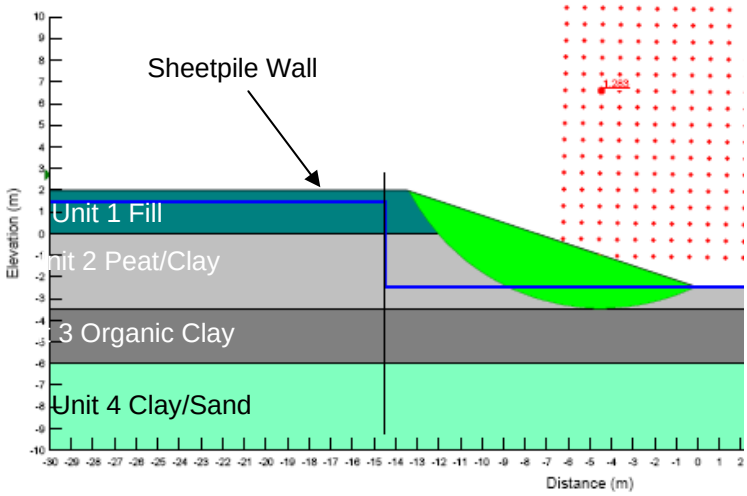

Figure 3: Stability Analysis for Internal Berm (fully drained).

As the design progressed, space constraints became significant so the internal berm was replaced by anchors, except in the area of the eastern entry ramp. Two types of sheet pile section were adopted (Larssen LX 16 and LX6W), depending on the retained height and proximity to sensitive structures. A schematic design in the vicinity of existing structures is shown in Figure 4.

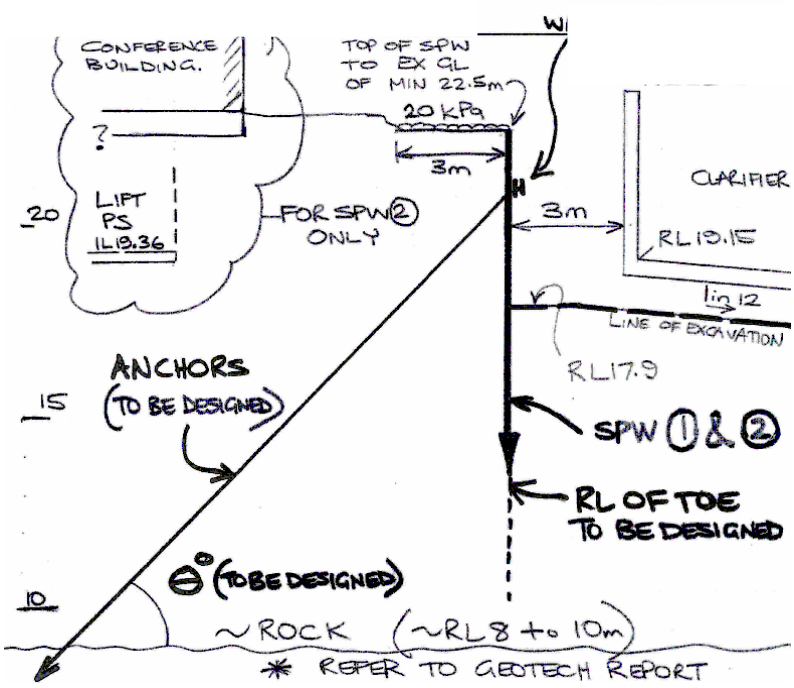

Figure 4: Schematic design of anchored wall (Note: Sydney Water datum used +20 m AHD).

The main design tool used to assess anchor and wall behaviour was WALLAP software. Groundwater behaviour near excavation works was analysed using the finite element package SEEP/W. Stability assessments for the berm and cantilevering wall options were checked using SLOPE/W.

Two main analyses were carried out:

- Case 1 – LX16 anchored sheetpile wall, as used near existing structures and
- Case 2 – LX6W cantilevering sheetpile wall with buttressing berm near location of haulage ramps.

Drained conditions in cohesive materials were not expected to occur within the construction timeframe for excavation Stage 1. Stage 2 was checked using drained and undrained soil parameters, because effective stress conditions had the potential to develop over the expected construction period of 6 months.

Checks were then carried out on wall displacement, safety factors, bending moment, shear force and wall buckling capacity. The whole design optimisation process and sensitivity assessment involved running over 100 WALLAP models to examine the effect of variables such as soil strength, drainage condition, wall toe level, anchor pre-stress and live load at each key cross section.

6 DESIGN OUTCOMES

For brevity only Case 1, incorporating the anchored sheet pile wall driven to rock, is discussed further in this paper. The results of critical WALLAP analyses are shown in Figure 5 and are discussed further below.

The factor of safety using a gross pressure method was calculated to be consistently above 1.8, and the controlling factor in the design was the management of wall movements to avoid impacting nearby structures – particularly along the northern wall.

Due to the low soil stiffness values used, wall deflections were found to be highly sensitive to surface loading and anchor pre-stress. Application of a full 20 kPa surcharge (i.e. large tracked excavator) during the cantilever Stage 1 excavation was predicted to cause unacceptable movements at nearby structures, and hence a construction plant exclusion zone within 3m of the wall crest was established along the critical northern anchored wall.

Key design findings are summarised below:

- Horizontal design waler loading at RL 0.5m AHD was approximately 130 kN/m run, based on a 30º inclination from horizontal, assumed anchor stiffness and pre-stress to 50% of anchor load.
- Sheet piles were not required to be driven to rock for stability or groundwater cut-off reasons, but were extended to sandstone rock surface to reduce the risk of wall movement under the vertical component of anchor loading.
- Anchor pre-stress of 50% working load (rather than 100%) was specified in order to accommodate additional anchor loads that WALLAP predicted would occur as excavation proceeded and reduce predicted movements back into retained soil. All temporary anchors were proof load tested to a minimum 125% working load.
- Estimates of vertical and horizontal ground movements away from the sheet pile wall were carried out using empirical design envelopes (Clough *et al.*, 1990). Limiting the maximum wall movement to 100 mm was found to result in acceptable movements at sensitive nearby structures which had to remain operational during the works.
- During construction, survey monitoring was used to check ground movements outside the excavation and wall crest movements. Anchor load behaviour was also monitored by a hydraulic load cell (See Section 8).

Seepage analyses indicated that groundwater cut-off was required through permeable fill around most of the excavation perimeter to reduce groundwater inflow to less than the required 1 ML/day. This flow rate was inferred to be the maximum amount that could be pumped into the sewage treatment plant. The tank design incorporated under-tank drainage to prevent buoyancy forces when tanks are emptied for periodic maintenance. To reduce the amount of under-tank drainage required, each tank incorporated a circumferential clay cut-off wall extending below the tank and under-tank drainage fill layer.

The SEEP/W seepage model extended about 50 m laterally westwards from the excavation crest to include the tidal creek, which flowed along the western site boundary and acted as a source of groundwater. The recharging effect of the dune aquifer and sea some 200 m to the east, was modelled using free and fixed head conditions at an infinite boundary. The actual response of the eastern boundary may lie somewhere between these conditions. A SEEP/W output showing the cut-off effect of the sheet pile wall with berm is shown in Figure 5.

Various sheetpile and berm configurations were modelled to establish cut-off depths and inflows during excavation and periodic dewatering of the under-tank drainage layer during maintenance. The key findings of the seepage analyses are presented below:

- It was found unnecessary to extend sheet piles to rock surface for adequate seepage cut-off, however there were overriding requirements to provide sufficient embedment for wall stability and to control displacements.
- During excavation, perimeter sheet pile walls installed near to rock reduced predicted steady state inflows into the clarifier from 2.2 ML/day for no cut off, 1.75 ML/day for 80 m of sheetpile wall, 1 ML/day for 220 m of sheet pile wall and 0.02 ML/day for full perimeter cut-off. Approximately 300 m of sheet pile wall was eventually installed, which resulted in estimated inflows of 0.01 to 0.1 ML/Day during excavation, based on intermittent use of a 50 mm diameter petrol powered submersible pump.

- Post construction steady state flows into tank drainage during operational maintenance were expected to be low at approximately 180-220 Litres/Day/Tank depending on whether full perimeter cut-off works were used. On this basis, permanent sheet piling was not necessary for the periodic, post-construction dewatering of the clarifiers. The design of the under-tank layer and drainage system included further work to optimise the size and layout of drainage pipes, control the grading of drainage fill and reduce clogging on the underside of the drainage layer.
- Groundwater drawdown and associated settlements outside the excavation were not significant for sheet piled options, which effectively prevented ingress into the excavation and limited impacts on external groundwater conditions. The volume of water pumped from the excavation was sufficiently low so that it could be treated on-site as part of normal effluent acid sulfate run-off.

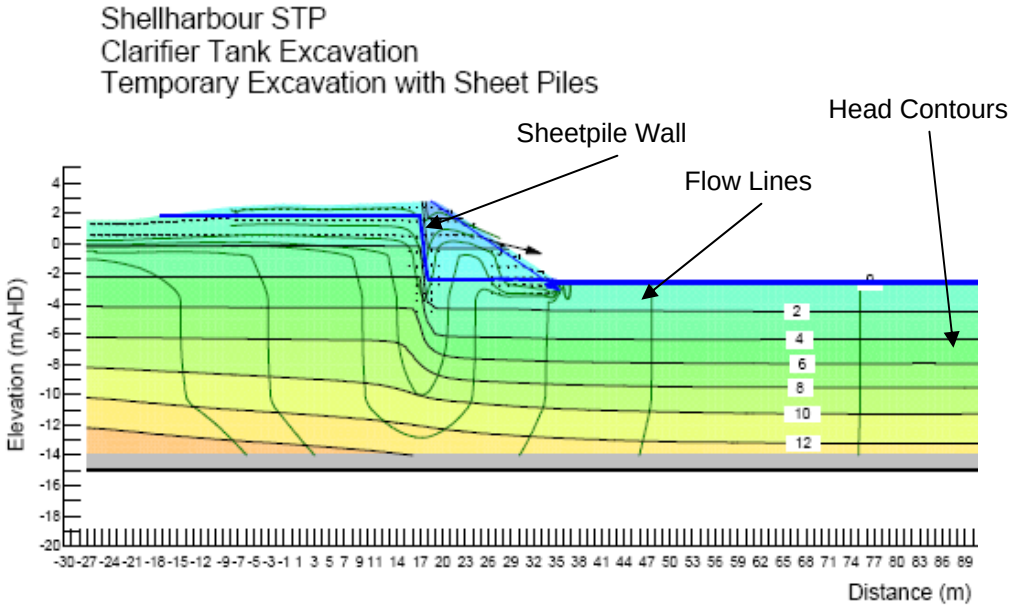

Figure 5: SEEP/W output.

Other design issues included providing suitable details for 'floating' (or un-piled) inter-tank pipework and thrust blocks taking lateral load. In particular, there were concerns that backfilling to higher site levels would cause significant loading of pipes between piled supports due to downdrag as underlying soils consolidated.

Load transfer from overlying soils onto to the ‘bridging’ pipe sections was estimated by considering both 'pull out' wedge mechanisms of material above the pipe and local pipe bearing capacity failure in uplift. The latter was analogous to the resistance available to laterally loaded piles. In all such cases, it was assumed that pipe bedding and trench details were in accordance with the Sydney Water specifications for Standard Trench Details.

7 CONSTRUCTION ISSUES

As excavation for the clarifier tanks and other subsurface structures was underway, it was observed that groundwater inflows through the gravelly fill layer were significantly less than anticipated. Excavations in fill for the chlorination tanks did not incorporate groundwater cut-off yet steady state recharge was low and manageable by intermittent pumping from a single sump point once the fill aquifer was drained. It was inferred from these observations that the hydraulic connection between the permeable fill layer and sources such as the tidal creek were not as well established as initially thought. It is thought that the original slurry wall may also have helped to reduce inflow and hydraulic connection. On this basis, a decision was made to replace a 60 m length of the sheet piled wall with a 1V:4H berm where space constraints and sensitive structures were not critical.

Figure 6 shows the clarifier excavation close to formation level.

A flood event also disrupted the initial excavation works, as a strategic decision had been made to set the wall crest at an elevation close to the 1 in 2 year flood event. However, the topography of the site was such that construction of a low embankment behind the wall crest along the western boundary provided significantly improved flood mitigation.

Additional analysis was then carried out to assess what the potential impact of embankment construction would be on the anchored wall. The geometry and location of the flood control embankment was adjusted to reduce the impact on the wall to an acceptable level and construction proceeded without further flooding.

Figure 6: Approaching final excavation level.

In regard to the design and installation of ground anchors, a preliminary anchor design featuring a fixed length in rock was carried out in order to finalise the anchored wall design and for cost estimation purposes. The successful anchor contractor put forward a non-conforming design which included multi-stage grouting of soil anchors in Unit 3 and 4 soils. Suitability tests on these anchors resulted in poor capacity, and they were rejected at an early stage. Further discussion on the effects of anchor pre-stress is contained in Section 8.

Special attention was also given to the design of the construction platform which was formed at the base of the clarifier excavation to provide support for piling rigs and to act as an under-tank drainage layer during periodic, post-construction tank dewatering. The platform was constructed from the gravelly coal wash reject material ("chitter") which was subjected to a range of laboratory tests to assess strength, durability, grading and resistance to weathering/breakdown. Tests included Particle Size Distribution Test (AS1289 3.6.1), a Slake Durability Test (ISRM) Point Load Strength Tests on Aggregate Samples (ISRM, 1985) and an Accelerated Weathering Test (RTA T103).

Interpretation of the test results indicated that nearly half of the material would breakdown under repeated wetting, drying and abrasion. It was inferred that the upper part of the as-placed construction platform would behave in a similar way under construction traffic, piling rig disturbance, etc. Based on the expected deterioration of the uppermost chitter material under trafficking, a 900 mm thick chitter layer was specified with an additional 300 mm sacrificial layer in areas trafficked by piling rigs. Following analysis, two layers of SS30 geogrid and geofabric were included in the platform.

8 OBSERVATION AND MONITORING

A monitoring plan was developed to include survey monitoring and anchor load monitoring. The plan included trigger levels which were divided into three levels of severity, based on a traffic light analogy (Green, Yellow and Red), in order of increasing severity. Corresponding mitigation actions were then tailored to reflect the sensitivity of particular structures. As with any monitoring plan, the purpose was to:

- Enable checking of actual versus predicted performance;
- Provide early warning of unexpected behaviour;
- Facilitate a managed response strategy (i.e. escalating trigger levels) and
- Protect stakeholders in the event of a dispute.

Following baseline and dilapidation surveys, monitoring was carried out during excavation and construction, at a frequency which was reviewed regularly and which was linked to the performance of the works. The initial frequency of displacement and anchor load monitoring took place on a two-weekly basis over the duration of excavation until movements and loads stabilised.

Trigger criteria were established to provide a framework of limiting thresholds, against which measured displacements/loads could be compared to determine what action would be needed to facilitate safe excavation. The

assessment of tolerable ground and structural movements was based on numerical analyses and commonly adopted serviceability criteria for structures. Traffic light criteria were defined as follows:

- Monitoring results in the "green" range are acceptable and require no action, beyond continuation of monitoring, if appropriate.
- Results in the "yellow" range require immediate investigation to determine the cause of the deformations and possibly more frequent or additional monitoring.
- Movements or loads in the "red" zone require stoppage of work until the nature of the deformations and their potential effects have been fully assessed. In this case remedial works may be required, which could potentially include installation of additional anchors.

The specific trigger level criteria adopted for this project are shown in Table 3:

Table 3: Monitoring Criteria.

Item	Green	Yellow	Red	
			Max. Displ. (mm)	Max. Angular Distortion (Δl/l)
Lateral movement at crest of northern anchored wall (near structures)	<100 mm	101-150 mm	>150 mm	N/A
Lateral movement at crest of other walls	<100 mm	101-200 mm	>201 mm	N/A
Structures - high sensitivity (e.g. PST, Chlorination Channels, Tank Structures)	<5 mm	5 – 10 mm	>10	1/500
Structures: low sensitivity (e.g. Conf. Centre)	<15 mm	15 – 40 mm	>40	1/350
Road / footpath Areas	<30 mm	30 – 50 mm	>50	1/100
Anchor load	< 100% working load	100-120% working load	>120% working load	

Selected wall crest displacements are shown on Figures 7 and 8.

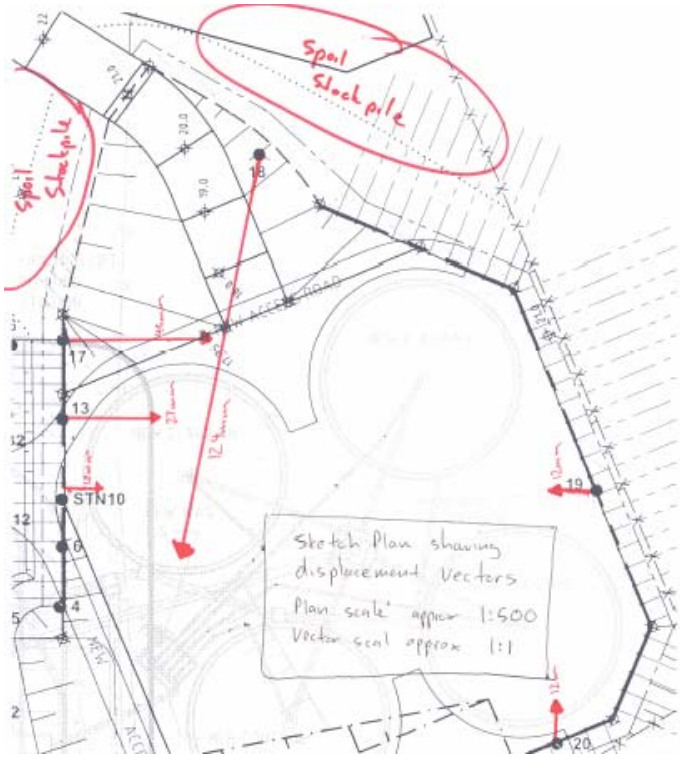

Figure 7: Measured displacements around clarifier excavation.

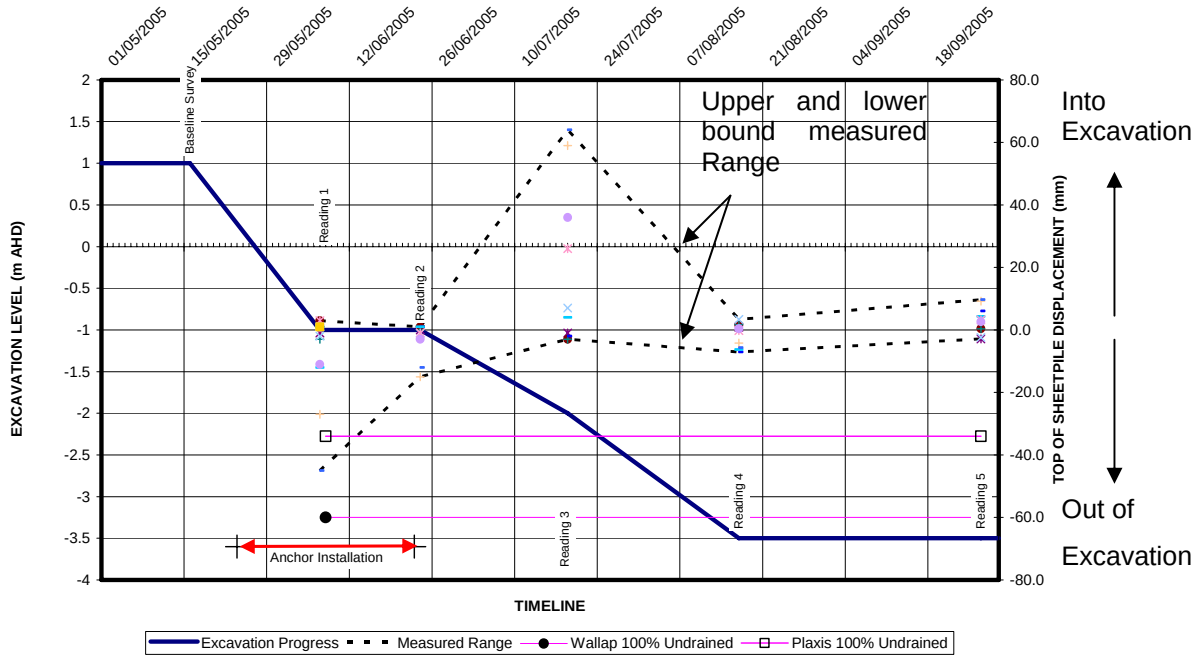

Figure 8: Measured and Predicted Displacements along Northern Wall.

Notable outcomes from the monitoring exercise are summarised below:

- Measured displacements and loads were all within the green or yellow range and no additional monitoring was necessary after the excavation phase. A plot showing the range of recorded movements is shown in Figure 8, which shows that actual crest movements were less than predicted.
- The anchor load cell was initially fitted to an anchor on the northern side of the excavation which was pre-stressed to 100% of working load. Load dropped 15% then recovered slightly, during a period of no excavation. This load change is inferred to be due to compression of retained soil and fill near anchor level.
- Due to a change in excavation programming, the load cell was relocated and the anchor only stressed to 50% of working load, in accordance with design recommendations. About 8 weeks after installation, following excavation to full depth, the anchor load had increased by 20%.
- The highest wall crest displacements of up to 124 mm were recorded in the vicinity of the cantilevering sheet pile walls at the eastern haulage ramp. The trend of data correlated well with proximity to the large spoil stockpiles, which were in the order of 5 m high (See Figure 7). Recommendations were provided at investigation stage to limit the height, slope and position of the spoil stockpiles and were reiterated during construction.

Figure 9 shows how the corresponding anchor loads varied over time, compared to loads predicted by PLAXIS and WALLAP software.

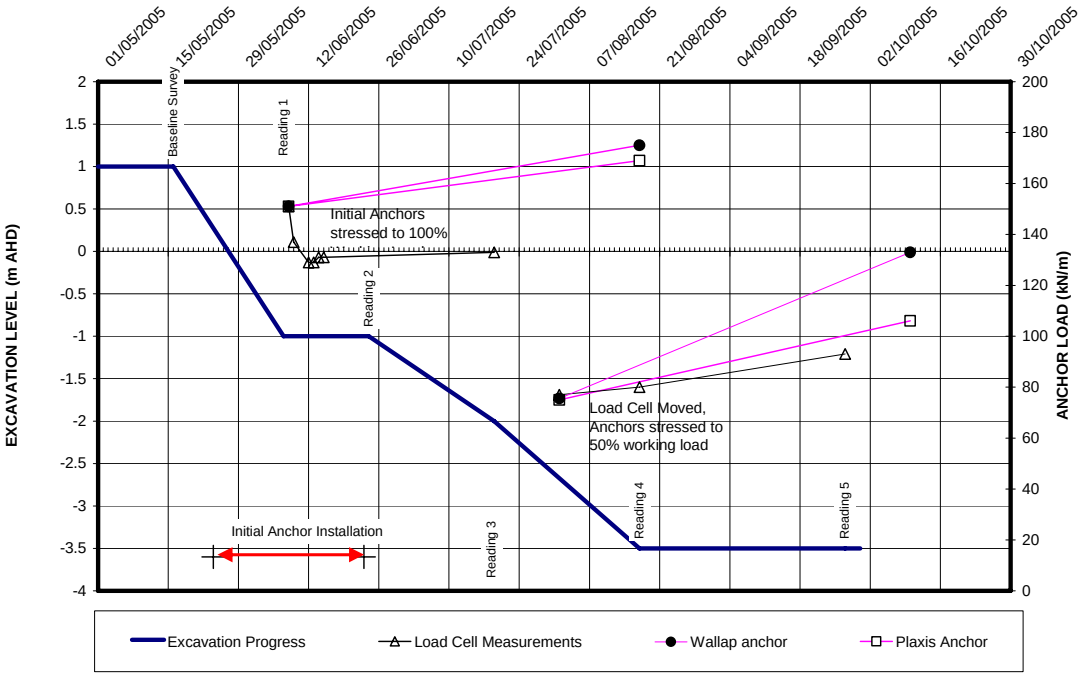

Figure 9: Measured and Predicted Anchor Loads.

9 PLAXIS COMPARISON

The authors felt it worthwhile to explore the issue of anchor behaviour and carry out a comparison against WALLAP, using PLAXIS finite element software. Where possible, the same input parameters were used for both programs (based on Table 2), although some judgment was necessary when considering input conditions such as wall/soil friction and constitutive model (elasto plastic, mohr coulomb used in PLAXIS).

Results for the two main construction stages comprising initial excavation to anchor level (Stage 1) and subsequent excavation to full depth after anchor installation are shown on Figure 10.

It can be seen from Figure 10 that the predicted movements at the initial cantilevering wall excavation stage are very similar and close to the upper range of measured wall displacements. Only results from undrained analyses are shown at Stage 1, due to the relatively short timeframe of this stage. Following anchor installation and excavation to full depth (Stage 2), the familiar anchored wall deflection profile is generated, although with a wide range of possible displacements depending on the amount of anchor pre-stress used and drainage condition.

Intuitively, the lower pre-stress value of 50% working load results in greater movement into the excavation. In these soft soil conditions, using 100% pre-stress resulted in large movements back into the retained soil. In order to limit the potential for such movement and to allow some spare capacity for the predicted rise in anchor loads as excavation proceeded, a 50% anchor pre-stress was specified on construction drawings. Interestingly, WALLAP predicted significantly larger movements into the retained soil than PLAXIS.

Initially, the anchor contractor stressed all anchors to 100% working load, and hence the applicable curves on Figure 10 (Stage 2) are those with negative value crest movements. The range of predicted wall movements (-30 mm to -80 mm) exceed the range of measured net crest movements along the northern wall (+/- 10 mm), although almost all of the 40 mm movement into the excavation was recovered.

The lack of movement back into retained materials may be due to a number of factors including higher-than-modelled soil stiffness, inappropriately modelled soil/wall friction in the anchor induced passive zone and the fact that large forces are required to initiate significant yielding in the passive anchor zone.

It is interesting to note that anchors installed with higher pre-stress lost load, whereas those with lower pre-stress picked up load (Figure 9). Loss of load may be partly due to consolidation of retained materials under highly pre-stressed anchor loading. Unfortunately no excavation occurred before the anchor was relocated, so we do not know whether loads would have increased as excavation took place. Conversely, the uptake of load in more lightly loaded anchors appears to support the modelling work, which may be a significant factor when considering appropriate pre-stress values and anchor capacity in deep soft ground excavations.

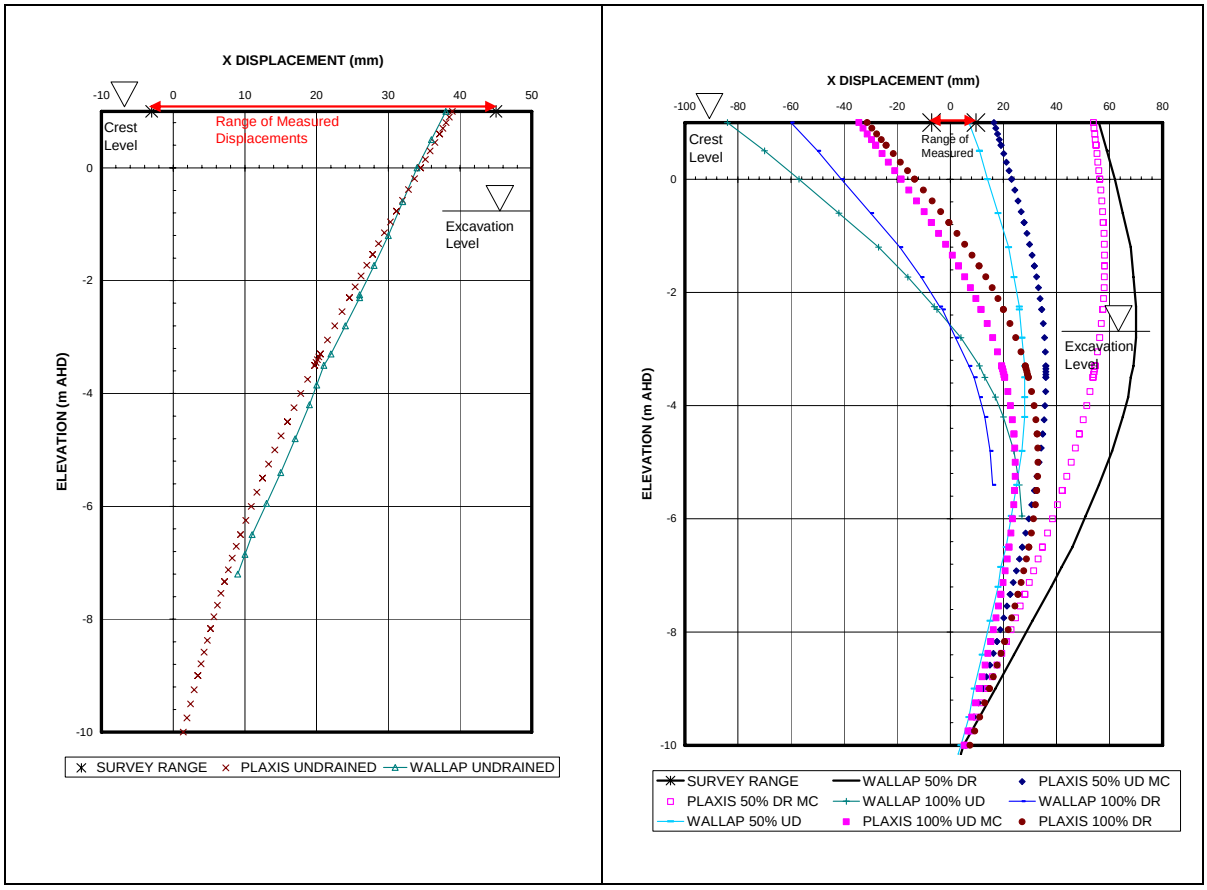

Figure 10: Measured and Predicted Displacements at Cantilever (Stage 1) and Full Depth (Stage 2).
Note: percentage relates to amount of anchor working load mobilised at installation.

10 CONCLUSIONS

This paper presents the findings of a case study on the investigation, design and construction of a large excavation as part of the upgrade of Shellharbour Sewage Treatment Plant (STP). The key outcomes of the case study are summarised below:

- The site is located in a former low-lying swamp, which has been filled over a wide area. A thorough site investigation provided a sound basis for design and revealed that the ground profile comprised gravelly fill (slag and coal wash reject) above organic peat and clays, overlying soft estuarine clay and progressively stiffer alluvial sandy clays. Bedrock surface (Tuffaceous Sandstone) occurred between RL-8 m and -14 m AHD.
- Groundwater was found at shallow depth throughout the low-lying site, and the surrounding tidal creeks influenced its behaviour. Actual inflows into excavations were significantly less than anticipated, which may be associated with the presence of an old slurry wall. An extended pump test using data loggers may have identified this at an early stage. Inflows were manageable during construction and under-tank drainage has performed well during post-construction dewatering.
- Selection of excavation support systems utilised WALLAP, SLOPE/W and SEEP/W numerical models. Both packages matched cantilever movements well, although over-predict movements into retained soil due to anchor loading. Post installation anchor loads varied by up to 20%.
- The authors consider that the use of the latter “one stop” design software incorporating stability, seepage and soil-structure interaction analyses would be used on similar future design tasks for convenience. In this case, further consideration of the most appropriate constitutive model would have been needed.
- Risks to existing infrastructure were successfully managed through the implementation of a monitoring plan incorporating red/yellow/green “traffic light” criteria. Measured displacements and loads were all within green or yellow range and no additional monitoring was necessary after the excavation phase.

- Construction issues were successfully resolved through the continuing, close involvement of geotechnical engineers through the construction stage. Examples include:
  - Flooding, which was successfully managed through construction of an additional embankment;
  - Construction platform, which involved thorough materials testing to verify the suitability of on-site materials for re-use as structural fill with good drainage properties; and
  - Reduced groundwater flow and monitoring, meaning savings could be achieved by replacing a significant section of sheet pile wall with an open cut slope.
- The response of displacements and anchor loads to the level of anchor pre-stress is of interest. The limited data in these soft soil conditions supports the adoption of reduced pre-stress so as to provide spare anchor capacity, although mobilising high pre-stress led to less uptake of load and did not appear to cause significant movement into the retained soil. Further research into the response of anchor loads in soft soil conditions would help to clarify these mechanisms and guide future design.

11 REFERENCES

Clough, G.W. and O'Rourke, T.D. (1990), Construction induced movements of *in situ* wall. Design and Performance of Earth. Retaining Structures (ASCE 25:439–470.

Hazelton, P.A. (1992), Soil Landscapes of the Kiama 1:100,000 Sheet. Soil Conservation Service of NSW, Sydney.

Geological Survey of NSW (1974), 1:50,000, Geological Series Sheet 9028-1, 1st Ed, 1974, "Kiama"

Soil Conservation Service of NSW, Soil Landscape Map (1:100,000), Soil Landscape Series Sheet 9028, 1993, "Kiama"

Department of Land and Water Conservation 1:25,000 Acid Sulfate Soil Risk Map 9028N1 (Albion Park)

Central Mapping Authority of NSW 1:4,000 Series Orthophotomap W8270 – V (The Lake Illawarra)

NSW ASSMAC Technical Committee and Queensland Acid Sulfate Soils Investigation Team (QASSIT) (1998) The Acid Sulfate Soils Management Guidelines.

JET GROUTING FOR LISAROW RAIL BRIDGE RENEWAL

Paul Hewitt[1] and Charles Spaulding[2]
[1]Parsons Brinckerhoff, [2]Austress Menard

ABSTRACT

This paper describes the design and installation of a jet grouted deep foundation system to support a rail bridge on the Main North Line, just north of Lisarow in New South Wales, as part of a bridge renewal. The adopted method of jet grouting is a replacement/mixing technology that uses a high pressure jet to erode and hydraulically excavate soils, to form a grouted soil mass. This is understood to be the first application of the jet grouting technique to support a rail bridge in Australia.

Parsons Brinckerhoff provided a specification, reference design, construction surveillance and certification for the works. Following consideration of alternatives, including driven piles, compaction grouting and mini-piles, Austress Menard was selected to construct the works on a design and construct basis, using jet grouting.

The project was completed on schedule, during limited track possession time, under low headroom conditions. The specification requirements, design, installation, monitoring and post-construction performance of the successful footing system are outlined in this paper.

1 INTRODUCTION

A railway bridge built in 1911 on one of Australia's major railways has been given a new life through the first application of jet grouting to support a rail bridge in Australia. Jet grouting technology is growing in popularity in various parts of the world due to its cost-effectiveness and proven performance, but it had never before been used by an Australian transportation authority to support a bridge.

The bridge spans about 19 m across Cut Rock Creek, 90 km north of Sydney between Gosford and Wyong. It was originally built of masonry piers on timber piled foundations, with about 2.3 m clearance between the steel superstructure and the creek. Originally designed for steam-powered trains, the aging foundations needed to be upgraded to support today's heavier rail traffic and to reduce ongoing maintenance costs. For the Rail Corporation of New South Wales (RailCorp), the choice was between shifting the existing structure to new piers at a higher cost and significant disruption to train traffic, or finding a way to strengthen the existing foundations to support a new bridge.

After evaluating a number of options, Parsons Brinckerhoff and RailCorp concluded that ground treatment would be the preferred solution. Following consideration of alternatives including piles, compaction (displacement) grouting and minipiles, jet grouting was adopted. A load transfer slab and culverts support the bridge loads applied to the 23 metre deep foundations.

2 SITE DESCRIPTION

The site is located at Cut Rock Creek, just north of Lisarow, which is 88.815 km north of Sydney on the Main North Railway Line (see Figure 1).

The previous bridge structure was a two span, transom topped bridge supported on a brick pier and abutments (see Figure 2). The creek bed reduced level is 19.7 m AHD at CPT2 (see Figure 3), and the 100-year flood level is 22.7 m AHD.

2.1 SITE INVESTIGATION

Site investigations were carried out by RailCorp and Austress Menard. Fieldwork included borehole drilling and sampling, cone penetration testing (CPT) and pressuremeter testing. The exploration locations are shown in Figure 3.

The boreholes were drilled with truck-mounted drilling rigs using open hole augering and concrete coring techniques, and air track drilling. Standard penetration testing (SPT) and U50 (50 mm) tube sampling were carried out. The CPT probes were performed using an electric 100 kN truck-mounted rig, without pore pressure measurement. The pressuremeter testing used a Menard GA pressuremeter.

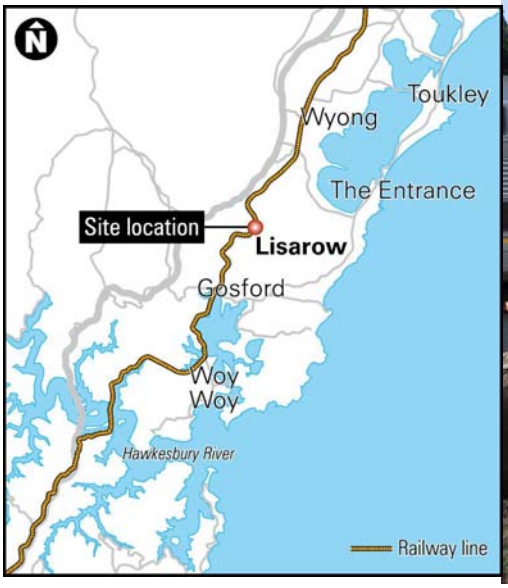

Figure 1: Site location plan.

Figure 2: Previous bridge showing jet grout installation.

2.2 SUBSURFACE CONDITIONS

Subsurface conditions at the site comprised compressible sand and clay alluvium to depths of about 17 m to 20 m, overlying siltstone. The alluvium was highly variable and comprised an upper, very loose to loose clayey sand layer to about 5 m to 6 m depth, over a stiffer, soft to firm, silty clay layer. The CPT probes indicated that the alluvium contained sandy and clayey layers. Soft to firm, silty clay existed from about 5.5 m to the limit of the auger boreholes at 16 m depth. The pressuremeter tests showed that the soil elastic modulus from the first unload-reload cycle ranged from 13 MPa to 20 MPa.

Figure 4 shows a simplified, inferred ground profile, showing the cone resistance (q_c) and friction ratio (F) in the creek bed at CPT2, and an envelope of the cone penetration resistance against reduced level.

The CPT and pressuremeter test results indicate that the subsurface conditions comprised, in descending order:

- 3 m to 4 m of loose silty sand that provides little resistance and has a very low limit pressure (Pl) typically in the range of 100 to 200 kPa; defined as, the point where the Menard pressuremeter tests become asymptotic on a pressure versus volume curve.
- a layer of firm to stiff clay/silty clay from RL 16.5 m to 8.5 m with higher cone resistance (between 0.5 MPa and 2 MPa) and higher limit pressure (600 kPa to 800 kPa).
- interbedded thin layers (about 1 m thick or less) of hard clay/dense sand or gravel from RL 8.5 m to 12 m
- a layer of firm to stiff clay from RL 7.5 m to 1.5 m with limit pressure of 600 kPa to 800 kPa
- a competent founding stratum at a depth of about 17 m to 19.5 m.

CPT3 gave a refusal depth of 16 m. The two air track holes, which penetrated 4 m into siltstone, confirmed weathered rock levels of RL 1.3 m and RL 0.9 m on the western and eastern side of the bridge respectively. The characteristics of the rock improved with depth. The drill rig experienced refusal at RL -4m in both holes in material identified on site as “blue shale”, which was inferred to be representative of the regional siltstone bedrock.

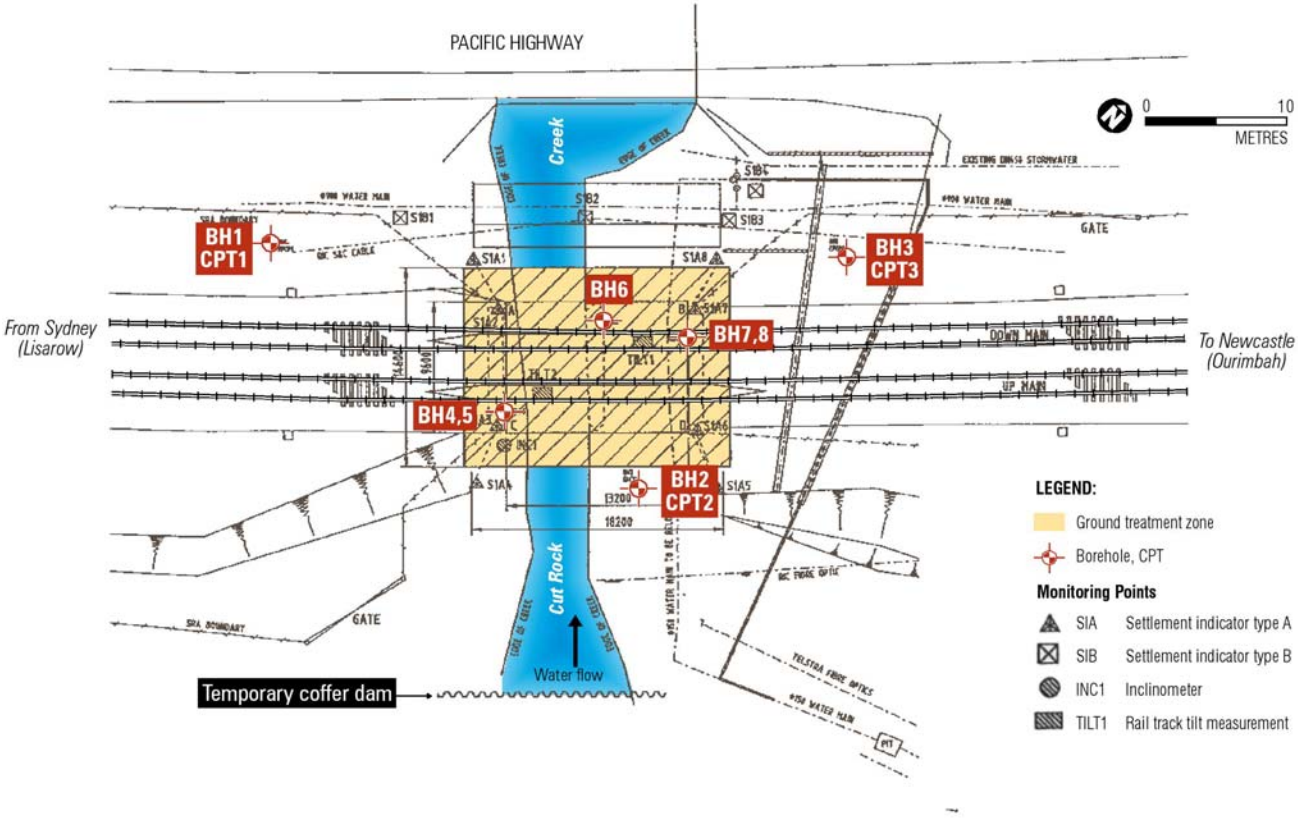

Figure 3: Exploration and monitoring location plan.

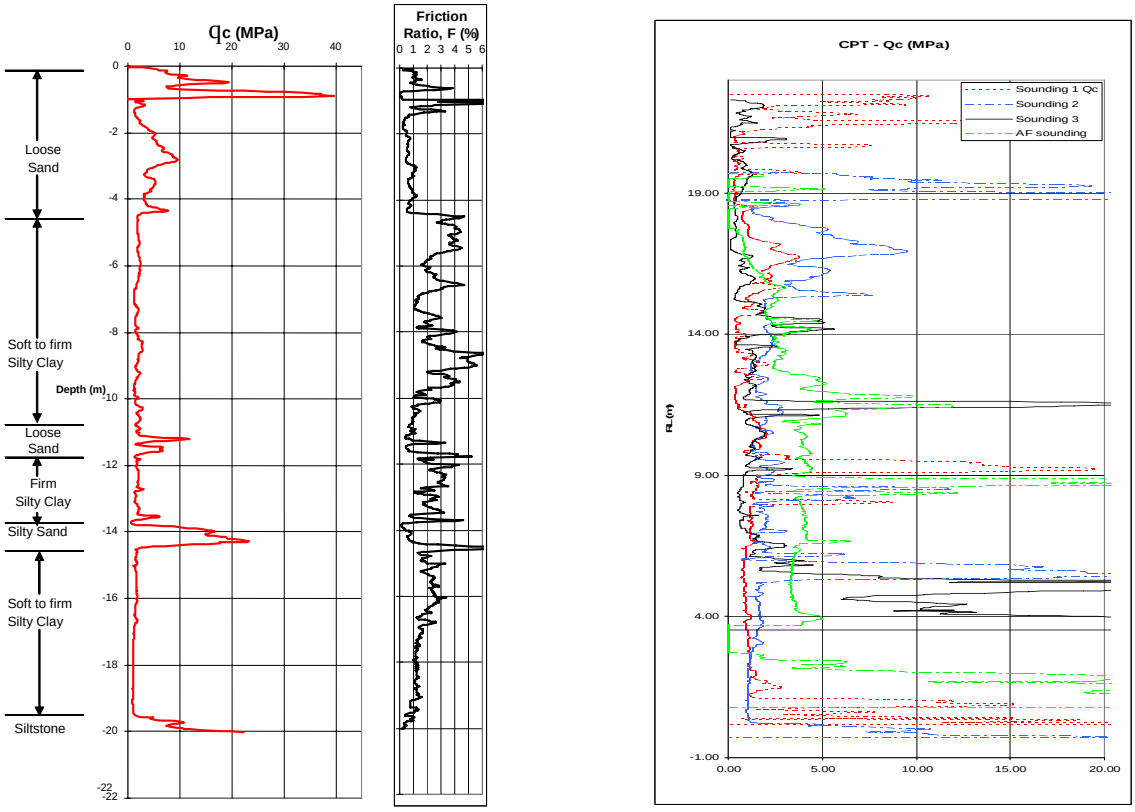

Figure 4: Inferred ground profile and CPT data.

3 FOUNDATION SELECTION

RailCorp's preferred option for replacement of the existing bridge was a concrete box culvert (see Figure 5). However, due to poor ground conditions, the site offered a very low bearing capacity and the prospect of unacceptable settlement, hence the use of conventional culvert foundations was not possible without piling or ground treatment.

Without ground treatment or deep foundations (piles), the bridge was predicted to settle up to 200 mm under a serviceability load of 100 kPa. Piles were not considered suitable due to the existence of adjacent, vibration and settlement-sensitive utilities, including fibre-optic cables, rail communications, a water main and limited clearance of 2.3m beneath the existing bridge.

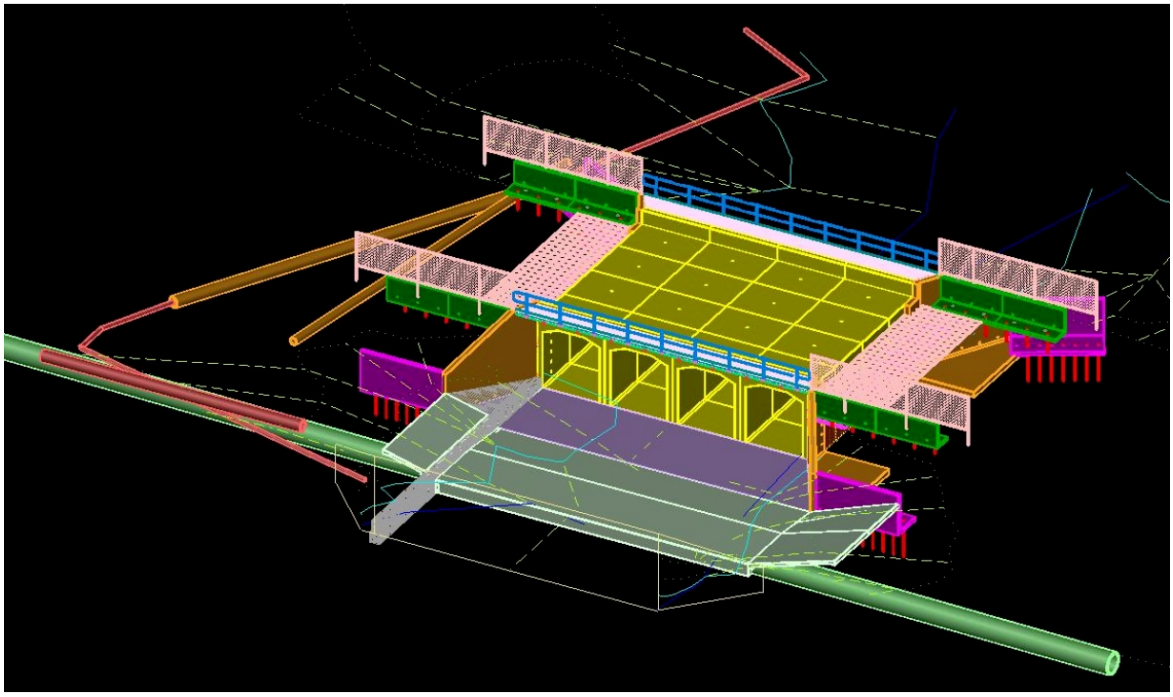

Figure 5: Bridge replacement concept.

Alternative foundation solutions considered by RailCorp at tender stage included:

- piles to transfer loads to stiffer ground at depth
- a large rigid slab to distribute the pressure to acceptable levels
- soil improvement of the compressible soils to support the bridge loads and control settlement.

Tender documents were targeted at achieving the required performance, based on a minimum volume of ground treatment, assessed to comply with design criteria.

4 OPTIONS CONSIDERED

Since a conventional deep foundation system was not considered practical, specialist ground treatment contractors were selected to tender for the works on a design and construct basis, based on tender documents prepared by RailCorp and Parsons Brinckerhoff. Six tenders were received from three tenderers. Details of the proposed methods submitted by the tenderers are summarised in Table 1 and described further in the following sections.

Table 1: Ground treatment methods submitted by tenderers.

Method	Schedule	Tender Details	Relative cost	Comments
Jet grouting	4-5 weeks	18, 1100mm diameter jet grout columns to about 20 m depth. Replacement ratio 6% on 3.3 m x 3.6 m grid – see Figure 9.	1.0 -1.2	Jet grout columns to rock using a mono-fluid system. Predicted settlement complies with design criteria.
Compacting (displacement) grouting	10 weeks	Compaction grouting to the surface of the stiffer soils at about 6 m depth. Involves controlled injection of mortar as an expanding bulb, to displace and compact loose soils, without causing hydrofractures, using low-slump mortar injected under pressure.	1.1 -1.4	Addresses substantial expected settlement in top 6 m. Risk of differential settlement below ground treatment zone. About 160 mm settlement predicted with no ground treatment. Treatment of upper 6m reduces predicted bridge settlement to 25-30 mm.
Minipiles	-	Grout injected minipiles – 150 mm diameter to 20 m depth at 1m centres.	2.0 -2.3	Long construction program and comparatively expensive.

4.1 JET GROUTING

Jet grouting is a partial replacement/mixing technology that uses a tool equipped with one or more high pressure jets to erode and hydraulically excavate soils, while mixing cement grout with the insitu soils, creating soil-cement columns or soil-cement panels (Bruce, 2005). The soil-cement columns are designed to carry loads to the siltstone at between 17m and 20m depth, thereby mitigating the risk of settlement in the alluvium (see Figure 6).

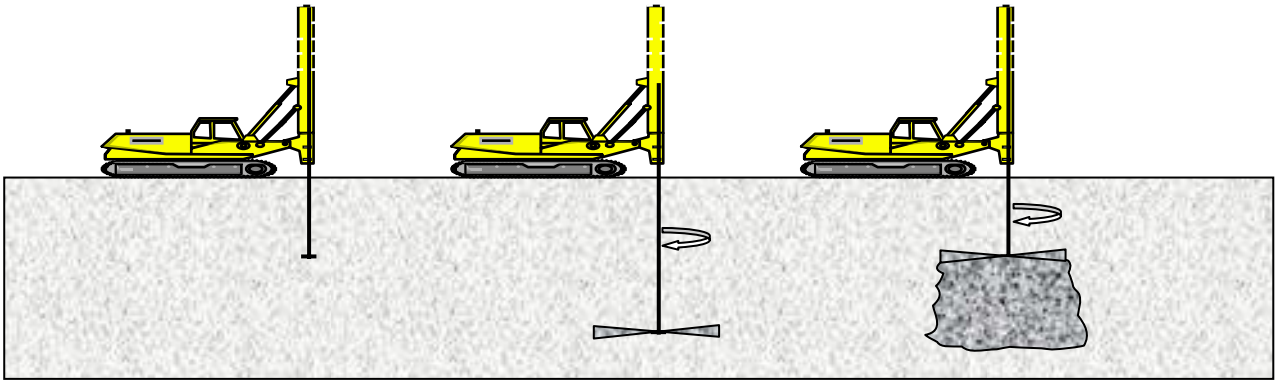

Figure 6: Schematic of jet grouting construction procedure.

4.2 COMPACTION GROUTING

Compaction or displacement grouting is a technique of injecting very low slump grout under high pressure to densify or controllably displace mostly granular soils (see Figure 7). Because the grout is thick, it is unable to enter the pore space of the soil allowing displacement to compact the surrounding soil. This process can be used to minimise the effects of subsidence and settlement caused by underground construction; to arrest sinkhole development; and for large scale site improvements in which loose soil strata preclude the use of alternative methods of support. Bruce (2005) defined compaction grout as grout injected with less than 25 mm slump. The compaction grouting alternative was designed to take foundation loads to the surface of the stiffer silty clay at about 6m depth but carried some additional risk, as it might not meet the stringent settlement performance criteria.

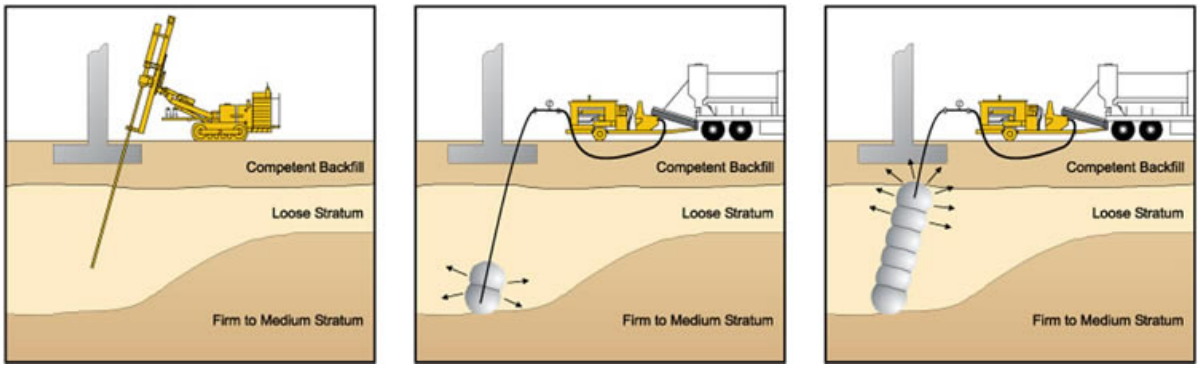

Figure 7: Schematic of compaction grouting (Hayward Baker, 2004).

4.3 MINI-PILES

A solution comprising the use of 150 mm diameter mini-piles, capable of being installed in the low headroom conditions to the underlying siltstone, was also considered. However, this option was rejected on the basis of the likely extended installation time, the lack of sufficient design information on which to assess the tender and cost.

4.4 SELECTION OF THE PREFERRED OPTION

Following a rigorous tender evaluation process, Austress Menard was selected from a group of three competitors and awarded the performance criteria based, design-construct ground treatment contract using jet grouting. Advantages of the jet grouting scheme were as follows:

- All soil types were groutable
- Ability to work around buried active utilities
- Can be performed in limited workspace/ headroom
- Specific in situ replacement possible
- Treatment to specific subsurface locations
- Designable strength and stiffness
- Only inert components
- No harmful vibrations
- Maintenance-free
- Faster than alternative methods and
- Design addressed performance criteria.

5 JET GROUTING DESIGN

The jet grouting construction process employed a high kinetic energy jet of fluid to break down the soil formation, wash the fine particles into suspension, and combine the coarser *in situ* soils with a fluid grout. This process of hydrodynamic washing of the soil and mixing the residual material with grout forms an *in situ* soil-grout mix (Hewitt, 1994). Therefore jet grouting reworks the soils in three distinct physical processes:

- breaking down the soil formation using a very high-velocity (energy) jet
- removing spoil to the surface via the return flow
- introducing and incorporating a binder in the form of a grout.

5.1 DESIGN CRITERIA

Performance criteria for evaluating the method of preferred treatment, including compliance with RailCorp track maintenance specification and British Standard BS EN 12716:2001, "Execution of special geotechnical works – Jet grouting", were:

- immediate settlement of less than 20 mm
- residual settlement limited to a maximum of 50 mm over a 10-year maintenance period
- maximum settlement of 15mm over any 12 month period following construction completion
- differential settlement (change in grade) of : $\leq$ 0.3% longitudinally
  <0.1% transversely
- compliance with RailCorp track maintenance limits.

5.2 DESIGN METHOD

A realistic design of a jet column network can only be developed with a calculation that takes into account both stress and deformation. This calculation should include laws for the behaviour of the soil, the jet column and ground and ground/ grout interaction. In particular, computer programs using simple failure analysis, which are commonly used for routine geotechnical calculations, are not appropriate.

The design process involved determining for a given diameter, the centre-to-centre spacing and anchorage (bond) length of the column, the distribution of stresses between the soil and columns and the corresponding settlement of the structure. The calculation was based on the French Laboratoire Central des Ponts et Chaussees (LCPC) design method for a mixed shallow/deep foundation (Combarieu, 1990). This involved the use of:

- the Combarieu (LCPC) method to evaluate the negative skin friction and neutral point effect (negative skin friction limited to the upper part of the column length)
- the Frank and Zhao (1982) method to evaluate the settlement of the columns in the surrounding soil.
- Hooke's law for the column material (elastic behaviour).

Checks were made to establish whether the calculated values of the stresses were acceptable for the slab-on-grade and were compatible with the material of the jet column and if the settlements were acceptable for the structures.

An important initial assumption was that of the distribution of load between the soil and the columns. From there, the settlements of the soil and of the columns were calculated separately. An iterative calculation was then conducted until an equal deflection of the soil and of the columns was obtained.

The steps of the calculation were as follows:

- The knowledge of the stresses at the toes of the columns allowed the calculation of the settlement, $w_t(H)$,of the toe of the columns.
- The settlement of the shallow footing, $w_s(0)$, could be calculated, if the linear compression of the jet was neglected, by $w_s(0)=w_t(H)$.
- The stress distribution under the shallow footing and the settlement, $w_{soil}(z)$, at depth, z, within the soil could be deduced from $w_s(0)$.
- At any levels of the column, the relationship between the relative settlement soil/jet, $w_r(z)=w_{soil}(z)-w_t(z)$, and the mobilised skin friction, $q_s(z)$, allowed the calculation of $q_s(z)$.
- The linear compression of the jet columns created, over the whole length of the columns, additional settlements Δw_t, to the settlement of the footing. This total settlement, $w_s(0)=w_t(H)+\Delta w_t$, allowed definition of the stress distribution under the shallow footing.

The iterative calculation was undertaken for the relationship between the tip resistance of the jet column, the distribution and transmission of shear over the length of the column and the stress modified under the footing. The combination of these three components represented the total loading of the mixed foundation. The corresponding settlements at the tops of the columns were calculated as $w_s(0)=w_t(H)+\Delta w_t$ and the settlements at the toes of the jet columns were calculated as $w_t(H)$.

An explanation of some of the terms used is given in Figure 8 (Combarieu, 1990).

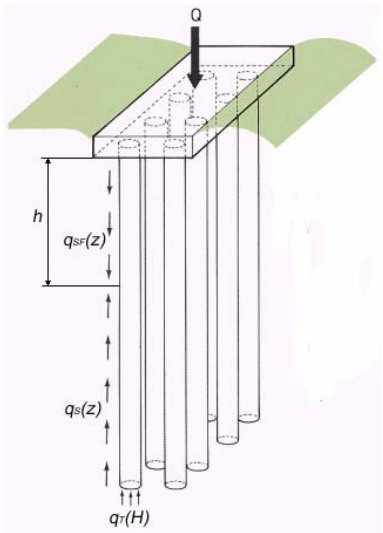

Figure 8: Stress distribution and negative skin friction.

5.3 SETTLEMENT CALCULATION (JET GROUTING COLUMN)

Due to the layout of the columns (see Figure 9), and the transfer of load through the culvert walls, the area of soil and load per column varied across the area to be treated. The information is summarised in Table 2 based on a compression service load of 495 kN at each column, as supplied by RailCorp. The total predicted settlement at the top of the piles was less than 20 mm, with a peak service stress in the column of 2.3 MPa.

Table 2: Jet column layout and calculated settlement.

Row		1	2	3	4	5	6
A	Area (m)	3 m*1.9 m	3 m*2.6 m	3 m*2.2 m	3 m*2.2 m	3 m*2.6 m	3 m*1.9 m
	Settlement (mm)	4.8	10.6	5.6	5.6	10.6	4.8
B	Area (m)	3.6 m*1.9 m	3.6 m*2.6 m	3.6 m*2.2 m	3.6 m*2.2 m	3.6 m*2.6 m	3.6 m*1.9 m
	Settlement (mm)	5.9	13.1	6.9	6.9	13.1	5.9
C	Area (m)	3 m*1.9 m	3 m*2.6 m	3 m*2.2 m	3 m*2.2 m	3 m*2.6 m	3 m*1.9 m
	Settlement (mm)	4.8	10.6	6.9	6.9	10.6	4.8

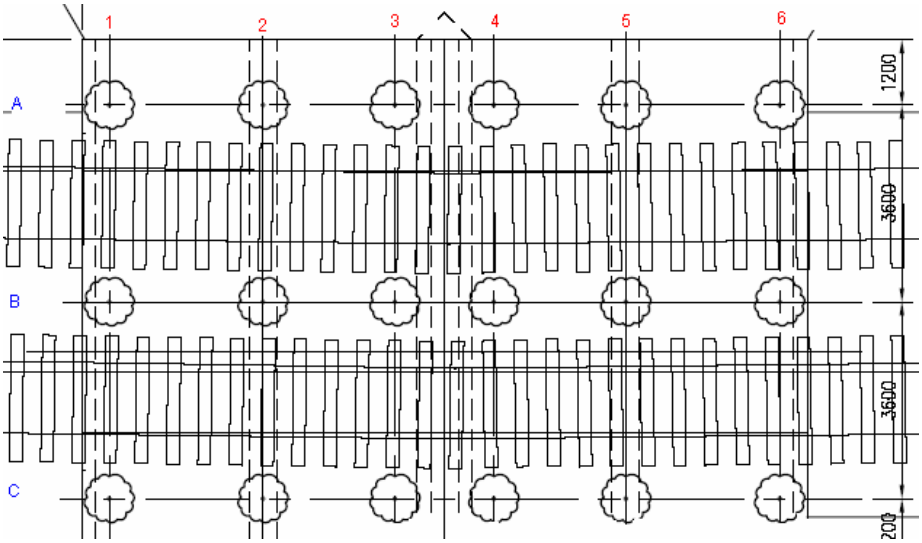

Figure 9: Jet column layout.

5.4 SEQUENCE OF OPERATIONS

Following construction of a coffer dam, to protect the site against inundation, and a working platform, the treatment was performed as follows:

- a small diameter drill hole (90 mm to 150 mm) was drilled to the depth to be treated (see Figure 6).
- a high speed jet of fluid propelled by a high pressure pump was introduced through one or several small diameter nozzles positioned on a 'monitor' at the foot of a series of rods of 70 mm to 120 mm diameter. The jet grouting pump delivery rate was typically 250 L/min.
- the rods were extracted whilst they were slowly rotated, to form a column of soil-grout mix (or "soilcrete") with the grout evenly distributed throughout the treated volume.
- during the jetting process, the excess of the soil-cement mix (referred to as 'spoil') exited freely to the top of the borehole and was removed as work proceeded.

The result (diameter, composition and strength of the columns) depended on the:

- treatment parameters (i.e. the speed of extraction of the monitor, the pressure generating the flow of the fluid grout)
- ground characteristics (nature, density, composition and grain size distribution)
- grout composition
- jetting method used.

The cement used was a low shrinkage portland cement. The resulting composition of the soil cement mix related to the jetting parameters (flow and grout lifting speed) and to the degree of displacement of soil by grout, in order to obtain the target strength of 4.5 MPa specified for the soil-cement mix columns. The grout dosage typically ranged between a water/cement ratio of 0.8 and 1.0.

The soil improvement works were performed using a mini jet grouting rig with a hydraulic 3.0 m height mast to execute the works from underneath the bridge apron (see Figure 2). A total of 18, 1100 mm-diameter columns were constructed between 16 June and 15 July 2005, to a maximum depth of 27.5 m at column B4. The adopted layout is given in Figure 9. The columns' average depth was 23 m, not 19 m as envisaged in the original design. This greater depth allowed for variability of the depth at which suitable weathered rock for founding was encountered.

The jet grouting parameters as well as the work sequence had to be adjusted almost daily to minimise any impact on the live railway structure, particularly in terms of movement, especially ground heave.

Changes in work method involved pre-cutting from top-down or bottom-up using water or cement grout and at medium to high pressure (25 MPa to 45 MPa typically), with a particular emphasis on monitoring the spoil returns to prevent any pressure build-up in the ground. Loss of spoil meant interrupting the column or the pre-cut and repeating the pre-cutting of the column, top down.

Management of the spoil generated by pre-cutting and jet grouting sought to prevent any contamination of the groundwater. Temporary platforms on each side of the bridge central pier were used to divert the flow away from the platform. The spoil was then funnelled away from the working area using a system of clay bunding and a 4 inch pump, before dredging into a stockpile area.

6 OBSERVATIONS, MONITORING AND TESTING

6.1 EFFECTS ON ADJACENT GROUND

Effects on adjacent structures were closely monitored during the jet column installation, because of risks associated with the presence of soft clay combined with the use of high-flow injection techniques. At one stage, the centre pier was lifted 38 mm which disrupted train running.

As a result of the monitoring, the jet grouting column installation was progressively refined using an observational approach, until "zero movement" was observed at the monitoring points.

6.2 STRUCTURE AND GROUND MONITORING

An instrumentation and monitoring program was specified to monitor ground and structure movement in the vicinity of the works to measure:

- ground movements
- angular distortion of the track
- settlement of structures
- settlement of utilities.

The following points were monitored:

- settlement points situated on the bridge piers and abutment (monitored against a local benchmark)
- reference points on the abutments and piers (to monitor possible rotation of the bridge supports)
- settlement points at rail levels (to check against RailCorp criteria).

Monitoring included settlement indicators, inclinometers and rail track tilt measurements.

6.3 COLUMN TESTING

Testing of the soil-cement columns was essential, because accurate design and prediction methods for column properties and load-deformation characteristics are currently limited. Before the final columns were constructed, one short (3 m) sacrificial demonstration column was installed at a point where relatively soft/loose alluvium existed. Compressive strength tests on sample cubes of the injected grout revealed strengths ranging from 10.5 MPa to 30.0 MPa, after 17 to 23 days curing, and strengths of between 5 MPa and 8 MPa in samples obtained from the soilcrete in completed jet columns B2 and B5.

7 PERFORMANCE

Monitored instruments confirmed that soil-cement columns were effectively supporting the bridge. The data showed:

- less than 5 mm horizontal movement of the brick pier and abutment during jet grout installation
- less than 5 mm settlement following construction completion
- movement at the bridge (six points): controlled heave of between 3 mm and 44 mm
- relative movement of pier/abutments (rotation): less than 5 mm (precision of instrument)
- heave at rail level: less than 5 mm measured on a weekly basis between 27 June and 12 July 2005.

The bridge remained open during the soil improvement works and the new section was opened to traffic in November 2005. The completed bridge is shown in Figure 10.

Figure 10: Completed rail bridge.

8 CONCLUSIONS

Although jet grouted foundations have a history of being relatively expensive, the total cost of the jet grouting was significantly less than the cost of constructing new bridge foundations and piers, and less disruptive to train operations and adjacent utilities. Other benefits included that, unlike other types of piles installed by pile-driving techniques, jet grouted pile installation did not endanger the existing bridge structure through vibration, nor did it affect nearby fibre-optic cable installations. It could also be done in the tight workspace and low headroom conditions present beneath the underbridge.

The rail bridge renewal was done with minimal disruption to train traffic and minimal environmental impact, demonstrating the viability of this technology and its suitability as a solution for this situation. Successful construction and performance of the jet grouted deep foundation is proof of the success of the adopted solution.

The innovative use of jet grouting enabled the project team to:

- avoid disruption of the railway operations
- reduce construction costs and
- advance the state-of-the-art.

9 ACKNOWLEDGEMENTS

This paper is based on the design and construction work of RailCorp, Parsons Brinckerhoff and Austress Menard. The authors acknowledge the support of Glen Xuereb, Ed Johnson, Grant Gilligan and Joe Muscat from RailCorp in supporting innovative practices in bridge foundation construction.

10 REFERENCES

British Standard BS EN 12716:2001. Execution of special geotechnical works – Jet grouting,

Bruce, D.A. (2005). *Glossary of grouting terminology.* J. Geotech and Geo.Eng. ASCE, 131(12) 1534 - 1542

Combarieu, O. (1988). *Calcul d'une foundation mixte semelle-pieux sous charge vertical centree* (Calculation of shallow footing – pile mixed foundation– single pile under concentric vertical surcharge), Ministere de l'equipment Laboratoire central des Ponts et Chaussees. LCPC Paris.

Combarieu, O. (1988). *Amélioration des sols par inclusions rigides verticales – application à l'édification de remblais sur sols médiocres* (Soil improvement using vertical rigid inclusions – application to the construction of embankments on poor soils) Revue Française de géotechnique n°44: 57-59.

Hewitt, P. (1994). *Design Considerations for Jet Grouting*. Soil Improvement Seminar, Drainage and Irrigation Dept. Wilayah Persekutuan, Kuala Lumpur, 1 June 1994.

Frank, R. and Zhao, S.R. (1982). *Estimation par les parametres pressiometriques de l'enfoncement sous charge axiale des pieux fores dans les sols fins* (Estimate of settlement of bored piles in fine grained soils under uniaxial loading using pressuremeter test results) Bulletins de liaison des Laboratoires des Ponts et Chaussees, 119, May-June 1982, pp. 17-24.

EFFECT OF CLAY STRUCTURE DEGRADATION ON SETTLEMENT OF EMBANKMENT

[2]Jidong Zhao, [1]Daichao Sheng, [1]Andrew J. Abbo, [1]Scott W. Sloan
[1]*Geotechnical Research Group, University of Newcastle, NSW 2308,* [2]*Corresponding author*

ABSTRACT

Due to the degradation of initial structures, soft clays can experience significant settlement without much change of pore pressure. Such a phenomenon has recently been observed at a fully instrumented trial highway embankment near the town of Ballina (New South Wales, Australia). In contrast, the displacements in saturated soils without structure (such as a fully remoulded clay) are always associated with the dissipation of excess pore pressure through the effective stress principle. This paper demonstrates the effects of clay structure degradation on the settlement of embankments, through numerical analysis of a trial embankment on soft clay. A constitutive model that accounts for destructuration of soils is used to characterise the behaviour of the soft clay. The material parameters are derived from conventional oedometer and triaxial tests for the structured constitutive model. It is shown that the settlement and the dissipation of excess pore pressure during construction of the embankment are closely related with the destructuration of the soft clay. With appropriate choice of the constitutive model and material parameters, the lag between the settlement and pore pressure dissipation can be well predicted by the coupled finite element method based on the effective stress principle and consolidation theory.

1 INTRODUCTION

As part of the upgrade of the Pacific Highway along the east coast of Australia, a substantial length of raised embankment is required to be constructed over areas of soft clay. Fully instrumented trial embankments have been constructed on estuarine clay deposits along the proposed alignment to acquire observational data on the settlement and stability of the highway embankments during and following the proposed construction. Extensive data on vertical settlements, lateral displacements and pore pressures have been obtained, and detailed field and laboratory tests on the clay deposits have also been carried out. This provides a useful opportunity to verify finite element codes for elastoplastic consolidation analysis, which in turn can be used to analyse the performance of the highway embankments under different design scenarios.

A distinct feature of natural soft soil that makes it behave differently from the corresponding reconstituted soil is the presence of initial structure in it. Compared to the reconstituted soil, the existence of initial structure in a natural soil may always lead to a higher void ratio. When it is subjected to loading process, the breakdown of the initial structure will lead to a destructuration process (e.g., Mitchell, 1976; Smith *et al*., 1992). This process renders the natural soil exhibiting extra strength than the corresponding reconstituted one at a given stress (Burland, 1990; Leroueil and Vaughan, 1990) and at the same time results in a significant settlement without much change of pore pressure in the soft soil. Such a phenomenon has been observed at a fully instrumented trial highway embankment near the town of Ballina (New South Wales, Australia).

Even though the Modified Cam-Clay model can be used to characterise typical behaviour in soils, like nonlinear elasticity and isotropic hardening, its deficiency in accounting for the structure in soft soils leads to the disagreement of some of its predictions with the field-monitored data as mentioned above. A specific constitutive model that is capable of addressing the initial structure and destructuration process in soft clays is thus desirable for the analysis. Fortunately, several models have been proposed to rationalise the behaviour of natural soils in literature (see e.g., Rouainia and Muir Wood, 2000; Liu *et al*., 2003; Asaoka, 2003; Baude and Stallegrass, 2004). We have successfully implemented two of them (Rouainia and Muir Wood, 2000; Asaoka, 2003) into the Newcastle Finite Element code, SNAC, and applied it to the prediction of some boundary value problems (see Zhao *et al.,* 2005).

In this paper, the model proposed by Rouainia and Muir Wood (2000) is employed to verify the settlement of the embankment by the finite element code. The model parameters are determined from a set of field and laboratory data from soft soils in Eastern Australia. Coupled analysis of deformation and pore pressure is adopted in the finite element implementation to predict the consolidation behaviours. The accuracy in settlement prediction using the consolidation theory of classical soil mechanics is also evaluated and compared with the finite element model predictions.

2 BRIEF DESCRIPTION OF THE STRUCTURE MODEL

In this section, the model proposed by Rouainia and Muir Wood (2000) that considers the structure degradation in soils is briefly described. This model has been developed to account for initial structures, small strain stiffness, stiffness degradation with strain history and hysteretic response in cyclic loading. The response associated with the elastic part in this model is expressed in terms of the bulk modulus and shear modulus, *K* and *G*, which are assumed to depend linearly on the pressure p':

$$K = \frac{dp'}{d\varepsilon_v^e} = \frac{p'}{\kappa^*}, G = \frac{3(1-2\mu)}{2(1+\mu)}K \quad \textbf{(1)}$$

where ε_v^e denotes the elastic volumetric strain; μ is the Poisson's ratio; κ^* is the slope for the swelling line in a volumetric strain-logarithmic mean stress compression plane. p' is the mean stress.

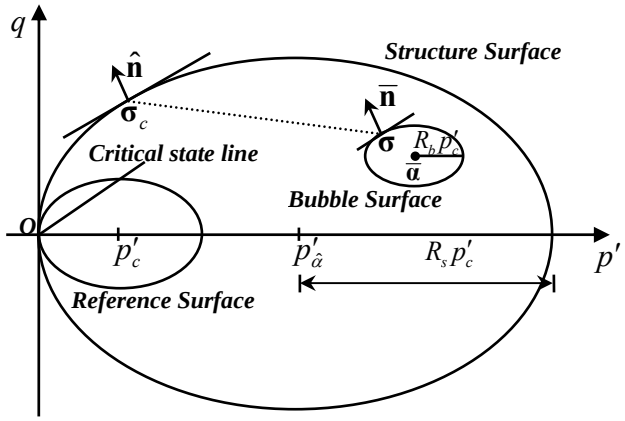

Figure 1: Illustration of yield surfaces for the structure model of Rouainia and Muir Wood (2000).

Three yield surfaces (the reference surface, the bubble and the structure surface as shown in Figure 1 are employed in this model, which, respectively, present the following analytical expressions:

$$\begin{cases} \text{Reference surface}: & f_r = g_r = \left(\dfrac{q}{M(\theta)p'_c}\right)^2 + \left(\dfrac{p'}{p'_c} - 1\right)^2 - 1 \\ \text{Bubble surface}: & f_b = g_b = \left(\dfrac{q - q_{\bar{a}}}{M(\theta)p'_c}\right)^2 + \left(\dfrac{p'}{p'_c} - \dfrac{p'_{\bar{a}}}{p'_c}\right)^2 - R_b{}^2 \\ \text{Structure surface}: & f_s = g_s = \left(\dfrac{q}{M(\theta)p'_c}\right)^2 + \left(\dfrac{p'}{p'_c} - R_s\right)^2 - R_s{}^2 \end{cases} \quad \textbf{(2)}$$

Where M denotes the slope of the critical state line (CSL), and is expressed as a function of the Lode angle θ as follows in this paper:

$$M = M_{\max}\left(\frac{2\alpha^4}{1+\alpha^4-(1-\alpha^4)\sin 3\theta}\right)^{1/4} \quad \textbf{(3)}$$

By setting the parameter α with $\alpha = (3-\sin\phi)/(3+\sin\phi)$, this yield surface coincides with the Mohr-Coulomb hexagon at all vertices in the deviatoric plane (where ϕ is the friction angle of the soil at critical state), while setting $\alpha = 1$ recovering the Von Mises circle. Note in Figure 1 that p'_c and $p'_{\hat{\alpha}}$ denote, respectively, the centres of the reference surface and structure surface; R_s and R_b denote, respectively, the initial structure and the relative ratio of the bubble size for the soft clay.

3 FINITE ELEMENT ANALYSIS

The study will focus on the data from one of the two trial highway embankments near the town of Ballina, referred to here as the *Teven Road embankment*. The alluvial and estuarine soils in the Ballina region are typical of those that prevail in coastal flood plain environments found in many parts of the East Coast of Australia. Figure 2 depicts the soil profile under the Teven Road embankment. The identified layer of silty sand (Layer 3 in Figure 2) is crucial in consolidation predictions as it will allow some degree of two-way drainage in the overlying compressible clay deposit, and at the same time it is also most susceptible to consolidation settlement. The trial embankment is 84 m long and 54 m wide at its base. A thin layer of geofabric, a 750 mm layer of fine crushed rock and a 250 mm layer of aggregate were firstly placed in an upward sequence over the entire embankment footprint and this provided a free draining surface for the underlying clay. Monitoring instruments for settlement and pore pressure were then installed over them. After covering by a further layer of geofabric, the embankment was filled gradually with ripped, weathered rock and aggregate to a maximum hight of 1.6 m over a period of 70 days (the embankment fill was placed in a stepwise manner as shown in Figure 3). The completed embankment is 44 m wide at the top.

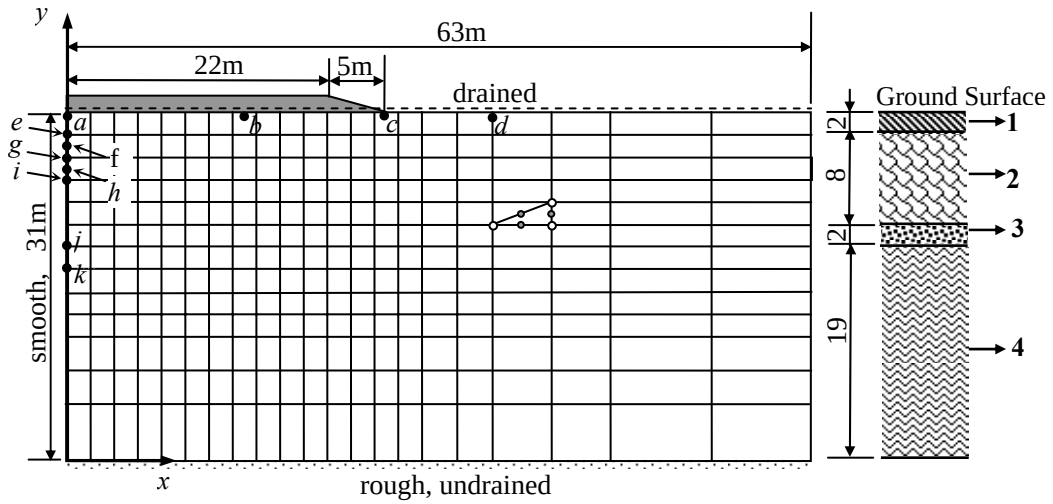

1 *Surface crust, silty CLAY, firm, brown, estuarine Lowest ground water table 1.2 m*
2 *CLAY, soft, structured, high plasticity, dark grey brown, saturated, shell fragments, estuarine*
3 *Clayey silty SAND, saturated, grey, dense, fine to medium grained*
4 *Silty CLAY, firm, dark grey, shell fragments, estuarine*

Figure 2: Typical soil profiles under the Teven Road trial embankment and the Finite element mesh for analysis (1161 nodes, 546 elements; a-k are reference points).

Figure 2 also shows the finite element mesh used to represent the soils under the embankment. Due to symmetry, only half of the embankment is considered. The embankment is represented by vertical loads which increased over time to a constant value of 30 kPa from x=0 m to x=22 m and linearly decreasing to zero from x-22 m to x=27 m. Each grid square in Figure 2 consists of two triangular elements with 6 displacement nodes and 3 pore pressure nodes. Nodes along the bottom boundary are restrained both vertically and horizontally, representing a rough boundary condition. The left and right boundaries are restrained in the horizontal directions, representing smooth contact vertically. The top boundary is set to be free drained to zero pore pressure, while the bottom boundary is set to be undrained. Four reference points on the ground surface, namely '*a*' (x=0.0 m), '*b*' (x=15.0 m), '*c*' (x=27.0 m) and '*d*' (x=34.0 m), are chosen to monitor the settlements of the trial embankment. Two other points, '*f*' (depth at 3 m or y=28.0 m) and '*h*' (depth at 5 m or y=26.0 m), are chosen to monitor the excess pore pressures. Four other reference points, '*e*'(y=29.0 m), '*g*'(y=27.0 m), '*i*' (y=25.0 m), '*j*'(y=19.0 m) and '*k*'(y=17.0 m), as shown in Figure 2, are marked for later use in FEM computations.

The experimental data, monitored from Teven Road trial embankment, are obtained by a number of triaxial tests on undisturbed samples taken from a nearby site (Robert Carr & Assoiciates Pty Ltd, 2000). These tests include consolidated undrained compression (CUC) tests, consolidated undrained extension (CUE) tests and consolidated

drained compression (CDC) tests. Appropriate optimization procedures have been used to obtain the model parameters listed in Table 1 for the finite element analysis.

Table 1: Model parameter selection optimized from the test data of Teven Road trial embankment

Layer	Depth (m)	Soil Features	λ^*	k^*	ϕ	μ	ρ	OCR	R_s	R_b	ω	A_d	B	ψ	k_p (10^{-4} m/d)
1	0~2	Desiccated clay crust	0.075	0.015	33.3°	0.20	1.81	6.65	1.0	0.1	4.0	0.9	1.8	1.4	10.2
2	2~10	Soft structured clay	0.17	0.014	33.3°	0.16	1.45	1.70	4.0	0.1	4.0	0.9	1.8	1.4	0.45
3	10~12	Clayey silty sand	0.21	0.017	33.3°	0.20	1.40	1.00	1.0	0.1	4.0	0.9	1.8	1.4	0.11
4	12-31	Firm clay	0.05	0.007	33.3°	0.20	1.62	1.06	1.0	0.1	4.0	0.9	1.8	1.4	0.25

In Table 1, λ^* and k^* denote the slopes of the Normal Compression Line (NCL) and the Unloading-Reloading Line (URL) in the plane of $\ln v - \ln p'$, respectively; ϕ is the effective frictional angle of the soil; μ and ρ are the Poisson's ratio and the density of soils, respectively; k_p is the permeability coefficient. ω, the destructuration parameter; A_d, the weight coefficient; B and ψ are, respectively, the stiffness interpolation parameter and exponent for the model (details see Rouainia and Muir Wood, 2000).

SNAC, a finite element code developed at the University of Newcastle, is used to conduct the analysis of the trial embankment. The resulting system of ordinary differential equations in term of displacement and pore pressure is treated by coupled displacement and pore pressure analysis and an adaptive time integration scheme with error control. For detailed formulation and numerical algorithms for the analysis in SNAC refer to Sloan and Abbo (1999), Sloan *et al.* (2001), Sheng and Sloan (2002) and Zhao *et al*. (2005). The initial stresses and pore pressures in the soil are generated using body loads corresponding to the bulk unit weight. Once the initial stresses are established, the initial yield surface locations are determined from the overconsolidation ratio OCR. Construction of the embankment is simulated by applying a pressure load, corresponding to the total embankment weight, over a period of 70 days. The final total weight of the embankment is 30 kPa beneath the full thickness of fill, and it is assumed to decrease linearly to zero at the toe. During the loading stage, the pore pressures at the ground surface are kept to zero and the vertical gradients of the pore pressures at 31 m depth are kept at 0 (representing an undrained boundary). The lateral boundary is taken to be impermeable. The bottom boundary at 31 m depth is fixed in both horizontal and vertical movements, representing a rough boundary. The left and right boundaries are fixed only in the horizontal movement, representing smooth boundaries in the vertical direction. After construction of the embankment, the soil layers are allowed to consolidate under the same boundary and loading conditions. The analysis is continued to a total time period of 1000 years.

4 RESULTS AND DISCUSSION

Since the construction of the embankment began, settlements and pore pressure data under the trial embankment have been measured over a 1300 day period. The predicted settlements at the ground surface and excess pore pressures at depths of 3 m and 5 m beneath the embankment centre are compared to the measured data in this section. The process of structure degradation in the soft clay will also be demonstrated.

4.1 SETTLEMENTS

The settlements at the ground surface (Reference Point *a, b, c* and *d* as in Figure 2 predicted by the finite element computation are compared against the measured data In Figure 3.

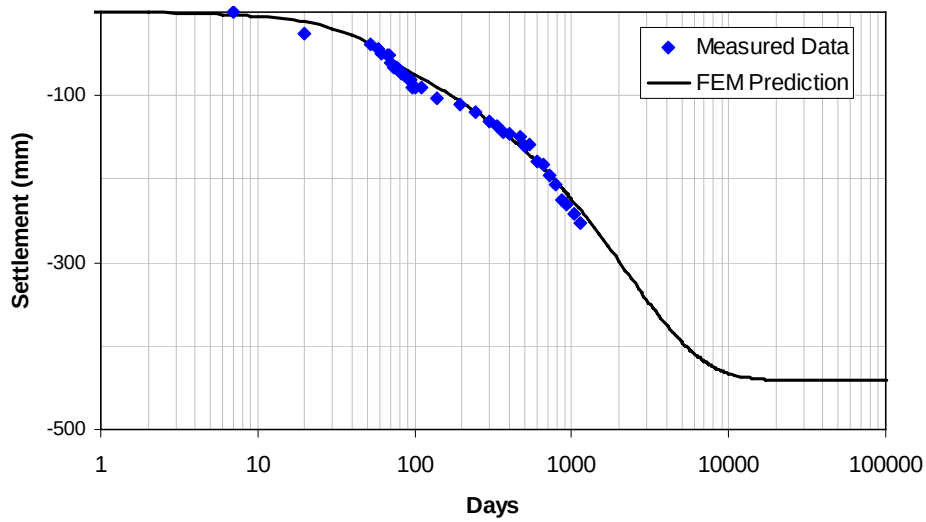

(a) Reference Point *'a'* (x=0.0 m)

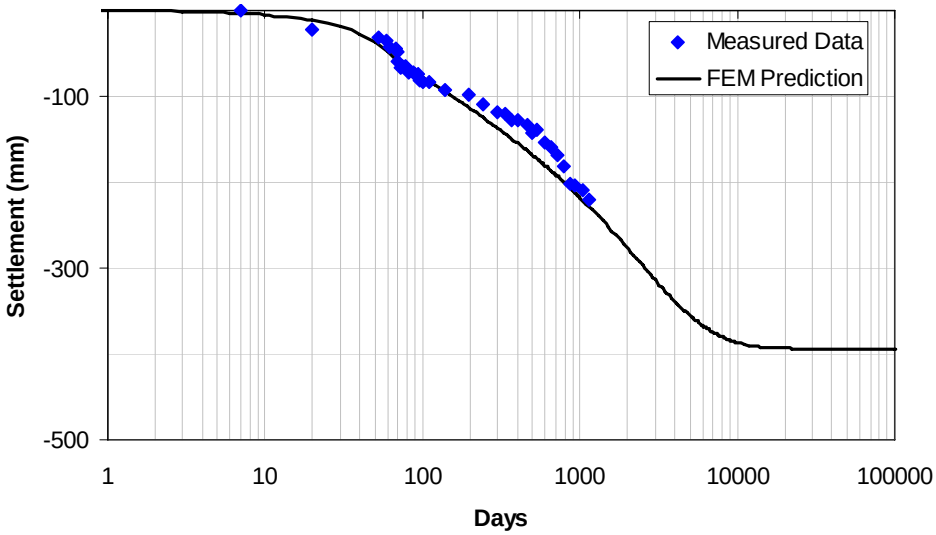

(b) Reference Point '*b*' (x=15.0 m)

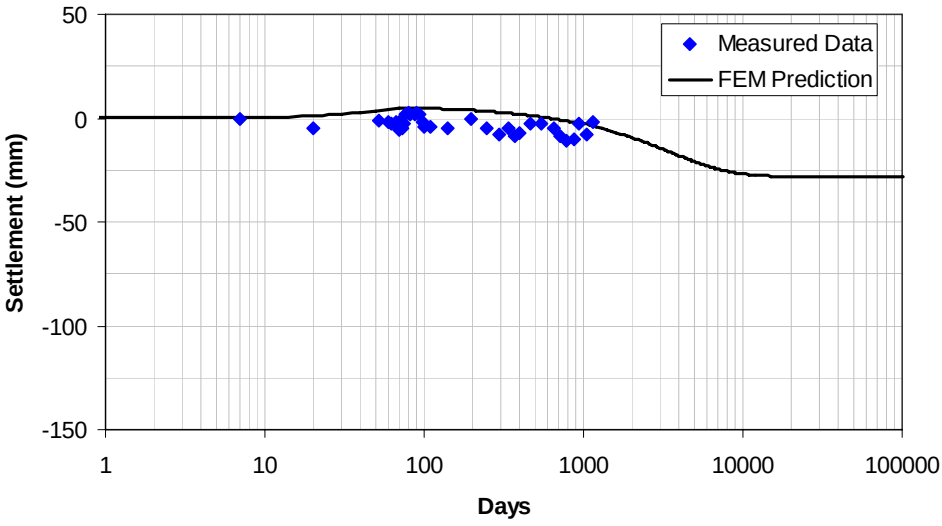

(c) Reference Point '*c*' (x=27.0 m)

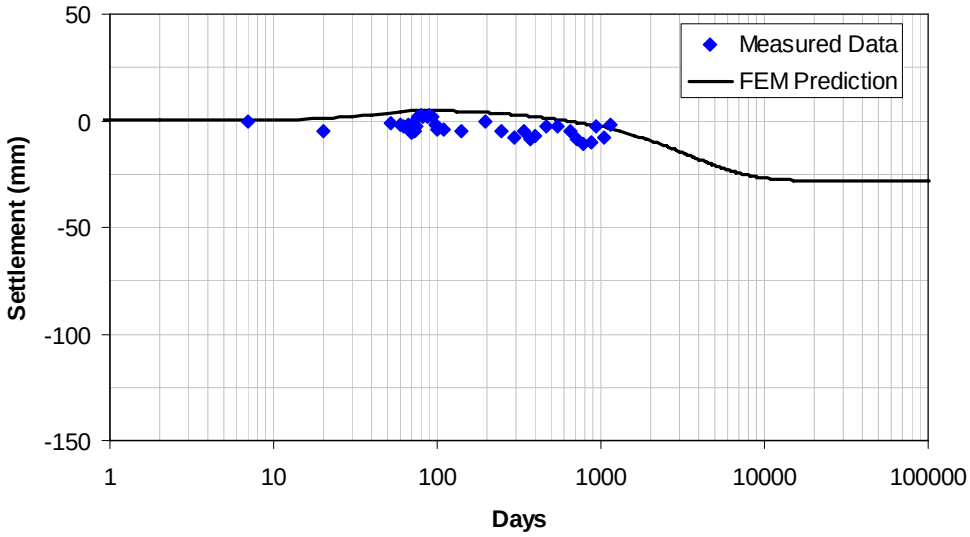

(d) Reference Point *'d'* (x=34.0 m)

Figure 3: Measured and predicted surface settlements for four reference points.

As can be seen from Figure 3(a), the finite element prediction of the time dependent settlements under the centre of the embankment (Reference Point '*a'*, x=0.0 m) agrees very well with the measured data. Only slightly smaller settlements are predicted by FEM than measured after 20 days and around 100 days. These differences are no larger than 10%. Figure 3(b) shows the ground surface settlements at the Reference Point '*b'* (x=15.0 m). The FEM predicted settlements for point '*b'* generally match well with the observed ones, except that the former underestimates the settlement up to 10% during the period between 200 days and 800 days. Figure 3(c) and Figure 3(d) depict the predicted surface settlements at the edge of the embankment (Reference Point '*c',* x=27.0 m from the centre) and outside the embankment (Reference Point '*d'*, x=34.0 m from the centre) in comparison with the observed data. The agreement between the predicted and observed responses is not as good as that shown for Reference Points *'a'* and '*b'*. The finite element method generally over-predicts the settlements at the two locations than the observed ones. Compared with the measured settlement data of Reference Points '*a'* and '*b',* those observed at location '*c'* and '*d'* are much smaller and scattered. Thus the comparisons for '*c'* and '*d'* are not as significant as for '*a'* and '*b'*. Generally, the predicted settlements by the finite element analysis using the structure model, with parameters derived from triaxial and oedometer tests, are relatively accurate.

4.2 EXCESS PORE PRESSURE

The predicted pore pressure dissipation at depths of 3 m and 5 m beneath the embankment centre (Reference Points '*f"* and '*h'*) are compared to the measured data in Figure 4. Due to difficulties in matching the boundary condition at the ground surface, and the fluctuating ground water table in the FEM computations with the actual behaviours, the computed and measured absolute values of excess pore pressures cannot be directly compared. Thus in Figure 4 the predicted and measured excess pore pressures are normalised against their maximum values respectively, resulting in a plot of the percentages of generation and dissipation of the excess pore pressures. It is shown that the times at which the maximum excess pore pressures occur are well predicted. At about 1000 days since the construction of the embankment, around 60% of the excess pore pressure generated at a depth of 3 m has been dissipated according to the field data, while the finite element analysis predicts a dissipation of around 20%. The predicted dissipation of the excess pore pressure generated at a depth of 5 m is about 20% less than the field data at time around 1000 days. In general, compared to the settlements, the excess pore pressures predicted by the finite element method appear much less accurate, which is in accordance with those reported by Wroth and Simpson (1979).

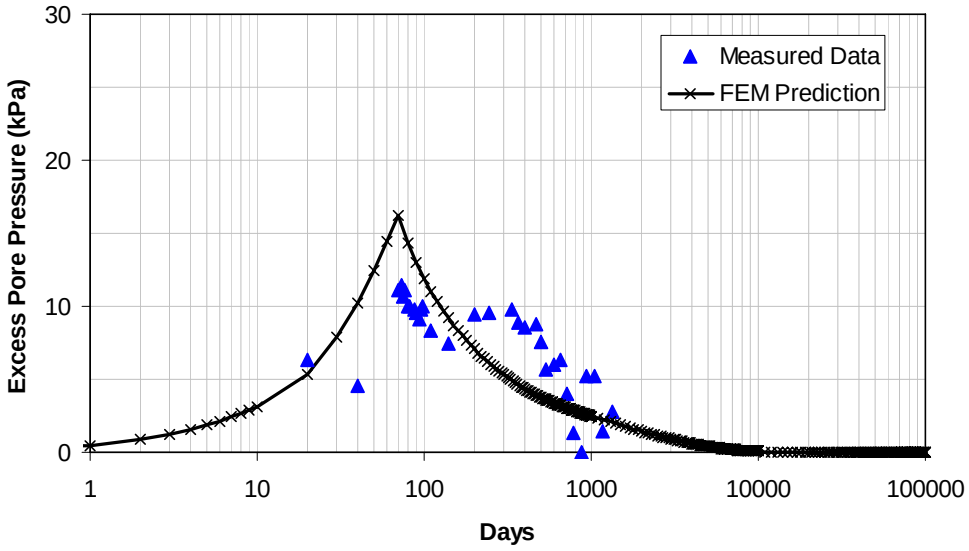

(a) Reference Point '*f*' (depth at 3 m or y=28.0 m).

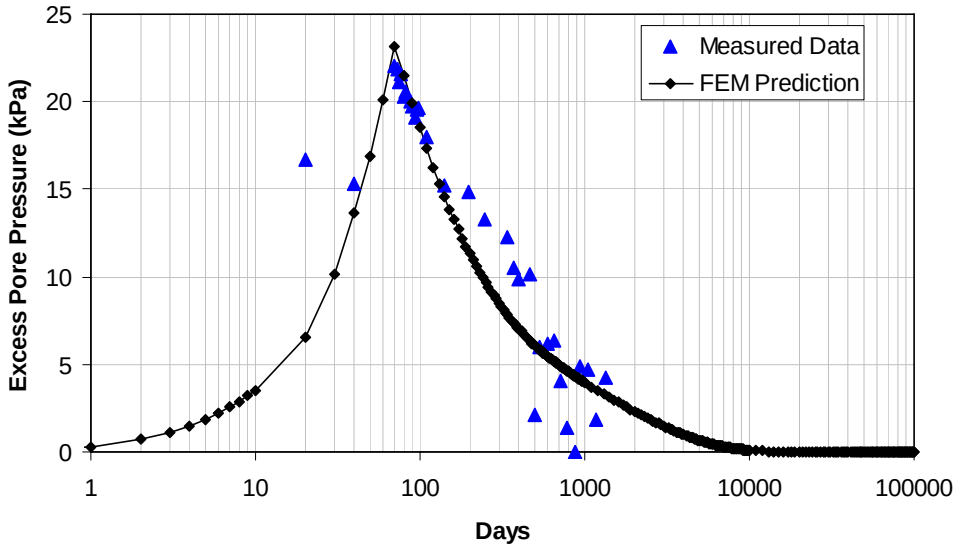

(b) Reference Point '*h*' (depth at 5 m or y=26.0 m).

Figure 4: Comparison between measured and FEM predicted excess pore water pressures beneath the centre of the embankment.

Though there are no measured data at other reference points (*e, g, i, j* and *k*) for comparison, we present the FEM predicted excess pore pressures for these points in Figure 5. As can be seen from, the peak pressures appear at around 70 days of the construction for all the reference points. And the shallower the point is the smaller the peak excess pore pressure is obtained. There is an exception, however, for points '*j*' and '*k*', as the peak pressure for '*j*' is slightly larger than that of '*k*'. This is because the reference point '*j*' is located at the boundary of the layers 3 and 4, while '*k*' is in layer 4. As it is known, layer 3 is mainly constituted of silty sand, which has very good draining properties, whereas layer 4 is composed of silty clay with poor drainage properties. Thus, on the boundary of these two layers the excess pore pressure will dissipate slower than at other places. This leads to the peak of '*j*' being higher than that of *'k'*. Another feature that may be observed from Figure 5 is, the shallower the point is, the more rapid the dissipation of excess pore pressure after peak undergoes. Comparatively, point '*e*' exhibits the most dramatic dissipation rate of excess pore pressure after the peak. On the other hand the curves after the peak for '*j*' and '*k*' show completely different features from those for *e, g* and *i.* The downward curves for *e, g* and *i* imply the dissipation rates at these locations decrease gradually over time, whereas the upward curves for '*j*' and '*k*' depict a clear increasing dissipation rate over time. However, no matter how the dissipation evolves, the excess pore pressures at all locations will decay after 10000 days.

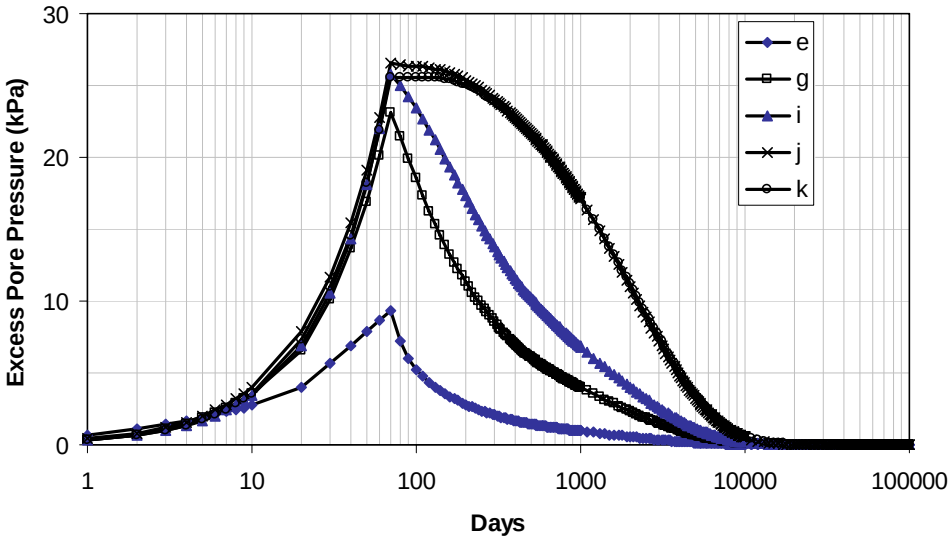

Figure 5: FEM predicted excess pore water pressures for Reference Points *e, g, i, j* and *k*.

4.3 CLAY STRUCTURE DEGRADATION

The behaviour of clay structure degradation during the embanking process can also be illustrated. The results are demonstrated in Figure 6, and observations may be made in conjunction with figure 4 and 5. As can be seen from Figure 6(a), the destructuration process is initiated just after the construction of the embankment. The shallower the point is located, the earlier this process begins. For all the four points, however, the damage caused to structure is inappreciable until 70 days of the construction. This time precisely corresponds to the point where abrupt settlements begin in Figure 3(a) and 3(b), or the point peak excess pore pressure appears in Figure 4. This coincidence is not surprising since the decay of structure in the soft clay always implies the failure of organic structure in the soil and thus leads to volumetric contractions. These volumetric contractions will unavoidably result in the settlement of ground surface of the embankment. Meanwhile, volumetric contractions will drain out water previously stored in the soil, which cause the dissipation process of excess pore pressure. Moreover, the more dramatic the decay of initial structure is, the quicker the latter two processes may be observed. Among the four points, it can be observed that the largest decay of initial structure appears earlier for the shallow points as '*f*' and '*g*' than the deeper ones as '*h*' and '*i*'. As also can be seen, none of the four points completely lose their initial structure. After 10000 days of the construction of the embankment, the structure index R_s is stable for all points and this value is greater than 1. This implies there is still some residual structure in the clay. Moreover, the points in shallow depth exhibit lower residual structure than those deeper ones.

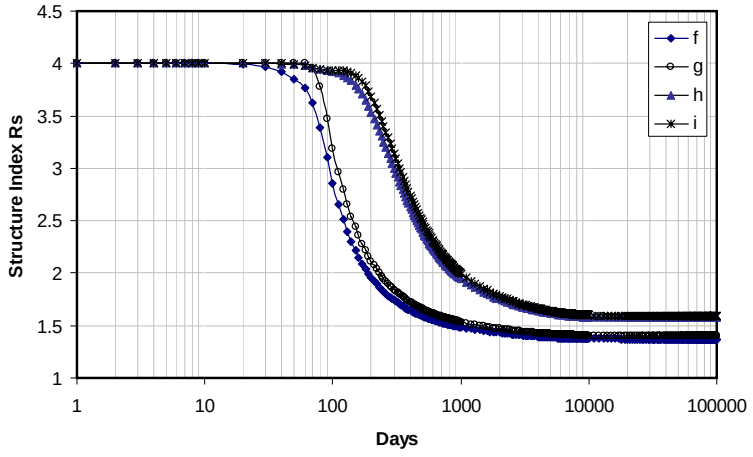

(a) Process of destructuration for Reference Points *f, g, h* and *i*.

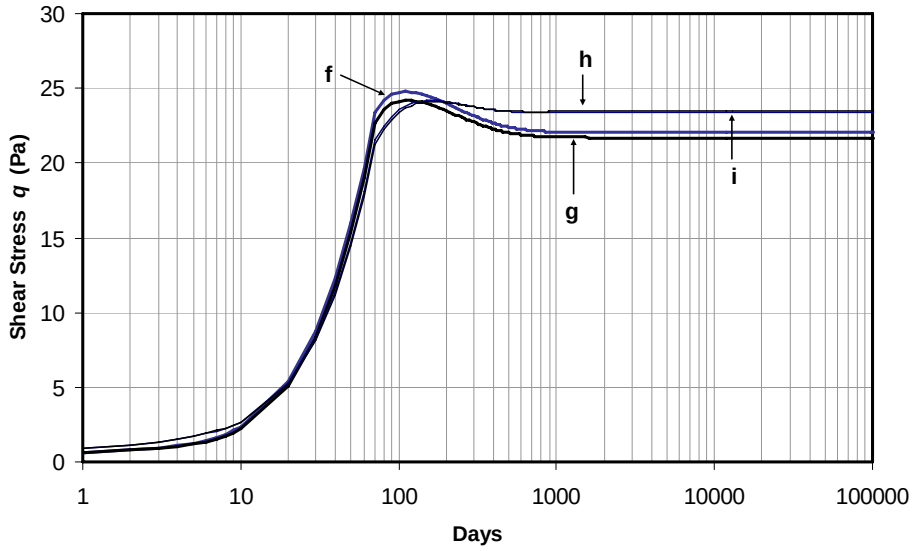

(b) Development of shear stress at Reference Points *f, g, h* and *i*.

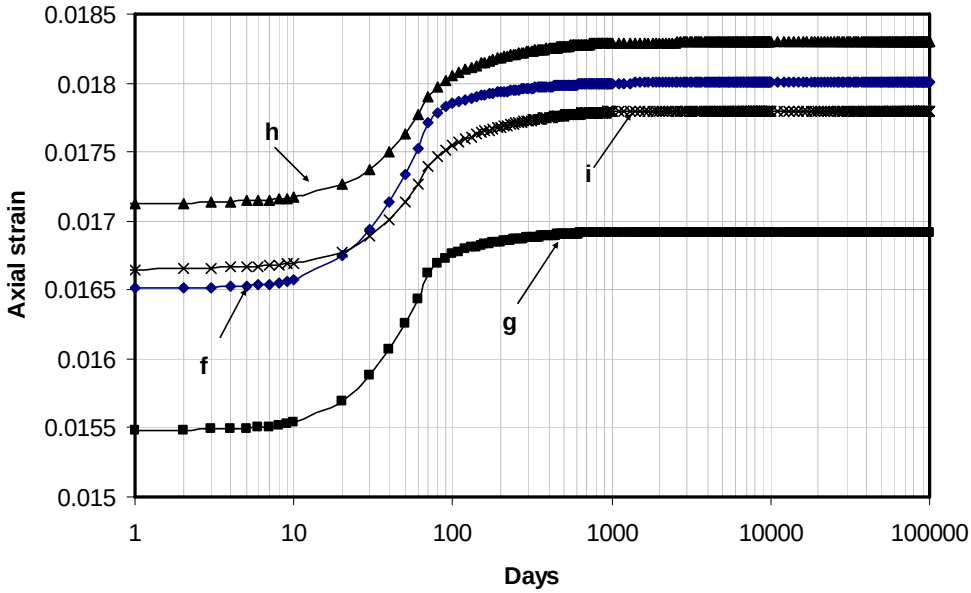

(c) Development of axial strain at Reference Points *f, g, h* and *i.*

Figure 6: Destructuration processes and stress-strain behaviour at reference points.

In Figure 6(b) and 6(c), the developments of shear stress and axial strain for the four points are depicted. In conjunction with Figure 6(a), we can observe that dramatic stress and strain increase occur before the destructuration process of the soil, which results in the accumulated plastic strain exceeding the threshold for the breakdown of the initial structure, and consequently the destructuration process is activated and the obvious decay of the initial structure in the soil is observed. This process also enables the soil to sustain some extra load, so that peak shear stress can be observed for all the four points before the stress curves go to stably horizontal.

5 CONCLUSIONS

The performance of a fully instrumented trial highway embankment on thick estuarine clay deposits is studied using the finite element method and a soil model that considers structure degradation. The performance of the numerical model in predicting the load response behaviour of soft soils found on the East Coast of Australia is evaluated. The settlements predicted by the FEM computations compare well with the data obtained from the embankment site. However, the numerical model tends to slightly under-predict the dissipation of excess pore pressure, even though the predicted rate of the settlement is relatively accurate. This discrepancy is attributed partly to the highly variable boundary conditions

in situ and partly to the inadequacy of the soil model. This paper also shows that the settlement and the dissipation of excess pore pressure are closely related to the destructuration process in soft clays. This proves the necessity of using constitutive models that take into account the effects of structure degradation to analyse geotechnical problems related to natural soft soils.

6 ACKNOWLEDGEMENTS

The authors gratefully acknowledge the provision of field and laboratory data by the Roads and Traffic Authority of New South Wales. This research was partly supported by the Australian Research Council.

7 REFERENCES

Asaoka, A. (2003) "Consolidation of clay and compaction of sand – an elastoplastic description". *12th Asian Regional Conference on SMGE*, August 2003, Singapore

Baude, B. and Stallegrass, S. (2004) "A constitutive model for structured clays". *Géotechnique* **54**(4), 269-278.

Burland, J.B. (1990) "On the compressibility and shear strength of natural clays". *Géotechnique* **40**(3), 329-378.

Leroueil, S. and Vaughan, P.R. (1990) "The general and congruent effects of structure in natural soils and weak rocks". *Géotechnique* **40**(3), 467-488.

Liu, M.D., Carter, J.P. Airey, D.W. and Liyanapathirana, D.S. (2003) "A Cam Clay-type Model for Structured Soils". *Proceedings 3rd International Symposium on the Deformation Characteristics of Geomaterials*, Lyon, France. A.A. Balkema, Lisse, Netherlands, pp1155-1160.

Mitchell, J.K. (1976). *Fundamentals of soil behaviour*. New York: John Wiley & Sons.

Robert Carr & Associates Pty Ltd, (2000). *Report on site investigation and instrumentation for the Cumbalum and Teven Road trial embankment*. Report No. 336T, Carrington, NSW, Australia

Rouainia, M. and Muir Wood, D. (2000) "A kinematic hardening constitutive model for natural clays with loss of structure". *Géotechnique* **50**(2), 152-164.

Sheng, D. and Sloan, S.W. (2003) "Time stepping schemes for coupled displacement and pore pressure analysis", *Computational Mechanics*. **31**:122-134

Sloan, S.W. and Abbo, A.J. (1999) "Biot consolidation analysis with automatic time stepping and error control, Part 1: Theory and implementation", *International Journal for Numerical and Analytical Methods in Geomechanics*, **23**, 467-492.

Sloan, S.W., Abbo, A.J. and Sheng, D. (2001) "Refined explicit integration of elastoplastic models with automatic error control", *Engineering Computations*, **18**, 121-154.

Smith, P.R., Jardine, R.J. and Hight, D.W. (1992) "The yielding of Bothkennar clay". *Géotechnique* 42(2), 257-274.

Zhao, J.D., Sheng, D.C., Rouainia, M. and Sloan, S.W. (2005) "Explicit stress integration of complex soil models". *International Journal for Numerical and Analytical Methods in Geomechanics*. **29**(12), 1209-1229.

ASSESSMENT OF IMPACTS OF GROUND MOVEMENTS ON EXISTING STRUCTURES ADJACENT TO EXCAVATIONS

Jeff Hsi
SMEC Australia Pty. Ltd., Australia

ABSTRACT

A cut and cover tunnel is being constructed in soft marine clay as part of the 12 km long Kallang and Paya Lebar Expressway in Singapore. The width of the excavation ranges approximately between 40 m and 60 m and the maximum depth is up to 25 m. Such extensive excavation inevitably causes substantial ground movement in the surrounding areas. The structures identified to be affected by the excavation induced ground movements include the bored piles beneath the base of the excavation, several multi-storey buildings supported on deep foundations and a cluster of warehouses on shallow foundations. This paper presents the methodology and analysis techniques employed for the prediction of ground movements and assessment of impacts on the adjacent structures. The role of monitoring is discussed and selected field data is included.

1 INTRODUCTION

Contract 421 (C421) of the 12 km long Kallang and Paya Lebar Expressway (KPE) in Singapore involves the design and construction of a 1.5 km vehicular tunnel from East Coast Parkway (ECP) to Nicoll Highway. The key project features comprise a 4 lane dual carriageway within a tunnel box, a river crossing including cofferdams during construction, a ventilation building, the KPE/ECP interchange, etc. The project layout plan of KPE C421 is shown in Figure 1. The tunnel is constructed by the cut and cover method using sheet piles and internal bracing for support of the excavation. The bored piles installed below the excavation are designed for both the permanent loads from the tunnel structures as well as for temporary forces induced during construction. Tension piles are used to assist the tunnel structure against floating. Both the top-down and bottom-up construction methods have been adopted.

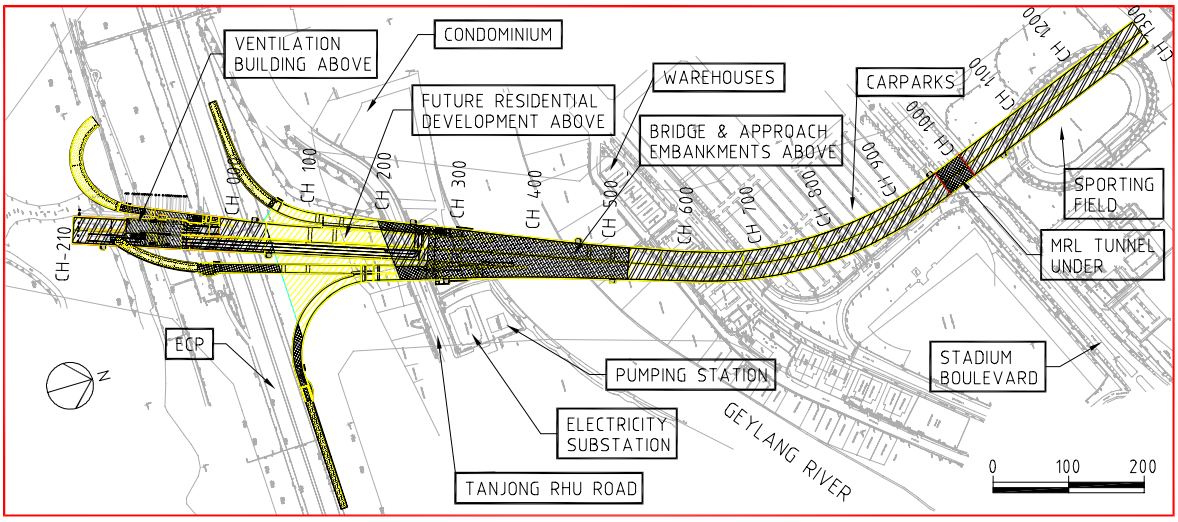

Figure 1: Project layout plan of KPE C421.

The project site is located on recently reclaimed land which is still settling. The fill is underlain by a series of soft marine clays and fluvial/alluvial deposits up to 50 m depth before reaching dense sands. Excavation is generally carried out in soft marine clays which presents particular challenges to the designer and the contractor for maintaining the stability of the excavation and limiting the ground movement in the surrounding area. The width of the excavation ranges approximately between 40 m and 60 m and the maximum depth is up to 25 m.

The tunnel generally traverses flat terrain in a greenfield site with several permanent structures all located within 50 m of the main excavation. These include a 20 storey Camelot condominium, a 5 storey electricity sub-station, and a single

storey pumping station, all supported on pile foundations. There is also a cluster of warehouses supported on shallow foundations. Figure 2 shows the location of these structures in relation to the cut and cover KPE tunnel.

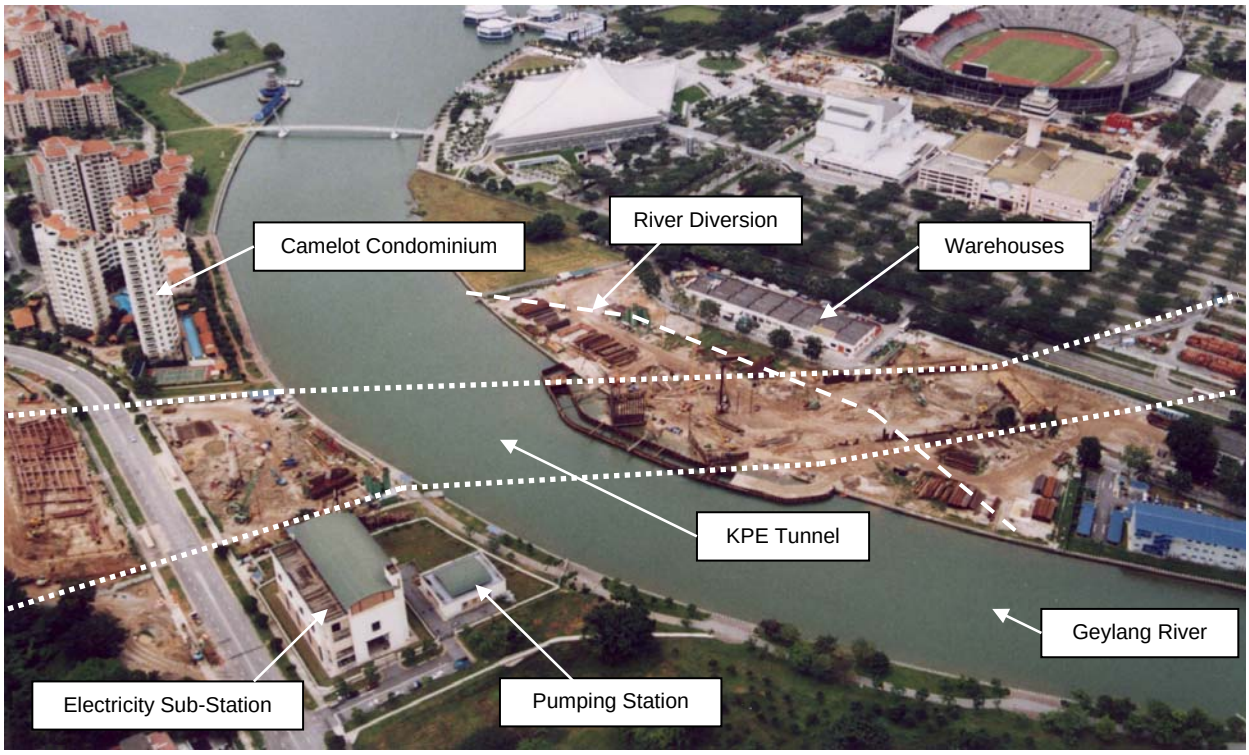

Figure 2: Aerial photo of structures adjacent to KPE C421 alignment.

Extensive numerical modelling has been used for the design of the temporary support systems, to ensure that the ground movements due to the excavation will not adversely impact the buildings adjacent to, and the bored piles below, the excavations. This paper focuses on the methods adopted for the prediction of the excavation induced ground movements and the assessment of impacts on the adjacent structures. The instrumentation and monitoring plan for critical structures are discussed and selected field monitoring results are presented.

2 SUBSURFACE CONDITIONS

The project site is located in an area where bedrock is inferred to be at a depth of greater than 70 m. The soils underlying the area have been divided into three main units comprising fill, overlying Kallang Formation, then overlying Old Alluvium. The measured groundwater levels are generally within 1 m to 1.5 m below the ground surface level.

Fill is present over the entire site except on the riverbed of the Geylang River. This fill is part of the reclamation works over the former low lying swampy land adjacent to the river. The material varies from sandy to clayey. The sandy fill is generally uncompacted with densities ranging from very loose to loose and medium dense. The clayey fill is generally soft to firm in consistency.

The Kallang Formation consists of sediments of fluvial or marine origin. The fluvial sediments can be sub-divided into cohesive and non-cohesive soils. The non-cohesive fluvial soils (F1) comprise sandy silts, silty sands and clayey sands. The F1 soils are loose to medium dense. The cohesive fluvial soils (F2) comprise sandy clays, silty clays and clayey silts. The F2 layer, which separates the two marine clays, is of high plasticity and is firm to stiff in consistency.

The two units of high plasticity marine clays have high compressibility, medium to high sensitivity and very low permeability. The upper marine clay (AuM) forms a near continuous layer along the tunnel route and ranges from 4 m to 18 m thick. The AuM is generally very soft to soft in consistency. The lower marine clay (ALM) forms several discontinuous layers ranging from 2 m to 18 m thick. The ALM is generally soft to firm in consistency. The field and laboratory test results indicate that the undrained shear strength (S_u) of the marine clays increases with depth. For design purposes S_u is taken to range between 10 kPa and 60 kPa. Due to the soft consistency, the marine clays have

particular significance to the design and construction of the KPE tunnel. Typical material properties are shown in Figures 3, 4 and 5.

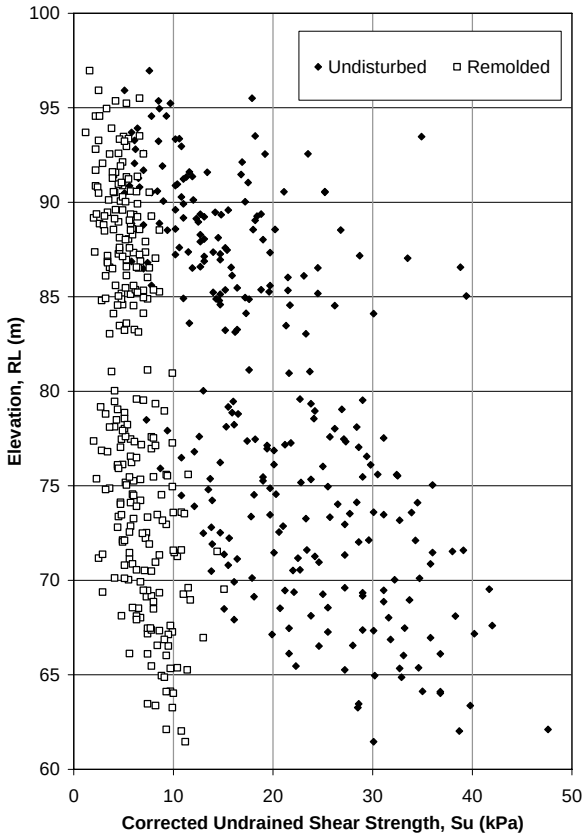

Figure 3: Undrained shear strength of marine clays from vane shear tests.

The Old Alluvium (OA) is a deposit of over-consolidated and cemented silty clays and silty sands, which range from medium dense or stiff, when weathered, to very dense or hard, where cemented. The depth of weathering is irregular varying from 0 to 21 m from the top of the unit. The OA layer is further sub-divided into a weathered unit OA-W1, two slightly weathered units OA-SW1 and OA-SW2 and the cemented unit OA-CZ.

The interpreted subsurface profile along the KPE C421 alignment is shown in Figure 6, and the geotechnical parameters adopted for the analysis are given in Table 1.

3 BORED PILES BENEATH EXCAVATION

3.1 GENERAL CONDITIONS

Permanent bored piles are installed under the base of the tunnel excavation to support the tunnel box, including overlying fill. The bored piles are typically 1 m diameter reinforced concrete piles, except at sections with heavier loads where 1.2 m diameter piles are used. In general, pile spacing of 3 m c/c or 6 m c/c is adopted to minimize the group effect. Piles in pure compression require reinforcement for the top 12 m only. Piles are installed prior to excavation.

3.2 DESIGN CONSIDERATIONS

The reduction of overburden pressure as excavation progresses results in heaving of soils at the base of the excavation which introduces tensile forces in the piles. Further, excavation causes lateral movement of the temporary sheet pile walls as well as lateral movement of soils below the excavation. The piles are subjected to additional lateral forces resulting from the lateral soil movement.

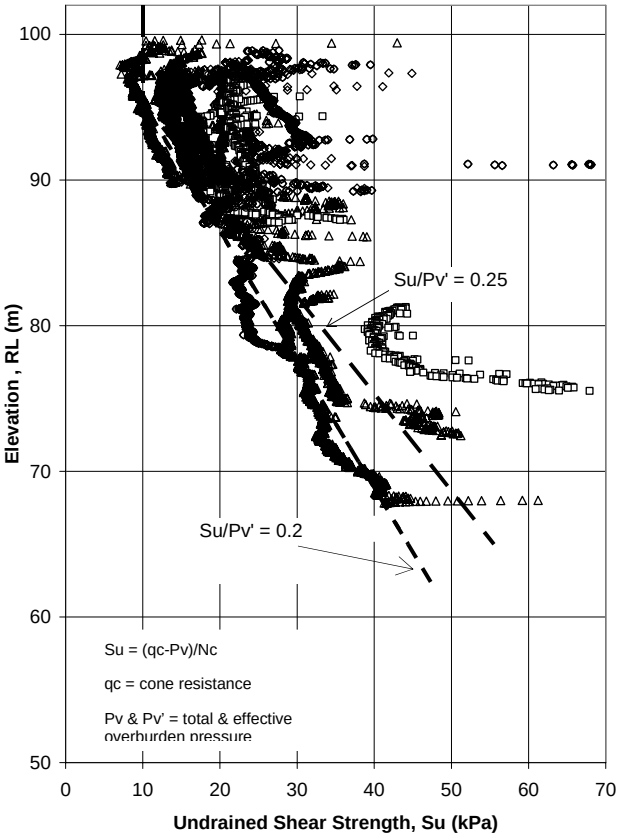

Figure 4: Undrained shear strength of marine clays from piezocone tests.

Table 1. Geotechnical design parameters.

Soil Unit	γ_t kN/m^3	Undrained Condition		Drained Condition			K_0	k cm/s
		S_u kPa	E_u kPa	c' kPa	ϕ' deg	E' kPa		
Fill (Clayey)	19	40	20,000	0	25	17,000	0.5	10^{-5}
Fill (Sandy)	19	-	-	0	30	10,000	0.5	10^{-4}
F1	19	-	-	0	30	10,000	0.7	10^{-3}
AuM	16	z≤6.7m, 10 6.7m<z≤40m, 10-60	z≤6.7m, 3000 6.7m<z≤40m, 3000-18,000	0	22	z≤6.7m, 2600 6.7m<z≤40m, 2600-15,600	1.0	10^{-7}
F2	19	50	15,000	0	26	13,000	1.0	10^{-6}
ALM	16	z≤6.7m, 10 6.7m<z≤40m, 10-50	z≤6.7m, 3000 6.7m<z≤40m, 3000-15,000	0	22	z≤6.7m, 2600 6.7m<z≤40m, 2600-13,000	1.0	10^{-7}
OA-W1	19	100	30,000	10	30	26,000	1.0	10^{-5}
OA-SW1	20	200	60,000	20	32	52,000	1.0	10^{-5}
OA-SW2	20	400	120,000	25	34	104,000	1.0	10^{-6}
OA-CZ	20	600	180,000	35	35	156,000	1.0	10^{-6}

where, γ_t = total unit weight of soil; S_u = undrained shear strength; E_u = undrained Young's modulus; c' = effective cohesion; ϕ' = effective friction angle; E' = drained Young's modulus; K_0 = at rest earth pressure coefficient; k= permeability; and z = depth below ground surface.

The possible additional lateral and axial tensile loads on piles as a result of unloading in the soil and the movements of soil during excavation are considered in the design.

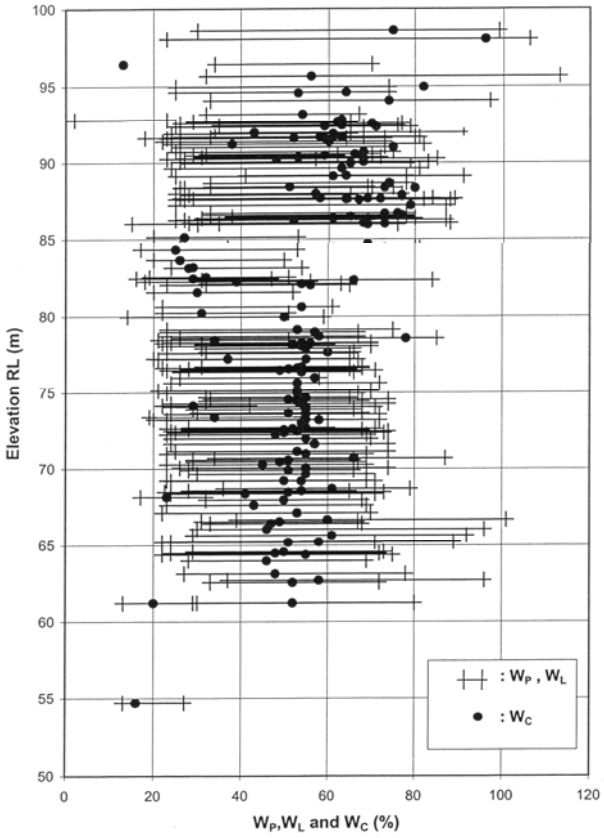

Figure 5: Plastic limit W_P, liquid limit W_L and moisture content W_C of marine clays.

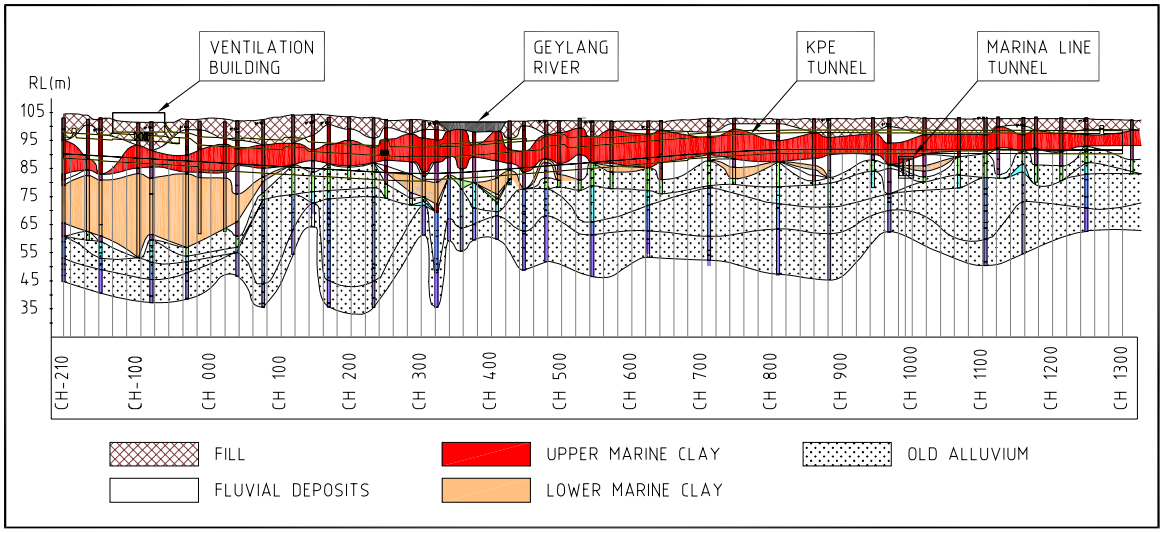

Figure 6: Interpreted subsurface profile along KPE C421.

3.3 ASSESSMENT METHODOLOGY

The methodologies suggested by Hull (1998), and Poulos (1989) are adopted for the assessment of bending moments and tension forces in piles associated with excavations.

A two dimensional finite element analysis program, PLAXIS (Version 7, 1998), is employed to calculate the ground movements without the presence of piles, i.e., the "greenfield" ground movements. PLAXIS considers the soil-structure interaction, the time dependent behaviour, the pore pressure response, the construction sequence and the appropriate constitutive soil model. The generation and dissipation of excess pore water pressure around the boundary of the excavation is simulated by PLAXIS in the form of consolidation using effective stress parameters and Mohr-Coulomb soil model. The rate of pore pressure dissipation is controlled by the permeability of the soil. Figure 7 is an output from the PLAXIS analysis for an excavation section at Ch +180 showing the displacement vectors when excavation reached its final stage. Note that the vertical lines below the excavation indicate the locations of the bored piles.

Figure 7 shows that the piles located under the centre of the excavation are mainly subjected to vertical soil movements whereas the piles located close to the edge of excavation are subjected to both vertical and lateral movements. The lateral soil movements are introduced in the program PALLAS (Hull, 1998) to calculate the induced bending moments in the piles. The vertical movements are entered in the program PIES (Poulos, 1989) to derive tensile forces in the piles. Both PALLAS and PIES allow soil to move past the piles, i.e. the soil and pile do not need to have identical movements.

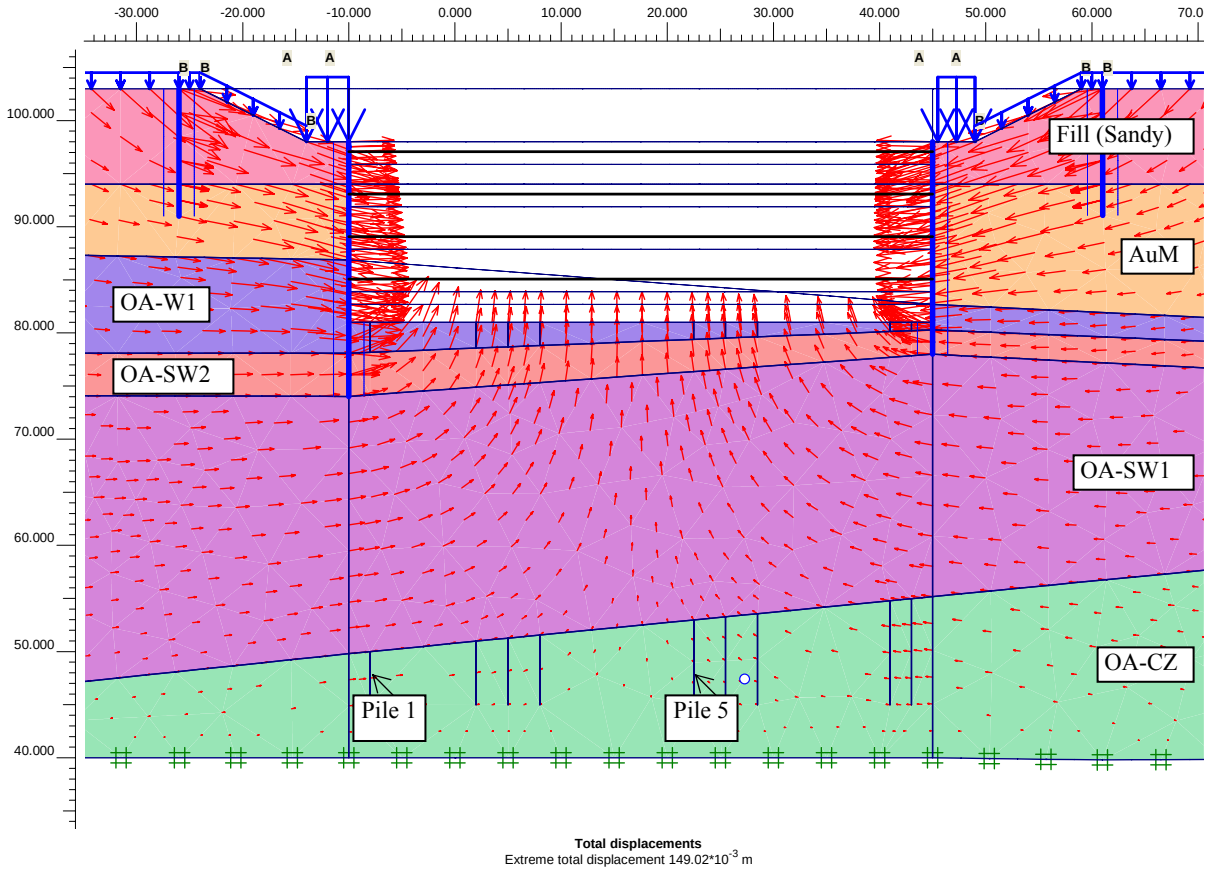

Figure 7: PLAXIS output at Ch +180 showing displacement vectors.

3.4 RESULTS OF ANALYSIS

The response of an edge pile at Ch +180 (Pile 1 on Figure 7) to lateral soil movement and the resulting bending moment induced in the pile are shown in Figure 8. The response of a central pile at Ch +180 (Pile 5 on Figure 7) to vertical soil movement and the resulting axial force induced in the pile are shown in Figure 9. These bending moments and axial forces are incorporated into the design of the bored piles. In Figure 9, the uniform pile has reinforcement extending to the toe of the pile, whereas for the non-uniform pile, reinforcement extends to the depth where axial stress is less than 1 MPa (tensile capacity of plain concrete), thus leading to a more optimized design.

4 BUILDING ON DEEP FOUNDATIONS

4.1 GENERAL CONDITIONS

There are three buildings located within 50 m of the tunnel excavation, which are supported on piles. The buildings include a 20 storey Camelot condominium, a 5 storey electricity sub-station, and a single storey pumping station. A similar methodology was adopted to assess the potential impacts the excavation may have on the foundation piles. In this paper, the assessment details and results for the most critical building, the 20 storey condominium, are discussed.

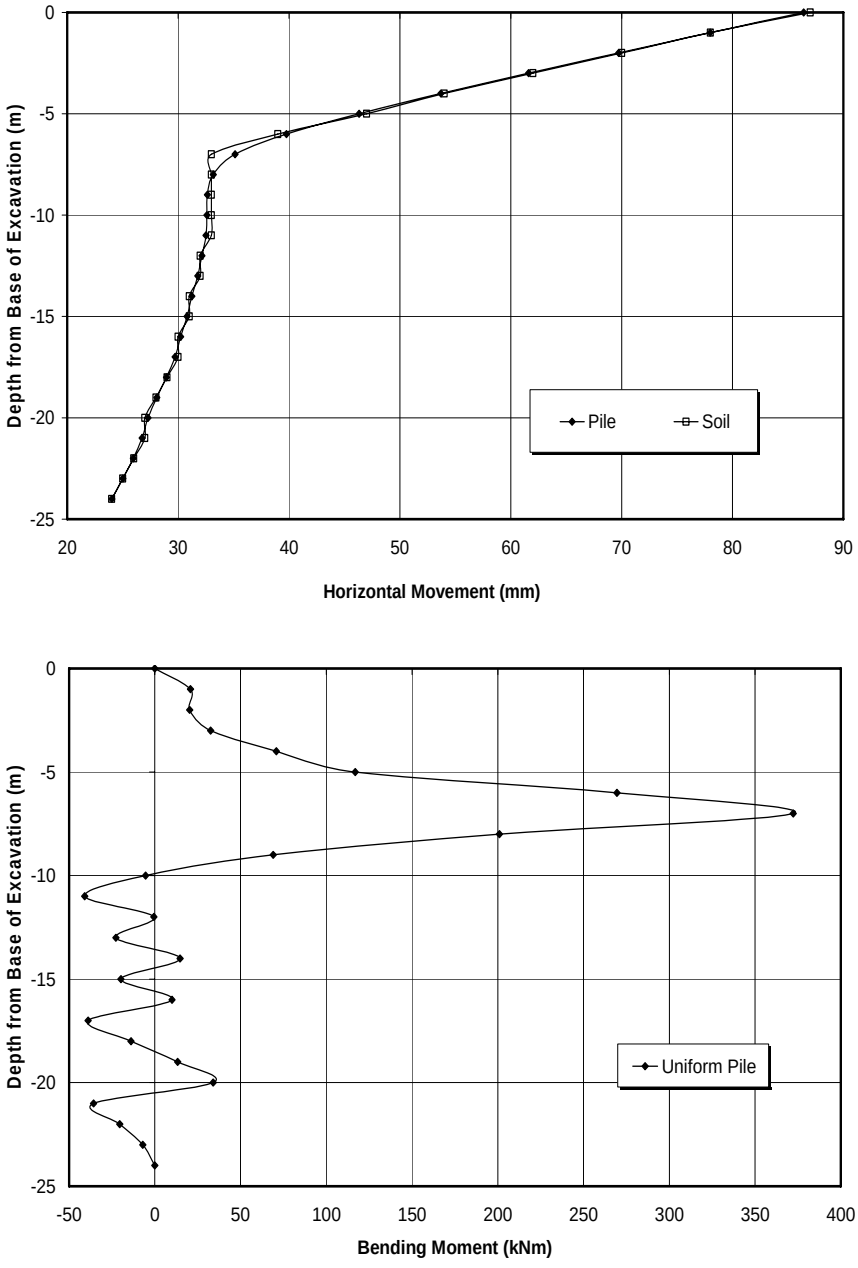

Figure 8: Response of an edge pile (1m dia.) to lateral soil movement.

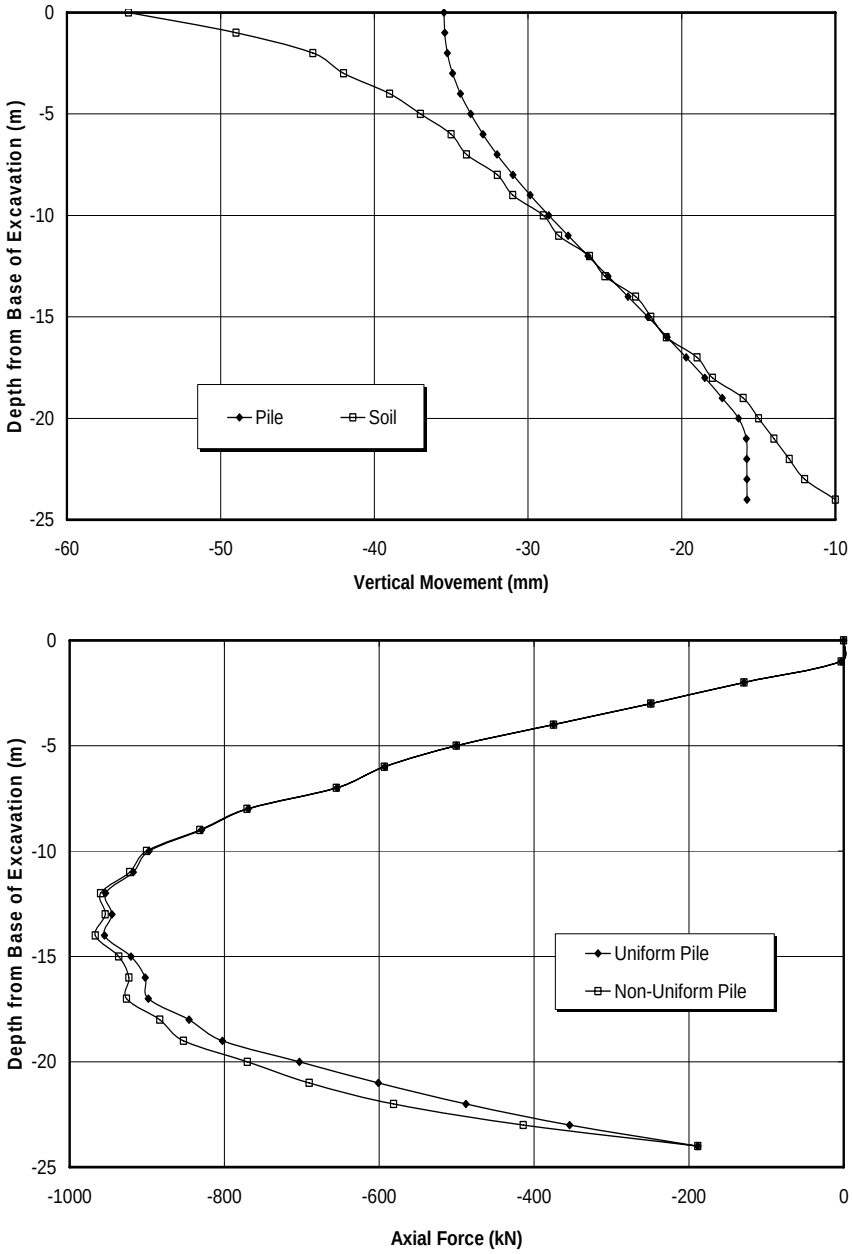

Figure 9: Response of a central pile (1m dia.) to vertical soil movement.

Camelot condominium is a 5 years old residential property, comprising a block of 20 storey flats and a block of flats from 3 storeys to 15 storeys complete with a club house, a swimming pool and a tennis court at the location as shown in Figure 2. The minimum distance of the building to the tunnel alignment is 30 m. The perimeter wall/fencing of Camelot condominium in relation to the temporary works is shown on the instrumentation and monitoring plan in Figure 10. The excavated area here is up to 84 m wide and 22.5 m deep.

The building structure is founded on driven precast pre-tensioned spun concrete piles with pointed pile shoes. The pile size consists of 450 mm, 500 mm, 600 mm diameter. The recorded pile length is 35 m from the pile cut off level. Based on the longitudinal geotechnical section, it is considered that the piles are founded in the OA stratum. An extensive 250 mm thick reinforced concrete slab constitutes the basement floor, which connects the buildings and extends under the tennis court. The near side of the tennis court is 31 m from the KPE excavation. The 20 storey building is located on the far side of the tennis court, approximately 35 m away from the excavation. The piles selected for damage assessment are located under the tennis court due to their close proximity to the excavation and sensitivity to ground movement.

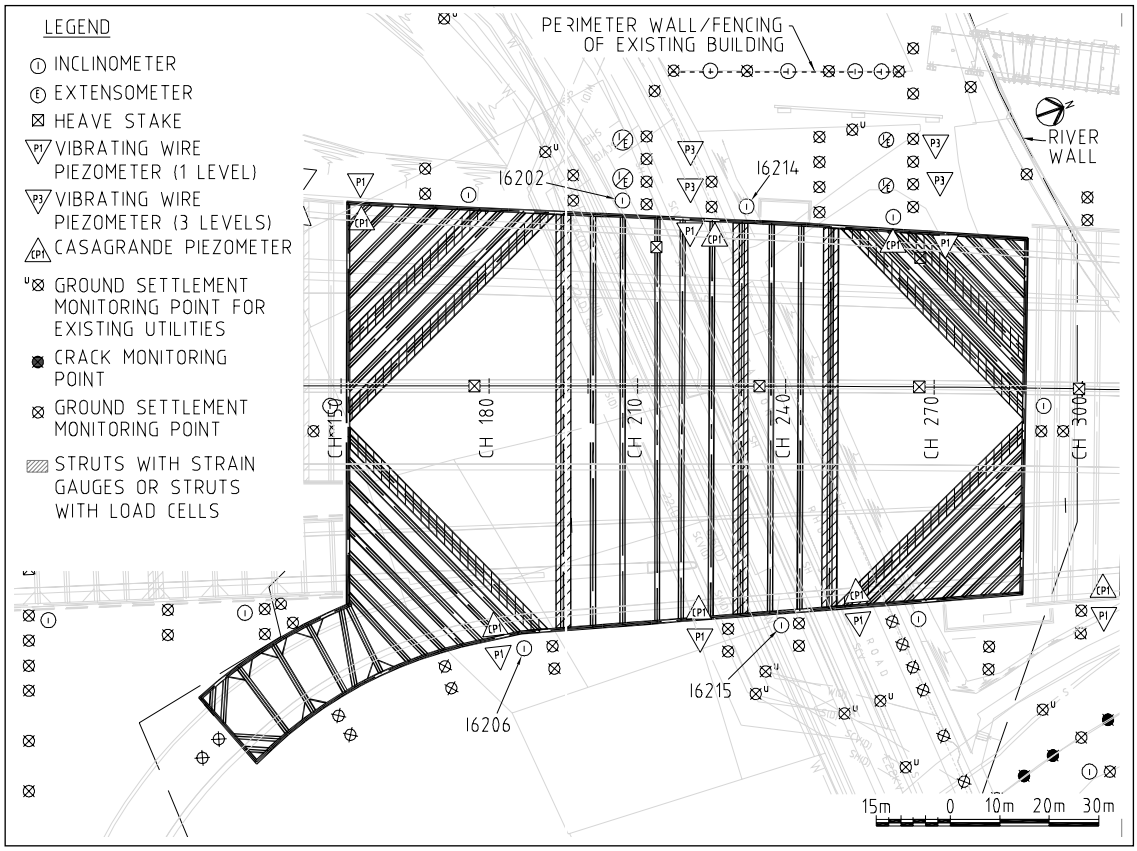

Figure 10: Instrumentation and monitoring plan of KPE C421 alignment adjacent to Camelot.

The excavation for the KPE tunnel involves a 5 m pre-cut prior to sheet piling. This pre-cut causes some horizontal ground movement before any bracing is installed to the sheet pile walls. The design is developed to control any further horizontal movement within the total limits for the prevention of damage to the Camelot building piles.

4.2 DESIGN CONSIDERATIONS

Due to the compressible and low strength nature of the underlying soils, most structures along the project alignment are founded on piles. As the project site is located in a reclaimed area where the whole area is undergoing consolidation settlement, the pile design for the existing structures is expected to have allowed for additional loading from negative skin friction (NSF). The excavation works will only speed up the settlement process and will not add additional vertical loads onto the piles of existing structures.

However, excavation would also result in lateral soil movements which would induce additional bending moments on the piles, compromising the pile performance. The impacts of lateral soil movement on the piles are considered in design of the temporary sheetpile walls.

Another important consideration is the plastic flow of the Marine Clay "squeezing" between the piles, i.e. horizontal ground movement can occur without this translating to a similar degree of movement of the piles. Lateral loads applied to the piles due to lateral soil movement will be distributed over the length of the whole pile group beneath the buildings.

4.3 ASSESSMENT METHODOLOGY

The horizontal ground movement at pile locations caused by the adjacent excavation is estimated using the program PLAXIS. The induced bending moments at pile locations are calculated using the program PALLAS. The induced bending moment is compared with the flexural capacity of the pile to determine the possibility of pile damage during excavation. This approach captures the complexity of the subsurface soil-structure interactions and is similar to that described in Section 3 above.

4.4 RESULTS OF ANALYSIS

PLAXIS modelling reveals that lateral soil movements of approximately 30-50 mm around the basement are expected at the position of piles closest to, and located at approximately 35 m away from, the excavation. This is indicated in Figure 11, in which green field horizontal movements are shown. The basement is considered to be fully restrained from horizontal and vertical movement. The associated bending moment induced by this lateral soil movement does not exceed the pile capacity based on the results of PALLAS and will not adversely affect the performance of the piles. It is further assessed that the pile is able to tolerate a lateral soil movement up to 100 mm without its structural capacity being exceeded.

An observational approach has also been implemented based on site monitoring data to assess the performance of tunnel excavation. The support system for the tunnel excavation is designed so that the resulting ground movements will not induce bending moments in the pile that exceed the pile capacity. Inclinometers are installed along the perimeter wall of Camelot (see Figure 10) and the measured movements for each pre-excavation stage are reviewed before excavation to the next level can proceed. Should the measured values exceed the pile tolerance and indicate future movements could damage the piles, a contingency system would be implemented to prevent further ground movements from impacting the piles.

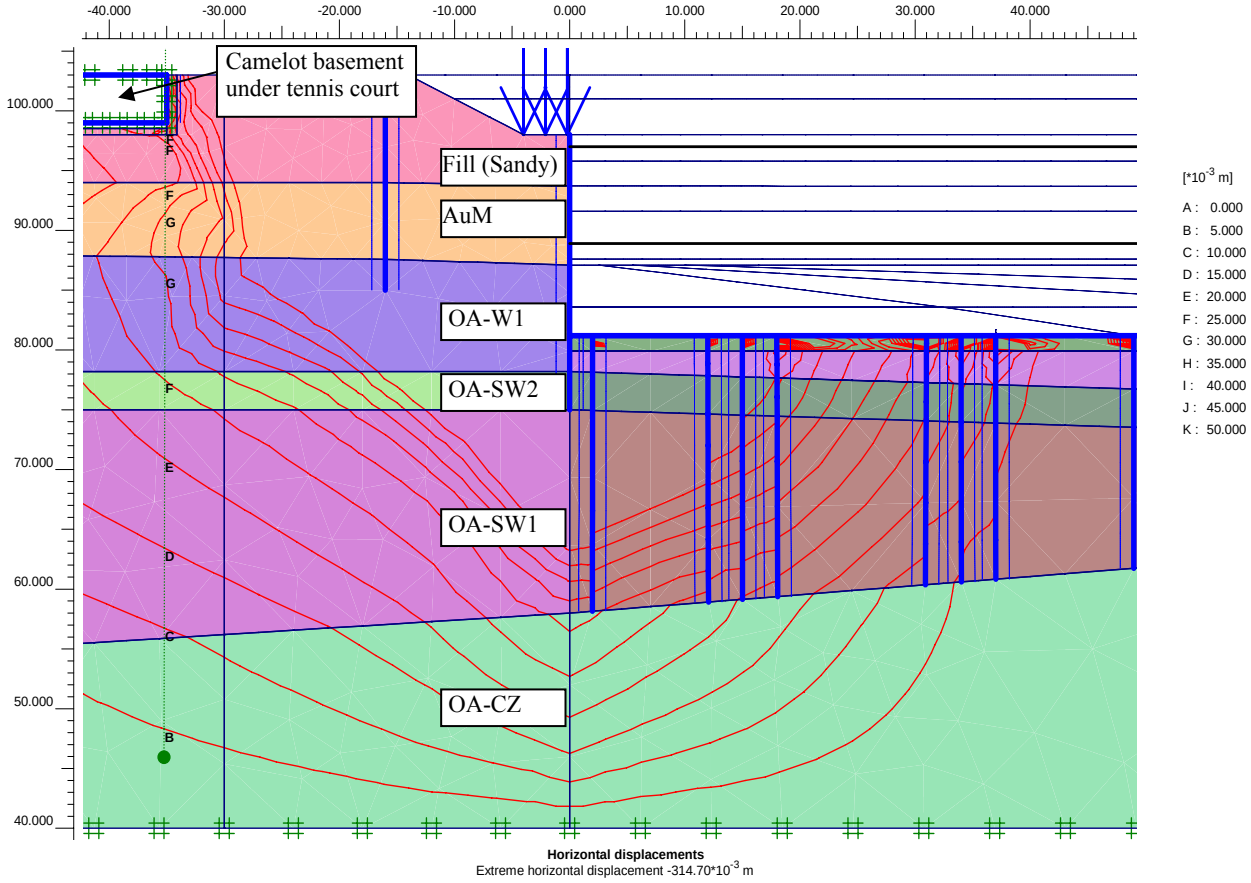

Figure 11: Horizontal soil movements at Ch +230.

4.5 PERFORMANCE

Four inclinometers have been installed at the perimeter of the Camelot condominium and have measured lateral ground movements up to 80 mm resulting from the tunnel excavation, as shown in Figure 12. These movements are within the structural capacity of the piles and are considered acceptable.

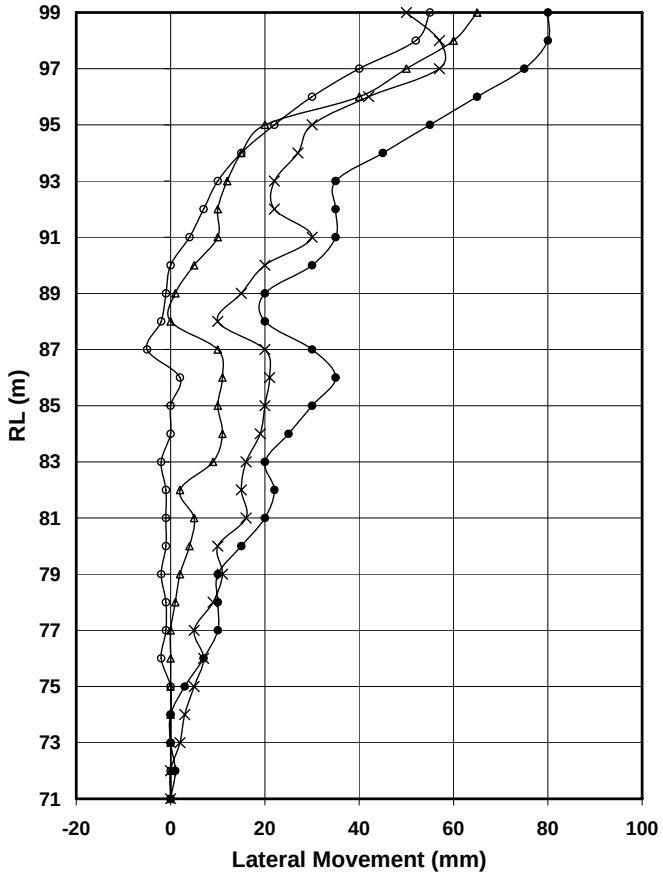

Figure 12: Measured lateral movements at perimeter wall after last excavation stage.

5 WAREHOUSES ON SHALLOW FOUNDATIONS

5.1 GENERAL CONDITIONS

Warehouses supported on shallow foundations are located to the north of the Geylang River as shown in Figures 1 and 2. In addition to the excavation works for the main tunnel at a distance of approximately 22 m away from the warehouses, a temporary river (Stage B) is to be excavated approximately 13 m in front of the warehouses as shown in Figure 13. This diversion of the Geylang River is required for the construction of the KPE section from Ch +280 to Ch +430.

5.2 DESIGN CONSIDERATIONS

It is envisaged that ground movements associated with excavation works carried out at such close proximity to the warehouses may induce damaging tensile strains in the structure. Analysis is carried out to determine the potential damage to the warehouses as a result of the ground movements caused by the adjacent excavation works.

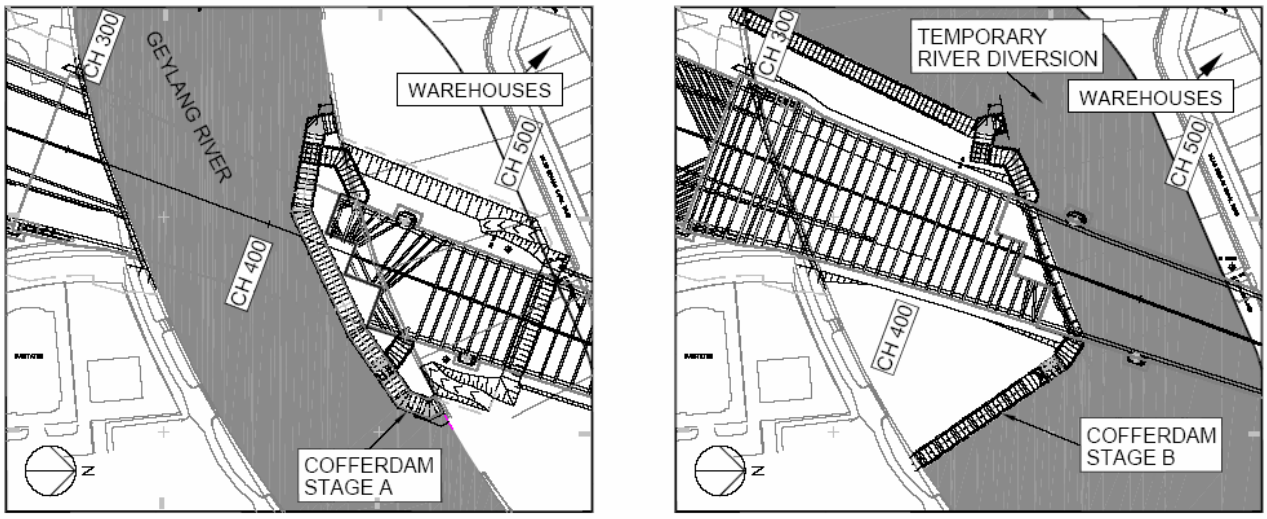

(a) Stage A (1st stage) (b) Stage B (2nd stage)

Figure 13: River crossing works.

5.3 ASSESSMENT METHODOLOGY

The vertical and horizontal ground displacements due to excavation are predicted using PLAXIS. Vertical and horizontal displacements are calculated for the main tunnel and temporary river excavations. The displacements are superimposed to obtain the vertical and horizontal ground movements due to both excavations.

The methodology used to assess the category of potential damage to the warehouses is based on limiting tensile strains (Burland *et al.*, 1977). The building is treated as an idealized beam and assumed to have no stiffness. The strains in the building due to the predicted relative settlements are calculated over its hogging and/or sagging spans.

The horizontal ground strain is combined with the bending and diagonal strains to give the total tensile strains using superposition suggested by Boscardin and Cording (1989).

The maximum tensile strains calculated are used to assess the potential damage to the building according to the relationship between tensile strains and categories of damage developed by Burland and Wroth (1974), Boscardin and Cording (1989) and Mair *et al*. (1996).

5.4 RESULTS OF ANALYSIS AND PERFORMANCE

The calculated vertical and horizontal displacements below the warehouse from PLAXIS are presented in Figure 14. Based on the methods described above, the damage category to the warehouses due to excavation works is assessed to be severe.

Due to the proximity of the warehouses to the excavations and the magnitude of predicted ground movements, it is considered uneconomical and impractical to minimize ground movements as a means to reduce the damage category to the warehouses. In reality the inherent stiffness of the warehouse will reduce the strains and the resulting damage of category will be less severe. A site construction procedure is developed that maintains the structural integrity and serviceability of the warehouse, during and following the occurrence of ground movement.

The procedure involves close monitoring of the amount of ground movement and structural movement of the warehouse and close inspection of the warehouse structure for evidence of any unacceptable loss of strength and serviceability. If such loss of strength and serviceability occurs, prompt remedial action is taken to recover this loss. Upon completion of the river diversion and excavation works, no severe distress of the building structure has been observed.

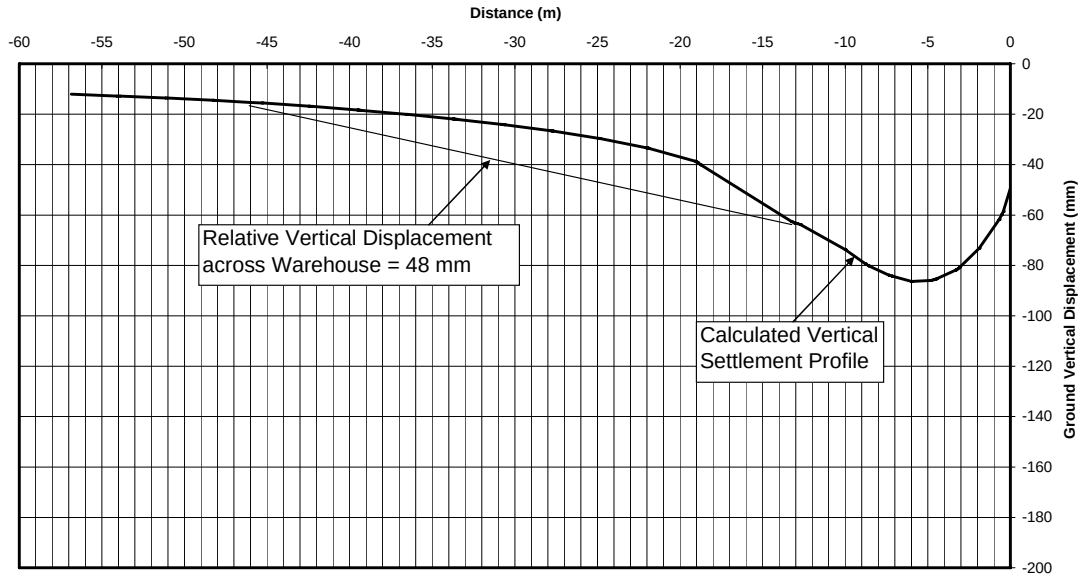

(a) Vertical displacement

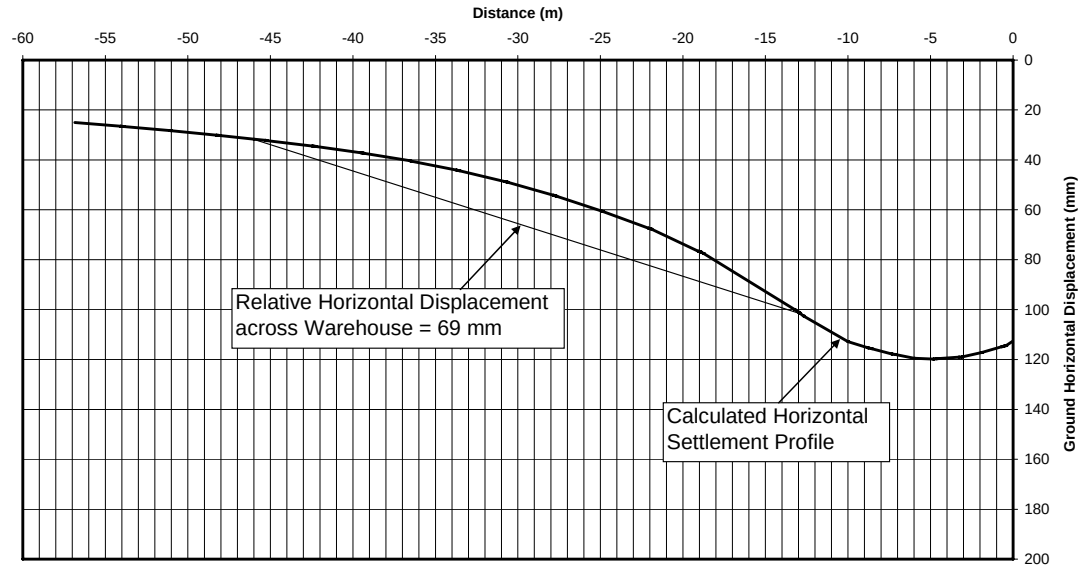

(b) Horizontal displacement

Figure 14: Calculated vertical and horizontal displacement of warehouse foundation.

6 CONCLUSIONS

It is prudent to properly predict the likely ground movements associated with large scale excavations in order to adequately assess the resulting impacts on the adjacent structures. The additional vertical loading and bending moment induced in the bored piles constructed below the tunnel due to excavation are considered during the design. An observational approach comprising prediction and monitoring of ground movements is adopted to evaluate the performance of foundation piles of a high rise building located close to a deep excavation. The presented building damage assessment procedure for warehouses sitting on shallow foundations follows well established practice.

7 REFERENCES

Boscardin, M.D., and Cording, E.G. (1989). Building Response to Excavation Induced Settlement. Journal of Geotechnical Engineering. ASCE, Volume 115, pp.1-21

Burland, J.B., Broms, B.B., and De Mello, V.F.B. (1977). Behaviour of Foundations and Structures. State of the Art Report, Session 2, Proceedings of the 9th International Conference on Soil Mechanics and Foundation Engineering, Tokyo.

Burland, J.B., and Wroth, C.P. (1974). Settlement of Buildings and Associated Damage. State of the Art Review. Conference on Settlement of Structures, Cambridge, Pentech Press, London.

Hull, T.S. (1998). Piles And Lateral Loading AnalysiS (PALLAS). Center for Geotechnical Research, Department of Civil Engineering, University of Sydney.

Mair, R.J., Taylor, R.N. and Burland, J.B. (1996). Prediction of Ground Movements and Assessment of Risk of Building Damage due to Bored Tunnelling. Geotechnical Aspects of Underground Construction in Soft Ground, Mair and Taylor (eds), 1996 Balkema, Rotterdam.

PLAXIS, Version 7, (1998). Finite Element Code for Soil and Rock Analysis, Brinkgreve and Vermeer (eds.), A.A. Balkema/Rotterdam/Brookfield.

Poulos, H.G. (1989). PIES. Centre for Geotechnical Research, Department of Civil Engineering, University of Sydney.

Poulos, H.G. (1998). The Effects of Ground Movements on Pile Foundations. Prof. R. Katzenbach and Prof U. Arslan (eds.), International Conference on Soil-Structure Interaction in Urban Civil Engineering 8-9 October 1998. Darmstadt Geotechnics No. 4 Vol 2. Darmstadt University of Technology, Germany.

SENSITIVITIES OF BRACED DEEP EXCAVATIONS TO JET GROUT PILE APPLICATIONS

Christopher Daniel
Parsons Brinckerhoff

ABSTRACT

In poor ground, jet grout pile (JGP) slabs may be used as preinstalled struts in deep excavations, to bring significant benefits to the earth-retention system. Based on the author's experience, top-down construction projects may require JGP slab usage to enable serviceability design criteria to be met at all construction stages, and to reduce base heave, ground settlement and soil loads on retaining walls during construction. This paper discusses parametric finite element sensitivity studies performed to predict qualitatively the performance of JGP slabs in reducing retaining wall loads, deflections, and associated ground movements.

1 INTRODUCTION

Jet grouting is a partial replacement/mixing technology that uses a tool equipped with one or more high pressure jets to erode and hydraulically excavate soils, while mixing cement grout with the *in situ* soils, creating soil-cement columns or soil-cement panels (Bruce, 2005).

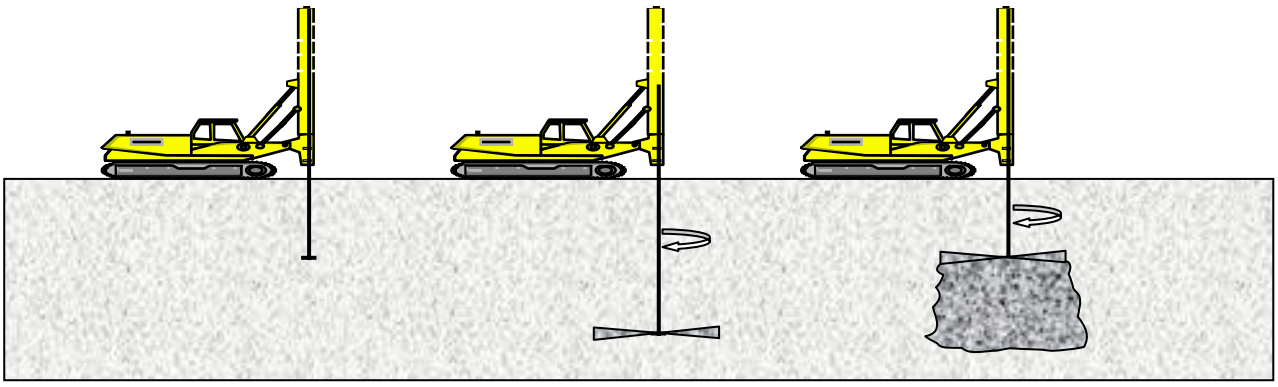

Figure 1: JGP construction stages (Hewitt *et al.*, 2006).

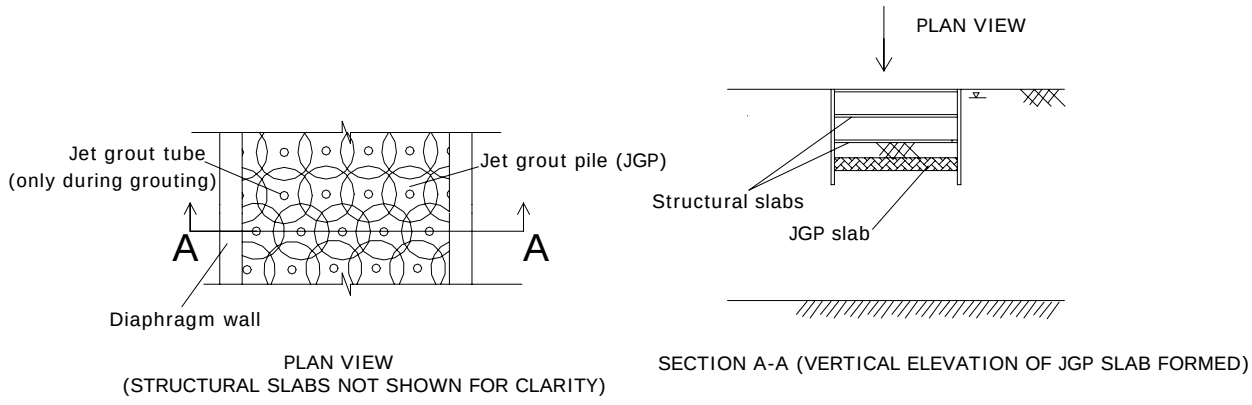

Figure 2: JGP grid, completed piles viewed in plan and elevation (slab).

When this grouting is done in a grid arrangement within structural walls (Figure 2), the end result is a slab composed of these piles. The principle, in this paper's context, is to introduce these slabs as lateral restraints, or struts, to walls at depth, prior to excavation commencement. Generally, this reduces the effective unbraced lengths of walls as excavation progresses and also counters base heave.

In addition, braced deep excavation walls often rely on some fixity in ground below formation level, for stability and deflection control. Where poor soils constitute deep layers (of the order of 60 m) below the proposed formation level, the wall depths required to attain this fixity can be economically prohibitive. JGP slabs can effectively fix such walls by acting as preinstalled struts, before excavation commences, thereby stabilising the deep excavation system.

2 THE JGP METHOD

2.1 CONSTRUCTION ASPECTS

From constructors' or specialist sub-contractors' perspectives, the following are the key issues in JGP slab applications:

- JGP diameter selection – concerns bore diameter and type of grout jets used;
- JGP single, double or triple tube drill bit usage - elaboration is beyond this paper's scope;
- JGP consistency – concerns the mix proportions of pre-existing soil and injected grout in the resulting piles;
- Jetting pressures - up to around 400 bars (40, 000 kPa) in the author's experience;
- JGP diameter –can range up to about 3 m (Bowles, 1996);
- JGP location – the targeted depth band;
- Jetting damage to temporary works - many deep excavation systems in densely built-up areas utilise temporary structural steelwork. The effects of high-pressure grouting in their immediate vicinity must be considered with regard to their continued functionality, eventual removal for reuse and construction sequencing;
- Jetting damage to buried services - pressure relief trenches excavated between the services and the JGP area are often used to provide paths of reduced soil resistance. Significant proportions of the jetting force at upper soil depths are dissipated via ground heave in these trenches. Alternatively, the pressure relief trenches can be around the services themselves, which are temporarily supported to keep them clear of the base heave and
- Jetting damage or adverse effects on tunnels in the vicinity – requires in-tunnel monitoring and a performance-based approach to grouting.

2.2 DESIGN ASPECTS

For design, the following are the key parameters of the JGP slab:

- Its stress-strain modulus;
- Its cross-sectional area;
- Its cohesion - derived from the unconfined compressive strength of grout samples tested. This value is of interest when modelling the JGP strut as an improved soil layer, as opposed to an elastic strut (foreign to the soil);
- Its depth below final formation level;
- The flexural rigidity and axial stiffness of the braced excavation system comprising walls and slabs and
- Surrounding soil parameters.

3 TOP-DOWN CONSTRUCTION IN THIS PAPER'S CONTEXT

Top-down construction may be used for underground metro stations, rail tunnels, building basements and underpasses, among others. These structures may be multi-levelled below the ground, involving a roof slab, several floor slabs, and a base slab. Geotechnically, the walls and slabs perform the following functions:

- Temporary earth-retention during construction;
- Permanent earth-retention during the structure's life-cycle and
- Resisting downward vertical loads and uplift due to floatation and heave.

With conventional top-down construction, the walls are typically installed first, followed by excavation, with slab casting at the requisite levels. Once each slab attains the requisite axial and bending strength, excavation proceeds below it, and the procedure repeats until base slab completion. The slabs generally act as struts throughout the structure's life.

Due to the walls deflecting within the temporary construction stage, prior to its permanent in-service stage, there can be difficulties keeping within the respective serviceability limit state criteria (crack widths) - a significant design criterion for tanked structures in poor soils.

Furthermore, deep excavations in cities are often constrained by physical and statutory limitations, precluding the use of ground anchors and soil nails. Examples include:

- Proximity of existing structures like basements, foundations or tunnels;
- Proximity of statutory 'reserves' surrounding them, within which works are either forbidden or permitted under very rigorous constraints and
- Land acts, building or environmental statutes forbidding the installation of temporary works under or at the perimeter of adjacent properties, when these cannot be reliably, safely and completely removed later. Where safe removal techniques exist, their cost and program implications may be prohibitive.

For these reasons, only braced top-down excavations are considered in the analysis here.

4 FINITE ELEMENT MODELLING OF JGP APPLICATIONS

The finite element program PLAXIS Version 8 was used in this analysis, with the following modelling considerations, and as shown in Figure 3:

- The structure is two-tiered with cell heights of 5.4 m, to examine the effects of JGP struts on generic multi-level structures like underground expressways, metro stations and basement car-parks;
- The construction method (Figure 4) is top-down with the priority to minimise existing road disturbance – the first excavation (Stage 3) is just to enable roof slab casting, so that traffic flows can be resumed quickly, while construction proceeds below the roof;
- Diaphragm walls (generally regarded as the stiffest walls available) with rectangular panels are assumed;
- From the structural serviceability perspective, the wall deflection profile is considered. This, together with the predicted base heave, are used by construction teams for monitoring purposes;
- From the environmental impact perspective, ground settlements immediately behind the wall and around 25 m away are captured to provide a basis of comparison for the effects of various JGP applications;
- A 50 m thick layer of firm clay is considered here as a generic representative of deep soil layers like alluviums estuarine and marine clays. The following parameters were assumed:
  - Unit weight - 16 kN/m³
  - Permeability - 8.64E-05 m/day
  - Poisson's ratio - 0.34
  - Stress-strain modulus - 20 MPa
  - Cohesion - 50 kPa and
  - Internal angle of friction - 0°.
- The groundwater table was at 2 m depth;
- Construction surcharge of 20 kPa was applied everywhere behind the walls. It was applied at the same first stage as diaphragm wall installation, and deformations were reset to zero from the second stage onwards, to clarify relevant construction-related settlements;
- Modelling and parametric application were carried out in accordance with Brinkgreve *et al.* (2004);
- Key output criteria taken are wall bending moment profiles, slab-strut axial loads, wall deflection profiles, base heave and ground settlement, to evaluate the effects of the JGP strut arrangements. The effects on the ground water table are also qualitatively observed and
- Bending moment envelopes also provide indications of areas where serviceability criteria, like 0.2 mm crack widths for tanked structures, may govern structural design considerations.

The objectives of the modelling were to examine the effects of JGP slab usage, compared to conventional top-down construction, then to consider the optimal location, thickness, unconfined compressive strength and stiffness of JGP slabs, to minimise deflections, settlements and heave.

4.1 CONTROL MODEL IN FIRM CLAY (MODEL 1) - NO JGP

This basic model, without JGP slab application, was set up using the construction and dewatering sequences as shown in Figure 4.

Ground settlement immediately behind the wall, and 24.6 m away were 66 mm and 125 mm respectively. Maximum base heave was 177 mm, and the groundwater table dropped 1.5 m behind the wall.

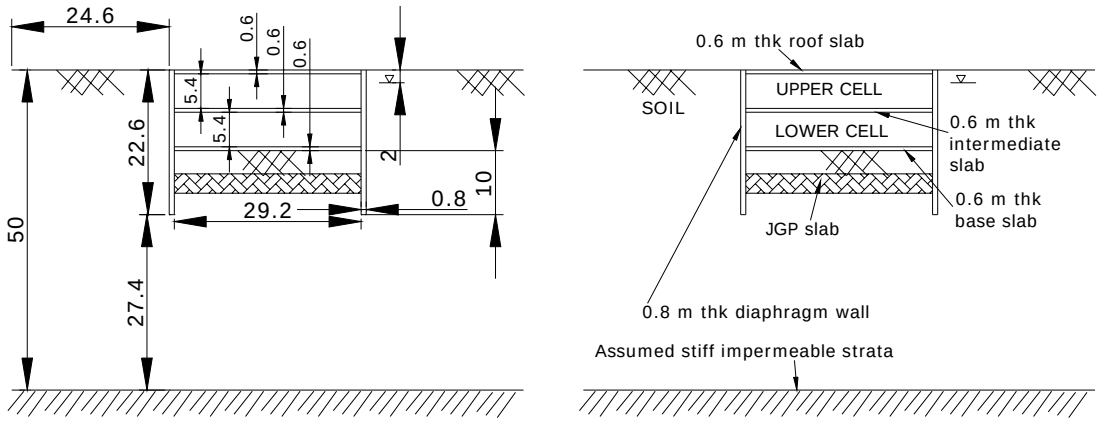

Figure 3: Geometrical and structural details of finite element top-down model.

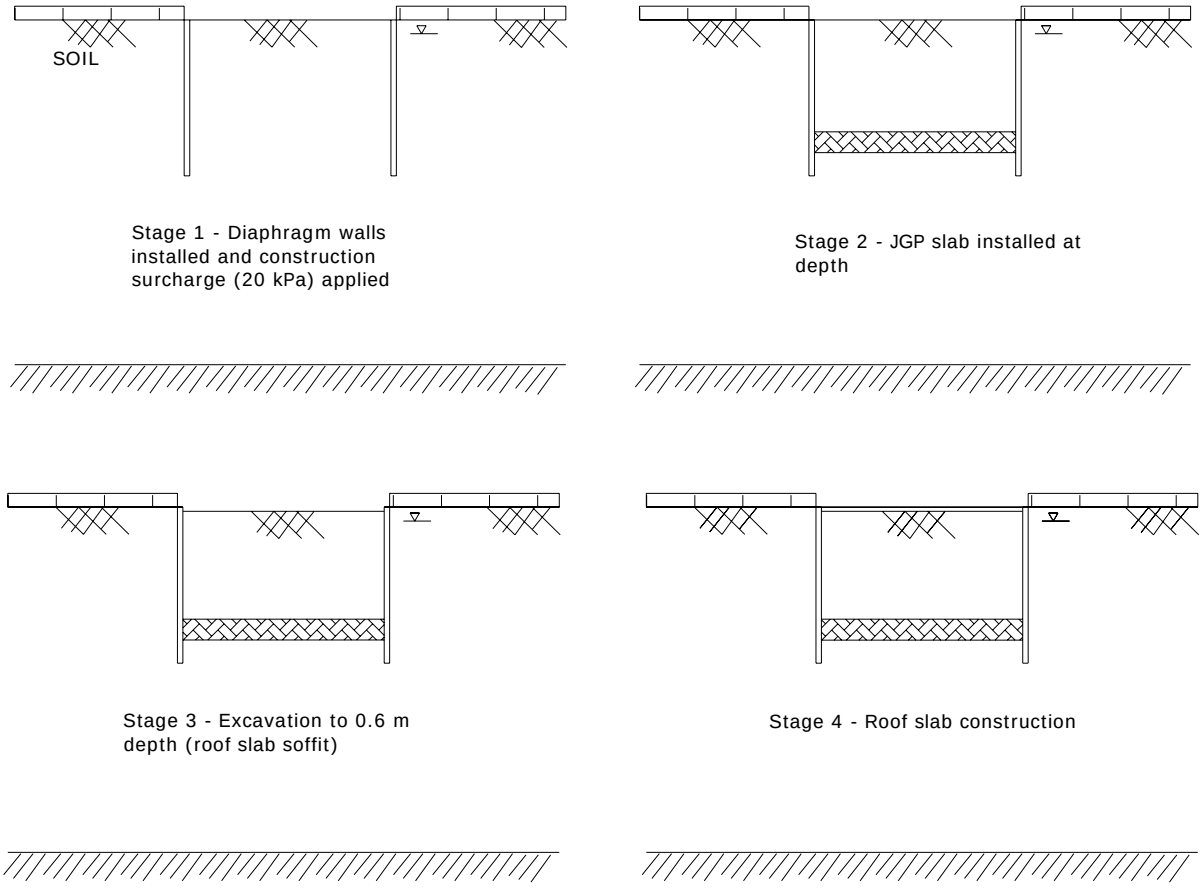

Figure 4: Finite element top-down model construction sequence Stages 1 to 4.

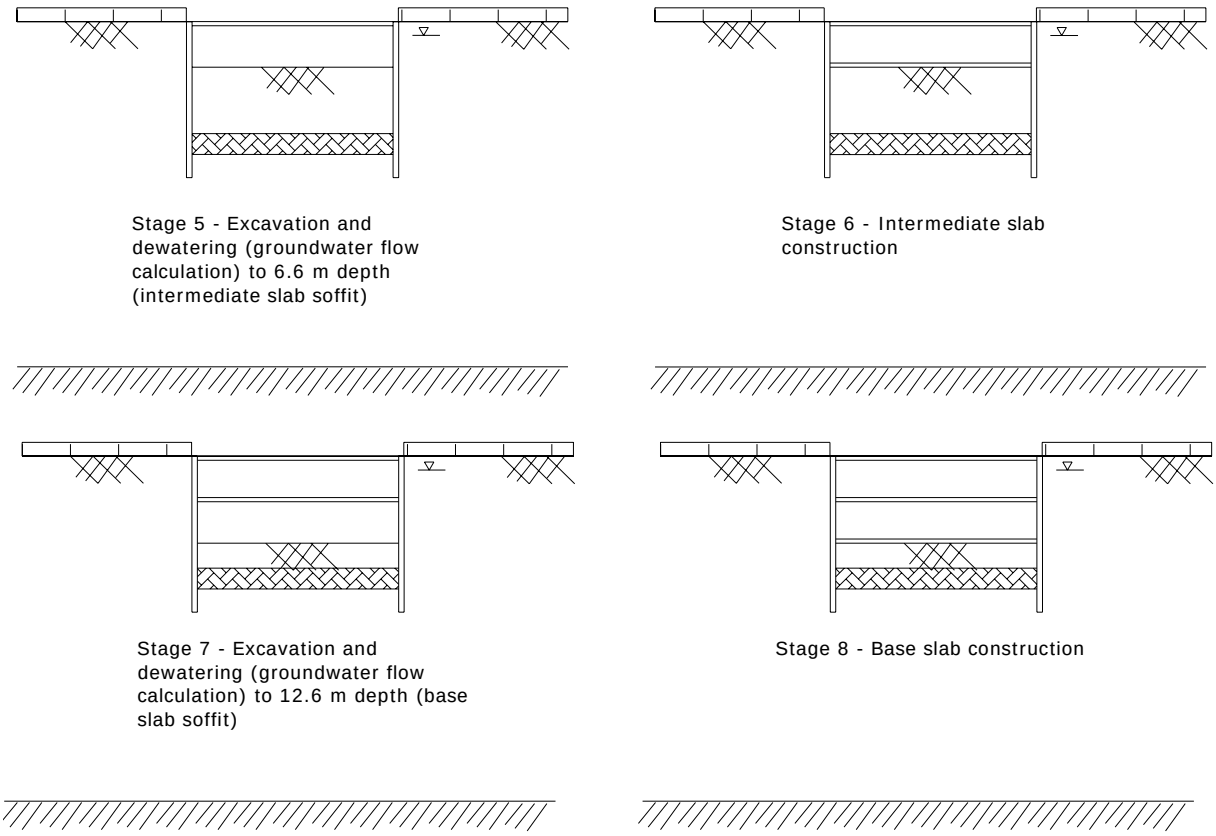

Figure 4: Finite element top-down model construction sequence Stages 5 to 8 (continued from previous page).

Note the following pertinent wall depths, for subsequent graph interpretation, and clarified in Figure 5:

- 3.3 m – mid-height of wall in upper cell above intermediate slab;
- 6.3 m – mid-height of intermediate slab;
- 9.3 m – mid-height of wall in lower cell above base slab;
- 12.3 m – mid-height of base slab;
- 15.1 m – wall depth at 2.5 m below base slab soffit;
- 18.1 m – wall depth at 5.5 m below base slab soffit;
- 22.6 m – wall toe depth.

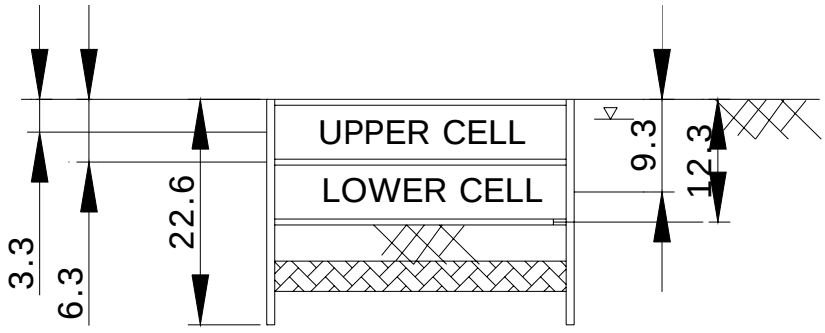

Figure 5: Pertinent wall depths as referenced by subsequent graphs.

Figure 6 gives the bending moment envelope (positive and negative) through all construction stages, for the left wall.

The following are salient points:

- Peak moments are at the slab support points, with relatively high bending at mid-height of the upper cell;
- The maximum moments at upper cell mid-height are significantly higher than at mid-height of the lower cell;
- Below the mid-height of the lower cell, there is no moment reversal and

- Moments reduce almost linearly with depth between base slab and toe – reasonable fixed cantilever behaviour.

As expected, the intermediate slab takes the maximum axial load of 1271 kN/m in compression. The roof slab takes 115 kN/m in tension, while the base slab effectively takes nothing (1.1 kN/m in compression), because of its late installation stage.

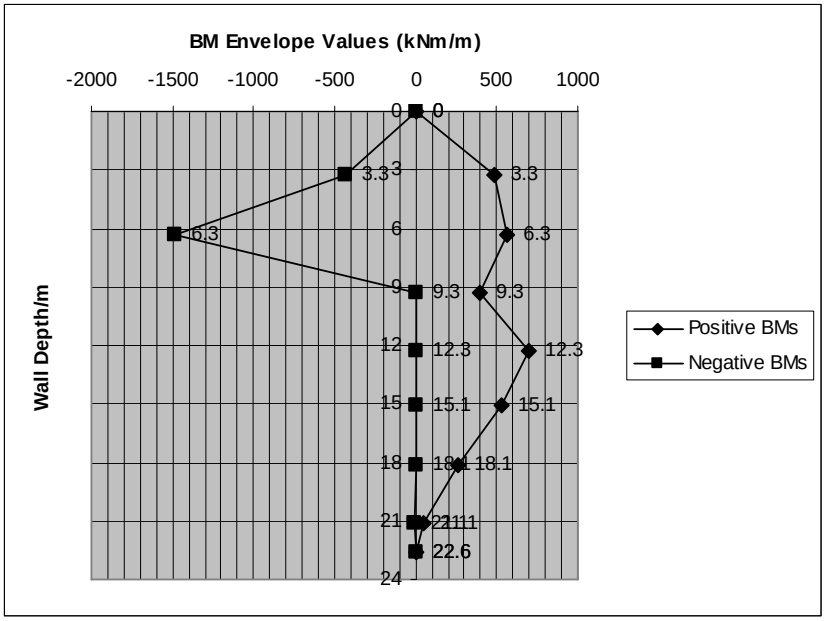

Figure 6: Bending moment (BM) envelope for left wall with wall depth (Model 1 - no JGP).

4.2 MODELS PERFORMED

The following is a summary of the models that were set-up and run:

Table 1: Summary of PLAXIS models run.

MODEL	SOIL	JGP SLAB LOCATION DEPTH (m)	JGP SLAB STRENGTH	JGP SLAB THICKNESS/M
1	Firm Clay	NONE	-	-
2	Firm Clay	12.6 -14.6	c_{ref} = 100 kPa; E_{ref} = 50 MPa	2
3	Firm Clay	14.6 - 16.6	c_{ref} = 100 kPa; E_{ref} = 50 MPa	2
4	Firm Clay	20.6 – 22.6	c_{ref} = 100 kPa; E_{ref} = 50 MPa	2
5	Firm Clay	12.6 -14.6	c_{ref} = 300 kPa; E_{ref} = 150 MPa	2
6	Firm Clay	14.6 - 16.6	c_{ref} = 300 kPa; E_{ref} = 150 MPa	2
7	Firm Clay	20.6 – 22.6	c_{ref} = 300 kPa; E_{ref} = 150 MPa	2
8	Firm Clay	12.6 -14.6	c_{ref} = 600 kPa; E_{ref} = 300 MPa	2
9	Firm Clay	14.6 - 16.6	c_{ref} = 600 kPa; E_{ref} = 300 MPa	2
10	Firm Clay	20.6 – 22.6	c_{ref} = 600 kPa; E_{ref} = 300 MPa	2
MODEL	**SOIL**	**JGP SLAB LOCATION/ DEPTH IN M**	**JGP SLAB STRENGTH**	**JGP SLAB THICKNESS/M**
11	Firm Clay	12.6 – 16.6	c_{ref} = 100 kPa; E_{ref} = 50 MPa	4
12	Firm Clay	12.6 – 18.6	c_{ref} = 100 kPa; E_{ref} = 50 MPa	6
13	Firm Clay	14.6 – 20.6	c_{ref} = 100 kPa; E_{ref} = 50 MPa	6
14	Firm Clay	12.6 – 18.6	c_{ref} = 300 kPa; E_{ref} = 150 MPa	6
15	Loose to Medium-Dense Sand	NONE	-	-

Note : c_{ref} and E_{ref} denote cohesion and Young's Modulus respectively (Brinkgreve *et al*., 2004).

For brevity, JGP slabs with c_{ref} = 100, 300 and 600 kPa will be referred to as low-strength (LS), medium-strength (MS) and high-strength (HS) JGP slabs respectively henceforth.

4.3 MODEL OUTPUT

4.3.1 The effect of the presence of a 2 m thick LS JGP slab (comparison between Models 1 and 2)

The LS JGP slab clearly has a beneficial effect on the bending moment envelopes (Figure 7). At intermediate slab level, the maximum negative moment falls from 1488.5 to 1180.3 kNm/m – a reduction in excess of 20 percent. Similarly, at base slab level, the maximum positive moment falls by 29 percent, from 703.1 to 501 kNm/m.

Figure 8 shows that the toe deflection is reduced by 22.4 mm from 107.9 to 85.5 mm – an improvement of 21 percent. As expected, the deflection reduction within the cells is lower than at the toe, due to the fixity provided by the slabs.

Both models have similar roof slab tensile forces of 115 (Model 1) and 113 (Model 2) kN/m, while base slab loads in both are insignificant compressions of 1.1 (Model 1) and 2.2 (Model 2) kN/m. However, the intermediate slab, which bears the greatest force, enjoys a reduction of 14 percent, from 1271 (Model 1) to 1094 kN/m (Model 2).

Maximum ground settlements immediately behind the wall and 24.6 m away drop from 125 mm and 66 mm respectively in Model 1 to 108 mm and 39 mm respectively in Model 2. Base heave falls from 177 to 161 mm, and the groundwater table is not significantly affected in Model 2, while it falls 1.5 m behind the walls in Model 1.

It is suggested, therefore, that, even a low-strength JGP slab of relatively small thickness (2 m) placed immediately below final formation level, is likely to be significantly beneficial to a top-down braced excavation in firm clay with a high groundwater table.

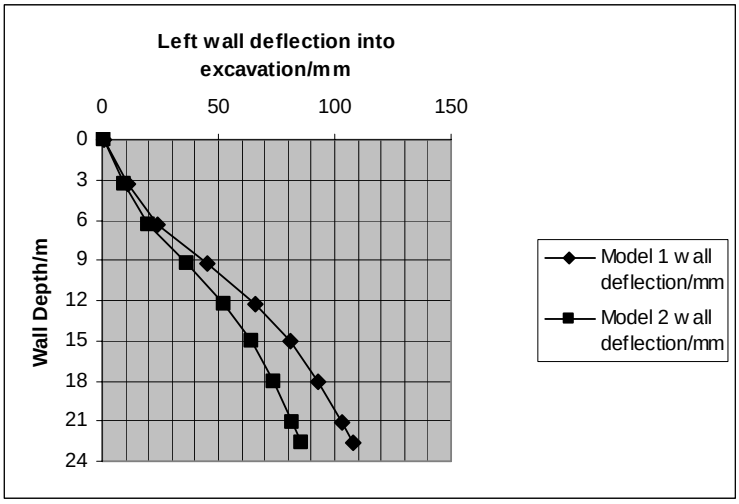

Figure 7: Bending moment (BM) envelope comparison between Models 1 and 2 (left walls).

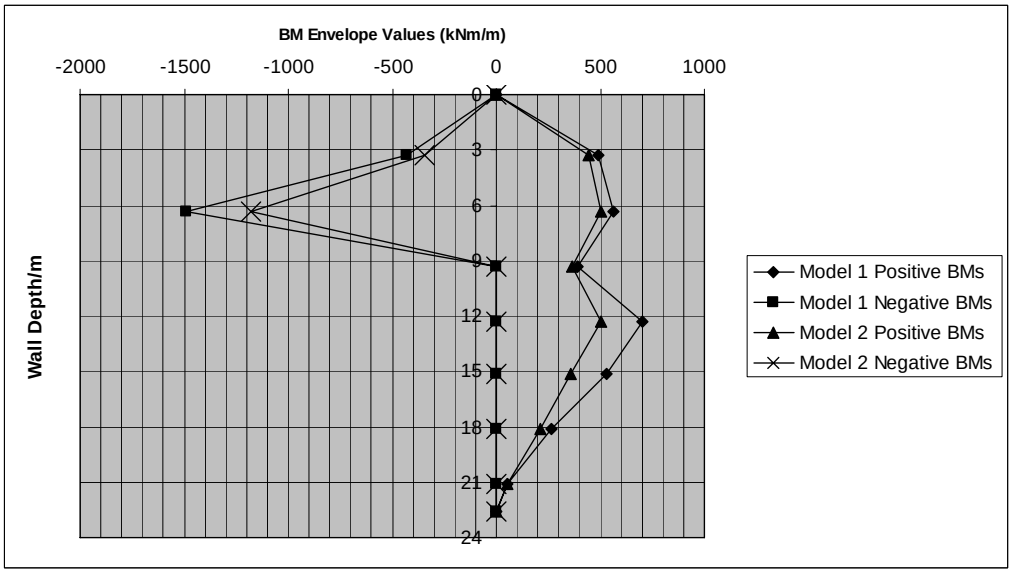

Figure 8: Left wall deflection profile comparison between Models 1 and 2.

4.3.2 The positional effects of a 2 m thick LS JGP slab (comparison between Models 1, 2, 3 and 4)

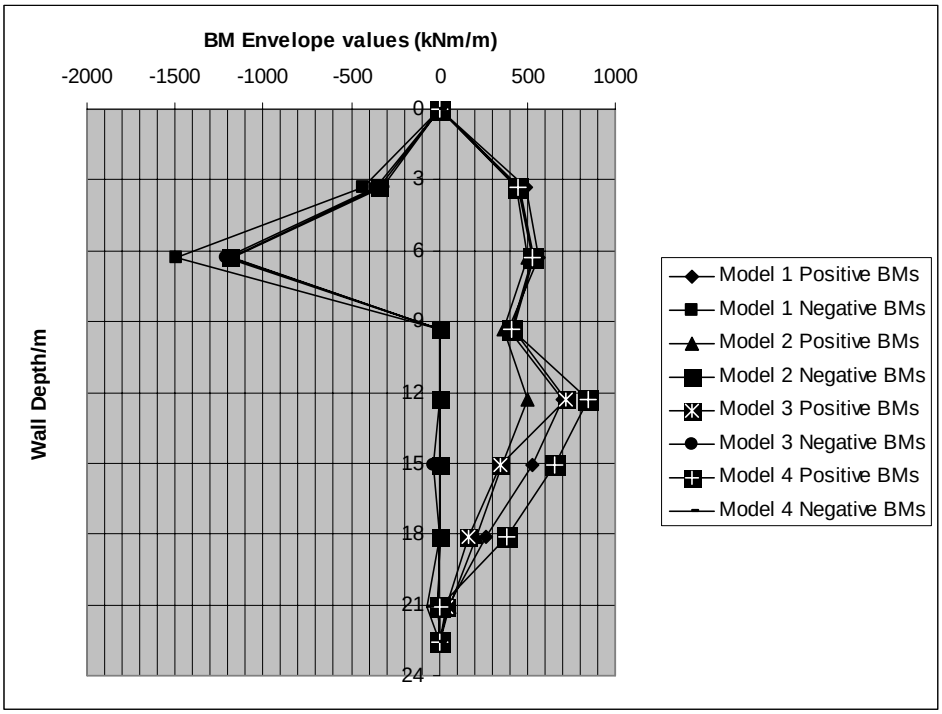

Figure 9: Bending moment (BM) envelope comparison between Models 1, 2, 3 and 4 (left walls).

Based on Figure 9, all modelled locations of the 2 m thick LS JGP slab provide similar reductions in the maximum negative moment at intermediate slab level (6.3 m depth) and mid-height of upper cell (3.3 m depth). As per Figure 7, there is no other area of significant negative bending moment envelope reductions.

Overall, Model 2 is the most effective at positive moment reduction, particularly above final formation level. However, below about 15 m depth, Model 3 tends to provide the greatest moment reduction.

Below the mid-height of the lower cell, Models 3 and 4 actually tend to increase the positive bending envelope values therein, greater than Model 1 values, with Model 4's envelope values being the most severe.

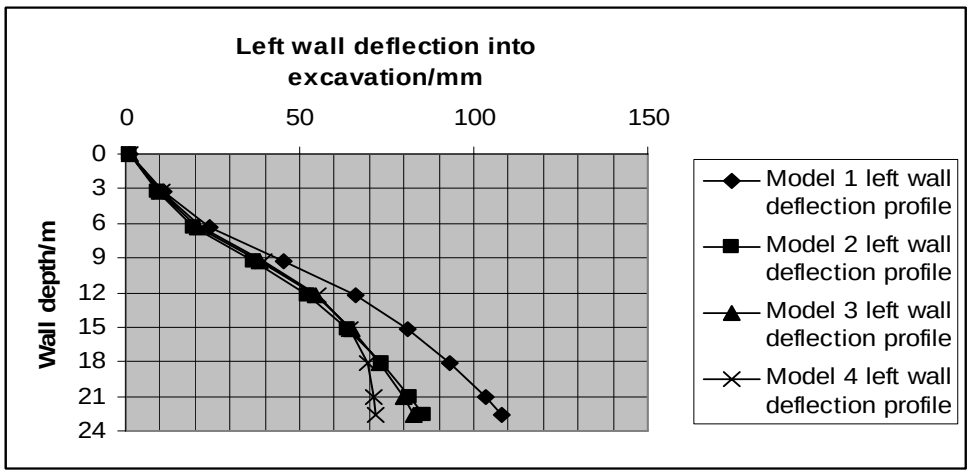

Figure 10: Left wall lateral deflection profile comparison between Models 1, 2, 3 and 4.

Based on Figure 10, all modelled JGP slab locations would reduce lateral deflection by approximately the same quantity above 18.1 m depth.

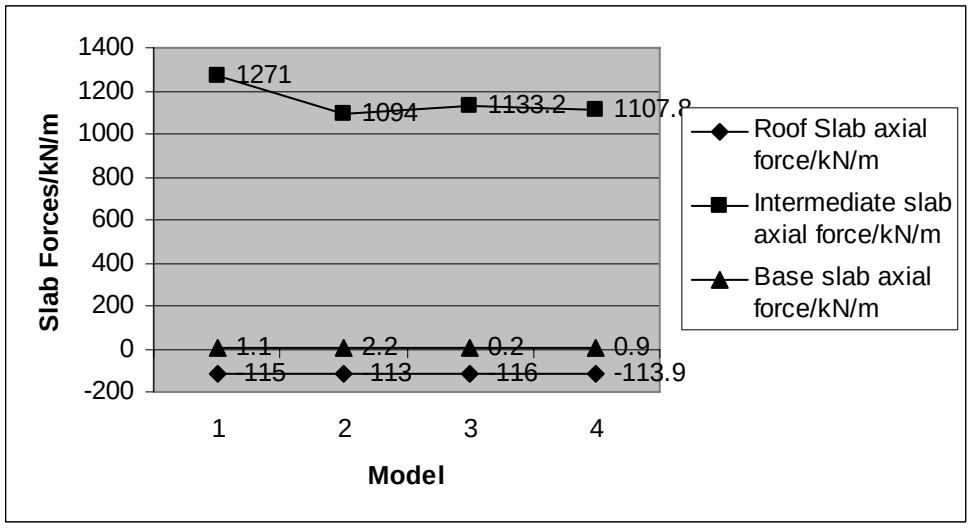

Figure 11: Slab axial force comparison between Models 1, 2, 3 and 4.

Base and roof slab forces appear largely unaffected by the presence of any JGP slab, let alone its position (Figure 11). However, the JGP slabs do reduce the intermediate slab axial forces somewhat.

Ground settlement is apparently unaffected by JGP slab location (Figure 12). However, Model 4's result suggests that the lower the JGP slab between walls, the lower the base heave.

The data suggests that, overall, the most effective JGP slab location is immediately below final formation level.

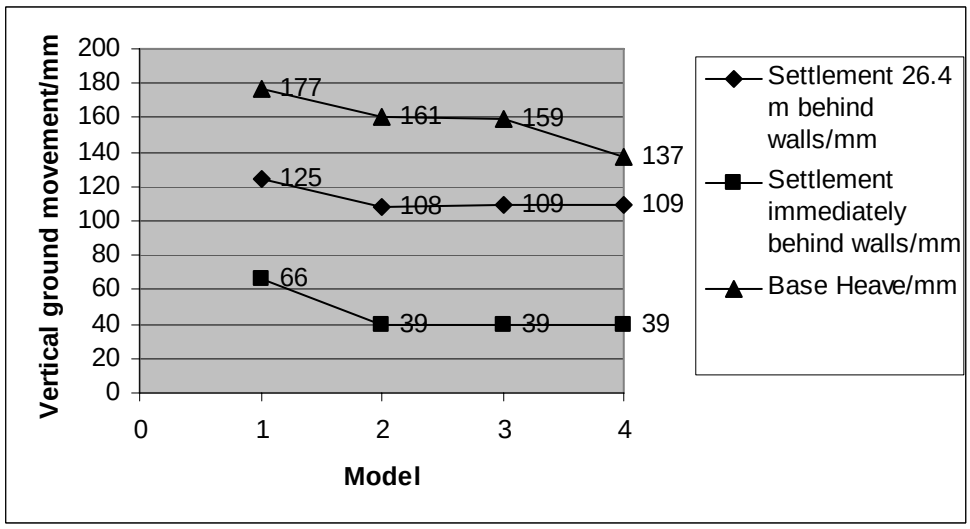

Figure 12: Vertical ground movement comparison between Models 1, 2, 3 and 4.

4.3.3 The strength effects of a 2 m thick JGP slab (comparison between Models 1 to 10)

Interestingly, Figure 13 suggests that increasing JGP slab material strength in factors of 3 and 6 does clearly reduce maximum positive moments above the mid-height of the lower cell (9.3 m depth), but not dramatically so. The dramatic reductions only occur between depths 9.3 m and 18.1 m (5.5 m below base slab soffit).

The opposite is true for the negative bending moment envelope - reductions are dramatic above 9.3 m depth. However, below that, the stronger the grout, the greater the magnitude of the negative bending moment.

This suggests that increasing grout strength is not a straightforward solution to reducing wall bending loads.

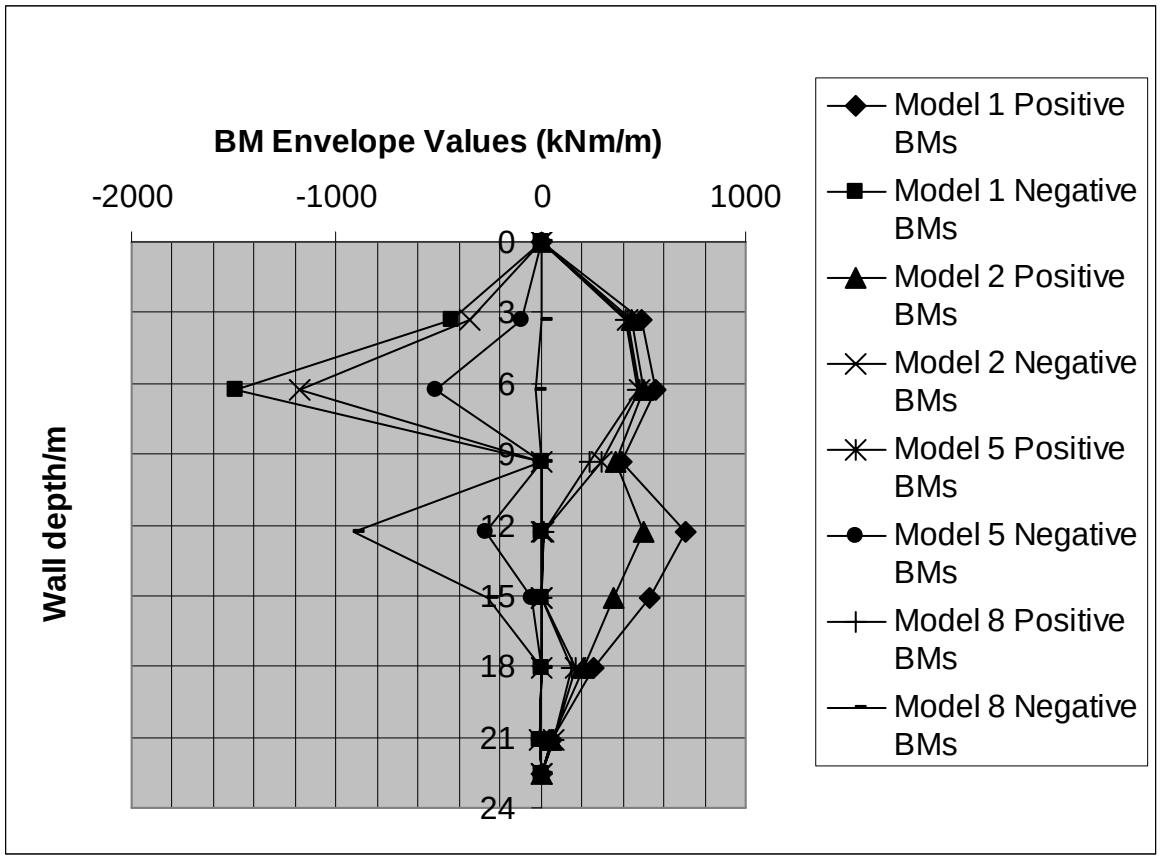

Figure 13: Bending moment (BM) envelope comparison between Models 1, 2, 5 and 8 (left walls).

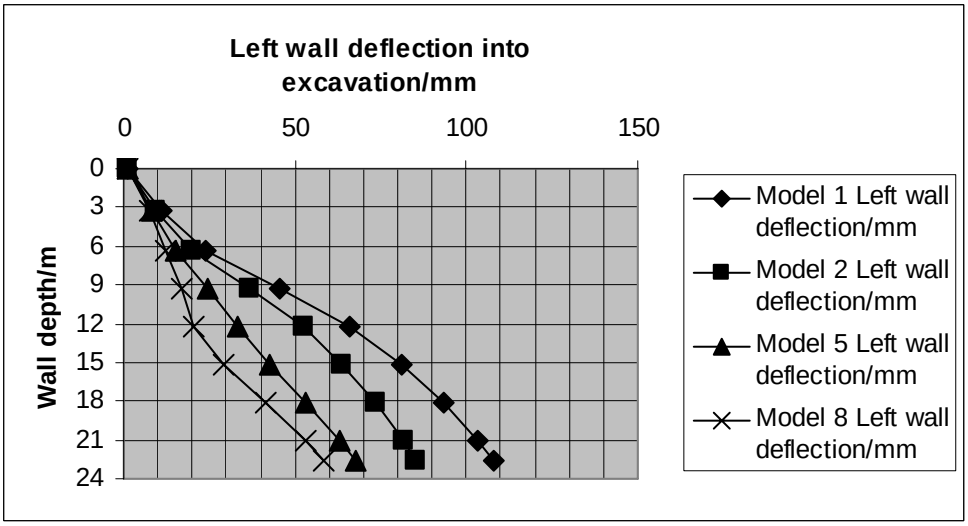

Figure 14: Left wall lateral deflection profile comparison between Models 1, 2, 5 and 8.

Figure 14 shows that as grout strength increases, wall lateral deflection clearly reduces, from intermediate slab depth (6.3 m) downwards. Figure 15 suggests that the magnitudes of roof and intermediate slab forces reduce with increasing grout strength. In addition, the roof slab axial force changes from tensile to compressive.

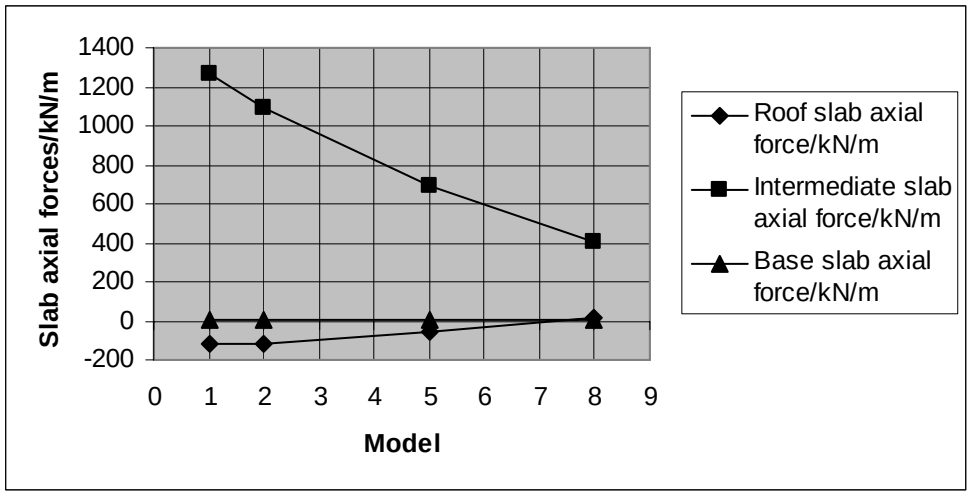

Figure 15: Slab axial force comparison between Models 1, 2, 5 and 8.

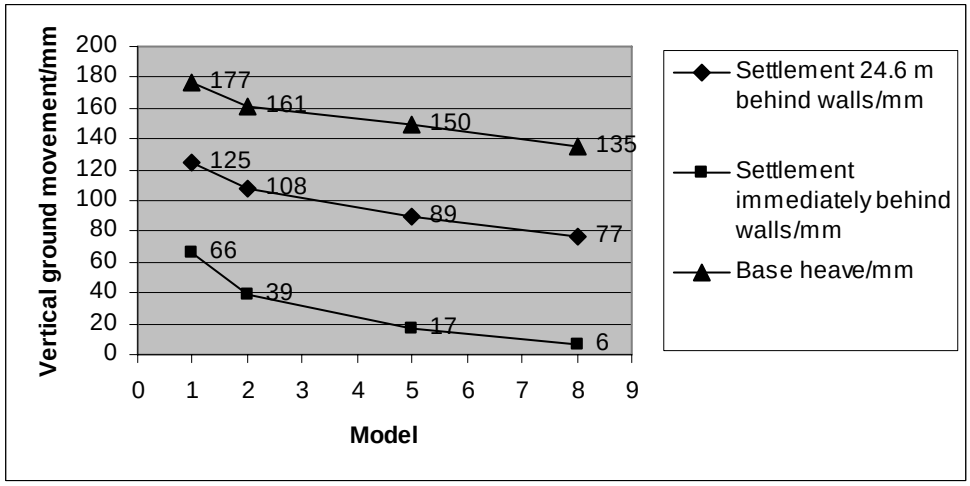

Figure 16: Vertical ground movement comparison between Models 1, 2, 5 and 8.

Figure 16 suggests that increasing grout strength may be a reliable method of ground settlement control around excavations.

Comparative inspection of the numerical output of Models 6, 7, 9 and 10 confirms the trends mentioned in Section 4.3.2 above - that, even for higher-strength slabs, ground settlement is not significantly affected by lowering the JGP slab, though base heave is significantly lowered. The slab force relationship with depth is also verified to match Figure 11 above.

The inspection also suggests that lowering the position of high-strength JGP slabs increases the bending moments, both positive and negative, especially above mid-height of the lower cell. The same is observed between JGP slabs at the same depth - increasing the grout strength significantly increases bending moments both positive and negative.

The conclusion here is that increasing JGP slab strength may achieve ground settlement, lateral wall deflection and slab axial load reductions, but significantly increases the required bending moment capacity of the wall, at almost all depths.

4.3.4 The effects of thickness of LS/MS JGP slab (comparison between Models 2, 11, 12 and 14)

Clearly, increasing the thickness of the LS JGP slab from 2, to 4, to 6 m reduces the negative bending moments in the upper cell, but nowhere else (Figure 17). In fact, below the base slab, negative moments actually increase around 15 m depth – the approximate centre of the JGP slabs in Models 11 and 12.

On the other side, increasing the JGP slab thickness significantly reduces the positive bending moment envelope only from around base slab soffit (12.6 m) downwards to around 19 m depth. In fact, above lower cell mid-height (9.3 m), moments actually increase marginally with increasing JGP slab thickness. Overall, only significant thickness increases from 2 m to 6 m result in significant moment reductions.

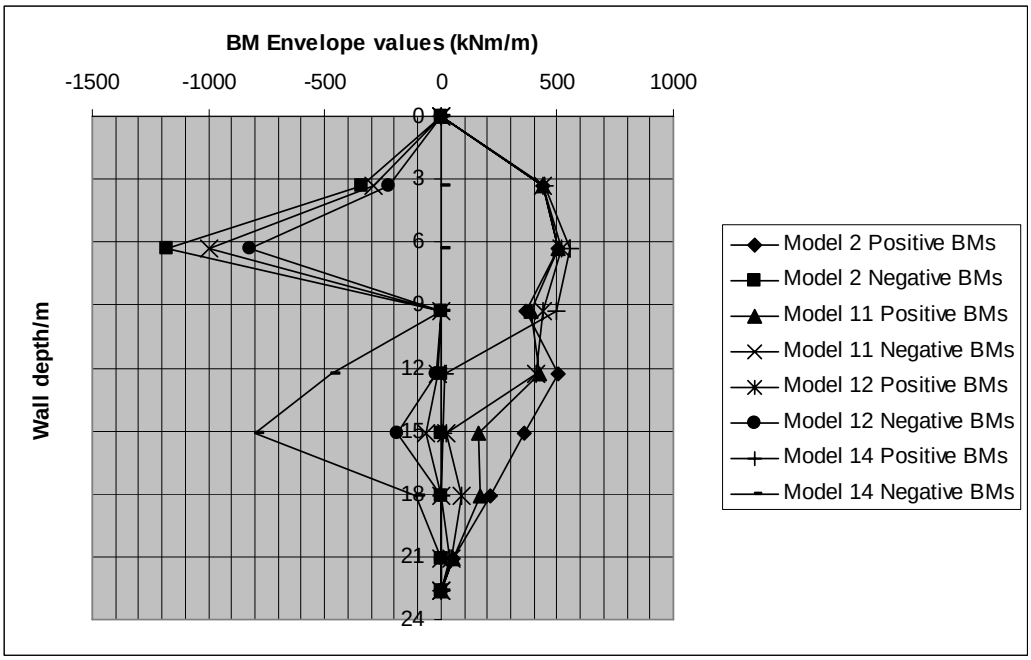

Figure 17: Bending moment (BM) envelope comparison between Models 2, 11, 12 and 14 (left walls).

Interestingly, by tripling the strength and stiffness of the 6 m thick JGP slab, the maximum positive bending moments marginally reach their maximums above 9.3 m depth, and then dramatically drop to zero all the way down to toe level. It is basically the reverse with the corresponding negative moment profile.

The conclusion here is that increasing JGP slab thickness does generally reduce moments everywhere, with low-magnitude local exceptions. Optimising the combination of grout strength and thickness increases can be effective in significantly reducing moments in critical areas.

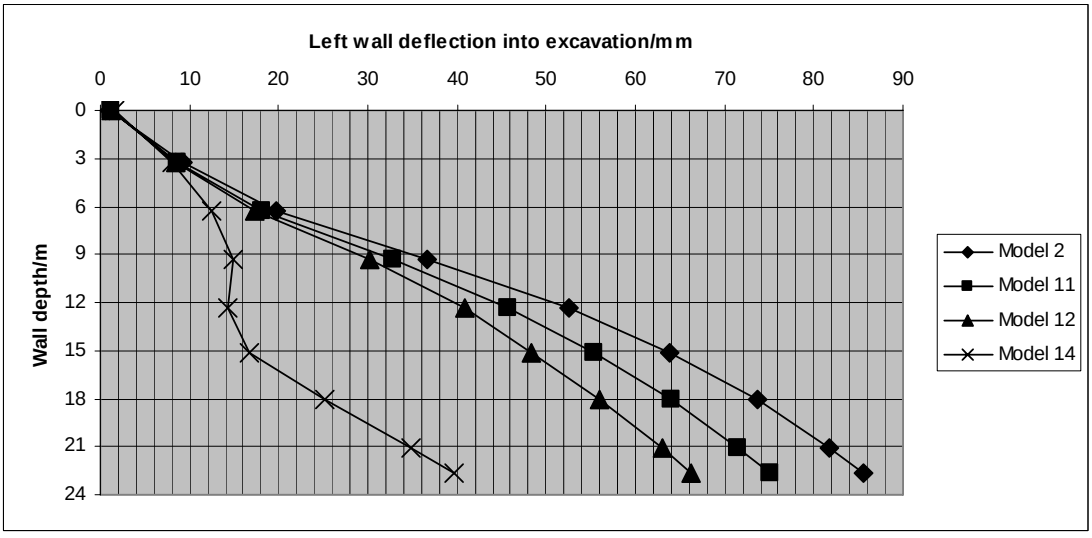

Figure 18: Left wall lateral wall deflection profile comparison between Models 2, 11, 12 and 14.

Figure 18 shows a clear trend of smaller lateral deflections with increasing JGP slab thickness. The reduction effects increase with depth, starting from mid-height upper cell (6.3 m depth).

Furthermore, as concluded earlier, grout strength increases do reduce deflection, and this effect may be magnified by thickness increases – note the large difference between Models 12 and 14, from upper cell (3.3 m depth) downwards.

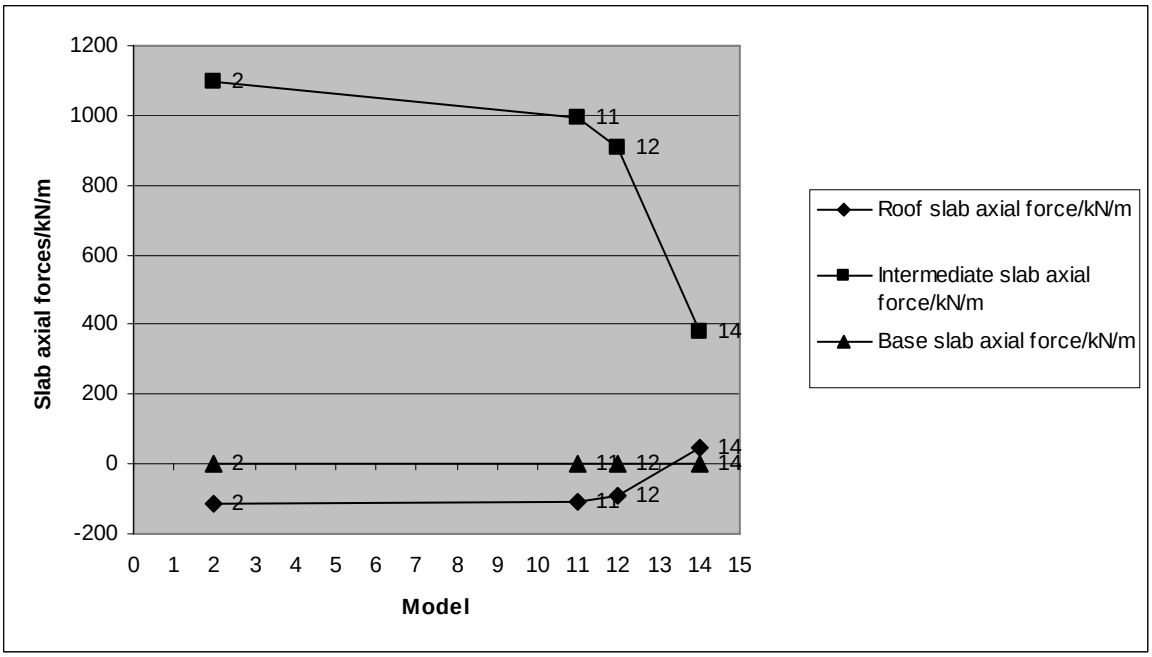

Figure 19: Slab axial force comparison between Models 2, 11, 12 and 14.

Figure 19 shows that intermediate slab axial loads reduce with increasing JGP slab thicknesses. Furthermore, increased JGP slab thickness, coupled with a strength increase (Model 14), results in a dramatic drop in intermediate slab loads, as well as reverses roof slab loads from tensile to compressive.

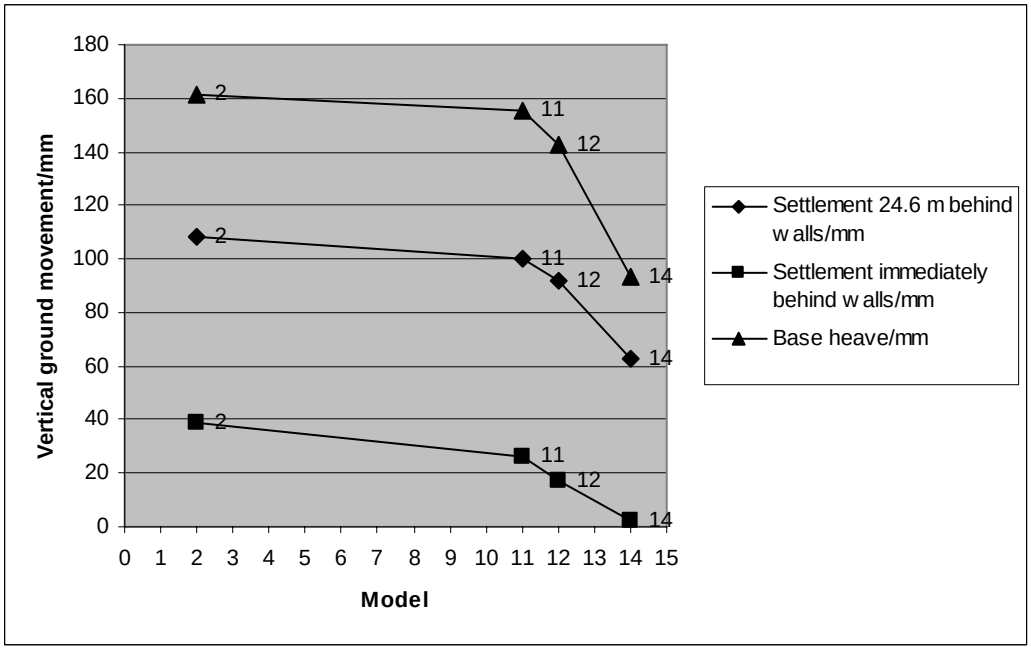

Figure 20: Vertical ground movement comparison between Models 2, 11, 12 and 14.

Increasing JGP slab thickness does reduce ground movements generally, but substantial reductions require substantial slab thickness increases (Figure 20). Coupling and increase in JGP slab strength and thickness dramatically reduces ground movements, with the strength increase being the driver.

Concluding this section, it is suggested that increasing JGP slab thickness generally reduces bending moments, wall lateral deflections, slab axial loads and ground movements. However, except for bending moments, it is not as effective as increasing JGP grout strength.

4.3.5 Comparing soils (comparison between Models 1 and 15)

The loose to medium-dense sand modelled had the following parameters:

- Unit weight - 17 kN/m³
- Permeability - 0.0086 m/day
- Poisson's ratio - 0.30
- Stress-strain modulus - 25 MPa
- Cohesion - 1 kPa and
- Internal angle of friction - 32°.

By inspection of the numerical output, the following observations were made regarding the same top-down excavation without JGP slabs, in loose to medium-dense sand and firm clay:

- In sand, both positive and negative moments are significantly less than their corresponding values in clay above intermediate slab (6.3 m depth), while the reverse is true below;
- In sand, lateral wall deflections into the excavation are about half those in clay, at all depths;
- In sand, roof and intermediate slab axial forces are significantly lower than in clay, though the reverse is true for the base slab and
- In sand, ground settlement is dramatically lower than in clay, although base heave is significantly greater.

5 CONCLUSIONS

The following general conclusions may be drawn, regarding top-down braced excavations in firm clay with high groundwater tables:

- Even a low-strength JGP slab of relatively small thickness (2 m) placed immediately below final formation level is likely to be significantly beneficial in terms of reducing wall/slab loads and vertical ground movements;
- The optimum JGP slab location is likely to be immediately below final formation level, though the lower it is (away from final formation level), the greater the base heave reduction;
- Increasing the strength and stiffness of JGP slabs is advantageous in reducing structural slab axial loads, wall deflections and vertical ground movements. However, it significantly increases wall bending moments;
- Only significant JGP slab thickness increases produce significant wall bending moment and vertical ground movement reductions. Wall lateral deflections and slab axial loads reduce with increasing JGP slab thicknesses, though the deflection reductions become more significant with increased proximity to the JGP slab itself. Increasing a JGP slab's thickness is not as effective as increasing its strength and stiffness and
- For qualitative purposes, based on the trends noted, simple approximate correlations between various parameters may be observable, but further work would be necessary to incorporate other factors like wall toe depth, wall stiffness and excavation width to confirm them.

6 ACKNOWLEDGEMENTS

The author gratefully acknowledges the support and contributions of Paul Gunson, Alan Garrard and Paul Hewitt of Parsons Brinckerhoff.

7 REFERENCES

Bowles, J.E. (1996) Foundation Analysis and Design, Fifth Edition, 364

Brinkgreve, R.B.J. and Broere, W. (2004) Plaxis 2D - Version 8

Bruce, D.A. (2005) Glossary of grouting terminology. *J. Geotech and Geo. Eng*. ASCE, 131(12) 1534-1542

Hewitt, P. and Spaulding, C. (2006) Jet Grouting for Lisarow Rail Bridge Renewal, Australian Geomechanics Society Sydney Chapter, Symposium on “Soft Ground Engineering”, 11 October 2006.

MODELLING OF SOIL IMPROVEMENT INDUCED BY TREE ROOT SUCTION

B. Fatahi[1], B. Indraratna[2], and H. Khabbaz[3]
[1]*PhD Candidate, Civil Engineering, University of Wollongong, NSW 2522, Australia*
[2]*Professor of Civil Engineering, University of Wollongong, NSW 2522, Australia*
[3]*Lecturer, Civil Engineering, University of Wollongong, NSW 2522, Australia*

ABSTRACT

Vegetation contributes to weak soil stabilisation through reinforcement of the soil, dissipation of excess pore pressures, and increasing the shear strength by induced matric suction. This paper is concerned with the way vegetation influences soil matric suction, shrinkage, and ground settlement. A mathematical model for the rate of root water uptake that considers ground conditions, type of vegetation and climatic parameters, has been developed. Based on this proposed model, the distribution of moisture and the matric suction profile adjacent to the tree are numerically analysed. Field measurements taken from literature are compared with the authors' numerical model. The predicted results calculated using the soil, plant, and atmospheric parameters implemented in the numerical model, compared favourably with the measured results, justifying the assumptions upon which the model was developed. Furthermore, through the parametric study and sensitivity analysis, the required accuracies of the model parameters are determined. The findings of this study indicate that due to significant reduction in soil moisture content induced by tree roots, the shear strength of the soil will be enhanced.

1 INTRODUCTION

Throughout the world soil conditions on construction sites have become worse than ever due to the overpopulation in the metropolitan areas. These conditions have compelled engineers to construct earth structures, major highways, and railways over expansive clays and compressive clay deposits. According to Nelson and Miller (1992), expansion and shrinkage are the result of changes in the soil water system that disturb the internal stress equilibrium. Retarding evaporation, heavy rainfall, and growth of trees and shrubs are the most important factors which result in a noticeable change in the ground moisture. Trees, shrubs, and grasses deplete moisture from the soil through transpiration.

Australia's railway network covers a vast area of land over very variable land forms and soil types, and the freight transportation is growing rapidly. The maintenance expenditure is influenced greatly by the large distances covered and the poor quality of the subgrade encountered; therefore, there is pressure to find appropriate methods to reduce the maintenance cost. Following heavy rains, water collection in depressions underneath the rail tracks will result in further track settlement. Continuous ballast resurfacing and replacement and costly track drainage following heavy rains is a large component of the maintenance cost. In design and construction of new railway lines, consideration of an appropriate drainage system is the most viable method to reduce the maintenance cost.

New maintenance observations show when trees are beside railway tracks, their localised undrained failure is minimised. Using native vegetation, to stabilise existing railway corridors built over expansive clays and compressive soft soils, in remote railway lines has become increasingly popular in Australia. Figure 1 shows an example of existence of native trees along railway lines. Properly selected and implemented vegetation, including native trees and shrubs, can reduce soil moisture by root water uptake. Moreover, vegetation can increase the shear strength and stiffness of soil by increasing matric suction and control erosion as a secondary effect.

In modelling of vadose zone behaviour influenced by vegetation, detailed consideration of root water uptake is required to develop a realistic model. Existing models, predicting the effects of vegetation on the ground, consider only the root reinforcement effects or a highly simplified approach for estimating the tree root water uptake. For example, Fredlund and Hung (2001) in their analysis to predict volume change in expansive soils, as a result of vegetation, did not consider the realistic root zone. It was assumed that the root water uptake rate is time-independent, which is not a realistic assumption. The extent and shape of the root system play a major role in determining uptake patterns. Biddle (1998) has reported the most comprehensive field observations for predicting the pattern of soil drying in proximity of trees on clay soils involving 60 different cases. As noted by Gardner (1961) tree root density distribution influences the pattern of moisture redistribution in vicinity of a tree. However, Biddle (1998) did not report the effects of root distribution.

Many attempts (e.g. Cameron, 2001; Jaksa *et al*., 2002; and Blight, 2005) have been made to establish a relationship between tree roots and soil moisture content. However, the previous experimental investigations could not offer a

complete model to include ground properties, vegetation specifications and atmospheric conditions. The main objective of this study is to establish a rigorous formula for estimating root water uptake, and then develop an integrated two-dimensional transient model considering soil water extraction by roots within vadose zone to simulate the ground under the influence of vegetation. The associated mathematical model is implemented in a numerical model to analyse and predict the movement of water in soil. The results are compared with field measurements to verify the numerical predictions. In addition, a sensitivity analysis is carried out to study the influence of the model parameters on the model outputs as well as to identify and evaluate important variables that affect the ground conditions under transpiration.

Figure 1: Trees planted along railway lines, Coalcliff, NSW, Australia

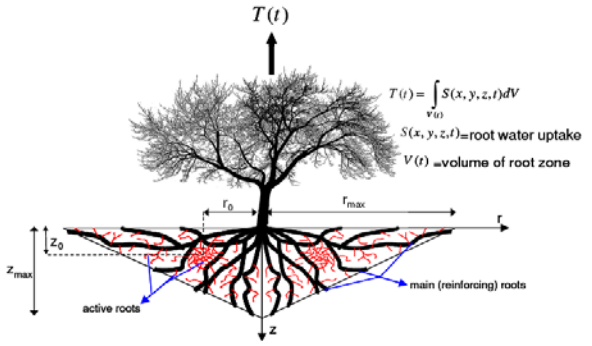

Figure 2: Schematic sketch of soil-plant-atmosphere system

2 ROOT WATER UPTAKE MODEL

Defining microscopic interaction between soil and root system needs detail of each single root and its interaction with the surrounding soil (Figure 2). Due to the complexity of this system, it is preferred to apply the macroscopic approach the integrated properties of the entire root system. In other words, in macroscopic approach it is assumed that both soil and roots are continuous media. Therefore, the entire root zone is assumed to extract moisture from small differential volumes of the root zone, and the water uptake by roots is represented by a volumetric sink term in the unsaturated flow equation;

$$\frac{\partial \theta}{\partial t} = \nabla.(k\nabla\psi) - \frac{\partial k}{\partial z} - S(x, y, z, t) \quad \textbf{(1)}$$

where, θ $(= V_W / V)$ is the volumetric moisture content, (V_w = volume of water, V = total volume), ∇ is the divergence vector, ψ is the soil suction, k is the hydraulic conductivity, z is the vertical coordinate (downward is positive) and $S(x, y, z, t)$ is the root water uptake at point (x, y, z) at time t.

A previous study by Indraratna *et al.* (2006) presented a mathematical model for the tree root water uptake distribution within the root zone. The proposed model combines the effects of soil matric suction, root density and potential transpiration, where the rate of tree root water uptake is given by:

$$S(x, y, z, t) = f(\psi).G(\beta).F(T_P) \quad \textbf{(2)}$$

where, $G(\beta)$ is the root density factor, $f(\psi)$ is the soil suction factor, and $F(T_P)$ is the potential transpiration factor. The most appropriate function for $f(\psi)$ is suggested by Feddes et al. (1978) as follows:

$$\left\{\begin{array}{ll} f(\psi) = 0 & \psi < \psi_{an} \\ f(\psi) = 1 & \psi_{an} \le \psi < \psi_d \\ f(\psi) = \dfrac{\psi_w - \psi}{\psi_w - \psi_d} & \psi_d \le \psi < \psi_w \\ f(\psi) = 0 & \psi_w \le \psi \end{array}\right\} \quad \textbf{(3)}$$

where, ψ_w is the soil suction at wilting point, ψ_d and ψ_{an} are the highest and lowest values of ψ at $S = S_{\max}$, respectively, where $S_{\max}$ is the maximum rate of root water uptake. The following two equations have been suggested by Indraratna *et al.* (2006) for the root density factor and the potential transpiration factor, respectively:

$$G(\beta) = \frac{\tanh(k_3 \beta_{\max} e^{-k_1|z-z_0|-k_2|r-r_0|})}{\int_{V(t)} \tanh(k_3 \beta_{\max} e^{-k_1|z-z_0|-k_2|r-r_0|}) dV} \quad \textbf{(4)}$$

$$F(T_P) = \frac{T_P(1 + k_4 z_{\max} - k_4 z)}{\int_{V(t)} G(\beta)(1 + k_4 z_{\max} - k_4 z) dV} \quad \textbf{(5)}$$

In the above equations, k_1 and k_2 are two empirical coefficients depending on the tree root system and type, k_3 is an experimental coefficient, z is vertical coordinate, r is radial coordinate, $\beta_{\max}$ is the maximum root length density which is located at the point $(r,z) = (r_0, z_0)$, T_p is the rate of potential transpiration, k_4 is an experimental coefficient to represent the effect of depth on the potential transpiration distribution, and $V(t)$ is the root zone volume at time t.

3 VERIFICATION OF THE ROOT WATER UPTAKE MODEL

To verify the model developed for root water uptake rate, a case history reported by Biddle (1983) has been considered for a lime tree grown in Boulder clay. The estimated parameters, based on the available literature, are shown in Table 1. Figure 3 illustrates the mesh and element geometry and boundary conditions of the finite element model. Using ABAQUS software, a two-dimensional plane strain mesh employing 4-node bilinear displacement and pore pressure elements (CPE4P) was considered.

Table 1: Parameters applied in the finite element analysis.

Parameter	Value	Reference	Comments
ψ_{an}	4.9 kPa	Feddes *et al*. (1978)	Clayey soil with air content of 0.04
ψ_w	1500 kPa	Feddes *et al*. (1978)	$1500 < \psi_w < 2000$ kPa
ψ_d	40 kPa	Feddes *et al*. (1978)	$40 < \psi_d < 80$ kPa
γ	21 kN/m^3	Powrie *et al*. (1992)	Typical value for Boulder clay
$r_{\max}$	9m	Biddle (1983)	Estimated from field measurements $(7m < r_{\max} < 11m)$
$z_{\max}$	1.5m	Biddle (1983)	Estimated from field measurements
k_s	10^{-10} m/s	Lehane and Simpson (2000)	Typical value for Boulder clay
PI	23	Biddle (1983)	Measured
e_0	0.60	Powrie *et al*. (1992)	Typical value for Boulder clay
C_c	0.13	Skempton (1944)	Typical value for Boulder clay

The authors' theoretical model representing the rate of root water uptake distribution within the root zone was included in the FE analysis through appropriate Fortran subroutines. The overall mesh consisted of 1326 nodes and 1250 elements. The boundary conditions of the finite element model are illustrated schematically in Figure 3. The flux boundary at the surface is controlled by both climatic conditions and soil properties. In this study, it is assumed that rainfall and evaporation are in balance and thus a "no water in-flow" condition is applied at the surface. According to the field measurements reported by Biddle (1983), the initial pore water pressure can be assumed as hydrostatic with the watertable located 13m below the surface.

This numerical analysis is based on the basic effective stress theory of unsaturated soils incorporated in the ABAQUS finite element code. The effective stress in the unsaturated soil is given by Bishop (1959):

$$\sigma'_{ij} = \sigma_{ij} - u_a \delta_{ij} + \chi(u_a - u_w)\delta_{ij} \quad \textbf{(6)}$$

where, σ'_{ij} is the effective stress of a point on a solid skeleton, σ_{ij} is the total stress in the porous medium at the point, u_a is the pore air pressure, u_w is the pore water pressure, δ_{ij} is Kronecker's delta ($\delta_{ij} = 1$ when $i = j$ and $\delta_{ij} = 0$ when $i \neq j$), and χ is the effective stress parameter attaining a value of unity for saturated soils and zero for dry soils. Bishop's effective stress concept for predicting shear strength and volume change in unsaturated soils has recently been discussed and validated by Khalili *et al*. (2004).

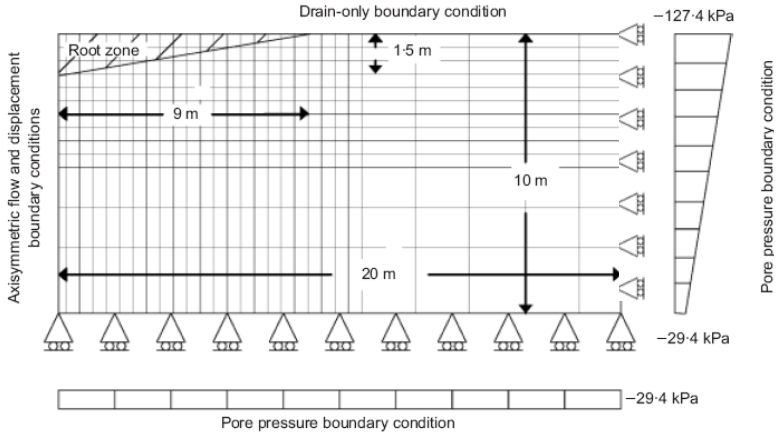

Figure 3: The geometry and boundary conditions of the verification model (after Indraratna *et al*., 2006)

The soil-water characteristic curve employed in this study is shown in Figure 4. A family of curves for different values of $w \times PI$ is shown in Figure 4, where w is the fraction of soil passing sieve #200 (75 μm)as an index between 0 to 1, and PI is the plasticity index (Zapata *et al*., 2000).

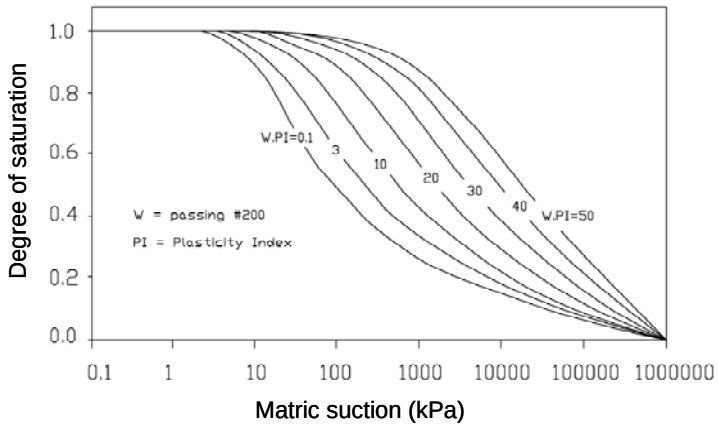

Figure 4: Predicted soil water characteristic curve based on $W \times PI$ (after Zapata *et al*., 2000).

The finite element analysis is conducted in two stages: (i) geostatic and (ii) consolidation. The first stage is to ensure that the analysis commences from a state of equilibrium under geostatic loading. The consolidation stage is to avoid non-physical oscillations and possible divergence problems caused by non-linearities. This stage includes a transient analysis of partially saturated soil under transpiration, starting with 1-day intervals and then continued for 1–year, with continuous root water uptake.

The coefficient of unsaturated soil permeability has been calculated based on Brooks and Corey (1964), thus:

$$k = k_s(e) S_e^{\frac{2+3\lambda}{\lambda}} \quad \textbf{(7)}$$

$$S_e = \left[\frac{S_r - (S_r)_{residual}}{1 - (S_r)_{residual}} \right] \quad \textbf{(8)}$$

where, $k_s(e)$ is the saturated coefficient of permeability estimated based on the well known Kozeney-Carman equation, S_e is the effective degree of saturation, S_r is the degree of saturation, $(S_r)_{residual}$ is the residual degree of saturation, and λ $(= \Delta \log S_e / \Delta \log \psi)$ is the slope of the soil water characteristic curve on a log-log plot.

As fluid passes through a porous medium, a coupled flow-deformation analysis of unsaturated soil is required to capture the 3-phase interaction among the soil, air, and water. The governing equations for pore fluid diffusion and deformation are a combination of Equation (1) and the relevant deformation equations. The soil is Boulder clay whose behaviour can be defined by

$$de^{el} = C_c \ln\left(\frac{p_0 + dp}{dp}\right) \quad \textbf{(9)}$$

where, de^{el} denotes the change of void ratio in the element, C_c is the compression index, p_0 is the initial mean effective stress, and dp is the mean effective stress change on the soil skeleton. The effect of osmotic suction is assumed to be negligible. The material properties and parameters used in the finite element analysis were given earlier in Table 1, and the additional assumed parameters are given in Table 2.

Table 2: Parameter values assumed in the finite element analysis in the verification model

Parameter	Value	Comments
r_0	6 m	Radial coordinate of the maximum root density point
z_0	0.50 m	Vertical coordinate of the maximum root density point
$\beta_{\max}(t)$	25 m^{-2}	Taken from the general shape or root suggested by Landsberg (1999)
k_3	0.0874 m^{-1}	As above
k_4	0.014	Coefficient of potential transpiration distribution
k_1	10	Coefficient of vertical root distribution
k_2	0.30	Coefficient of horizontal root distribution
ν	0.30	Typical Poisson's ratio for clayey soils
T_P	3 mm/day	Estimated average potential transpiration rate for U.K. (UNEP World Atlas of Desertification)
Passing #200	55%	Typical value for Boulder clay

A comparison between the field measurements and the FEM predictions for moisture content reduction around the lime tree is presented in Figure 5. The numerical model results are in accordance with the field observations reported by Biddle (1983). The main differences noted between field data and the predictions are observed at 6-8 m distance away from the tree trunk. This discrepancy is attributed to the simplicity of the assumed root zone shape. In addition, the foliage prevents uniform distribution of rainfall around the tree. As a result, moisture content can increase at the canopy edges, thereby further contributing to this disparity

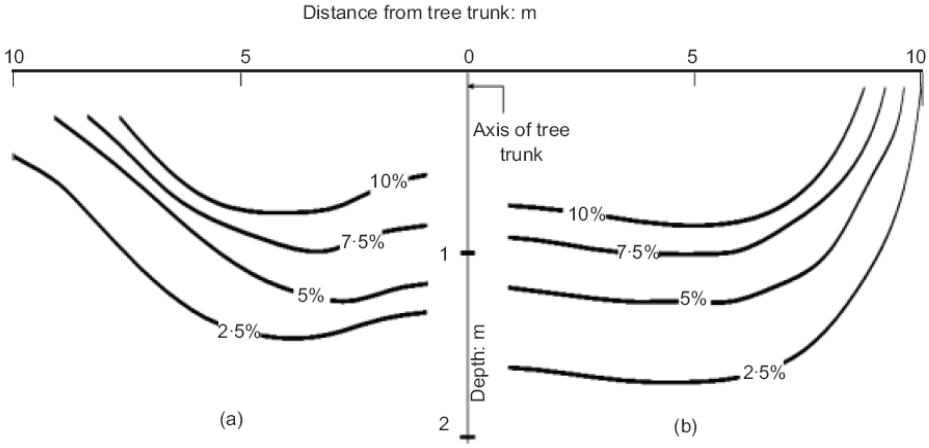

Figure 5: Contours of volumetric soil moisture content reduction (%) close to a lime tree: (a) Biddle (1983), (b) FEM predictions (Indraratna *et al*., 2006)

The maximum change in the soil matric suction from the finite element analysis (Figure 6) is found at about 0.5m depth, which coincides with the same location of the maximum root density. Figure 7 shows the ground settlement at various depths. In this analysis, only the suction related settlement was considered. On the surface, the predicted 80mm settlement beside the tree trunk decreases to less than 20 mm, at a distance 10 m away from the trunk. As shown in Figure 7, the location of the maximum settlement is closer to the trunk at shallower depths, which tends to coincide with the points of maximum change in suction (Figure 6).

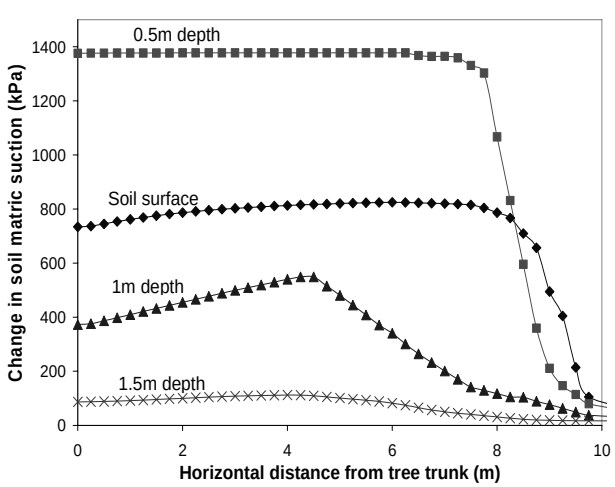

Figure 6: Predicted soil matric suction in different depths.

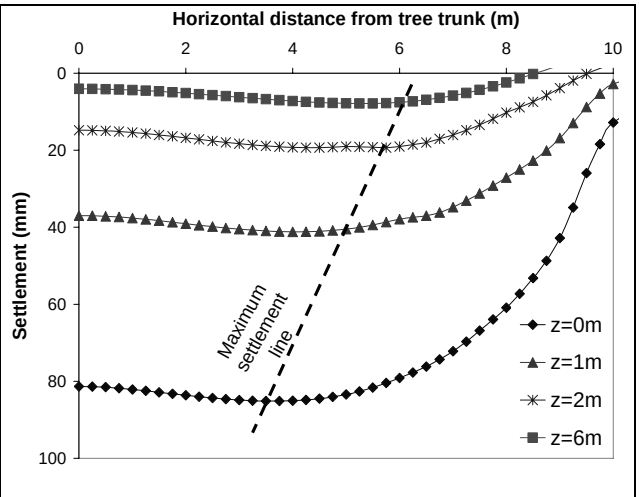

Figure 7: Ground settlement at various depths.

It was shown that the numerical analysis incorporating the proposed model could predict the variation of moisture content surrounding the tree trunk. Knowing the moisture content variation, the development of matric suction can be predicted reasonably well using the soil water characteristic curve. Native biostabilisation improves the shear strength of the soil by increasing the matric suction, and also decreases the soil movements. This contribution from trees grown along rail corridors and rail slope is of immense benefit for improving track stability in problematic soil. In other words, native vegetation generating soil suction is comparable to the role of prefabricated vertical drains with vacuum pressure, in terms of improved drainage (pore water dissipation), and associated increase in shear strength. In addition, the tree roots provide a natural reinforcement effect, which the current model has not simulated thus far.

4 PARAMETRIC STUDY AND SENSITIVITY ANALYSIS

4.1 DESCRIPTION OF REFERENCE PROBLEM AND PARAMETRIC STUDY

A two dimensional finite element analysis is used to conduct a sensitivity analysis of the relevant model variables. The finite element mesh, along with the specific boundary conditions, are shown in Figure 8. Because of symmetry, a zero flux boundary was applied along the left boundary. Root water uptake was modeled as a moisture flux boundary, applied along the top surface of all elements within the root zone. The mesh used in this simulation consists of bilinear strain quadrilateral element (CPE4P) with 4 displacement and four pore pressure nodes positioned at the corners of each element. The entire FE mesh consists of 13,041 nodes and 12,800 elements. In the numerical model, only the matric suction component was considered, and the osmotic suction component was neglected. During the parametric study, the magnitude of one parameter was varied while keeping the other parameters constant at their initial values. The initial values of all parameters considered here are summarised in Table 3. Also, it is assumed that a steady state condition is reached when the rate of change in matric suction $(d\psi / dt)$ is less than or equal to $10^{-6} kPa/s$.

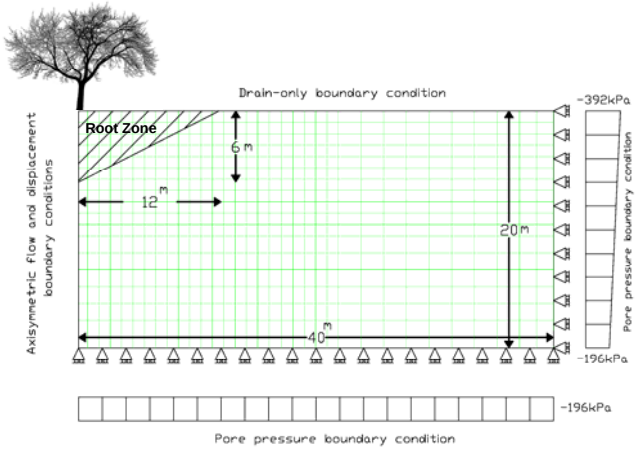

Figure 8: The geometry and boundary conditions of the FE model

Table 3: The initial assumed parameter values in the numerical parametric study.

Parameter	Value	Comments
(r_0, z_0)	(4m, 2m)	Corresponding to radial and vertical coordinate of gravity centre of root zone
$\beta_{max}(t)$	25 m^{-1}	Taken from the general shape suggested by Landsberg (1999)
$k_1 = k_2$	2 m^{-1}	Applied by Knight (1999)
k_3	8.74×10^{-2} m^{-2}	Taken from the general shape suggested by Landsberg (1999)
k_4	0.014 m^{-1}	Assuming $H_{root} = -76.5m$ and $R_c = 0.05$ *
(r_{max}, z_{max})	(12m, 6m)	Root zone boundary
ψ_{an}	4.9 kPa	Feddes et al. (1976), Clay soil and air content of 0.04
ψ_d	40 kPa	Feddes et al. (1976; 1978), $40 < \psi_d < 80$ kPa
ψ_w	1500 kPa	Feddes et al. (1976; 1978), $1500 < \psi_w < 2000$ kPa
γ_d	18 kN/m^3	Typical earth soil
C_s	0.05	Average value for clay soils in vicinity of building foundations
k_s	5×10^{-8} m/s	Typical value for clay soils in vicinity of building foundations (e=1)
passing #200 × Plasticity Index	20	-
T_P	8 mm/day	Myers and Talsma (1992), Pinus Radiata tree (ACT, Australia)
Initial void ratio (e_0)	1	Typical clay soil

*by comparing Equations (5) and Nimah and Hanks (1973) model, k_4 can be estimated by $k_4=-(1+R_c)/H_{root}$, where H_{root} is the effective water potential in the root at the soil surface where z is considered zero and R_c is the flow coefficient in the plant root system.

Considering the initial parameters, the predicted profile of the steady state soil matric suction is presented in Figure 9. The matric suction varies from a maximum value of 1081 kPa at point (r_0, z_0) to 196 kPa at 20 m depth. As expected, the maximum matric suction change is at the centre of gravity of the root mass (r_0, z_0) and it decreases with distance away from this point. The deformation of the soil profile due to the root water uptake is predicted through a coupled flow-deformation analysis, considering the stress-deformation equations. The ground settlement at various depths under steady state conditions is shown in Figure 10.

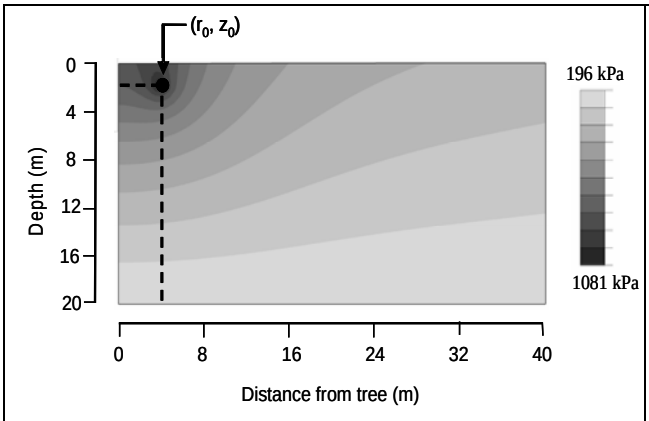

Figure 9: Matric suction profile in steady state condition

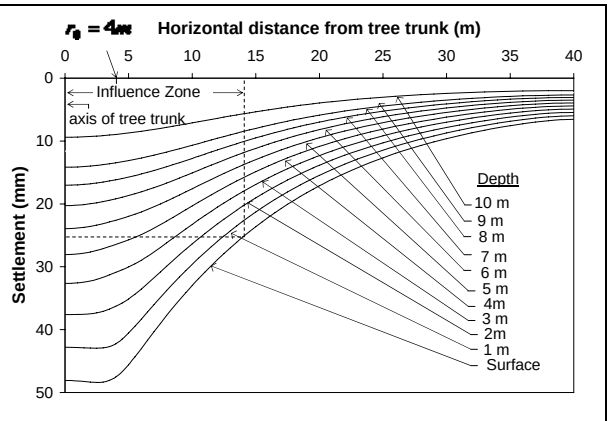

Figure 10: Ground settlement profile at various depths.

The radius of the influence zone for which the surface settlement is at least 25 mm (i.e. change of curvature of the settlement plots) is shown to be about 14 m. The ground settlement decreases rapidly with the horizontal distance from the tree trunk, and beyond 30 m, the predicted settlement is not significant.

4.2 EFFECT OF WILTING POINT VALUE (ψ_w)

It seems that the value of the soil suction at wilting point (ψ_w), based on Feddes *et al.*'s (1978) formula, strongly influences the value of the $f(\psi)$. To confirm this point, six analyses are performed similar to the reference case, except for the value of suction at wilting point, which changes from 1500kPa to 3000kPa (see Figures 11 and 12).

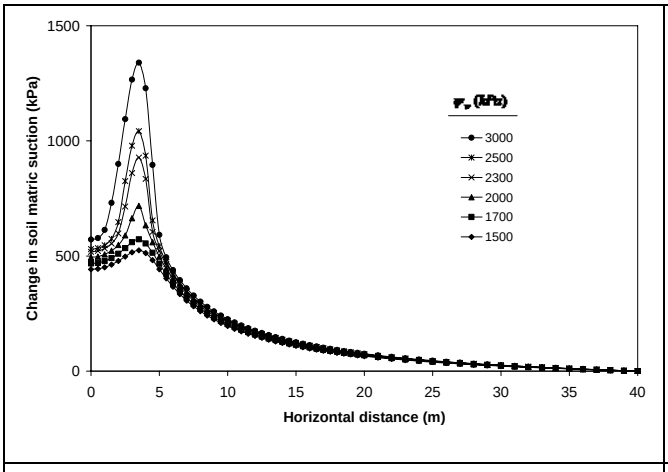

Figure 11: Effect of ψ_w on matric suction change at soil surface.

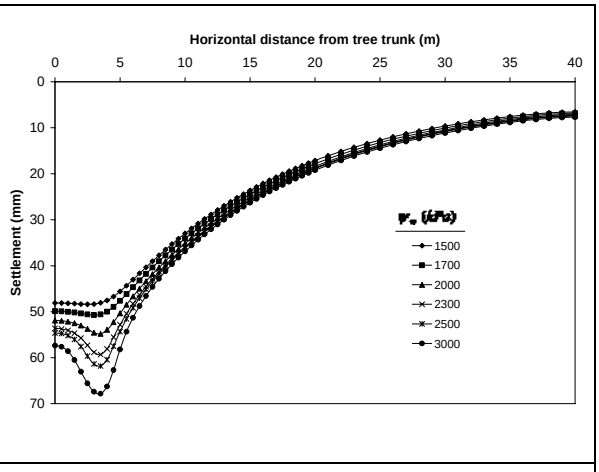

Figure 12: Effect of ψ_w on soil surface settlement.

When ψ_w increases, the value of $f(\psi)$ (in the range of $\psi_d \le \psi \le \psi_w$) increases and consequently the rate of root water uptake increases. As Figures 11 and 12 present, soil matric suction change and soil settlement increase by ψ_w. It can be noted that the maximum suction changes occur at point (r_0, z_0).

4.3 EFFECT OF VERTICAL ROOT DENSITY DISTRIBUTION FACTOR (k_1)

To evaluate the influence of vertical root density distribution factor (k_1), the results of four analyses with k_1 values equal to 0.1, 0.5, 1, and 5 are compared to each other. As Figures 13 and 14 show, the maximum soil suction change increases with k_1 value. Meanwhile, by decreasing the vertical root density distribution factor, the point of the maximum soil suction change moves toward tree trunk. On the other hand, the soil suction change at points away from the maximum point ($|r - r_0| > 1m$) decreases with the value of k_1. Thus, as Figure 14 clearly shows, the soil suction change under the tree trunk decreases with the value of k_1.

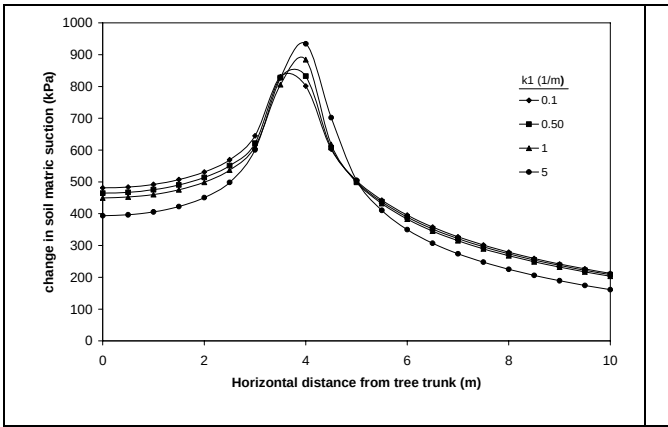

Figure 13: Effect of k_1 on soil matric suction change at 2 m depth.

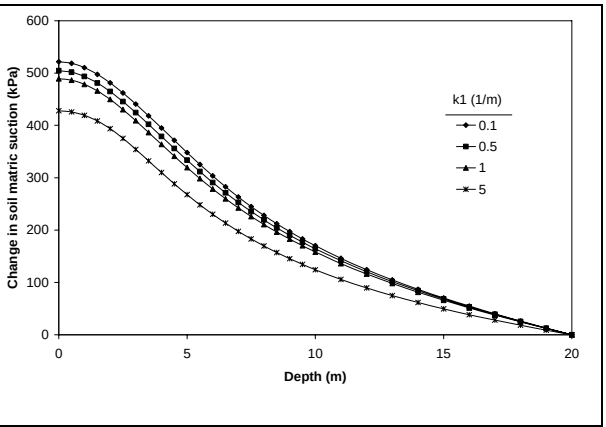

Figure 14: Effect of k_1 on soil matric suction change under the tree trunk.

4.4 EFFECT OF HORIZONTAL ROOT DENSITY DISTRIBUTION FACTOR (k_2)

The analyses to examine the effect of horizontal root density distribution factor are similar to the reference case except for the value of k_2 that changes from 0.1 to 5. Figure15 illustrates that the maximum soil matric suction change increases with the value of k_2, and the point of the maximum suction change moves towards the tree trunk and the soil surface. On the other hand, as Figure 16 shows soil suction on the surface decreases with k_2 value.

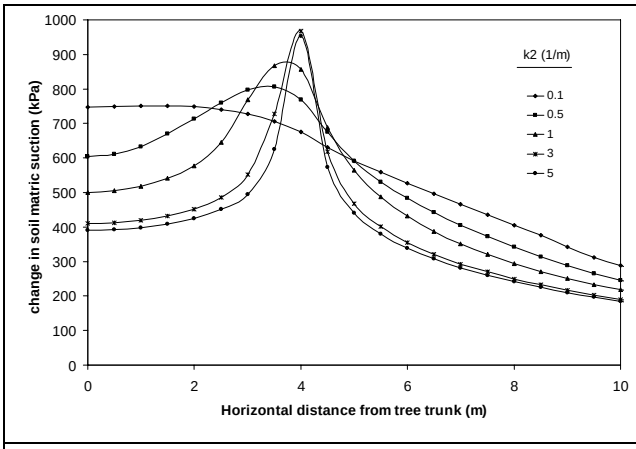

Figure 15: Effect of k_2 on soil matric suction change at 2 m depth.

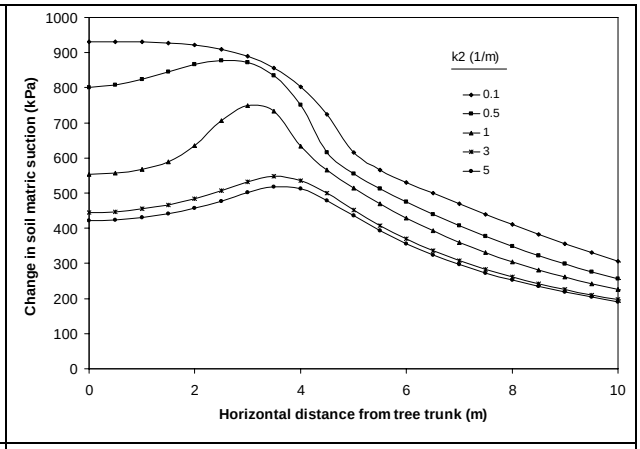

Figure 16: Effect of k_2 on soil matric suction change on soil surface.

4.5 SENSITIVITY ANALYSIS OF THE GROUND SETTLEMENT

The maximum allowable settlement is an essential criterion in foundation design. Accordingly, prediction of ground settlement induced by tree transpiration can enhance the design approach of foundations in the vicinity of tree roots. In this section, sensitivity of the maximum settlement with respect to a number of parameters is investigated employing sensitivity index defined by,

$$(I_S)_i = \frac{\dfrac{\partial D_{\max}}{\partial u_i}}{\dfrac{D_{\max}}{u_i}} \qquad \textbf{(10)}$$

where, $(I_S)_i$ is the sensitivity index of i th parameter, $D_{\max}$ is the maximum vertical deformation, and u_i is the parameter which influences the ground settlement. Based on the sensitivity index, parameters can be categorised as follows:

$$\begin{cases} 0\% < I_S < 20\% & \textit{Insensitive} \\ 20\% \le I_S < 50\% & \textit{Sensitive} \\ 50 \le I_S & \textit{Very sensitive} \end{cases} \qquad \textbf{(11)}$$

Figure 17 shows the results of the sensitivity indices of various parameters.

The sensitivity analysis results demonstrated in Figure 17 are based on the assumed initial parameters and the applied range of parameters. Table 4 summaries the sensitivity of the maximum ground settlement with respect to variation of the model parameters.

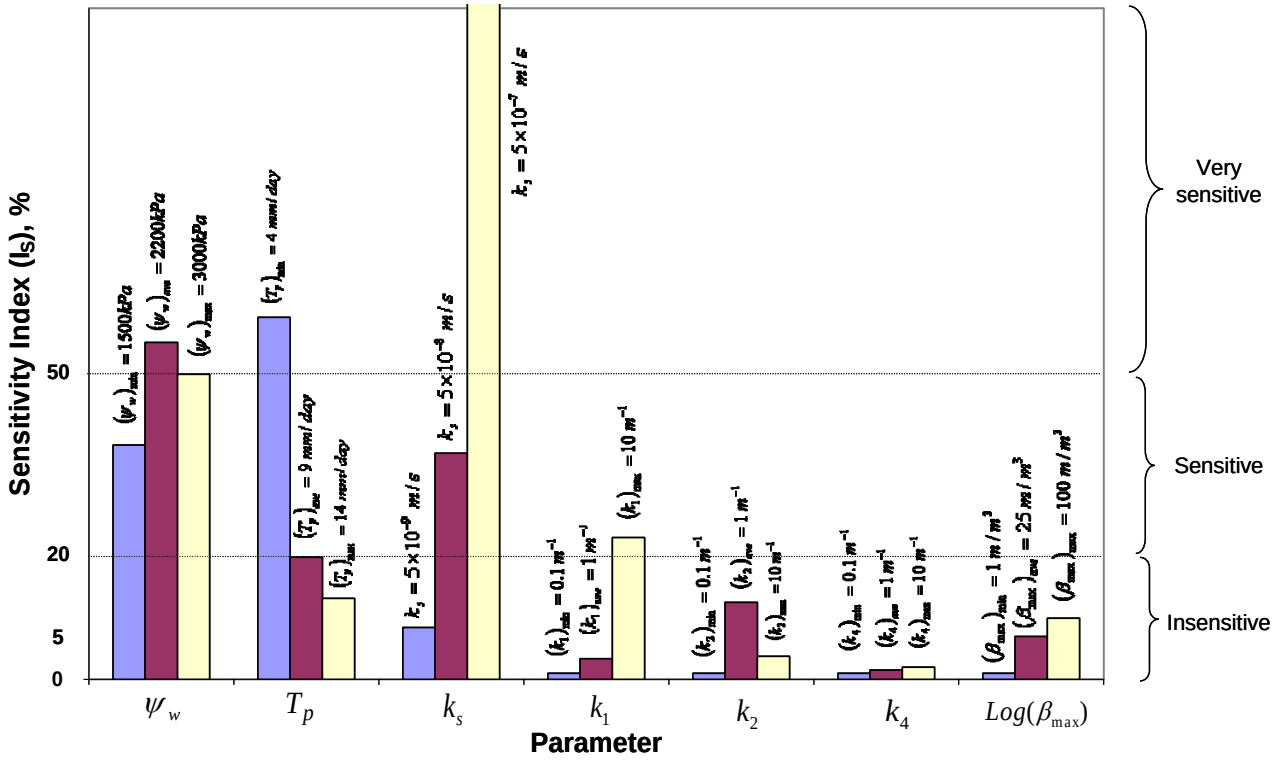

Figure 17: Results of the sensitivity analysis for the maximum ground settlement.

Table 4: Sensitivity of the maximum settlement to some of the parameters

	Insensitive	Sensitive	Very Sensitive
$\psi_w\ (kPa)$	-	1500 - 1900	1900 - 3000
$T_p\ (mm/day)$	9 - 14	5 - 9	4 - 5
$k_s\ (m/s)$	$5\times10^{-9} - 3\times10^{-8}$	$3\times10^{-8} - 7\times10^{-8}$	$7\times10^{-8} - 5\times10^{-6}$
$k_1\ (m^{-1})$	0.1 - 6	6 - 10	-
$k_2\ (m^{-1})$	0.1 - 10	-	-
$k_4\ (m^{-1})$	0.01 - 10	-	-
$Log(\beta_{max})$	0 - 2	-	-

The most sensitive parameters are: the wilting point suction, saturation permeability when the coefficient is relatively high ($>3\times10^{-8}\ m/s$), the rate of potential transpiration at lower values (i.e. $T_p < 9\ mm/day$), and vertical root distribution coefficient (k_1) when the coefficient is high ($>6\ m^{-1}$). Parametric studies have also been conducted for T_p and k_s, but not shown in this paper. As expected, a higher rate of transpiration creates a higher matric suction change, whereby the highest rate of matric suction change is at the point of maximum root density. Furthermore, soil permeability influences the soil moisture movement, thereby affecting the soil matric suction distribution. The analysis results show that the soil settlement decreases with the increasing value of permeability. When the permeability is smaller, the generated matric suction within the soil matrix is higher and, consequently, the effective stresses increase causing larger settlements.

5 CONCLUSIONS

In order to investigate the effects of tree transpiration on ground condition, a numerical model using the finite element analysis has been developed considering the coupled flow-deformation equations. The finite element mesh is formulated using partially or fully saturated soil elements, which are capable of capturing the role of unsaturated permeability and the degree of saturation at various levels of matric suction. Tree root suction was considered through

the model developed by Indraratna *et al.* (2006) which takes into account soil matric suction and distribution of root density and potential transpiration.

Existing data from previously published literature have been used to validate the analysis. It has been found that given the approximation of the assumed root geometry and model parameters, the agreement between predictions and field data is promising. The proposed root water uptake and transpiration model verifies that the suction induced by the tree roots contributes to a substantial gain in shear strength. Similar to prefabricated vertical drains, the tree roots induce good drainage, pore water pressure dissipation and in addition provide natural reinforcement of the soil. As the influence zone of each tree can be several meters in radius, the methodological planting of native trees along rail corridors at a practical distance away from the track is currently considered by rail organizations in Australia. Considering various soil conditions, the type of vegetation and atmospheric conditions, the proposed mathematical model for biostabilsation is most useful to predict the formation behaviour in a rail track environment.

An in-depth analysis of the effects of several important variables has shown that a complex interaction exists between tree and soil properties. The findings of this study confirm that a number of parameters are required to be measured or estimated accurately for a proper foundation design. The soil permeability, the wilting point suction, the root length density and the rate of potential transpiration significantly influence the ground behaviour. Other parameters including soil properties (e.g. consolidation parameters, strength parameters and soil water characteristic curve) should be measured accurately in laboratory or field as they are also important factors in the analysis.

6 ACKNOWLEDGEMENTS

This research has been sponsored by the Australian Cooperative Research Centre for Railway Engineering and Technologies (Rail-CRC). The contributions and feedback from various industry colleagues, particularly Wayne Potter and David Christie, are appreciated. The assistance of Dr. Don Cameron (University of South Australia) is also acknowledged.

7 REFERENCES

Biddle, P.G. (1983). Pattern of soil drying and moisture deficit in the vicinity of trees on clay soils. *Geotechnique*, 33, 2, 107-126.

Biddle, P.G. (1998). *Tree Root Damage to Buildings*. Wantage, Willowmead Publishing Ltd**.**

Bishop, A.W. (1959). The principle of effective stress. *Teknish Ukebadk*, Norway, No. 39, 859-863.

Blight, G. E. (2005). Desiccation of a clay by grass, bushes and trees, *Geotechnical and Geological Engineering*, Vol. 23, Springer, 697–720

Brooks, R.H., and Corey, A.T. (1964). *Hydraulic properties of porous media*. Hydrology paper 3, Colorado State University, Fort Collins, Colorado

Cameron, D.A. (2001). *The* Extent of Soil Desiccation Near Trees in a Semi-Arid Environment, *Geotechnical and Geological Engineering*, Vol 19, Issue 3-4, pp 357 –370.

Feddes, R.A., Kowalik, P.J. and Zaradny, H. (1978). *Simulation of field water use and crop yield*, *Simulation Monograph*. Pudoc, Wageningen, the Netherlands, 9-30.

Fredlund, D.G. and Hung, V.Q. (Vipulanandan C. *et al.*, eds.) (2001). Prediction of volume change in an expansive soil as a result of vegetation and environmental changes. *Expansive Clay Soils and Vegetative Influence on Shallow Foundations*, Geo Institute, U.S.A, 24-43.

Gardner, W.R. (1961). Soil suction and water movement. In *Proceedings of the Conference on Pore Pressure and Suction in Soils*. Butterworths, London, pp. 137–140.

Indraratna, B., Fatahi, B. and Khabbaz, H. (2006). Numerical analysis of matric suction effects of tree roots. *Proceedings of the Institution of Civil Engineers Geotechnical Engineering*, Vol 159 No. GE2, pp. 77–90.

Jaksa, M.B., Kaggwa, W.S. and Woodburn, J.A. (2002). Influence of large gum trees on the soil suction profile in expansive soils. *Australian Geomechanics Journal*, 37, 1, 23-33.

Knight, J.H. (Landsberg J.J. ed.).) (1999). Tree Water Use and its Implications in Relation to Agroforestry Systems, Appendix 2, *The Way Trees Use Water*, Rural Industries Research and Development Corporation (RIRDC), Australia, Water and Salinity Issues in Agroforestry No. 5, RIRDC Publication No. 99/37, RIRDC Project No. CSM-4A, 25-78.

Landsberg, J.J. (Landsberg J.J. ed.).) (1999). *Tree* Water Use and its Implications in Relation to Agroforestry Systems. *The Way Trees Use Water*, Rural Industries Research and Development Corporation (RIRDC), Australia, Water and Salinity Issues in Agroforestry No. 5, RIRDC Publication No. 99/37, RIRDC Project No. CSM-4A, 1-24.

Lehane, B.M. and Simpson, B. (2000). Modeling glacial till under triaxial conditions using a BRICK soil model. *Canadian Geotechnical J.*, 37, 1078-1088

Khalili N., Geiser F. and Blight G.E. (2004). Effective stress in unsaturated soils: review with new evidence. *International Journal of Geomechanics*, 4, 2, 115-126.

Nelson, J.D., and Miller, D.J. (1992). *Expansive soils: Problems and practices in foundation and pavement engineering*. John Wiley & Sons, New York, NY.

Nimah, M.N., and Hanks, R.J. (1973). Model for estimating soil water, plant and atmospheric interrelations. I. description and sensitivity. Proceedings *of Soil Science Society of America*, 37, 522-527.

Powrie, W., Davies, J.N., and Britto, A.M.A. (1992). Cantilever retaining wall supported by a berm during temporary work activities. *ICE conference on retaining structures*. Robinson College, Cambridge, 418-428.

Skempton, A.W. (1944). Notes on compressibility of clays. *Quarterly Journal of Geological Society*, London, 100, 2, 119-135.

Zapata, C.E., Houston, W.N., Houston, S.L., and Walsh, K.D. (Shackeford *et al.*, eds.) (2000). Soil-water characteristic curve variability. *Advances in unsaturated geotechnics*. GEO-Institute, ASCE, U.S.A, 84-124.

LARGE-SCALE CYCLIC TRIAXIAL TESTING OF SOFT CLAY

Anass Attya[1] and Buddhima Indraratna[2]
[1]PhD Candidate, [2]Professor of Civil Engineering
School of Civil, Mining and Environmental Engineering, University of Wollongong

ABSTRACT

The behaviour of saturated soft clays subjected to cyclic loading is of considerable importance in railway engineering. The use of prefabricated vertical drains (PVDs) with surcharge preloading is one of the popular methods of soft ground improvement as they accelerate the consolidation by shortening the drainage path. In this paper, the behaviour of a soft clay from North-eastern NSW subjected to cyclic loads is investigated using large-scale triaxial testing. Cyclic triaxial tests on remoulded soft clay samples with vertical drains were carried out using a large scale triaxial apparatus designed and built at the University of Wollongong, using samples of 300 mm in diameter and 600 mm in height. The samples were anisotropically consolidated under k_o condition to simulate the *in situ* stress history. Stress-controlled cycles were then applied to the soil samples. The results of the excess pore water pressure and settlement of the soft clay are presented. The advantages of soft subsoil stabilization with PVDs under cyclic loading conditions are discussed.

1 INTRODUCTION

A problem of considerable importance in geotechnical engineering is that of the prediction of the behaviour of soils under cyclic loading. The behaviour of soft clays subjected to cyclic loading is of paramount significance in both railways and roadway design. Due to the rapid increase in population and associated urbanisation, most new construction activities have to utilise the poorest of soft soils. Soft clays that exist in the coastal regions of Australia usually have low bearing capacity and high compressibility properties, affecting the performance of major transportation infrastructure. It is well known that failure in soft clays under cyclic loads occurs at strengths well below the undrained shear strength obtained from the standard static tests (Larew and Leonards, 1962; Sangrey *et al*., 1969). The rapidly generated excess pore water pressures due to cyclic loads play a key role in causing failure of the clay subgrade as it dramatically decreases effective stress under undrained cyclic loading.

Vertical drains with preloading have been widely utilised to stabilise soft soil deposits prior to construction (Indraratna *et al*., 1994), inducing most of the expected ultimate settlement under the given loading by promoting rapid radial consolidation (Richart, 1957). This results in a gain in the shear strength of the soft formation soil.

Although the theoretical and practical aspects of static preloading with prefabricated vertical drains (PVDs) has been well established (Barron, 1948; Hansbo, 1979; Hansbo, 1981) followed by even more rigorous analytical and numerical models together with experimental verifications and/or field case studies (Hird *et al*., 1992; Indraratna *et al*., 2005), the application of cyclic loading on soft clays with PVDs has not been investigated in the past, except some preliminary work reported by Indraratna *et al*. (2006). The purpose of the current study is to investigate the effect of cyclic load application to soft clay improved by PVD, and to discuss the potential advantages of PVDs under cyclic loading situations such as in railway environments.

2 LABORATORY INVESTIGATIONS

2.1 TESTING APPARATUS

A large-scale cylindrical triaxial equipment shown in Figure 1(a) was used (Indraratna, 1996; Indraratna *et al*., 1998). The apparatus utilises a hydraulic type dynamic actuator to apply the cyclic load. As shown in the schematic illustration of Figure 2(a), this apparatus consists of five main parts: the triaxial chamber, the axial loading unit, the air pressure and the water control unit, the pore pressure measurement system and the volumetric change measurement device. It has the capability of accommodating specimens of 300 mm in diameter and 600 mm in height as shown in Figures 1(b) and 2(a). The apparatus has been modified to measure the excess pore pressure at different locations inside the specimen by fitting miniature type pore pressure transducers through the base of the triaxial cell, as illustrated in Figure 1(c).

(a) (b) (c)

Figure 1: (a) Large-scale triaxial apparatus, (b) Soil specimen and (c) Miniature pore pressure transducers.

2.2 TESTING PROCEDURE

2.2.1 Sample Preparation

Reconstituted clay from North-eastern NSW was used in this test. The properties of this reconstituted clay obtained from standard consolidation testing and standard Atterberg limits test are summarised in Table 1.

Table 1: Soil properties of the reconstituted clay.

Specific Gravity, G_s	2.65
Liquid Limit, w_L (%)	66
Plastic Limit, w_P (%)	28
Compression Index , C_c	0.84
Swelling Index, C_s	0.14

The procedure for preparing the reconstituted sample was as follows:

- The clay was wet-screened through a # 40 sieve (0.425 mm opening size) to remove larger particles and any coarse organic materials.
- The rubber membrane was clamped into the base of the triaxial equipment and a geosynthetic filter layer was placed at the bottom to prevent clogging of the drainage line.
- Subsequently, the clay slurry was placed and lightly compacted in four layers (150 mm each) inside the membrane to a unit weight of about 15.5 kN/m^3.
- During the placement of the clay in the membrane, four pore pressure transducers were positioned at selected locations (Figure 2b).
- A vertical band drain was inserted into the clay specimen. A geosynthetic layer was placed at the top of the sample also, after inserting the PVD and prior to placing the top loading cap, in order to protect the top drainage holes from clogging.

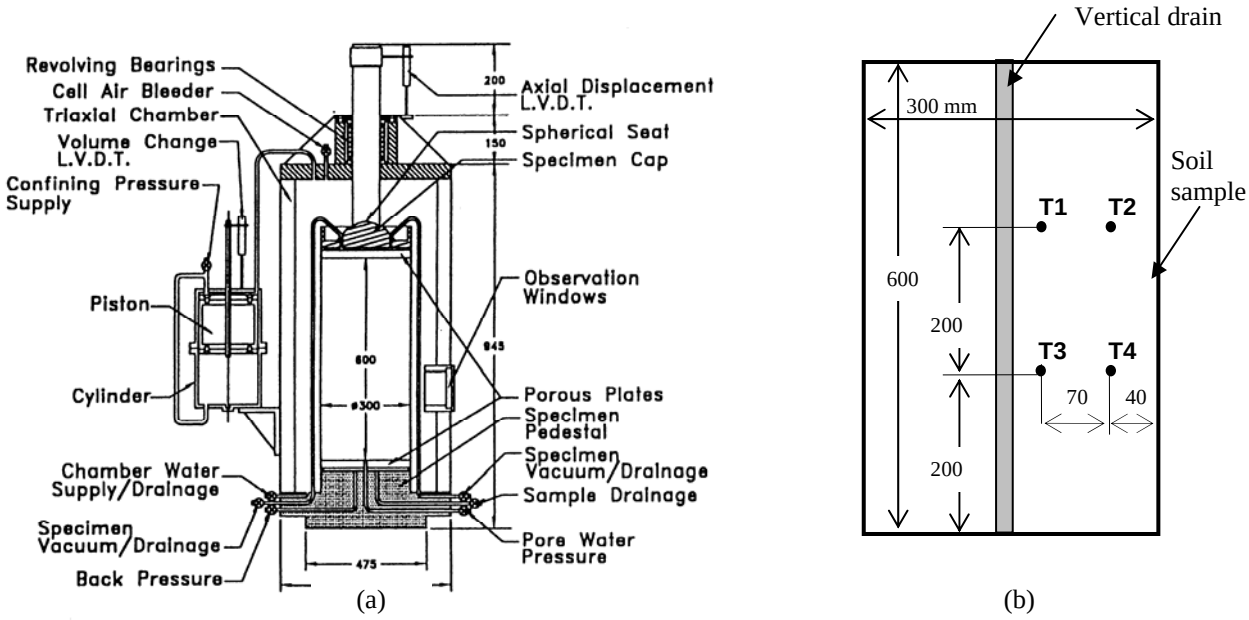

Figure 2: (a) schematic diagram of the large-scale triaxial cell, (b) location of pore pressure transducers inside the soil specimen.

2.2.2 Sample consolidation

The sample was anisotropically consolidated (k_o=0.6) to simulate the appropriate field conditions. The sample was then subjected to a vertical overburden pressure of 35 kPa and a horizontal pressure of 21 kPa. The consolidation process was carried out in 3 incremental stages to avoid shear failure. With the PVD, the consolidation process took about 8 weeks with both the top and the bottom drainage valves open.

2.2.3 Application of cyclic load

At the end of the consolidation stage, a cyclic load having a frequency of 5 Hz was applied to the soil sample. This specific frequency was chosen to simulate the loading frequency common on rail track environments in Australia, i.e. corresponding to train speeds of 80 to 100 km/h. The test was conducted at a cyclic stress ratio (CSR) of 0.6, where the cyclic stress ratio is defined by the ratio between the cyclic deviator stress q_{cyclic} to the effective initial overburden pressure σ_{vo}' (i.e. CSR= q_{cyclic} / σ_{vo}'). The corresponding loading pattern is shown in Figure 3.

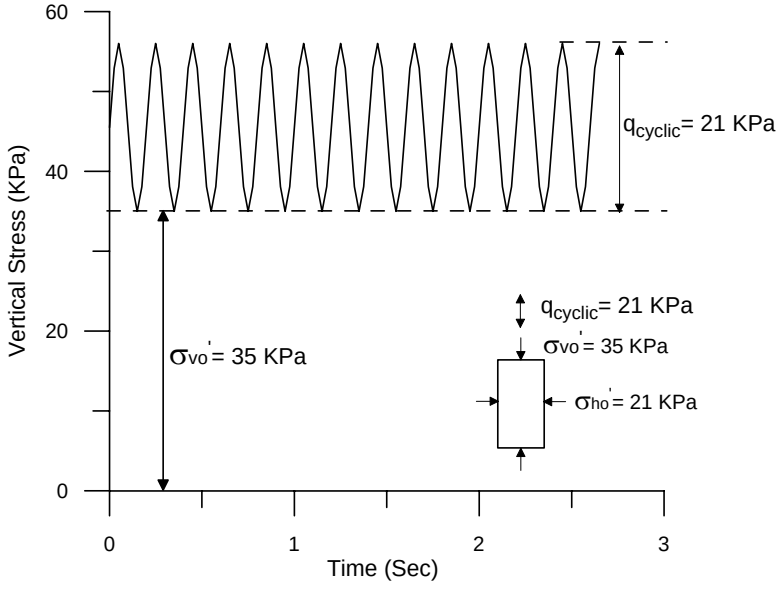

Figure 3: The pattern of cyclic loading.

A thousand cycles (N = 1000) was applied to the specimen to simulate a train passage time of about 3 minutes; the cyclic load was then terminated and followed by a drainage period to allow the dissipation of the excess pore water pressures thus developed. In this stage, the only drainage permitted was through the top of the sample, thereby simulating the actual field conditions encountered by a PVD installed in soft clay. The excess pore water pressures at the locations shown in Figure 2(b) were recorded during the period of cyclic loading and, also, the vertical deformations and the volume change were concurrently measured using linear variable differential transformers (LVDT).

2.3 TEST RESULTS

2.3.1 Pore pressure generation

The excess pore water pressure ratio u^* ($u^*=\Delta u/\sigma_{vo}'$, Δu, excess pore water pressure, σ_{vo}', effective initial overburden pressure) is defined for the purpose of analysis. The variation of u^* versus the number of loading cycles is plotted in Figure 4. The transducers T1 and T4 were chosen to show the effect of the drainage path length on the development of the cyclic pore pressures. T1 has the shortest drainage path as it is the closest to the central drain and the top drainage surface, whereas T4 has the longest drainage path. The results indicate that at the same number of cycles, T1 experienced a smaller excess pore pressure ratio than T4. At the end of the cyclic load application (N=1000 cycles), the excess pore pressure ratio at T4 is about 4 times greater than that of T1.

The residual vertical strains are plotted against the number of load cycles (Figure 5), which indicate that these strains are predominantly plastic. The results show that at the end of the cyclic load, the maximum plastic vertical strain was about 5.2%.

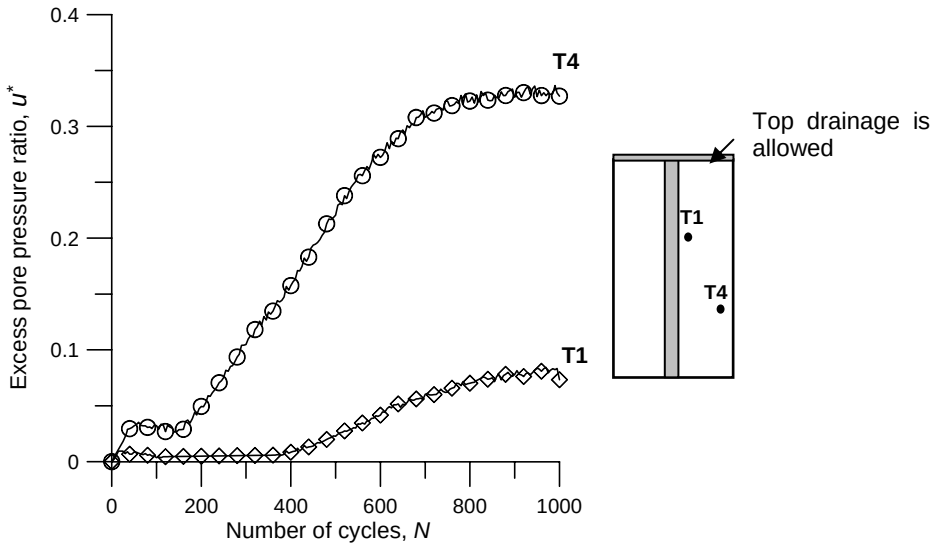

Figure 4: Pore pressure generation curves for transducers 1 and 4.

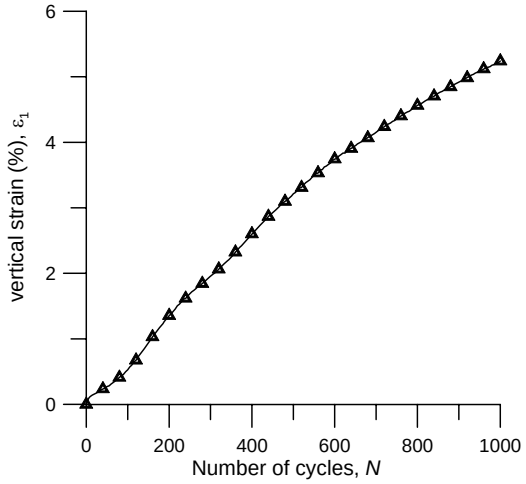

Figure 5: Vertical strains during cyclic load applications.

2.3.2 Comparison with undrained cyclic loading

Zhou and Gong (2001) carried out a series of undrained stress-controlled triaxial tests on Hangzhou normally consolidated clay under different cyclic stress ratios. Although no PVDs were used here, these tests provide a good idea about the expected behaviour of soft clays under cyclic loading conditions. In order to show how effective the PVDs are in dissipating the cyclic-generated excess pore water pressures, the results of T1 and T4 are plotted together with the results obtained by Zhou and Gong (2001) for stress ratios of 0.6, 0.5 and 0.35 in Figure 6. Comparison between these two sets of data indicates that the use of PVDs significantly controls the rate of excess pore water pressure buildup during cyclic loading. As shown in Figure 6, for a cyclic stress ratio of 0.6 with absence of PVD, the failure occurred quickly only after a small number of cycles. There is no doubt that a smaller cyclic stress ratio causes less pore pressure buildup.

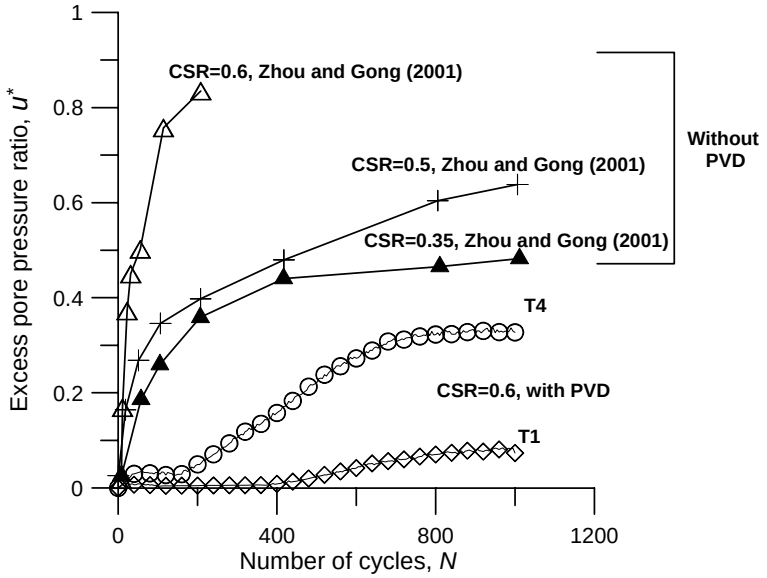

Figure 6: Cyclic excess pore pressures response of soft clay with and without PVD.

2.3.3 Post-cyclic loading dissipation

After termination of cyclic loading, the top drainage allowed the dissipation of the excess pore pressures developed and sustained during the loading cycles. The time-dependent excess pore water pressures for the 4 transducers are shown in Figure 7. The length of the drainage path plays a very important role and, as expected, the fastest dissipation rate was for T1 having the shortest drainage path length while the slowest rate was for T4. The responses of the other 2 sensors were observed to be between T1 and T4, with less pore pressure buildup indicated by T3 compared to T2 as the former was placed closer to the drain.

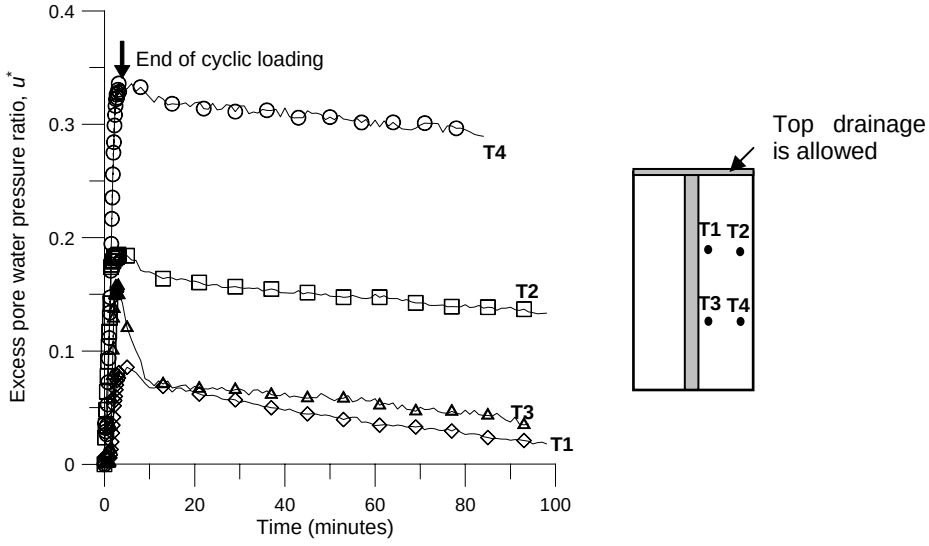

Figure 7: Dissipation behaviour after termination of cyclic loading.

The results clearly confirmed the expectation that the PVD assisted in the dissipation of the cyclically generated pore water pressures. This implies that having PVDs beneath rail tracks can lead to increased stability of the soft foundation and significantly reduces the risk of any potential shear failure. Especially during wet weather, having in-situ vertical drains will maintain continuing dissipation of excess pore pressure even after the passage of trains thereby making the track stable for the next loading stage by the forthcoming trains.

3 CONCLUSIONS

An experimental study was conducted to investigate the influence of prefabricated vertical drains (PVDs) on the cyclic behaviour of soft clay conducted using a large-scale triaxial equipment simulating typical cyclic loads encountered in railway environments. The excess pore water pressures ratio and the post-cyclic loading dissipation rate were considered in the assessment of the performance of PVDs.

During the application of cyclic loading, the PVDs reduced the rate of generation of excess pore water pressure, when compared to the case without PVD. Under the same cyclic stress ratio, the magnitude of the excess pore pressure generated was also significantly less. The paper also showed evidence that the buildup of excess pore pressure (both the rate and the magnitude) would increase if the cyclic stress ratio were to increase. As expected, irrespective of the magnitude of the cyclic stress ratio and the number of cycles, the development of excess pore pressure was the least for the part of the soil specimen nearest to the central PVD, as indicated by the transducer located closest to the PVD.

While further testing is still ongoing to study the cyclic behaviour of soft clay stabilised by PVD, the findings reported here clearly suggest that railway tracks will benefit considerably by having PVDs installed in the soft subgrade, by reducing the risk of undrained failure and soil slurrying under high excess pore pressures.

4 AKNOWLEDGEMENTS

The first author is grateful for the financial support from the Australian Commonwealth Government (IPRS) and the University of Wollongong (UPA). The assistance of Dr Cholachat Rujikiatkamjorn is appreciated. The support of the laboratory technical staff at University of Wollongong is acknowledged.

5 REFERENCES

Barron, R.A. (1948) Consolidation of fine-grained soils by drain wells, *Transactions of the American Society of Civil Engineers, ASCE,* 113**,** 718-742.

Hansbo, S. (1979) Consolidation of clay by band-shaped prefabricated drains, *Ground Engineering***,** 16-25.

Hansbo, S. (1981) Consolidation of fine-grained soils by prefabricated drains, Proceedings of the 10th International Conference on Soil Mechanics, Stockholm, Sweden, 677-679.

Hird, C.C., Pyrah, I.C. and Russell, D. (1992) Finite element modelling of vertical drains beneath embankments on soft ground, *Geotechnique,* 42 (3)**,** 499-511.

Indraratna, B. (1996) Large-scale triaxial facility for testing non-homogeneous materials including rockfill and railway ballast, *Australian Geomechanics,* 30**,** 125-126.

Indraratna, B., Balasubramaniam, A.S. and Ratnayake, P. (1994) Performance of embankment stabilized with vertical drains on soft clay, *Journal of Geotechnical Engineering, ASCE,* 120 (2)**,** 257-273.

Indraratna, B., Ionescu, I. and Christie, H.D. (1998) Shear behaviour of railway ballast based on large-scale triaxial tests, *Journal of Geotechnical and Geoenvironmental Engineering, ASCE,* 124 (5)**,** 439-449.

Indraratna, B., Rujikiatkamjorn, C., Sathananthan, I., Shahin, M. and Khabbaz, H. (2005) Analytical and numerical solutions for soft clay consolidation using geosynthetic vertical drains with special reference to embankments, Proceedings of the Fifth International Geotechnical Engineering Conference, Cairo University, Egypt.

Indraratna, B., Rujikiatkamjorn, C., Wijeyakulasuriya, V., Shahin, M. and Christie, D. (2006) Soft soil stabilisation with special reference to road and railway embankments, Fourth International Conference on Soft Soil Engineering (4th ICSSE), Vancouver, British Columbia, Canada, October 4 - 6, 2006 (accepted July 2006).

Larew, H.G. and Leonards, G.A. (1962) A strength criterion for repeated loads, Proceedings of the Highway Research Board, No. 41, 529-556.

Richart, F.E. (1957) A review of the theories for sand drains, *Journal of the Soil Mechanics and Foundations Division, ASCE,* 83 (SM 3)**,** 1-38.

Sangrey, D.A., Henkel, D.J. and Esrig, M.I. (1969) The effective stress response of a saturated clay soil to repeated loading, *Canadian Geotechnical Journal,* 6 (3)**,** 241-252.

Zhou, J. and Gong, X. (2001) Strain degradation of saturated clay under cyclic loading, *Canadian Geotechnical Journal,* 38**,** 208-212.

THE SENSITIVITY FRAMEWORK: BEHAVIOUR OF RICHMOND RIVER ESTUARINE CLAYS

Daniel Bishop and Stephen Fityus
Civil, Surveying and Environmental Engineering, University of Newcastle

ABSTRACT

The stability and long-term settlement behaviour of NSW estuarine clays under load has become increasingly significant as a result of the large-scale infrastructure development currently occurring in coastal NSW.

The Structured Clay Framework (SCF) developed by a number of authors over the past 20 yrs (Burland *et al.,* 1996; Chandler, 2000; Cotecchia and Chandler, 2000) and based on the work of Burland (1990), provides a general framework for understanding the behaviour of natural structured clays. This is analogous to the framework for remoulded soils provided by Critical State Soil Mechanics (CSSM).

The basis of the SCF is a normalised void ratio vs. effective stress relationship generated from oedometer tests on remoulded clay. The parameters used in the normalisation procedure are the intrinsic properties of e^*_o, e^*_{100} and e^*_{1000} the void ratios of the remoulded clay at the liquid limit, (e_o), σ'_{vo}=100kPa, (σ'_{100}, e^*_{100}), and at σ'_{vo}=1000kPa (σ'_{1000}, e^*_{1000}). The "intrinsic" properties represent the values of clay with no microstructure i.e. its baseline properties.

Unlike standard empirical correlations between geotechnical properties and Atterberg limits there is a rigorous analytical basis (i.e. CSSM) for these correlations (Burland, 1990). The behaviour of high quality undisturbed tests can then be compared and classified according to this intrinsic baseline. The SCF provides a quantitative measure of the structure component of the clays consolidation and shear behaviour above that predicted based purely on void ratio stress relationships (Burland, 1990).

The work presented in this paper describes the implementation of the SCF on Holocene estuarine clays from the Richmond River in Northern NSW. These geologically normally consolidated clays form a significant component of the foundations of the proposed Ballina Bypass and it has been noted, anecdotally, that a number of these clay deposits suffer from large (3 m under a 7 m embankment) settlements and have relatively high sensitivities (4-10, shear vane). Both these factors suggest micro-structure may play a significant role in the overall behaviour.

The initial results indicate that the SCF method provides a useful tool for relating mechanical behaviour, in terms of oedometer and shear vane results, to periods in the geological evolution of the estuarine deposits. Significantly, zones of high sensitivity clays, the deposition of which relates to a period of rapid flooding within the estuary, have been identified. They have much higher intrinsic values that can be accounted for under normal sedimentation conditions, suggesting that they are highly structured. This fact is not apparent when using the standard Atterberg correlations.

1 INTRODUCTION

The Critical State Soil Mechanics framework forms the basis of many of the soil models used in engineering practice. This framework is based on extensive testing on remoulded clays (Muir-Wood, 1990). However the behaviour of remoulded clay differs significantly from natural clays due to the presence of structure (Burland, 1990; Leroueil *et al.,* 1990a). This structure is a combination of the clay *fabric* or particle orientation that is imparted at the time of deposition, and the *stability* of this fabric resulting from electro- bio- and physiochemical bonds formed during and post-deposition. Subsequent void ratio changes due to burial consolidation do not alter this initial stability but improve the overall strength characteristics by increasing the degree of interparticle interaction. Together the *fabric* and fabric *stability* are defined as the *structure* of the sediment (Mitchell and Soga, 2005).

Both Terzaghi (1941) and Skempton (1970) investigated the Sedimentary Compression Curves (SCC) of normally consolidated marine sediments under gravitational loading. They showed that a log linear relationship exists between the void ratio and *in situ* effective stress, but also that, for a given void ratio, a gravitationally loaded soil will carry an *in situ* effective stress approximately 5 times higher than the equivalent remoulded clay. This difference is a measure of the enhanced deformation resistance of the natural clay fabric over the remoulded clay fabric.

It is generally assumed that the soil's *structure* evolves during burial and adjusts so that it will just support the overlying load, i.e. the soil is normally consolidated and the oedometer will detect the geological preconsolidation pressure. However for many recent normally consolidated clays the structure that forms as a result of the deposition process and post-depositional phenomena results in the soil's fabric attaining a degree of *stability* above that required to carry the

overburden load. These processes include bioturbation, thixotropy and precipitation of cements (Leroueil and Vaughan, 1990; Schmertmann, 1991). This extra structure will result in an increase in the soil's sensitivity, where the sensitivity (S_t) is defined as the ratio of undisturbed strength (S_u) of the clay to the strength of a fully remoulded sample ($S_{u\ remoulded}$). By definition, remoulded soils have a strength sensitivity of 1 (Mitchell and Soga, 2005). This *structure* should be considered as important as the *in situ* void ratio and stress history in defining the soils behaviour (Leroueil and Vaughan, 1990).

The problem in modelling or predicting the geomechanical behaviour of structured natural clay is that many of the behaviours observed are not predicted by the CSSM framework (Burland, 1990). The central tenant of CSSM is the direct link between void ratio, peak strength and effective stress (Muir-Wood, 1990). This relationship divides soil behaviour into two zones. Below the peak strength, or yield state, soils behave elastically and pore pressures rise uniformly in proportion to the applied load. At stresses above this peak state, soils behave in a plastic manner and plastic deformation results in the expansion of the soil's "yield surface" and improvement in its strength characteristics. The presence of *structural stability,* above that defined by the void ratio and *in situ* stress conditions in a ground, means that a soil can exist in a state outside the yield envelope predicted by CSSM. In other words the clay fabric is meta-stable (Mitchell and Soga, 2005).

It is important to realise that dramatic increases in clay sensitivity after burial occur due to a reduction in the remoulded strength of a soil rather than an increase in the undisturbed strength (Mitchell and Soga, 2005). A process that can cause this is a reduction of pore water salinity in marine sediments due to fresh water flushing (Torrance, 1975) This process plays an important role in the formation of the quick clays in Northern Europe (Bjerrum, 1967) and the highly sensitive Champlain Sea Clays in Canada (Leroueil *et al.,* 2003). The behaviour of these soils is considered unusual because their metastable fabric has a tendency to collapse (Cotecchia and Chandler, 2000) resulting in significant and dramatic pore pressure development (Hoeg *et al.*, 1969). Hoeg *et al.* (1969) noted that during embankment loading the excess pore pressure generated was significantly lower than expected below a critical embankment height ($\Delta u/\sigma_{vo}$= 15-20% predicted). Once this critical embankment load was reached (approximately equivalent to σ'_{vy}) the rate of excess pore pressure increased dramatically and continued to rise significantly up to a week after loading was complete. Another aspect of sensitive and quick clay behaviour is that at low confining stresses (Burland, 1990) and rapid strain rates (Leroueil and Hight, 2003) these soil have a tendency to behave in a brittle manner.

An important consequence of structure and sensitivity in soils is the fact that their behaviour cannot be described by CSSM. The CSSM framework is not able to predict the peak undrained shear strength, S_u, of normally consolidated sensitive clays, because this strength is a function of *structure* not the maximum *in situ* stress condition the profile has experienced. There are also significant implications for behaviour predictions using continuum models based on CSSM, since the observed brittle behaviour results from strain localisation and this cannot be modelled using continuum mechanics methods (Hight, 2006).

What appears to be poorly appreciated within the Australian geotechnical community is what constitutes sensitive soils and the possibility that they may be as prevalent in Australia as they are in northern European and Canadian deposits. Clays of high *in situ* sensitivities ($S_{u\ vane\ peak}/S_{u\ vane\ residual}$) in the region of 8-24 have been recorded in the Richmond River Estuary in Northern NSW. On a world scale, these are considered very sensitive to slightly quick soils (Mitchell and Soga, 2005).

The research presented in this paper applies the concept of the sensitivity framework in order to demonstrate the important role played by soil structure in controlling the geomechanical behaviour of east coast Australian estuarine clays.

2 SENSITIVITY FRAMEWORK

This section briefly reviews the concept of intrinsic parameters proposed by Burland (1990) and the sensitivity framework developed by Cotecchia and Chandler (2000), based on the use of intrinsic parameters. The sensitivity framework provides a semi-quantitative understanding of the degree of *structure* in a natural soil through a comparison of its natural behaviour to a baseline of its remoulded clay behaviour. The sensitivity framework is a behavioural framework for natural clays akin to CSSM for remoulded clays.

By remoulding a soil at a moisture content of between 1.25 and 1.5 times its liquid limit any natural structure is considered to be removed. The geomechanical properties of a soil reconstituted in this way are defined as its intrinsic properties (Burland, 1990). As in Burland (1990) the intrinsic properties presented here are denoted with an asterisk, *.

The intrinsic parameters are derived from a standard incremental oedometer test on the remoulded soil. The intrinsic compression index, C^*_c, is defined as the difference between the void ratio at 100kPa (e^*_{100}) and the void ratio at

1000kPa (e^*_{1000}) of the fully remoulded material. These values are represented schematically in Figure 1(a) for two remoulded clays of with different index properties. The values e^*_{100} and e^*_{1000} are determined directly from the curves.

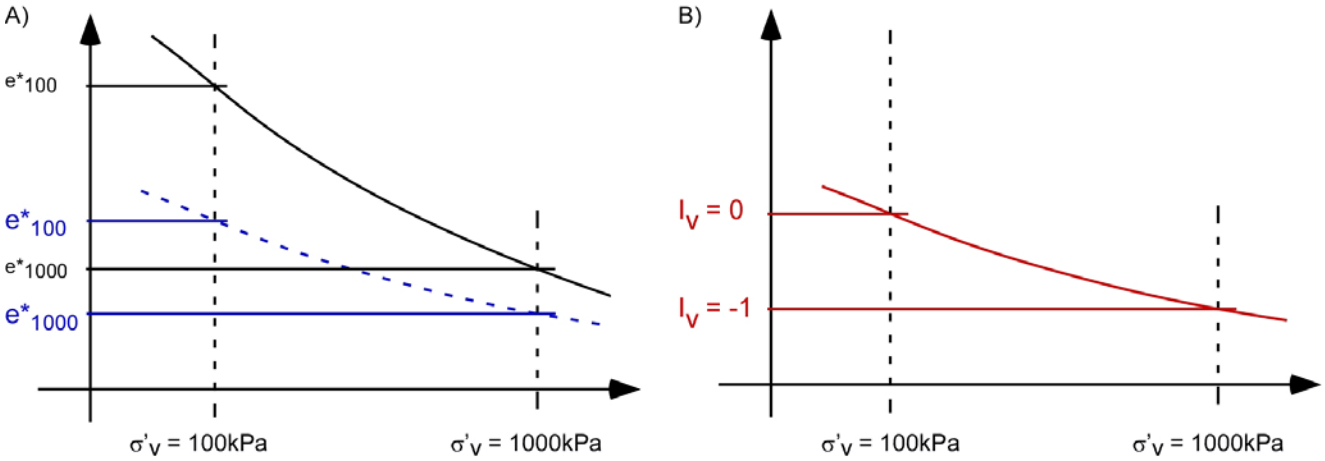

Figure 1: Derivation of the Intrinsic clay parameters (a) Oedometer curves of two remoulded clays with different LL (b) Same curves, normalised using intrinsic properties to produce the Intrinsic Compression Line.

The parameter, C^*_c, is used to normalise the particular e vs. $log\ \sigma'_v$ curve according to Equation (1). The resulting normalised value is defined the void index, I_v, and when plotted against σ'_v both curves fall onto a single curve as shown in Figure 1(b). This curve is defined as the Intrinsic Compression Line or ICL.

$$I_v = \frac{e - e^*_{100}}{C^*_c} \qquad \textbf{(1)}$$

A similar normalising effect can be achieved using the Liquidity Index as was demonstrated by Skempton (1970) for a range of natural clays. However, the Void Index is considered by a number of authors (Chandler, 2004; Hight and Leroueil, 2003) as a more rigorous basis for comparison of soil behaviour because it incorporates an explicit link between void ratio, stress and clay behaviour in the oedometer test, rather than the implicit relationship between plasticity and geotechnical properties represented by the Liquidity Index.

Burland(1990) proposed a second reference line within the intrinsic framework termed the Sedimentary Compression Line (SCL). This line is derived using the Void Index and Skempton's original data for normally consolidated clays (Skempton, 1970). The SCL and the ICL are approximately parallel, so that the ratio of stresses at a given void ratio is around 5 (Burland, 1990), as shown in Figure 2.

Within this framework, it is possible to compare the degree of structure in the clay being studied relative to both its intrinsic values and against the average line (SCL) of clays whose structure is purely a function of gravitational loading. The *in situ* state of the soil is defined by the *in situ* stress, σ'_{vo} and the *in situ* void ratio e_0. In this discussion the term σ'_{vc} will be used to define the past maximum *in situ* stress determined from the geological loading history. The oedometer curve for a normally consolidated[1] clay (OCR=1, $\sigma'_{vo} = \sigma'_{vc}$) that has a degree of structural resistance above that defined by the maximum *in situ* stress (i.e. 'metastable') will display the behaviour shown in Figure 2(a). The soil will have a yield stress, σ'_{vy}, greater than the *in situ* stress σ'_{vo}. The ratio of these two stresses, $\sigma'_{vy}/\sigma'_{vo}$, is termed the yield stress ratio or YSR (Burland, 1990). A measure of the available structural resistance above the ICL is provided by the ratio of the yield stress to the intrinsic stress, $\sigma'_{vy}/\sigma'_{ve}$*, called the Stress Sensitivity or S_σ(Cotecchia and Chandler, 2000).

The black oedometer curve in Figure 2(b) represents the behaviour of an over consolidated clay with no structural sensitivity (YSR =1). The curve approaches the SCL and begins to deflect at the point equivalent to the past maximum stress ($\sigma'_{vy} = \sigma'_{vc}$). The term yield (Chandler, 2004) or gross yield (Hight and Leroueil, 2003) is used to describe this point within an oedometer test. The idea of yielding may seem unusual in the context of the oedometer however it is actually appropriate in that it represents the onset of plastic deformations within the soil skeleton (Leroueil and Vaughan, 1990).

[1] In this discussion, reference to over consolidation ratio and preconsolidation pressure relate strictly to values based on the gravitational loading history of the clay, rather than inferred from the oedometer test results.

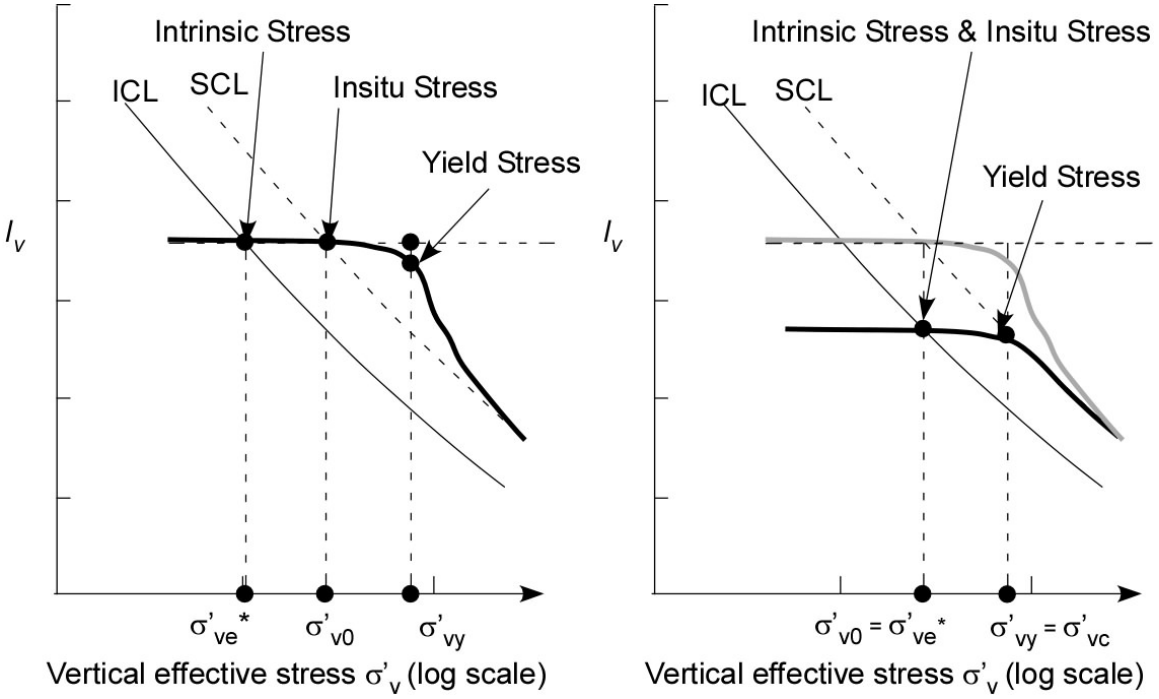

Figure 2: Sensitivity framework for oedometer curves of 2 clays (a) a normally consolidated clay with structure and (b) an over consolidated clay with only gravitational structure.

The most important distinction between the two clays represented in Figure 2 is in the post-yield behaviour. With the presence of structure, the clay in a) exists outside its limit state curve. Once this structure has been broken down the limit state curve will shrink, rather than expand as predicted by CSSM. There will be a decrease in the subsequent measured stiffness, peak shear strength and preconsolidation pressure. The pore pressure response of the post-yield clay will also be significantly different. Behaviour during yielding will also be different, the most significant variation being the pore pressure response. Since the structured clay is undergoing significantly greater plastic deformation in returning towards the SCL, the excess pore pressure will be higher than predicted for clay that was normally consolidated. As was described in the introduction these pore pressure responses are characteristic of the sensitive clays of Canada and the quick clays of Norway. A more important implication of a high degree of structure in a normally consolidated material is the fact that this clay has a greater tendency to deform in a brittle manner at low confining stresses (Burland, 1990) or higher strain rates (Leroueil and Hight, 2003). This has significant ramifications for the prediction of behaviours during embankment construction to end of primary settlement using continuum models based on CSSM.

As a substitute for detailed geological information, the oedometric yield stress (σ'_{vy}) is sometimes considered to represent the past maximum gravitational load (σ'_{vc}). It can be seen from Figure 2 that this assumption would lead to the prediction of the same over consolidation ratio for both clay samples in Figure 2(b). In turn, the structured, normally consolidated clay (grey curve in Figure 2b) could be mistaken for having the behavioural properties of the over consolidated material (black curve). The initial stiffness measured by the initial reload slope in the oedometer curve, may be taken as the recompression index of an over consolidated clay, when in fact this slope may represent the structural stability of a sensitive clay material.

The remainder of this paper will consider the results of oedometer tests conducted on soft soils from the Richmond River Estuary. A detailed geological history has been developed for this deposit (Bishop, 2006) that allows a comparison of the behaviours within the Sensitivity Framework.

3 RICHMOND RIVER: SITE CHARACTERISTICS

The lower Richmond River flows across a low floodplain (around 2 m AHD) that caps a mature (Roy *et al*., 2001) Holocene barrier-estuary fill sequence (Figure 2a). The sand barrier is shore parallel and extends between the rocky headlands of Evans Head to the south and Ballina to the north. This elongate, shore parallel barrier and back-barrier fill pattern is typical of the northern estuaries along the east coast of Australia (Roy, 1984). Below the 1 m thick floodplain deposits, the barrier-estuary sediments consist of a tidal delta sand system, a large area of central basin clays and silts, dominated by black shelly clays with considerable authigenic sulphides and coarse (silt-sand-fine gravel) fluvial delta deposits buried within the Emigrant and Duck Creek tributaries (Figure 3). The current tidal delta system is confined to

the main Richmond river and North creek channels but behind this, under the Ballina Township, is an extensive early-Holocene tidal sand delta (Figure 3). The fluvial deltas are confined to narrow bedrock-controlled tributary valleys (Macguires, Emigrant and North creeks). The central basin clays and silts range in thickness from 8 m to 25 m and underlie much of the current floodplain. They become thinner towards hills on the eastern margins of the floodplain and peter-out on the barrier sands.

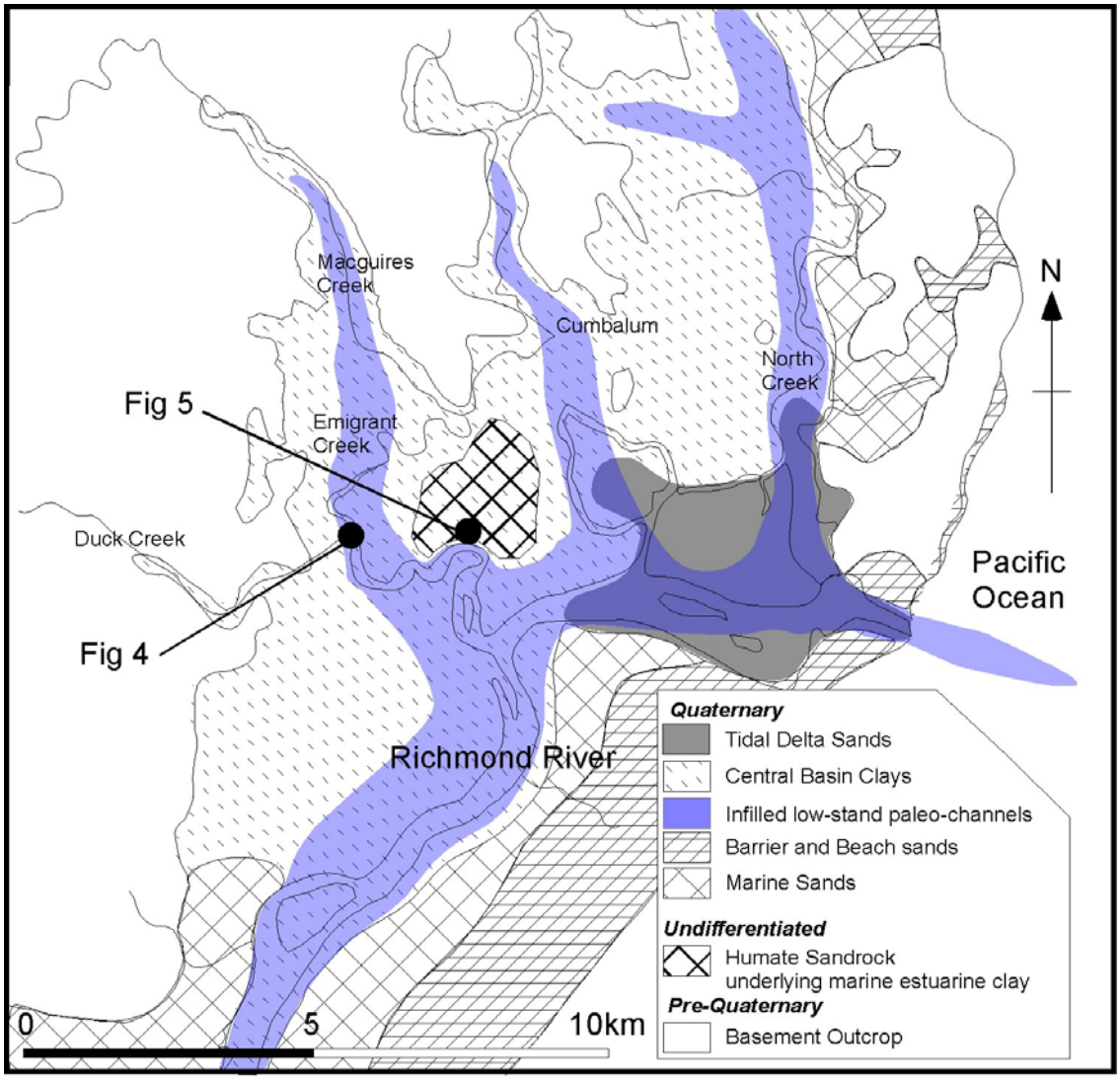

Figure 3: Map of Richmond River mouth with locations of Cumbalum and Teven and section.

The Holocene-Pleistocene sequence boundary defines the base of the Holocene estuary sediment. This boundary consists of a number of paleochannels carved into Pleistocene estuary deposits from the last highstand (120,000yrs BP) and possibly earlier highstand estuary deposits (Drury, 1982a). The paleochannels define the thalweg of the drainage system that would have existed at sea level lowstand around 18,000yrs BP. The channels are separated by interfluves that define terraces of stiffer sediments within the soft Holocene sediments. These terraces define the areas of thinner deposits of central basin mud.

The basement rocks consist of highly deformed interbedded metasediments of the Lower Proterozoic Neranleigh-Fernvale group (Packham, 1969). These rocks are overlain by Tertiary Volcanics of the Lamington Group (Packham, 1969). The basalts, rhyolites and tuffs belonging to this group dominate the outcrops that form the hills and headlands in the Ballina Study area (Figure 3) exposures. It is these rocks that are the dominant source material for the non-marine component of the estuary sediments.

The evolution of the coastal Richmond deposits has been defined by cycles of sea level rise and fall since the early Pleistocene. The presence of large amounts of humate sand rock (locally known as coffee rock) formed by the precipitation of humate substances from the groundwater flows is responsible from the preservation of older sediments. It also forms the substratum for the aggradation of the coastal sand barrier at a similar location during repeated sea level

highstands. The dominant depositional environment behind the barrier during highstand is the central basin: a brackish tidal mud and mangrove system (Hashimoto *et al.*, 2006). interspersed with tidal channels containing marine sand deposits (Bishop 2004). Areas of this system evolved under anaerobic conditions resulting in extensive post depositional alteration of the clays and formation of secondary sulphides and carbonates. A recent sea level fall of around 1m since 3000yrs BP (Goodwin *et al*., 2005) has seen the incision of the main drainage channels into the marine clays of the central basin. This has resulted in the formation of meander and point bar organic deposits as the river adjusted to the new flow conditions.

4 INTRINSIC BEHAVIOUR OF ESTUARY CLAYS

Sample disturbance has major implications for values interpreted from laboratory testing. Current standard practice of testing U75 tube samples in Australia does match that used in Northern Hemisphere projects. Extensive research has shown sensitive material sampled using U75 samples will cause excessive sample disturbance (Jamiolkowski *et al*., 1985) and interpreted oedometer results may underpredict the actual preconsolidation pressures by as much as 30% (Leroueil, 1996). Although the utmost care was taken with the samples during testing, this degree of disturbance must still be expected, even with the U100 sampling methods used. The oedometer yield stresses have been interpreted using Casagrande construction. Adjustments for the *in situ* conditions were also made according to the recommendations of Terzaghi *et al.* (1996). In order to obtain the actual yield stress accounting for sample disturbance, this value was adjusted by 30% in line with the values determine by Leroueil (1996) from oedometer tests conducted on samples obtained from high quality block samples compared to U75 samples. Importantly though, the sampling process only acts to reduce the peak values, so if high levels of *structure* are identified they are likely to be, if anything, lower bounds to the true values. That is, increased care in sampling will only reveal higher levels of structure still. It is important to remember that by normalising the oedometer data in the manner described in the previous section, the effects of soil composition and plasticity are removed and the clays are being compared on an equivalent basis.

Two methods for determining the intrinsic parameters are possible. The first and preferable method is to obtain the values from tests on the remoulded material. With regards to the data presented in this paper intrinsic tests have only been conducted on the floodplain clay, Figure 4a. The plot of this ICL is shown in Figures 4a and 4b (dashed blue line). Over the range of pressures, 10-1200 kPa, there is excellent agreement with the literature values as shown by relative positions of ICL (green and brown) and SCL (blue) reference lines from Burland (1990) and Chandler (2000). The deviation below 10 kPa is most likely to be due to restructuring that has occurred during the preparation of the reconstituted material. The second method for determining e^*_{100} and C^*_c is to use the correlation equations determined by Burland (1990). These equations relate the Index properties of the clay to its intrinsic values (see appendix). This method has been used to derive the intrinsic oedometer curves for the samples in Figure 4b and Figure 5.

One of the proposed uses of the sensitivity framework is in detecting variations in depositional environment (Chandler, 2000). In the conditions envisaged during the evolution of the Richmond Estuary (and other east coast Australian estuaries) some clay deposits will have evolved in shallow tidal flat environments while adjacent clays have evolved entirely in the deeper water within the open water portion of the central basin. The data in Figure 4 is derived from oedometer tests performed on two samples of grey shelly clay from different depths within the sample borehole (Figure 3). The sample in Figure 4a is of from 3.15 m below ground surface (w_n=74%, w_L=89%, PI=56%). The sample in Figure 4b is from 4.75,m below ground surface in the same location (w_n=107%, w_L=118%, PI=83%). The shallower clay (Figure 4a) lies to the left of the ICL while the deeper clay (Figure 4b) lies significantly to the right of the SCL. The deeper clay also has a more open yet just as stable structure, indicated by the higher void index but similar yield strength. The *in situ* stress conditions are only marginally different and, since both clays are normally consolidated from a geological perspective (Bishop, 2006), the difference is indicative of different depositional conditions. Within this framework, normally consolidated clays deposited in a tidal flat environment will plot on or to the left of the ICL (Chandler, 2000). This is due to the diurnal flooding they are subject to and, although they not become desiccated when aerially exposed, they are subject to negative pore water stresses during low tide periods. As a result, the structure that they evolve is more stable than deeper water sediments. The importance of this from a geological perspective is that once a particular clay environment becomes buried (e.g. during rising sea levels) the relative position of the *in situ* state to the ICL and SCL will remain fixed and the void index will evolve parallel to these lines.

The slope of the swelling path of the undisturbed sample compared to the remoulded sample in Figure 4b demonstrates an important element of the structure (Burland, 1990). The influence of the structure in the sample is to increase the ability of the sample to rebound relative to its remoulded counterpart. In this case it indicates that complete structural breakdown has not occurred through the first stage of the oedometer test. It is also apparent that there is a clear difference between the slope of the initial loading line compared to the reload line. This is further evidence of the degree of structural breakdown that occurs during primary consolidation of the undisturbed sample.

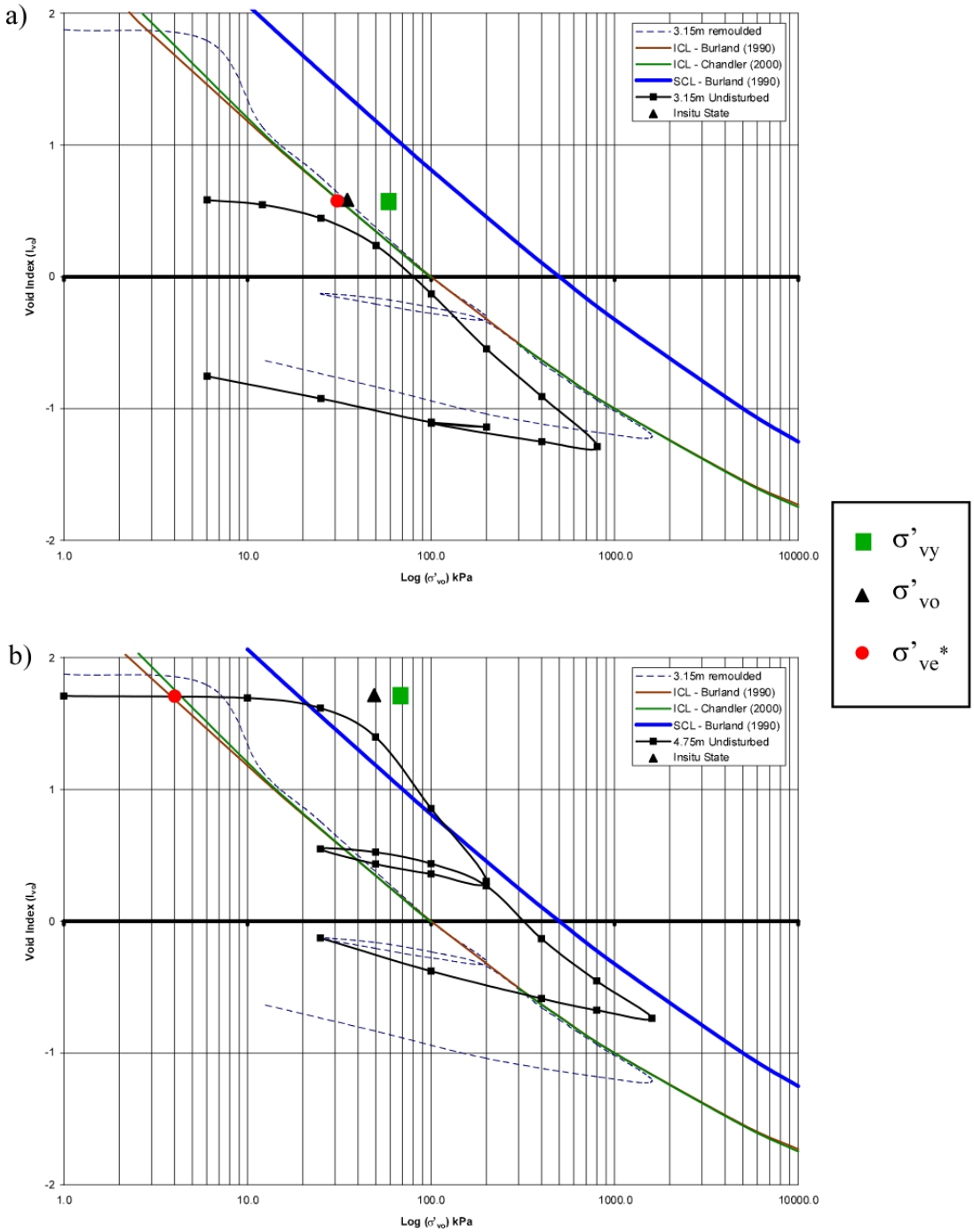

Figure 4: Intrinsic oedometer curves for samples from Bruxner (a) Central Basin Clay and (b) Floodplain clays.

Figure 5 shows the intrinsic oedometer plots for two clays from within a single profile (refer to Figure 3). The presence of a humate sand rock layer (Figure 3) separating the clays indicates that the lower clay is Pleistocene in age (Roy, 1984). The upper clay (4.2 m depth) is Holocene and has similar index properties to the Central basin Clay from Figure 4b. The lower clay has a natural water content of 60%, a liquid limit of 60% and a plasticity index of 37%. Both clays lie to the right of the ICL indicating a significant level of structure in both, however the lower clay lies on or just to the right of the SCL. In terms of deposition environments both clays were deposited in deeper water brackish marine conditions, evidenced by the presence of small quantities of shell hash and almost no sand. Both clays have natural water contents near their liquid limits and if they had been deposited in a continuous sequence they would both lie a similar distance to the right of the SCL. The fact that they do not supports the conclusion that the lower clay is Pleistocene. Sea levels at the time of deposition of the lower clay (112,000yrs BP) were approximately 5 m higher than present day conditions. This would imply an approximate additional overburden stress of at least 70 kPa (assuming 5 m extra marine clay at γ_{bulk} = 14 kN/m^3) that has since been removed. Stress of at least this magnitude is recorded in the

distance between the *in situ* condition σ'_{vo} and the yield stress σ'_{vy}. Since the lower clay is now under a lower overburden stress its *in situ* condition is shifted to the left. The upper clay, which is normally consolidated has a degree of structure that allows it to exist at a void index (read void ratio) and stress state (σ'_{vo}) well above the value that it should begin to collapse (σ'_{ve}*) Both clays undergo significant structural yielding during loading recognised by the fact that the slope of the loading curve is significantly steeper than the intrinsic and sedimentary curves.

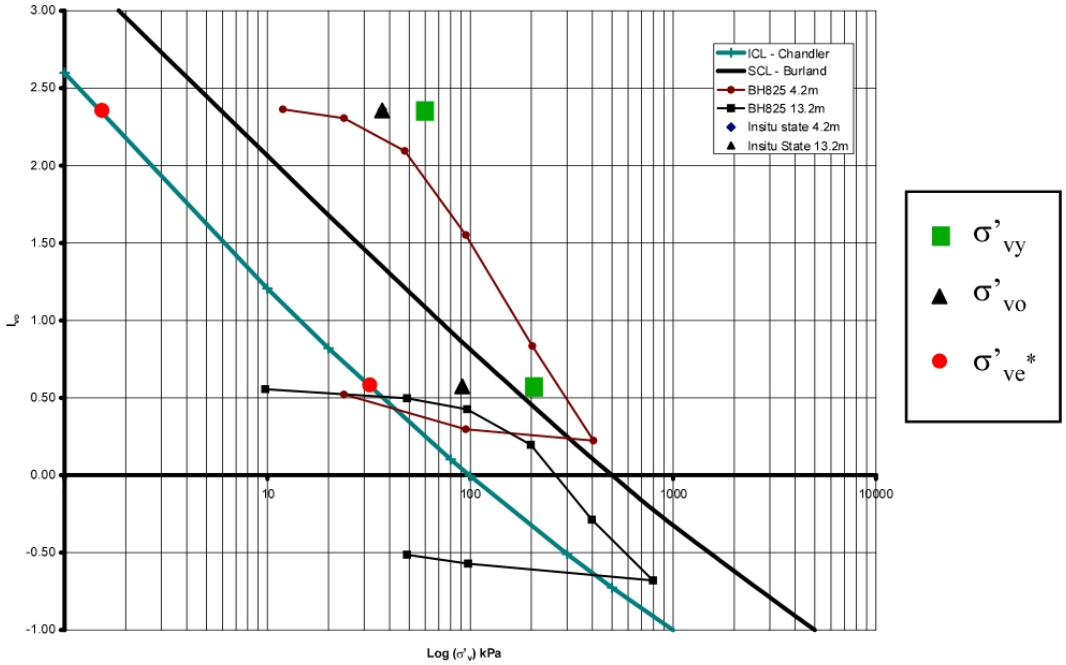

Figure 5: Intrinsic oedometer curves for a) Holocene Central Basin Clay (4.2m) b) Pleistocene Central Basin Clay (13.2m) both samples are from the same borehole (Figure 3).

5 SENSITIVE CLAYS IN NSW ESTUARIES

The important question to consider in this section is whether sensitive soils exist in Australia.

In order to examine this it is necessary to qualify both the definition of sensitivity and the scale used to quantify the sensitivity. The data set of *in situ* vane results with both peak and remoulded values is quite considerable for the Richmond region so this data will be used in conjuction with the oedometer results. Table 1 presents the Sensitivity Framework ratios defined previously in Section 3. These are the Yield Stress Ratio (YSR) and the Stress Sensitivity, S_σ. The *in situ* shear vane sensitivity ($S_{t\ vane}$) for the tested clays are given on the right of Table 1. Also included in this table are equivalent data from a deposit of sensitive marine clay from Onsøy in Norway. The data for the Onsøy clay was obtained from Lunne *et al.* (2003). Most importantly this is the same clay investigated by Bjerrum (1967) in his landmark paper investigating the behaviour and formation of the Drammen River quick clays.

Firstly, on the scale of shear vane sensitivities proposed by Rosenqvist (1953) values in the region of 6-8 are considered very sensitive. It is immediately apparent that these sensitivities are found in the Richmond clays (Samples highlighted by Bold type). Comparable stress sensitivities (S_σ) also occur in this material but it is interesting to note that some samples with high stress sensitivities do not have high shear vane sensitivities (BH825 4.2 m). This reflects the fact that although a soil may have an open structure signified by the high values of S_σ its remoulded strength can also be high thus reducing the measured sensitivity.

The behaviour of the clays in the oedometer and the values presented in Table 1 indicate that highly sensitive clays do occur and are common within the Richmond Estuary. The published data on Australian estuarine clays is very limited and few of the behaviours that characterise high sensitivity clays have been officially reported. It is highly likely that this is due to the nature of the projects which have been undertaken on the estuaries. Predominantly these projects have been large embankments for transport infrastructure in which issues of stability, even on sensitive materials, can be designed for (Leroueil *et al*., 1990b). The absence of projects in which stability is an issue means that the performance of these soils under critical conditions has not yet been tested.

Table 1: Intrinsic parameters and sensitivities for clays in the Richmond compared to Onsøy Clay (Norway), values in brackets are the values uncorrected for sample disturbance

Sample	Deposition Environment	σ'_{vy}(kPa)	σ'_{vo} (kPa)	YSR ($\sigma'_{vy}/\sigma'_{vo}$)	S_σ ($\sigma'_{vy}/\sigma'_{ve}$*)	$S_{t\ vane}$
3.15 m undisturbed	Floodplain	68 (52)	35	1.9 (1.6)	1.93 (0.92)	2
4.75 m undisturbed	**Central Basin**	**68 (52)**	**50**	**1.4 (1.1)**	**11.6 (8.91)**	**6.5**
BH825 4.2 m	Central Basin	63 (48)	37	1.7 (1.3)	30.7 (23.59)	2.6
BH825 13.2 m	Central Basin	209 (161)	90	2.3 (1.8)	4.1 (3.14)	N/A
BH832 10.2 m	Central Basin	93 (72)	57	1.6 (1.3)	(71.9)	2.21
BH809 4.2 m	**Central Basin**	**66 (51)**	**41**	**1.6 (1.2)**	**13.2**	**24**
BH809 7.2 m	**Central Basin**	**124 (95)**	**58**	**2.1 (1.6)**	**20.6**	**20**
Onsoy (Norway) 6.85 m	**Central Basin**	**85**	**54**	**1.4**	**42.3**	**6-8**

The above data illustrating the existence of sensitive clays in east coast Australian estuaries is consistent with the expectation derived from an understanding of the complex evolutionary processes in eastern Australian estuaries. The eastern Australian estuaries accommodate strikingly similar evolutionary processes to those under which all quick clay precursor material evolves. The Onsøy clay described above, the Champlain Sea clay from Canada (Leroueil *et al.,* 2003) and the estuarine clays of the Richmond River have all evolved in brackish to marine conditions. They all contain a component of shell material and organic matter concentrations in the order of 3-5%. Finally they all have evidence in the form of authigenic sulphides of anaerobic post-depositional alteration. This alteration also leaves the characteristic dark black colour relating to the presence of monosulphides. This final driver for the formation of quick clays in the case of the northern hemisphere clays is the leaching of salt from the pore fluid. With the melting of the glaciers the Canadian and Norwegian landscapes have lifted out of the ocean through isostatic rebound (Kenney, 1964). Progressively, fresh water flowing from higher in the landscape has leached salt from the marine clays thus reducing the remoulded strength and increasing the sensitivity.

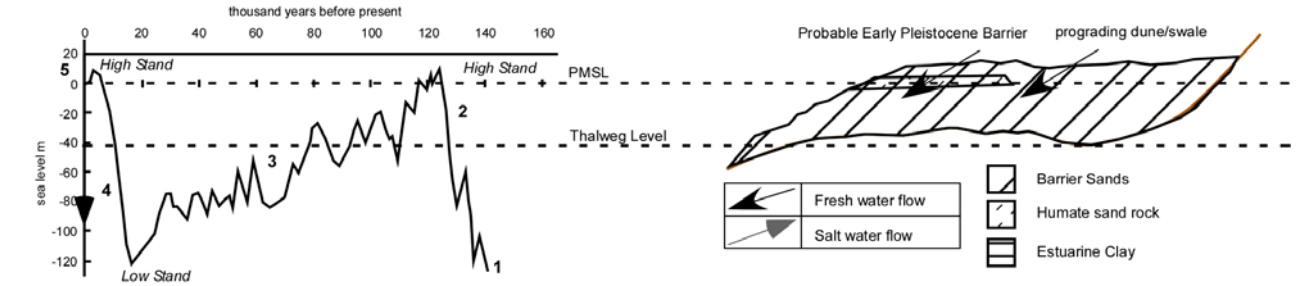

Stage	Process	Chemistry
1	Low stand:Erosion, local deposition of coarser terrestrial material. vegetation stabilizing nutrient rich deposits	Freshwater, well aerated aquifers, carbonate dissolution,
2	High Stand: River terrace to floodplain to central mud basin	Fresh water to saline, fresh and salt carbonates, high OM productivity, Reducing conditions dominate
3	Falling S.L.: Hydraulic gradient increasing,	Saline/reduced deposits flushed, elements become mobile. localized re-deposition
4	Holocene transgression: Marine deposits occur within the Pleistocene paleochannels	Freshwater aquifers are flushed with salt water. brackish conditions reappear
5	As for Stage 2; fluvial deposits at base, river terrace structure , transitioning to meanders and then central mud basin	Fresh to saline transition, carbonates deposited, high O.M. production, reducing conditions dominate

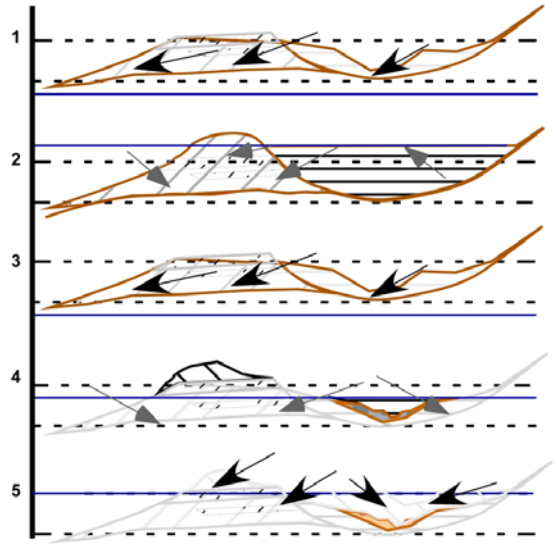

Figure 6: Mechanism for the alteration of marine clays within the Richmond River.

At first glance this last important factor may appear to be missing form the Australian situation. However Figure 6 presents the sequence of stratigraphic evolution for the Richmond Estuary relative to the regional sea level curve taken from Chappell *et al.* (1996). During two periods within the last 120,000 yrs, conditions have occurred in which fresh water gradients would exist in such a way as to flush salt water from marine deposited clays. These are at periods of relative sea level lowering. The first of these is from 120,000 yrs BP to 18,000 yrs BP. Most importantly, in the last 3000 yrs relative sea level has fallen by around 1 m. Marine clays deposited during the early Holocene transgression will have experienced a significant period of fresh water flushing. This process is being driven both by fresh water infiltration from the surface and through contact with confined fresh water aquifers that occupy previously saline tidal channel and barrier sand deposits within the clays. Initial investigations have shown that high sensitivity materials found in the Richmond River are in locations that have been exposed to fresh water flushing.

A very important difference between Australian Estuarine clays and those of the Northern Hemisphere lies in the climate and sediment supplied to the estuaries. In Australia the climate has been dominated by sub-tropical to temperate conditions and we have had no glacial periods. As a result Australian clays have evolved under intense chemical rather than physical processes and the estuarine clays (at least in the Richmond) are dominated by mixed layer clays and smectite. Since a major characteristic of extremely sensitive and quick clays is the presence of rock flour (Torrance, 1983) as the soil matrix. The rock flour is a product of mechanical abrasion by glaciers so it is unlikely that clays with this extreme sort of behaviour would occur in Australia. In terms of our future investigation into the estuarine clays of Eastern Australia and the likely development of future expensive infrastructure that may mobilise this element of the clay's behaviour it would seem necessary to reassess the way in which we look at them.

6 CONCLUSION

This paper has demonstrated presence and potential occurrence of structured clays with sensitivities ranging from low to very high in eastern Australian estuaries. A better understanding of estuary evolution allows the diverse range of complex evolutionary processes to be appreciated and the role played by them in generating structured clays. Experience with these materials in Europe and Canada gives insight into the significant phenomena associated with these clays and the possible shortcomings of CSSM for modelling the behaviour. At the same time it has been demonstrated that there are suitable differences in the composition that need to be considered when applying the northern Hemisphere experience to the Australian problem.

It is likely that many of the problems experienced in engineering infrastructure on east coast estuarine clays is related to the complex behaviours of structured clay and hence there is a need for additional research into their distribution and engineering behaviour.

7 APPENDIX

The determination of intrinsic values can also be achieved using the correlation equations proposed by Burland (1990). These correlations (Equation 2 and 3) relate the void ratio of the clay sample at the liquid limit e_L to e^*_{100} and C^*_c. The reader is referred to Burland (1990) and Chandler (2000) for the background into these derivations.

$$e^*_{100} = 0.109 + 0.679e_L - 0.089e_L^2 + 0.016e_L^3 \quad \textbf{(2)}$$

$$C^*_c = 0.256e_L - 0.04 \quad \textbf{(3)}$$

8 ACKNOWLEDGEMENTS

The authors would like to acknowledge the cooperation of The Roads and Traffic Authority NSW, Coffey Geosciences and RCA for making data available for this study. Financial support from the Australian Research Council is also acknowledged.

9 REFERENCES

Bishop, D. "A proposed geological model and geotechnical properties of a NSW Estuarine valley: A case study." *Proceedings of the 9th international conference on Geomechanics*, Auckland, 261-267.

Bishop, D. T. (2006). "The geotechnical evolution of the Richmond Estuary," University of Newcastle, Newcastle.

Bjerrum, L. (1967). "Engineering Geology of Norwegian normally-consolidated marine clays as related to settlements of buildings." *Geotechnique*, 17, 81-118.

Burland, J. B. (1990). "On the compressibility and shear strength of natural clays." *Geotechnique*, 40(3), 329-378.

Burland, J. B., Rampello, S., Georgiannou, V.N., and Calabresi, G. (1996). "A Laboratory Study of Four Stiff Clays." *Geotechnique*, 46(3), 491-514.

Chandler, R.J. (2000). "Clay sediments in depositional basins: the geotechnical cycle." *The Quarterly Journal of Engineering Geology and Hydrogeology*, 33(11), 7-39.

Chandler, R.J. "Geotechnical characterisation of Soils and Rocks: a geological perspective." *The Skempton Conference*.

Chappell, J., Omura, A., Esat, T., McCulloch, M., Pandolfi, J., Ota, Y., and Pillans, B. (1996). "Reconciliation of late Quaternary sea levels derived from coral terraces at Huon Peninsula with deep sea oxygen isotope records." *Earth and Planetary Science Letters*, 141(1-4), 227-236.

Cotecchia, F., and Chandler, R.J. (2000). "A general framework for the mechanical behaviour of clays." *Geotechnique*, 50(4), 431-447.

Drury, L.W. (1982a). "Richmond River Valley Groundwater Investigation." *90*, Water Resources Commision, Sydney.

Goodwin, I.D., Stables, M.A., and Olley, J.M. (2005). "Late Holocene wave climate, sediment supply and evolution of the Iluka-Woody Bay Sand Barrier, northern New South Wales, Australia." *Marine Geology*, SUBMITTED.

Hashimoto, T.R., Saintilin, N., and Haberle, S.G. (2006). "Mid-Holocene Development of Mangrove Communities Featuring Rhizophoraceae and Geomorphic Change in the Richmond River Estuary, New South Wales, Australia." *Geographical Research*, 44(1), 63-76.

Hight, D.W. (2006). "Continuum models." D. Bishop, ed., Guildford.

Hight, D.W., and Leroueil, S. (2003). "Characterisation of soils for engineering purposes." Characterisation and Engineering Properties of Natural Soils., T.-S. Tan, K. K. Phoon, D. W. Hight, and S. Leroueil, eds., A.A. Balkema, Tokyo, 255-362.

Hoeg, K., Andersland, O.B., and Rolfsen, E.N. (1969). "Undrained behaviour of quick clay under load tests at Asrum." *Geotechnique*, 19(1), 101-115.

Jamiolkowski, M., Ladd, C.C., Germaine, J.T., and Lancellotta, R. "New developments in the field and Laboratory testing of soils." *Proceddings of the XIth ICSMFE*, San Francisco, 57-153.

Kenney, T.C. (1964). "Sea-level movements and the geological histories of the post-glacial marine soils at Boston, Nicolet, Ottawa and Oslo." *Geotechnique*, 14, 203-230.

Leroueil, S. (1996). "Compressibility of Clays: Fundamental and practical aspects." *Journal of geotechnical engineering*, 122(7), 534-543.

Leroueil, S., Bouclin, G., Tavenas, F., Bergeron, L., and Rochelle, P.L. (1990a). "Permeability anisotropy of natural clays as a function of strain." *Canadian Geotechnical Journal*, 27, 568-579.

Leroueil, S., Hamouche, K.K., Tavenas, F., Boudali, M., Locat, J., Virely, D., Roy, M., La Rochelle, P., and Leblond, P. (2003). "Geotechnical characterisation and properties of a sensitive clay from Canada." Characterisation and engineering properties of natural soils, T.-S. Tan, K. K. Phoon, D. W. Hight, and S. Leroueil, eds., Balkema, Tokyo, 363-394.

Leroueil, S., and Hight, D.W. (2003). "Behaviour and properties of natural soft soils and soft rocks." Characterisation and engineering properties of natural soils, T.-S. Tan, K. K. Phoon, D. W. Hight, and S. Leroueil, eds., Balkema, Tokyo, 29-254.

Leroueil, S., Magnan, J.P., and Tavenas, F. (1990b). *Embankments on Soft Clays*, D. Muir-Wood, translator, Ellis Horwood Limited.

Leroueil, S., and Vaughan, P.R. (1990). "The general and congruent effects of structure in natural soils and weak rocks." *Geotechnique*, 40(3), 467-488.

Lunne, T., Long, M.M., and Forsberg, C.F. (2003). "Characterisation and Engineering properties of Onsoy Clay." Characterisation and Engineering Properties of Natural Soils, Swets & Zeitlinger, 395-427.

Mitchell, J.K., and Soga, K. (2005). *Fundamentals of soil behaviour*, John Wiley & Sons, New York.

Muir-Wood, D. (1990). *Soil behaviour and Critical State Soil Mechanics*, Cambridge University Press, Cambridge.

Packham, G.H. (1969). "The Geology of New South Wales." D. A. Brown, ed., Geological Society of Australia, Sydney, 654.

Rosenqvist, I.T. (1953). "Considerations on the sensitivity of Norwegian quick clays." *Geotechnique*, 3(5), 195-200.

Roy, P.S. (1984). "New South Wales Estuaries: Their origin and Evolution." Coastal geomorphology in Australia, B. G. Thom, ed., Academic Press, Sydney, 349.

Roy, P.S., Williams, R.J., Jones, A.R., Yassini, I., Gibbs, P.J., Coates, B., West, R.J., Scanes, P.R., Hudson, J.P., and Nichol, S. (2001). "Structure and Function of South-east Australian Estuaries." *Estuarine, Coastal and Shelf Science*, 53, 351-384.

Schmertmann, J.H. (1991). "The mechanical aging of soils." *Journal of geotechnical and geoenviromental engineering*, 119(9).

Skempton, A.W. (1970). "Consolidation of clays by gravitational compaction." *Q.J. Geol.Soc. Lond.*, 373-412.

Terzaghi, K. (1941). "Undisturbed clay samples and undisturbed clay." *Journal of the Boston society of civil engineers*, 28, 211-231.

Terzaghi, K., Peck, R.B., and Mesri, G. (1996). *soil mechanics in engineering practice*, Wiley Interscience, New York.

Torrance, J.K. (1975). "On the role of chemistry in the development and behaviour of the sensitive marine clays of Canada and Scandinavia." *Canadian Geotechnical Journal*, 12, 326-335.

Torrance, J.K. (1983). "Towards a general model of quick clay development." *Sedimentology*, 30(4), 547-555.

PERFORMANCE AND PREDICTION OF SOFT CLAY BEHAVIOUR UNDER VACUUM CONDITIONS

Cholachat Rujikiatkamjorn[1] and Buddhima Indraratna[2*]
[1]Research associate, [2]Professor of Civil Engineering, Department of Civil Engineering
*University of Wollongong, NSW, 2522 Australia,*Corresponding Author*

ABSTRACT

This paper describes the behaviour of soft soil foundation under vacuum-assisted preloading at the Second Bangkok International Airport, Thailand. An analytical solution considering the variation of soil permeability and compressibility is proposed. The associated settlement and excess pore pressure at the embankment centerline are predicted and compared with the available field measurement. The field data shows that the efficiency of this improvement technique depends on the magnitude and distribution of vacuum pressure as well as on the extent of air leak protection. The height of sand surcharge and consolidation time can be significantly reduced in comparison with the conventional method of surcharge alone.

1 INTRODUCTION

Many coastal regions of Australia and Southeast Asia contain very soft clays, which possess poor geotechnical properties such as high compressibility and very low bearing capacity (Indraratna *et al*., 1992). The construction of highway and railway embankments on normally consolidated soft soil deposits has been affected by excessive differential settlements, lateral displacements in the absence of an appropriate ground improvement prior to construction. To prevent the unfavorable conditions, the application of preloading with prefabricated vertical drains (PVDs) prior to the construction has been popularly employed in many large scale projects (Hansbo, 1979; QDMR, 1991; Indraratna and Redana, 2000; Chu *et al*., 2004) . This method accelerates the consolidation by providing a shorter drainge path (Figure 1). The gained shear strength of the foundation can be achieved due to rapid excess pore pressure dissipation. It is also well-known that the high outward lateral movement causing the embankment instability can also be reduced via this method.

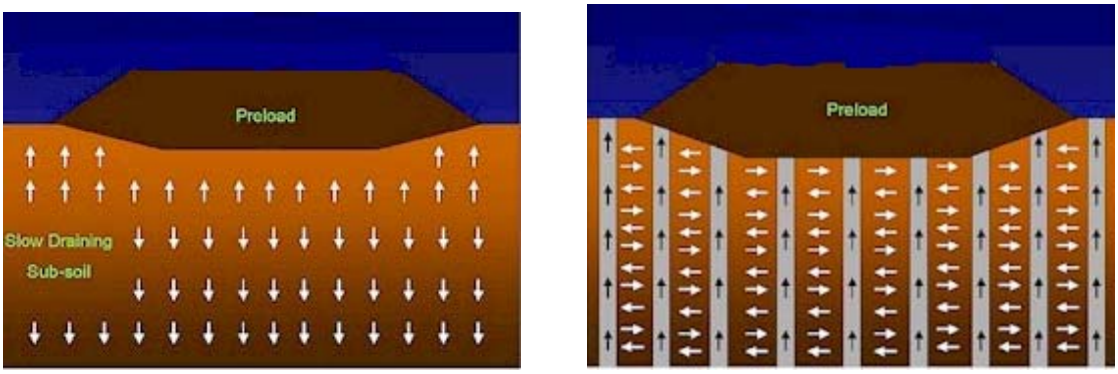

(a) (b)

Figure 1: Effect of vertical drain on drainage path; (a) without vertical drains and (b) with PVDs. (http://www.americandrainagesystems.com/wick_drains.htm).

In the case of hydraulic fill used in land reclamation projects where the height of surcharge is restricted due to the low shear strength of soft soil, vacuum-assisted consolidation is an ideal method for ground improvement (e.g. reclaimed land) (Shang *et al.,* 1998; Indraratna *et al*., 2004; Chu and Yan, 2005). The application of vacuum pressure as apparent surcharge load with PVDs can be used as a replacement of high embankment fill (Choa, 1990). Vacuum preloading method was first introduced by Kjellman (1952) to improve the strength of soft soil. The applied negative vacuum pressure is propagated along the PVDs length to deep subsoil layer, resulting in an increase in lateral hydraulic gradients ($i = \frac{1}{\gamma_w}\left\{\frac{\partial u}{\partial r} + \frac{\partial u_{vac}}{\partial r}\right\}$) and effective stresses in soil where u and u_{vac} are excess pore pressure generated by preloading and suction pressure generated by vacuum pump, respectively. Consolidation can be accelerated without increasing excess pore pressure (Cognon *et al*., 1994; Qain *et al*., 1992).

In this paper, rigorous analytical solutions for radial consolidation under vacuum condition incorporating non-linear soil properties (e.g. compressibility and permeability) are introduced. Subsequently, a case history constructed on soft Bangkok clay is analysed based on the current solution and compared to field measurements.

2 THEORETICAL BACKGROUND FOR VACUUM PRELOADING

2.1 VACUUM PRELOADING PRINCIPLES

In saturated soils, the total stress (σ) at any point within the soil mass is the combination of the effective stress (σ') and the pore pressure (u) (Terzaghi, 1943). Thus, the total stress at any point within the soil mass can be written as:

$$\sigma' = \sigma - (+u_{\Delta p}) \quad \textbf{(1)}$$

Under the surcharge load alone, the effective stress is gained by the dissipation of positive excess pore water pressure after the load application. In contrast, the effective stress is increased by the applied negative pore pressure ($-u_{vac}$) under the vacuum condition. Equation (1) can be rewritten based on the vacuum and fill preloading as:

$$\sigma' = \sigma - (+u_{\Delta p}) - (-u_{vac}) \quad \textbf{(2)}$$

It can be seen that the effective stress increases by negative suction, thereby reducing the risk of shear failure. The performance of this system depends on the vacuum condition under the airtight membrane (Indraratna *et al*. 2004). The intensive pore pressure measurement under membrane should be performed to verify the reliability of the vacuum system. Figure 2 shows the system of vacuum assisted preloading via PVDs.

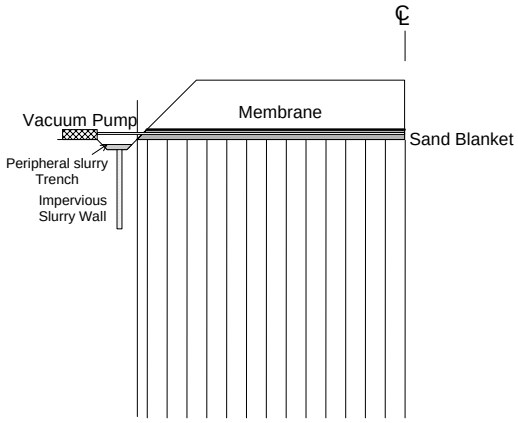

Figure 2: System of PVDs with sand blanket, airtight membrane and surcharge preloading (Indraratna *et al*. 2005).

2.2 ANALYTICAL SOLUTIONS FOR VACUUM PRELOADING

The unit cell theory is usually employed in the analysis of radial consolidation of soil around a single drain at the location of the embankment centreline where the lateral displacement is negligible (Barron, 1948; Hansbo, 1981). However, the solutions based on the surcharge load condition were simplified using the constant compressibility and permeability.

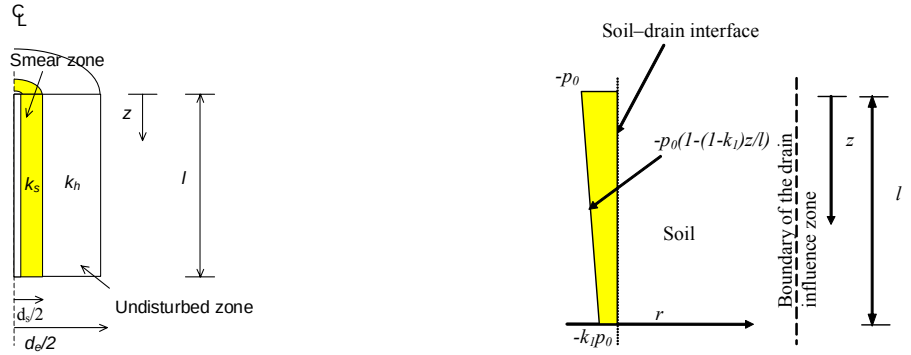

(a) (b)

Figure 3: (a) Unit cell and (b) Vacuum pressure distribution along the drain length.

Indraratna *et al*. (2005) proposed a comprehensive analytical solution for a unit cell under vacuum condition considering the constant soil compressibility and soil permeability. The details of the derivation were explained elsewhere in Indraratna *et al*., 2005. Figure 3a shows the unit cell and its dimension. Based on the laboratory observation by Indraratna *et al*. (2004) Figure 3b illustrates the linear variation of vacuum pressure distributed along the drain length interface.

The dissipation rate of average excess pore pressure $\bar{u}_t$ at any time factor (T_h) can be expressed as:

$$\bar{u}_t = \left(\Delta p + p_0 \frac{(1+k_1)}{2}\right)\exp\left(\frac{-8T_h^*}{\mu}\right) - p_0\frac{(1+k_1)}{2} \quad \textbf{(3)}$$

In the above expression,

$$T_h^* = P_{av}T_h \quad \textbf{(4)}$$

$$P_{av} = 0.5\left[1+\left(1+\Delta p/\sigma'_i + p_0(1+k_1)/2\sigma'_i\right)^{1-C_c/C_k}\right] \quad \textbf{(5)}$$

$$T_h = c_h t / d_e^2 \quad \textbf{(6)}$$

$$\mu = \ln\frac{n}{s} + \frac{k_h}{k'_h}\ln s - 0.75 \quad \textbf{(7)}$$

where, μ = a group of parameters representing the geometry of the vertical drain system and smear effect, $n = d_e/d_w$, s = d_s/d_w, d_e = equivalent diameter of cylinder of soil around drain, d_s = diameter of smear zone and d_w = diameter of drain well, k_h = average horizontal permeability in the undisturbed zone (m/s), k'_h = average horizontal permeability in the smear zone (m/s). Δp = preloading pressure, T_h is the dimensionless time factor for consolidation due to radial drainage, C_c = the compressibility indices, C_c = the permeability change index.

The average degree of consolidation (U_h) can now be evaluated conveniently by the equation:

$$U_h(\%) = \frac{1-\bar{u}}{1-\bar{u}_\infty}\times 100\ , \quad \textbf{(8)}$$

where, $\bar{u}_\infty$ can be calculated by Equations 1 and 6 when $t \to \infty$.

The settlement (strain) based on average degree of consolidation is defined by:

$$\rho = \rho_\infty U_h \quad \textbf{(9)}$$

where, ρ_∞ is the ultimate settlement when $t \to \infty$.

3 APPLICATION TO A CASE HISTORY

3.1 EMBANKMENT DETAILS AND SITE CHARACTERISTICS

The Second Bangkok International Airport is located at Samut Prakan province near the city of Bangkok, Thailand. At this site, soft clays, mainly marine or estuarine, often have construction difficulties such as excessive differential settlement and foundation failure due to insufficient shear strength of the soil. Therefore, a suitable ground improvement scheme is required prior to the infrastructure construction. Due to the scarcity of good fill material and time limitation, vacuum preloading combined with a very low height of surcharge fill via PVDs was selected to improve soft soil shear strength in this project.

Figure 4 shows the shear strength and compressibility ratio of sub-soil layers. The minimum undrained shear strength (C_u) of topmost weathered clay is about 18 kPa at a depth of 1 m. This value decreases to 8-15 kPa in the very soft underlying clay layer, which is highly compressible. The weathered crust is much less compressible due to its desiccation and compaction. The compression ratio of the soft clay layer varies from 0.3-0.5, whereas the weathered crust has a compressibility ratio of about 0.2. The soil layer at the crust is highly overconsolidated (OCR ~ 2.4-26) due to aging, desiccation and oxidation process.

At this site, Embankment TV2 was raised with 12 m PVDs at 1.0 m drain spacing and -70 kPa vacuum application (Figure 5). Total base area of each embankment was 1600 m^2 (Asian Institute of Technology, 1995). Perforated and corrugated pipes wrapped together in non-woven geotextile were placed under a membrane liner. Instrumentation included piezometers, surface settlement plates, multipoint extensometers, inclinometers, observation wells and benchmarks. The settlement, excess pore water pressure and lateral movement were measured for about 150 days. Figure 6 shows the fill loading history of the embankment.

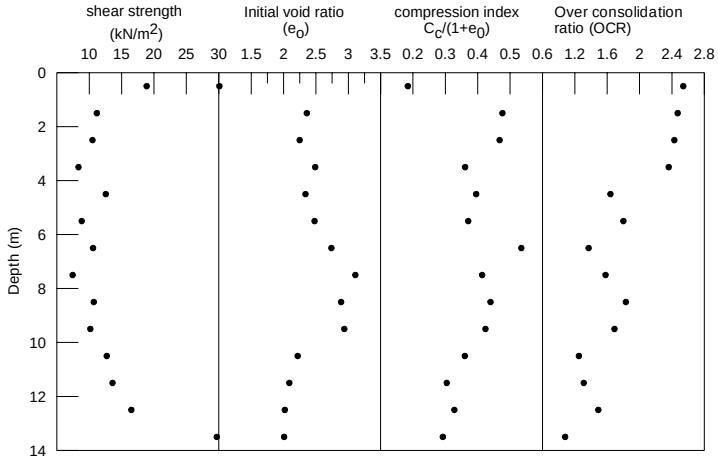

Figure 4: Average strength and compressibility indices (After Sangmala, 1997).

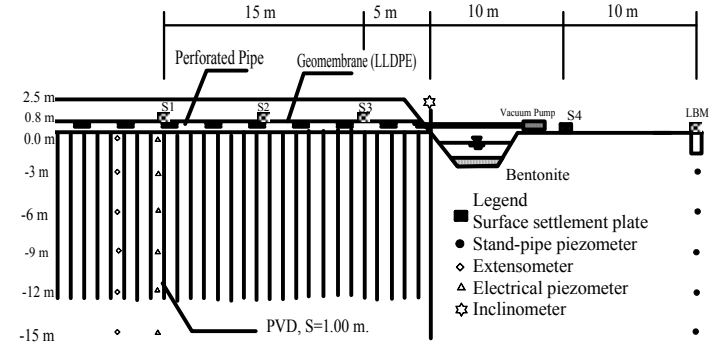

Figure 5: Cross section and location of monitoring system (after Indraratna and Rujikiatkamjorn, 2004).

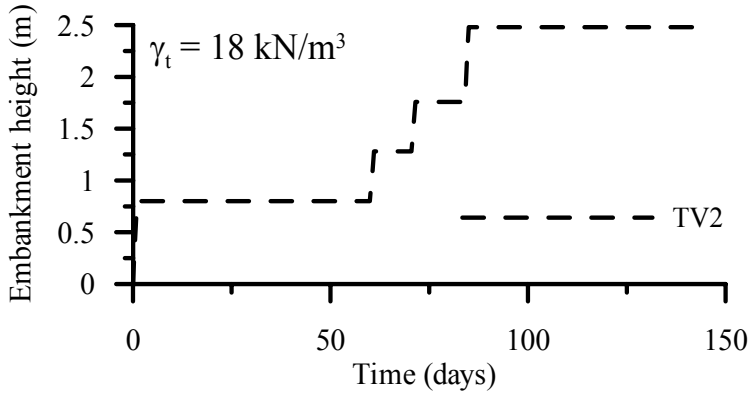

Figure 6: Construction schedule (after Indraratna and Rujikiatkamjorn, 2004).

3.2 SINGLE DRAIN ANALYSIS USING PROPOSED ANALYTICAL MODEL

In the field, at the embankment centreline, the condition of 1-D consolidation assumed in the proposed analytical model can be justified. The soil parameters, the *in situ* effective stress and the soil permeability for soft Bangkok clay subsoils are shown in Table 1. The relevant soil properties were obtained from CK_oU triaxial tests (AIT, 1995). The slope of e-logk_h (C_k) can be determined by (Tavenas *et al*., 1983, Indraratna *et al*. 2005):

$$C_k = 0.5e_0 \quad \textbf{(10)}$$

In the analysis, each subsoil layer was divided into 12 sub-layers (approximately 1 m thick) to obtain a more accurate effective stress distribution with depth. The value of soil compressibility indices (C_c or C_r) are related to the actual stress state, where the current effective stress must be considered in association with the pre-consolidation pressure of soil at that particular depth (Indraratna *et al*., 1994). The values of k_h/k_s and d_s/d_w for this case study were assumed to be 2 and 6, respectively.

The embankment loading was simulated using an instantaneous loading at the upper boundary. Settlement predictions were carried out at the embankment centreline using Equations (3)-(10). At the beginning of the subsequent stage, the initial *in situ* effective stress and soil permeability were calculated based on the final degree of consolidation of the previous loading stage. As the computation of consolidation settlement at the centreline is uncomplicated and follows the 1-D consolidation theory, the use of an EXCEL spreadsheet formulation for this purpose is sufficient. For the first stage loading, where the effective pre-consolidation pressure (p'_c) is not exceeded, the value of recompression index (C_r) may be used. In particular, the surface crust is heavily over-consolidated (up to about 2 m depth). Once p'_c is exceeded, the value of compression index (C_c) follows the normally consolidated line as indicated by the values in Table 1.

The following 4 models were analysed:

Model A: Application of surcharge load alone (i.e. no vacuum application).
Model B: Application of surcharge and time dependent vacuum pressure simulating vacuum loss according to the measured vacuum pressure under membrane (Figure 7). However, the soil compressibility and permability is assumed to be constant (Hansbo, 1981).
Model C: Similar to Model B. The nonlinear variation of soil compressibility and permeability proposed by the authors is employed.
Model D: Similar to Model C. There is no vacuum loss after 1 month.

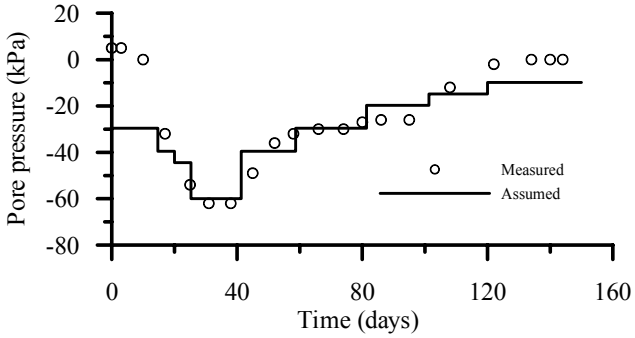

Figure 7: Measured and assumed pore pressure.

Table 1: Selected soil parameters for single drain analysis

Depth (m)	C_r	C_c	k_h ($\times 10^{-9}$ m/s)	e_0	□ (kN/m^3)	p'_c (kPa)
0.0-2.0	0.06	0.37	30.1	1.8	16	58
2.0-8.5	0.08	1.6	12.7	2.8	15	45
8.5-10.5	0.05	1.7	6.02	**2.4**	**15**	**70**
10.5-13.0	**0.03**	**0.95**	**2.56**	**1.8**	**16**	**80**
13.0-15.0	**0.01**	**0.88**	**0.60**	**1.2**	**18**	**90**

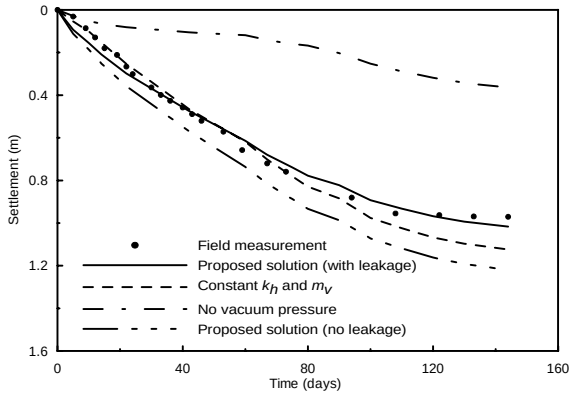

Figure 8: Surface settlement predictions at the centreline.

Figure 8 compares the predicted surface centreline settlement with the measured data. As expected, the predicted results based on the proposed solutions agree well with the measured results, whereas the prediction based on the constant k_h overestimates settlement after 80 days, because the actual soil permeability decreases considerably at higher stress levels. It was verified that the combined vacuum application and the PVDs system accelerates consolidation, while the vacuum pressure performs as an additional surcharge load. As shown in Figure 8, 'no leakage' conditions gain more settlement, whereas the prediction without any vacuum application yields less settlement. The efficiency depends

entirely on preventing airleaks and the distribution of vacuum pressure along the length of the drain. It is noted that the ultimate settlement can be obtained after 170 days.

4 CONCLUSIONS

A system of prefabricated vertical drains (PVDs) combined with vacuum preloading is an effective method for accelerating soil consolidation. In this study, a revised analytical model for vacuum preloading incorporating the compressibility indices (C_c and C_r) was proposed, and the variation of horizontal permeability coefficient (k_h) was represented by the e-logk_h relationship. The solution was employed to evaluate the performance of soft clay beneath embankment TV2 using spreadsheet software. The settlement predictions of the soft clay foundation agreed well with field observations when considering the actual field condition such as the varations of vacuum pressure, soil compressibility and permeabiltiy. It showed that the assumption of vacuum pressure distribution along the drain length could be applied to this site as evidenced by the monitored data. The effectiveness of the vacuum system depends on the protection against an air leak in the field.

5 REFERENCES

American Drainage Systems, Inc. (2006). Vertical wick drains [Online]. Available: http://www.americandrainagesystems.com/wick_drains.htm [Accessed 2006, May 16].

Asian Institute of Technology. (1995). *The full-scale field test of prefabricated vertical drains for the Second Bangkok International Airport: Final report*, Vol. 1, Asian Institute of Technology, Thailand.

Barron, R. A. (1948). The influence of drain wells on the consolidation of fine-grained soils. Diss., Providence, U S Eng. Office.

Choa, V. (1990). Soil improvement works at Tianjin East Pier project. *Proceedings 10th Southeast Asian Geotechnical Conference*, Taipei, 1: 47-52.

Chu, J., and Yan, S.W. (2005). Application of vacuum preloading method in soil improvement project. Case Histories Book (Volume 3), Edited by Indraratna, B. and Chu, J., Elsevier, London, 91-118.

Chu, J., Bo, M.W., and Choa, V. (2004). Practical considerations for using vertical drains in soil improvement project. *Geotextiles and Geomembranes*, 22, 101-117.

Cognon, J.M., Juran, I and Thevanayagam, S. (1994) Vacuum consolidation technology- principles and field experience, *Proc. of conf. on vertical and horizontal deformations of foundations and embankments deformations*, College station, Texas.

Hansbo, S. (1979). Consolidation of clay by band-shaped prefabricated drains. *Ground Engineering*, 12(5), 16-25.

Hansbo, S. (1981). Consolidation of fine-grained soils by prefabricated drains. In Proceedings of 10th International Conference on Soil Mechanics and Foundation Engineering, Stockholm, Balkema, Rotterdam, 3, pp. 677-682.

Indraratna, B., and Redana, I.W. (2000) Numerical modeling of vertical drains with smear and well resistance installed in soft clay. *Canadian Geotechnical Journal*, 37, 133-145.

Indraratna, B., and Rujikiatkamjorn C., (2004) Mathematical modeling and field evaluation of embankment stabilized with vertical drains incorporating vacuum preloading. *The Fifth International Conference on Case Histories in Geotechnical Engineering*. New York, Vol. 1, 2.01-2.08.

Indraratna, B., Balasubramaniam, A.S., and Balachandran, S. (1992). Performance of test embankment constructed to failure on soft marine clay." *J. Geotech. Eng., ASCE*, 118, 12-33.

Indraratna, B., Bamunawita, C., and Khabbaz, H. (2004). Numerical modeling of vacuum preloading and field applications. Canadian Geotechnical Journal, 41: 1098-1110.

Indraratna, B., Balasubramaniam, A. S., and Ratnayake, P. (1994). Performance of embankment stabilized with vertical drains on soft clay. J. Geotech. Eng., ASCE, 120(2), 257-273.

Indraratna, B., Rujikiatkamjorn C., Balasubramaniam, A.S. and Wijeyakulasuriya, V. (2005). Predictions and observations of soft clay foundations stabilized with geosynthetic drains and vacuum surcharge. Ground Improvement – Case Histories Book (Volume 3), Edited by Indraratna, B. and Chu, J., Elsevier, London, pp. 199-230.

Kjellman, W. 1952. Consolidation of clayey soils by atmospheric pressure. Proceedings of a conference on soil stabilization, Massachusetts Institute of Technology, Boston, 258-263.

Qian, J.H., Zhao, W.B., Cheung, Y.K. and Lee, P.K.K. (1992). The theory and practice of vacuum preloading. Computers and Geotechnics, 13: 103-118.

Queensland Department of Transport Registry (1991) Queensland Department of Transport, Sunshine Motorway Stage 2 – Area 2 *Geotechnical Investigation. Materials and Geotechnical Services Branch Report No. R1765*, June 1991.

Sangmala, S., (1997) Efficiency of drainage systems of vacuum preloading with surcharge on PVD improved soft Bangkok clay, ME Thesis, Asian Institute of Technology, Bangkok, Thailand.

Shang, J.Q., Tang, M., and Miao, Z. (1998). Vacuum preloading consolidation of reclaimed land: a case study. Canadian Geotechnical Journal, 35: 740-749.

Terzaghi, K. (1943). Theoretical soil mechanics, John Wiley & Sons, New York.

WHY ARE THERE SEASHELLS IN MY ALLUVIAL VALLEY? – THE COASTAL GEOLOGIST'S PERSPECTIVE OF VALLEY-FILL SEQUENCES.

T.L. Graham
GeoCoastal (Australia) Pty. Ltd., Brisbane, Queensland

ABSTRACT

For engineers tasked with placing infrastructure across alluvial valleys in eastern Australia the *mélange* of unconsolidated sand and silt/clay deposits encountered beneath modern floodplains must often appear baffling, particularly the juxtaposition of river derived and marine influenced deposits. However, it is this apparent anomaly that immediately alerts coastal geologists, for whom modelling these valley-fill sequences is their stock and trade, that they are dealing with an ancient 'drowned-valley estuarine' depositional environment.

Valleys that ultimately connect to the coast have experienced numerous cycles of erosion and deposition as a consequence of major sea level fluctuations through geological time. The last major phase of fill has occurred in response to marine inundation of coastal valleys by rising sea level which stabilized at approximately its present level some 6,500 years ago.

With the exception of the alluvial capping layer that supports human habitation of these valleys, the greater proportion of silt/clay sediments deposited during this last phase have remained beyond the influence of pedogenic processes and are therefore 'unripe'. This immaturity provides a number of challenging geomechanical and environmental aspects to working with these sediments.

Although local complexity may occur, stratigraphic models of 'drowned-valley estuarine' deposition provide a good general framework for understanding the distribution of both geomechanical and environmental properties of the valley-fill sequences.

1 INTRODUCTION

To engineers investigating the properties of unconsolidated sedimentary sequences in alluvial valleys, the presence of 'marine clays' must appear incongruous – 'alluvial' sedimentation having been generated by fluvial processes, while the 'marine clays', often bearing shells, exhibit an obvious connection with the sea. This mystery deepens when the subject valley-fill sequence is encountered many tens of kilometres from the coast. However, to a coastal geologist the very presence of sediments bearing the signature of both landward and seaward influences, immediately suggests that we are in an ancient estuarine environment.

In fact, drive across the level plain of any valley that is ultimately connected to the coast, and you can be reasonably certain that you are transecting an alluvial cap over an old 'drowned–valley estuarine' sequence. Coastal geologists have studied the genesis of these sequences extensively and, although there can be considerable complexity at the second and third order of investigation, general models of their evolution can bring some rhyme and reason to the stratigraphic architecture of these valley fills.

2 THE EVOLUTION OF [##]HOLOCENE DROWNED-VALLEY ESTUARIES

2.1 SEA LEVEL CHANGE

Fundamental to understanding the evolution of coastal environments is an appreciation of how coasts have responded to sea level change through geological time. Within geological timeframes sea level has been shown to fluctuate quite dramatically in response to water from the world's oceans becoming locked into large bodies of land-based ice during ice-age (or 'glacial') periods. While major sea level fluctuations have been numerous in the geological record, we generally need only concern ourselves with the changes that have occurred during the past 125,000 years when interpreting modern coastal plain evolution.

Changes in sea level during this period are illustrated in Figure 1.

[##] Holocene transgression – *Holocene* is the name of a geological time period (or 'epoch') commencing ~10,000 years ago and extending to present. *Transgression* is the term used to describe the progressive marine incursion of the land surface as sea level rises.

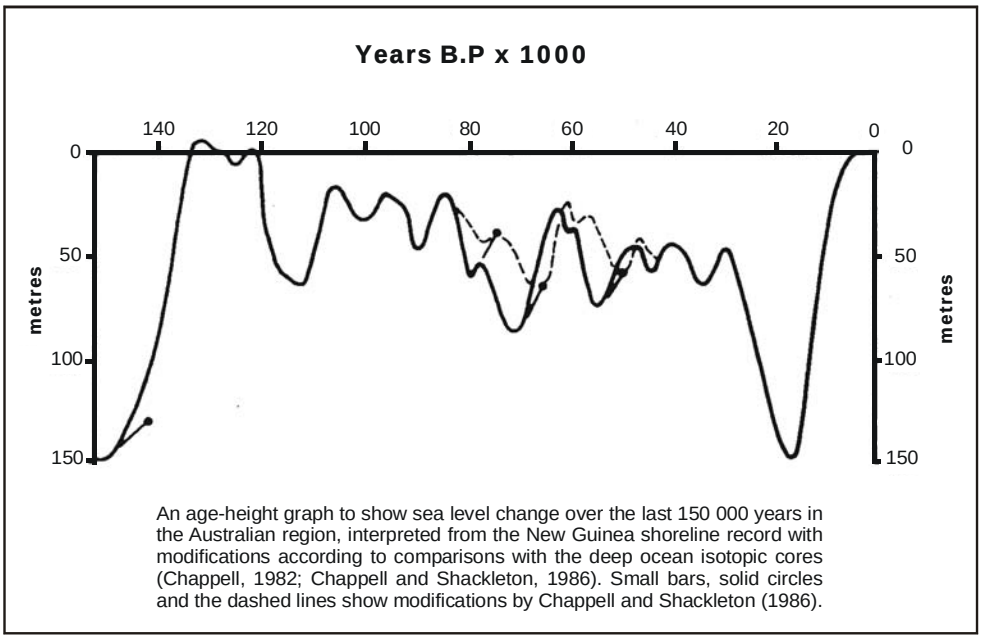

Figure 1: Age-height graph of sea level change (Chappell and Shackleton, 1986).

Approximately 125,000 years ago the world was experiencing a warm period between ice ages, similar to present. A number of studies have shown that sea level was higher than present at this time. In southeast Queensland, Pickett *et al*. (1985) reported evidence from old coral reefs on North Stradbroke Island of sea levels 1 m to 3 m above present. Originally, an age of 105,000 yrs ago was attributed to these corals, however they have since been reassessed as being in the range 120,000 to 130,000 (Chappell, 1987). During this period sediments were deposited at, or slightly above, the level of present coastal deposits and remnants of these older sequences are still found interspersed among younger deposits on present coastal lowlands.

2.2 GLACIAL LOW SEA LEVELS

As ice age conditions returned and sea level fell, the shoreline retreated seaward across the present continental shelf. Figure 1 shows several rises and falls of sea level during the period 125,000 to 30,000 years ago, however, none that resulted in the shoreline returning to the area we presently identify as the coast. Approximately 30,000 years ago sea level began to plummet, finally reaching a level some 130+ metres lower than present along the Queensland/NSW margin at the peak of the last ice-age (*circa* 18,000 years ago; Chappell, 1974). From this depth rapid sea level rise followed, which in its later stages, as it travelled landward across the present continental shelf, was termed the 'Holocene transgression'.

During the approximate 120,000 year interval where sea level remained below present, the processes of fluvial erosion were geared to a much lower base level and the valleys we presently comprehend as coastal were part of the more aggressive upper fluvial system. Consequently, they were extensively deepened by erosion (e.g. in larger coastal rivers of northern NSW and southeast Queensland these valleys achieved depths in excess of 40 m).

As had occurred cyclically through geological history, the setting of an erosionally-carved valley with some surviving remnants of previous coastal deposition, now formed the template for the next cycle of deposition.

2.3 THE HOLOCENE TRANSGRESSION

Aspects of sea level rise across a landscape can be understood by imagining slowly rising flood waters gradually enveloping an exposed land surface. However, the essential difference is that with sea level rise comes the translation of the dynamic shoreline systems and an associated array of shoreline environments. The rate of sea level rise is governed by the melting of major ice sheets, and the final extent of transgressive penetration of the sea across the land is determined by the completion of this melting. When sea level stabilised, a series of irregular embayments resulting from the flooding of old valley systems became the new template within which coastal and floodplain environments developed. As with floodwaters, the water first penetrated along the deeper river valleys, finally overtopping the confines of these deeper features and spreading across the landscape as a widespread sheet of water. Generally, the rate of sea level rise far outstripped the ability of coastal processes to fill these newly flooded valleys. The resultant large

tidal coastal water bodies became estuaries and much of our understanding of modern coastal evolution is based on models of estuarine sedimentary processes.

2.4 STILLSTAND AND DROWNED-VALLEY ESTUARINE SEDIMENTATION

Following the Holocene rise, sea level stabilised around its present level some 6,500 yrs ago (Thom and Roy, 1985), a condition termed stillstand. As sea level slowed and finally halted sedimentary processes were finally able to keep pace with, and ultimately outstrip, the production of new sub-aqueous space. The geological evolution of coastal floodplains can be explained within the broader framework of the infilling of this sub-aqueous 'accommodation' or 'drowned-valley estuary'. For many of us our image of an estuary is that of an areally-limited, near-coastal water body, however, in geological terms they are often very extensive features of which these small coastal waterbodies are only a final remnant. A fundamental model for the development of an estuary is illustrated in Figure 2.

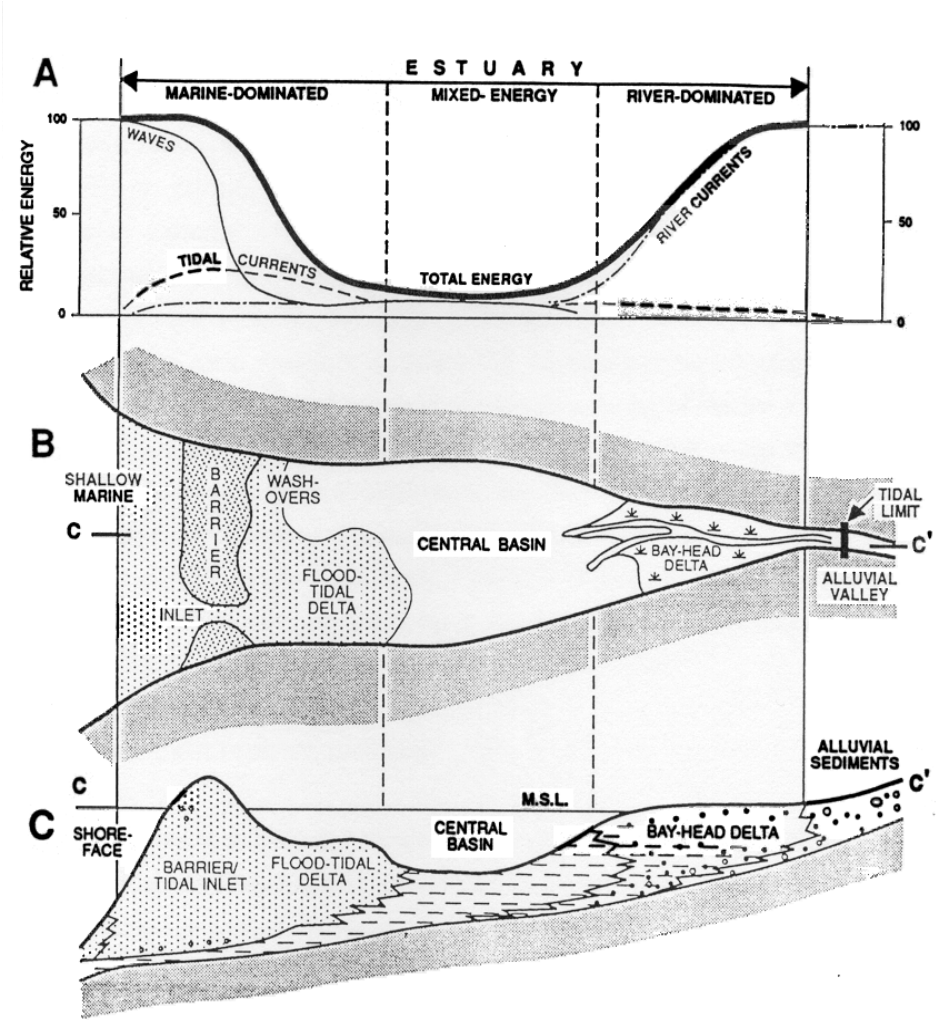

Distribution of A) energy types, B) morphological components in plan view, and C) sedimentary facies in longitudinal section with an idealized wave-dominated estuary. Note that the shape of the estuary is schematic. The barrier/sand plug is shown here as headland attached, but on low-gradient coasts it may not be connected to the local interfluves and is separated from the mainland by a lagoon. The section in C represents the onset of estuary filling following a period of transgression.

Figure 2: Lateral association of estuarine facies (Dalrymple, Zaitlin and Boyd, 1992).

3 HOLOCENE DROWNED-VALLEY ESTUARINE DEPOSITION

The following summary identifies the sequential stages of 'drowned-valley estuary' evolution, the sedimentary '[Φ]facies' that may be expected to be deposited, and some geomechanical attributes of these sediments.

3.1 STAGE 1- LOW SEA LEVEL ('GLACIAL') PERIOD

The shoreline retreated a considerable distance offshore relative to its present location. Consequently, the area now occupied by modern coastal floodplains was transformed to a river headwaters environment, characterised by an eroded, river-dissected landscape similar to that seen in present river catchment areas.

3.1.1 Resultant sedimentary facies

If the very thalweg of this antecedent valley is intersected by drilling, then a boulder stream bed may be intersected, however, far more commonly, a mature substrate clay that has developed in either residual parent material or in remnant former valley deposition, is encountered. These clays have experienced a minimum of ~120,000 years of pedogenic maturity, and consequently exhibit good compressive strength (e.g. in the order of 130+ kPa). Another relict Pleistocene-age deposit that may be encountered (particularly behind the present coast) is a degraded dune barrier, often easily identified by its distinctive humic B-horizon ('coffee' layer). These sands are generally well sorted, with an upper fine to lower medium grainsize, and are dense. The B-horizon of these low fertility soils may take the 'coffee' route where organic colloids have been present, which can vary between weakly cemented to strongly indurated hardpan (generally where iron is present), or alternatively be strengthened by a small percentage of mature clay matrix. The presence of a 'coffee' layer generally indicates that a water table has been maintained throughout the period of lowered sea level landscape exposure, and consequently Pleistocene-age acid sulfate soil (ASS) is commonly preserved at depth in these sands.

3.2 STAGE 2 – MARINE TRANSGRESSION

When rising sea level flooded a coastal river valley in this older landscape, it forced the retreat of the river mouth a substantial distance inland (e.g. in northern NSW the Clarence River mouth retreated some 60+ km inland).

3.2.1 Resultant sedimentary facies

There are three distinct facies types that may occur at the base of the valley-fill sequence as a result of the passage of the marine transgression:

i. toward the centre of the antecedent valley, a fining upward fluvial sand sedimentary sequence may be encountered representing the forced landward retreat ('backstepping') of the fluvial delta. These sands may be expected to be loose, and increase in sorting up-sequence as the site becomes more distal from the energy of the river mouth.

ii. away from the direct influence of the fluvial delta the passing of the transgression is often recognised by a thin sandy layer (often containing shells and/or organics) overlying the mature clay substrate. Although the transgression is preceded by the progressive creation of a series of familiar coastal environments such as dune, beach and backswamp environments, these are in turn generally cannibalised by the passage of shore processes, leaving little sedimentary evidence of its passing. A number of studies by the author have established that where these thin sandy lags are present, they often have a very high acid sulfate potential. Although the mechanism responsible for this elevated ASS potential is not entirely clear, it is thought that it may be due to the selective winnowing of pyrite (or its chemical antecedents) during the reworking of coastal sediments. Occasionally a thicker, more coarse-grained sand deposit will testify to the preservation of pockets of washover sands

iii. at casual scrutiny the third type, 'transgressive mangrove silt/clays', can be difficult to distinguish from the overlying 'marine clays' described in the following stage. These sediments deposit on low angle and/or protected locations (eg. embayments) where silt/clay accretion is able to support mangrove mantled shorelines. In more obvious examples mangrove debris may be present, however, where the sediments are deposited within nearshore proximity to mangroves they may contain a high percentage of very fine organics and appear to meld seamlessly into the overlying clays. Attributes of this depositional environment, such as

[Φ] Coastal sedimentary facies may be described as a 'mappable, areally restricted sedimentary body associated by either character or origin'.

anaerobic conditions, a constant interchange of sulfate and bicarbonate and substantial organic presence, provide ideal conditions for the bacteria that accelerate acid sulfate soil formation.

3.3 STAGE 3 – LATE MARINE TRANSGRESSION/SEA LEVEL STILLSTAND

During this phase a coastal sand barrier generally developed which substantially blocks the lower, or seaward end of the flooded valley creating essentially an extensive coastal tidal lake isolated from open marine conditions.

3.3.1 Resultant sedimentary facies

As sea level rise ceases, deposition can finally out-compete the creation of new subaqueous accommodation, and the main phase of valley-estuarine fill can begin. From the landward end filling occurs by stream sediments building a delta (i.e. a 'fluvial delta' or 'bay-head delta'). The rapid dissipation of energy as the fluvial discharge enters this estuarine 'lake' limits the extent to which sand size sediments can be transported. Similarly, from the seaward end the tidally transported marine sands invade through the passage to the sea building a 'flood-tide delta', but, again, the extent of this sand transport is curtailed by the dissipation of energy.

The centre of this large tidal lake, an area called the 'estuarine central basin' remains a large energy void, into which only fine suspension load sediments (i.e. fine silt and clay size sediments from fluvial sources) can be transported and settle. These sediments, commonly identified as 'marine clays' by engineers because of the shells present in them, are more correctly termed 'estuarine central-basin silt/clays'. Both the perception that these sediments are 'clays' and their apparent uniformity in appearance can be deceptive from an engineering point of view. These sediments commonly contain layers that have a high silt percentage (>50%), particularly toward the landward end of the system where they interface with the prodelta, presenting potential shear planes.

It should be noted that these deposits are not soils in the true sense, but rather virgin sediment that has not experienced pedogenesis, and consequently they have a poor compressive strength (e.g. ~20 kPa) prior to controlled loading and dewatering.

3.4 STAGE 4 – FINAL STAGES OF COASTAL FLOODPLAIN DEPOSITION

During the preceding stage estuarine deposition can be comfortably separated into three broad depositional entities (bayhead or fluvial delta, central basin, and flood tide delta). As the central basin area fills and the water body shallows, a platform is created for fluvial deposition to project itself across, creating the series of more complex fluvial and alluvial environments that support human occupation.

3.4.1 Resultant sedimentary facies

Simplistically, the model for this final phase of deposition can be seen as the main river passing centrally through the valley, developing levees which produce an alluvial wedge feathering toward the valley margins. Commonly swamps along these valley margins identify little or no alluvial cover over the old estuarine surface. Consequently, the draining of these swamps to extend grazing in many coastal valleys has generated a substantial acid sulfate soil problem. The initial return of the fluvial delta is generally signalled in the sedimentary sequence by occasional thin fine sandy layers in the upper estuarine basin clay deposits representing higher energy intrusions into the normally silt/clay dominated pro-delta facies. The arrival of the delta proper is often marked by a distinct boundary to sand dominated deposition. In a Doppler like analogy, this sand will generally coarsen up sequence as the fluvial energy source overtakes the site. As with the underlying central-basin silt/clay facies, this fluvial sand deposit is generally pedogenically immature, loose and flowing.

Commonly however, the stratigraphy of floodplain surface environments is considerably more complex than this simple model, due to factors such as river meandering and division of the primary channel into anabranches. Additionally, whereas the stages of estuarine development presented above provides a reasonable model for the main valley, there is often a series of subsidiary basins referred to as 'floodbasins' representing former tributary catchments in the drowned-valley system. These floodbasin environments exhibit a further set of characteristic sedimentary depositional environments. The Clarence Valley in northern NSW presents an ideal example of this with a series of 'floodbasins' at various stages of maturity.

The model for drowned-valley estuary evolution outlined above has good application in the large coastal rivers of NSW, but progressively loses application moving into Queensland where the southeast is influenced by large tidal basin estuaries developed behind an offshore sand barrier, and onward to northern Queensland where barrier reefs occupy broad continental shelves. Some of these differences are summarised in Table 1.

Table 1: Summary of the main differences in coastal lowland development between southern Australian states and northern Australian states.

S.E. QUEENSLAND + N.S.W. + VICTORIA	NORTHERN AUSTRALIA
narrow and steeper continental shelf = exposed high energy coastline	wider shallow continental shelf – major reef provinces = protected low energy coastline
deep sandy coastal barriers	vast [γ]chenier plains incorporating mangrove mud flats or low beach ridge plains with subtidal nearshore mud (possibly incl. mangroves) buried beneath.
generally estuaries still filling – very little fluvial discharge of sand size sediment into the marine environment	estuaries generally filled – large seasonal discharge of sediment into the marine environment
deep, extensive Holocene-age coastal estuaries buried beneath coastal lowlands	shallower, extensive Holocene estuaries buried beneath coastal lowlands and occupying large north facing embayments
largely temperate climate = less biological and chemical activity ∴ reduced acid sulfate soil intensity	warm wet tropical climate = greater biological and chemical activity ∴ increased acids sulfate soil intensity

4 CONCLUSION

The wealth of knowledge of coastal processes and depositional sequences accumulated within the discipline of coastal geology has a great deal to contribute to understanding the genesis and distribution of unconsolidated valley-fill sequences. Application of stratigraphic modelling and mapping can provide a practical framework within which to couch an understanding of engineering and environmental parameters.

5 REFERENCES

Chappell, J. (1974) Late Quaternary glacio- and hydro-isostasy on a layered earth. *Quaternary Research* 4:429-440.

Chappell, J. (1982) Sea levels and sediments: some features of the context of coastal archaeological sites in the tropics. *Archaeology in Oceania* 17:69.

Chappell, J. (1987) Late Quaternary sea-level changes in the Australian region. In, Tooley MJ and Shennan I (eds) Sea-level changes. Blackwell, Oxford, p. 296-331.

Chappell, J. and Shackleton, N.J. (1986) Oxygen isotopes and sea-level. *Nature* 324:137-40.

Dalrymple, R.W., Zaitlin, B.A. and Boyd, R. (1992) Estuarine facies models: conceptual basis and stratigraphic implications. *Journal of Sedimentary Petro*logy 62:1130-1146.

Pickett, J.W., Thompson, C.H., Kelley, R.A. and Roman, D. (1985) Evidence of high sea level during isotope stage 5c in Queensland, Australia. *Quaternary Research* 24:103-114.

Thom, B.G. and Roy, P.S. (1985) Relative sea levels and coastal sedimentation in southeast Australia in the Holocene. *Journal of Sedimentary Petrology* 55(2):257-264.

[γ] chenier - discrete, elongated sand and/or shell bodies stranded on a coastal mudflat or marsh.